Application of Electro-oxidation for the Degradation of Organics in Oil Sands Process Water (OSPW)

by

Abdallatif Satti Abdallatif Abdalrhman

A thesis submitted in partial fulfillment of the requirements for the degree of

Doctor of Philosophy

in

Environmental Engineering

Department of Civil and Environmental Engineering
University of Alberta

ABSTRACT

Large volumes of oil sands process water (OSPW) are generated during the extraction of bitumen from the mined oil sands ores in northern Alberta. The treatment of OSPW is currently considered a serious challenge facing the oil sands industry in the region. Among the different constituents in OSPW, naphthenic acids (NAs) are considered the most abundant and problematic organic pollutants. Enormous efforts have been implemented towards the development of strategies for OSPW treatment. However, highly effective and cost-efficient treatment approaches have not been found so far.

The main objective of this study was to investigate the effectiveness of applying electro-oxidation (EO) at low current densities as a treatment option for OSPW treatment. Combining EO with aerobic biodegradation was proposed as an effective and cost-efficient treatment train for OSPW. The study investigated the performance of EO by graphite anode for NAs degradation, biodegradability enhancement, and toxicity reduction. The degradation kinetics and structure-reactivity relation for NAs during EO by graphite anode were also investigated. The performance of EO by graphite anode for the degradation of organics in real OSPW was evaluated and compared with that by dimensionally stable $Ti-RuO_2/IrO_2$ anode (DSA). The effectiveness of EO for improving the biodegradability of NAs in OSPW was also evaluated.

In the first set of investigations, EO by graphite anode was applied for the degradation of a commercial NA mixture in water samples. At current densities of 0.5, 2.5, and $5\,mA/cm^2$, acid extractable fraction (AEF) was removed by 42.2%, 57.0% and 67.9%, respectively, while classical NAs were degraded by 76.9%, 77.6% and 82.4%, respectively. Oxidized NAs were also degraded effectively during EO. The biodegradability of the NA mixture was improved by up to

2.7 folds when the samples were pre-treated with EO. The aromatic NA fraction was degraded effectively by EO. Biodegradation alone reduced the acute toxicity of the NA mixture towards *Vibrio fischeri*; however, the combination of EO with biodegradation resulted in a complete removal of the acute toxicity, showing a synergistic effect for combining these two processes.

In the second set of investigations, the degradation kinetics and structure-reactivity relation for NAs during EO by graphite anode was investigated by using model NA compounds. The degradation of cyclohexanecarboxylic acid (CHA) increased steadily with increasing the applied current density from 0.25 to $20 \, mA/cm^2$ and followed pseudo first-order degradation kinetics with rates increased from 0.00091 to $0.01 \, min^{-1}$, respectively. The main oxidation mechanism for CHA during EO by graphite was through oxygenated species generated at the surface of anode. The structure-reactivity analysis showed that NAs with higher carbon number were preferentially degraded by EO. Branched NAs were more reactive than non-branched NAs only if the branch existed far enough from the carboxylate group. Monocyclic NAs were more reactive than linear NAs, but any increase in the cyclicity beyond one ring resulted in reduced reactivity. Aliphatic compounds were found to be more reactive than aromatic compounds and the existence of more than one carboxylate group in the structure hindered the reactivity.

In the third set of investigations, the performances of EO by graphite anode and DSA for the degradation of the recalcitrant organics in real OSPW were investigated and compared. EO by graphite anode was able to reduce the chemical oxygen demand (COD), AEF, classical NAs, oxidized NAs and aromatics in OSPW even at current density as low as $0.5 \, mA/cm^2$. The removal of organics by DSA, however, did not start until the applied current density reached $2 \, mA/cm^2$. Graphite anode showed higher NAs and AEF removals than DSA at current densities below $20 \, mA/cm^2$. The degradation of NAs by both anodes followed pseudo first-order kinetics.

The reactivity of NAs toward oxidation by both anodes increased with the increase in the cyclicity and carbon number. EO by DSA generated NAs with low-carbon number as byproducts of the oxidation of high-carbon NAs. Graphite anode maintained higher current efficiency at all applied current densities. Both anodes were able to remove the aromatic compounds with DSA being more selective toward aromatics especially those with multiple aromatic rings. Graphite was more effective at low current densities, but at high current densities DSA became superior.

In the fourth set of investigations, combining EO with biodegradation for real OSPW treatment was evaluated in terms of NA biodegradability enhancement. Qualitative analysis using ion mobility spectrometry (IMS) showed that EO by graphite was able to degrade the different NA clusters in OSPW including classical, oxidized and heteroatomic NAs. Applying EO even at current density as low as 0.2 mA/cm^2 resulted in reductions in classical NAs and AEF by 19% and 6.7%, respectively. Aerobic bio-incubation for 40 day was able to achieve reductions in NAs as high as 30.9% when the samples were pre-treated with EO. The removal of AEF during bio-incubation, however, was very slow. It was demonstrated that applying EO as pre-treatment before bio-incubation can increase the biodegradability of some classical NAs classes by up to 4.4 folds. The analysis for the microbial communities after bio-incubation showed differences between samples without EO pre-treatment and those with EO pre-treatments. The abundance of Alphaproteobacteria was higher in the samples with EO pre-treatment.

This research has shown that low-current EO by graphite anode can be a promising pre-treatment option for OSPW while being routed to in-pit lakes or wetlands where further biodegradation can take place. EO can lead to improved biodegradability and reduced acute toxicity of NAs. The lower voltages required, low-cost of graphite electrodes and exclusion of chemicals addition can result in a sustainable and environmental friendly process that can be run by renewable energy.

PREFACE

All of the research work described in this thesis was designed and performed by myself under the direct supervision of Dr. Mohamed Gamal El-Din in the Department of Civil and Environmental Engineering at the University of Alberta. This thesis was designed in a paper-based format with Chapters (2-5) represent stand-alone papers that have been published or will be submitted for publication. I conducted all of the experimental work as well as the data interpretation and analysis and the preparation of the manuscripts under the supervision of Dr. Mohamed Gamal El-Din. Some post-doctoral colleagues contributed to sample analysis or manuscript edits, and some of them were co-authors in the manuscripts. The contributions from different collaborators and coauthors are described below:

Chapter 2 has been published as "*Abdalrhman, A. S., Y. Zhang, and M. Gamal El-Din. 2019. Electro-oxidation by graphite anode for naphthenic acids degradation, biodegradability enhancement and toxicity reduction. Science of the Total Environment 671:270-279.*". Dr. Mohamed Gamal El-Din contributed to the research planning and manuscript revision. Dr. Yanyan Zhang and Dr. Pamela Chelme-Ayala contributed to the edit and revision of the manuscript. Dr. Rongfu Huang performed the detection of NAs using ultra-performance liquid chromatography time-of-flight mass spectrometry (UPLC TOF-MS).

Chapter 3 has been published as "*Abdalrhman, A. S., S. O. Ganiyu, and M. Gamal El-Din. 2019. Degradation kinetics and structure-reactivity relation of naphthenic acids during anodic oxidation on graphite electrodes. Chemical Engineering Journal 370:997-1007.*". Dr. Mohamed Gamal El-Din contributed to the research planning and manuscript revision. Dr. Soliu Ganiyu and Dr. Pamela Chelme-Ayala contributed to the edit and revision of the manuscript. Dr. Mingyu

Li and Dr. Selamawit Messele performed the measurement of NAs concentration using the liquid chromatography- mass spectrometry (LC-MS). Dr. Mingyu Li also helped with the sample preparation for scanning electron microscope (SEM) and X-ray photoelectron spectroscopy (XPS).

Chapter 4 will be submitted to Journal of Hazardous Materials as "*Abdalrhman, A. S. and M. Gamal El-Din. Degradation of the recalcitrant organics in real oil sands process water by electro-oxidation using graphite and dimensionally stable anodes.*". Dr. Mohamed Gamal El-Din contributed to the research conduction and manuscript edits. Dr. Pamela Chelme-Ayala and Dr. Soliu Ganiyu contributed to the revision of the manuscript. Dr. Rongfu Huang did the NA detection using UPLC-TOFMS.

Chapter 5 will be submitted to Water Research as "*Abdalrhman, A. S., Y. Zhang, and M. Gamal El-Din. Low-current electro-oxidation accelerates the biodegradation of the recalcitrant organics in oil sands process water*". Dr. Mohamed Gamal El-Din contributed to the research planning and manuscript revision. Dr. Yanyan Zhang and Dr. Pamela Chelme-Ayala contributed to the edit and revision of the manuscript. Dr. Yanyan Zhang also helped in performing DNA extraction, quantitative polymerase chain reaction (qPCR). Dr. Rongfu Huang performed the detection of NAs and IMS using UPLC-TOF-MS.

DEDICATION

To my parents; Amal & Satti

To my brother (Ali) and sisters (Sarah and Samah)

To all my family and friends

To the souls of my grandmother and uncle

To the souls of those who died fighting for freedom, peace and justice in Sudan

To the whole Humanity

ACKNOWLEDGEMENTS

TABLE OF CONTENTS

LIST OF TABLES

LIST OF FIGURES

ABBREVIATIONS

2mHPA	2-methylheptanoic acid
4mCHA	4-methyl-1-cyclohexanecarboxylic acid
4mHPA	4-methylheptanoic acid
AAA	1-adamantaneacetic acid
ADA	1, 3-adamantanedicarboxylic acid
AEF	Acid extractable fraction
AO	Anodic oxidation
AOPs	Advanced oxidation processes
BQ	1,4-benzoquinone
CHA	Cyclohexanecarboxylic acid
CHPA	5-cyclohexanepentanoic acid
COD	Chemical oxygen demand
DBE	Double bond equivalent
DCHA	Dicyclohexylacetic acid
DCM	Dichloromethane
DNA	Deoxyribonucleic acids

DO	Dissolved oxygen
DOC	Dissolved organic carbon
DSA	Dimensionally stable anode
EO	Electro-oxidation
EOAPs	Electrochemical advanced oxidation processes
FT-IR	Fourier transform infrared
GAC	Granular activated carbon
GEC	General current efficiency
H_2O_2	Hydrogen peroxide
HPA	Heptanoic acid
NAs	Naphthenic acids
O_3	Ozone
OCA	Octanoic acid
OSPW	Oil sands process water
PAHs	Polycyclic aromatic hydrocarbons
PVA	5-phenylvaleric acid
qPCR	Quantitative polymerase chain reaction

RNA   Ribonucleic acids

SEC   Specific energy consumption

SEM   Scanning electron microscope

TBA   Tert-butyl alcohol

TOC   Total organic carbon

TPCA   Trans-4-pentylcyclohexane carboxylic acid

UPLC-TOF-MS   Ultra-performance liquid chromatography time-of-flight mass
spectrometry

XPS   X-ray photoelectron spectroscopy

1. GENERAL INTRODUCTION AND RESEARCH OBJECTIVES

1.1 Background

Large amounts of fresh water are consumed by the industry for various purposes, which consequently results in the generation of huge amounts of wastewater. Industrial wastewaters are complex mixtures of various organic and inorganic compounds, depending on the nature of the industry, and some of them can be toxic and difficult to treat (Särkkä et al. 2015). With the continuous tightening of the environmental regulations in many different areas, and the growing social and economic pressures for a more sustainable development, adopting "zero-pollution" processes and developing more efficient technologies for industrial wastewater treatment have become a must (Panizza and Cerisola 2009). The oil sands industry in Alberta, Canada, is a typical case of an industry that is currently facing critical water demand and wastewater treatment challenges.

The bitumen reserves in the northern areas of Alberta are the third largest oil reserves in the world with proven reserves of 170 billion barrels of recoverable bitumen (Swart and Weaver 2012). The production rate from these reserves was 1.9 million barrels per day in 2012, it reached 2.3 million barrels per day in 2014, and the number is predicted to reach 4 million barrels per day by 2024 (Hooshiar et al. 2012, Swart and Weaver 2012). Surface mining and steam assisted gravity drainage (SAGD) are currently the commercially applied methods for the bitumen extraction from oil sands. Surface mining is applied in the case of shallow oil sands deposits (90 m or less) followed by alkaline hot water extraction (50-80 °C) (Pal et al. 2015). The overall recovery rate of bitumen from the oil sands ore through this process is usually higher than 90% (Hooshiar et al. 2012). For deeper oil sands deposits,

1

surface mining becomes uneconomical. In this case, the bitumen must be recovered without removing the ores through an in situ process known as steam assisted gravity drainage (SAGD). In SAGD, steam is injected through upper horizontal wells to reduce the viscosity of bitumen by heating the oil sands which will then moves into lower horizontal wells where it is recovered (de Klerk et al. 2014). Both bitumen extraction methods (i.e., surface mining and SAGD) depend mainly on water. However, surface mining is more water intensive (Masliyah et al. 2004, Allen 2008a, de Klerk et al. 2014).

The extraction of bitumen from the mined oil sand ores occurs through what is known as Clark process which consume huge amount of caustic hot water and results in the generation of huge volumes of process water known as oil sands process water (OSPW) (Masliyah et al. 2004, Allen 2008a, de Klerk et al. 2014, Pal et al. 2015). Despite the high water recycling rates, more than 80%, the fresh water intake for mined oil sands is still very high at around 2 to 3 barrels of fresh water for every barrel of upgraded bitumen (Masliyah et al. 2004). Currently, oil sands companies are not allowed to release their OSPW into the receiving environment. Instead, OSPW is sent to constructed tailings ponds in order to be stored for the long-term (Wiseman et al. 2013). Tailings ponds are growing in volume and number with an accumulated amount of OSPW estimated to be more than 1 billion m^3 covering an area of more than 170 km^2 (Pereira et al. 2013). As the oil sands mining is expanding, more fresh water will be needed and consequently more OSPW will be generated. The oil sands companies are obligated to remediate the OSPW in the future and reclaim the tailing ponds into sustainable ecosystems at the end of their operations according to their contract with the Government of Alberta (Masliyah et al. 2004, Allen 2008a). Considering the large volumes of currently impounded OSPW and the expected

increase, the development of effective treatment technologies for OSPW remediation is a critical need.

1.2 Oil sands process water (OSPW)

1.2.1 Alberta oil sands

Alberta oil sands are mixtures of 4–18 wt% bitumen, 55–80 wt% inorganic materials (mostly sands and clays) and 2–15 wt% water, depending on the quality and location of ores (Osacky et al. 2013). Bitumen is an extra-heavy crude oil that has higher density and viscosity compared to conventional crudes. Alberta oil sands bitumen has a density in the range of $1000-1029$ kg m^{-3}, carbon content in the range of $83.1-83.4$ wt%, and viscosity between 80 to12 000 Pa s (at 20 °C) (de Klerk et al. 2014).

1.2.2 Source and composition of OSPW

The initially generated waste slurries from the extraction process are mixtures of water (70 to 80%), solids (20 to 30 %) and residual bitumen (1–3 %) (Allen 2008a). The slurries then settle in the tailings ponds creating 3 layers: (i) the top layer is clarified water contains total suspended solids in the range 15–70 mg/L and residual bitumen and it is known as OSPW; (ii) the middle layer is an aqueous suspension with fine particles (silt and clay); and (iii) the bottom layer includes rapidly settled particles, such as sand (Allen 2008a, Han et al. 2009). The OSPW (top layer) is slightly alkaline, with a pH in the range of 7.8 to 8.7, and is known to be acutely toxic to aquatic organisms because of the organic compounds leached from bitumen during the extraction processes (Allen 2008a, Wang et al. 2013, Wiseman et al. 2013).

The properties of OSPW vary from one site to another depending on several factors such as the ore quality, extraction process and age (Allen 2008a, Kannel and Gan 2012, de Klerk et al. 2014). OSPW is considered brackish water with total dissolved solids (TDS) in the range of 2000-2500 mg/L and electrical conductivity of 3.0-3.7 mS/cm (Gamal El-Din et al. 2011, Kim et al. 2012). Among the different inorganics in OSPW, the dominant components are bicarbonate (800-1000 mg/L), sodium (500-700 mg/L), chloride (75-550 mg/L) and sulfate (200-300 mg/L) (Allen 2008a, Choi et al. 2014). OSPW is relatively hard with calcium and magnesium concentrations of 15-25 mg/L and 5-10 mg/L, respectively (Masliyah et al. 2004, Allen 2008a, Gamal El-Din et al. 2011, Pourrezaei et al. 2011).

A number of organic compounds have been detected in OSPW including bitumen, NAs, phenols, phthalates, benzene, ethylbenzene, toluene, asphaltenes, xylenes, creosols, polycyclic aromatic hydrocarbons (PAHs), and humic and fulvic acids (Rogers et al. 2002, Allen 2008a, Kannel and Gan 2012). Some of the properties of an OSPW sample that was collected from an active oil sands tailings pond in Fort McMurray, Alberta, Canada, were reported by Wang et al. (2015), as shown in Table 1.1.

Table1.1 Typical composition of OSPW

Parameter	Value
Turbidity (NTU)	135 ± 12
pH	8.4 ± 0.2
Alkalinity (mg/L)	776.9 ± 7.6
Color (CU)	11.3 ± 1.3
COD (mg/L)	211.0 ± 8.0
TOC (mg/L)	56.3 ± 6.0
DOC (mg/L)	45.3 ± 5.0
UV_{254} absorbance (cm^{-1})	0.494 ± 0.018
Classical naphthenic acids (NAs) (mg/L)	12.1 ± 0.8
Sodium (mg/L)	840.6 ± 1.7
Magnesium (mg/L)	8.6 ± 0.1
Calcium (mg/L)	10.1 ± 0.1
Potassium (mg/L)	14.7 ± 0.1
Titanium (mg/L)	0.09 ± 0.03
Gallium (mg/L)	0.001 ± 0.000
Iron (mg/L)	1.0 ± 0.0
Aluminum (mg/L)	2.1 ± 0.0
Manganese (mg/L)	0.02 ± 0.01
Nickel (mg/L)	0.01 ± 0.00

1.2.3 Naphthenic acids

Among the various organic constituents in OSPW, naphthenic acids (NAs) have gained great attention because of their high toxicity toward different organisms in addition to their corrosive behaviour toward the process equipment (Quinlan and Tam 2015). NAs occur naturally as a part of the bitumen mixture; they are the products of the incomplete degradation of petroleum hydrocarbons by the indigenous microbial communities in the reservoirs (Brown and Ulrich 2015). Generally, NAs account for around half of the total organic fraction in OSPW, and there are more than 200,000 possible NA structures associated with the OSPW (Garcia-Garcia et al. 2011, Rowland et al. 2011). NAs are defined as complex mixture of aliphatic, cyclic, acyclic, or polycyclic alkyl-substituted carboxylic acids with the general chemical formula $C_nH_{2n+z}O_x$, where n represents the carbon number and varies in the range of 7 to 30, z is either zero or a negative even integer ranging from 0 to -18 and represents the number of hydrogen deficiency and x represents the number of oxygen atoms (x = 2) for classical NAs and (x $\geq$3) for oxidized NAs (Clemente et al. 2003, Barrow et al. 2010, Wang et al. 2013).

The quantification and identification of NAs in OSPW is considered a challenging analytical task because of the high complexity of the OSPW mixture. A number of analytical methods have been developed for NA quantification and identification through using various analytical techniques, such as Fourier transform infrared spectroscopy (FTIR) (Scott et al. 2008a), gas chromatography (GC) (Holowenko et al. 2002), electrospray ionization–mass spectrometry (ESI–MS) (Martin et al. 2008), high performance liquid chromatography (HPLC) (Lu et al. 2013), in addition to various high resolution techniques including HPLC coupled with time of flight (TOF-MS) (Ross et al. 2012, Wang et al.

2016a), LC/MS/MS, Orbitrap-MS, and Fourier Transform Ion Cyclotron Resonance (FTICR) MS (Headley et al. 2013). FTIR spectroscopy had been used earlier during the development of a method for NA quantification. The issue with the FTIR method is that it detects all the organics that contain -CO, -CHO and -COOH groups; therefore, it overestimates the NA concentrations by detecting compounds that do not adhere to the strict chemical formula for NAs and will rather quantify which is known as the acid extractable fraction (AEF) of OSPW (Gamal El-Din et al. 2011).

1.2.4 Toxicity of OSPW

Since the beginning of the research on OSPW NAs, there has always been a connection between NAs and the toxicity of OSPW (MacKinnon and Boerger 1986). This was supported by the accumulation of studies suggesting that NAs are the principal cause of OSPW toxicity (Brown and Ulrich 2015). OSPW has been shown to be acutely, sub-chronically and chronically toxic to a variety of organisms (Wiseman et al. 2013, Li et al. 2017) including; phytoplankton (Woodworth et al. 2012), zooplankton (Frank et al. 2009), invertebrates (Hagen et al. 2013), mammals (Garcia-Garcia et al. 2011), fish (Hagen et al. 2013), plants (Armstrong et al. 2010), and bacteria (Wang et al. 2013). Despite the existence of a clear relation between the concentration of NAs and toxicity, determining the total NAs concentration is still insufficient to describe the exact toxic effects of NAs because the molecular structure and composition of the NA mixture can also play an important role (Clemente and Fedorak 2005, Wang et al. 2013). It is still not clear which NA structure in OSPW are more toxic, however, some researchers have suggested that the lower molecular weight compounds in a NA mixture correlate with higher toxicity for various organisms (Holowenko et al. 2002, Rogers et al. 2002, Brown and Ulrich 2015).

7

Recently, some studies have suggested that NAs, although they have the major contribution, are not the only cause of OSPW toxicity and that some of the other organic constituents may also contribute to the toxicity directly or through synergistic effects (Garcia-Garcia et al. 2011, Hagen et al. 2013).

1.2.5 OSPW treatment

1.2.5.1 Adsorption

Adsorption has been studied widely for contaminants removal from water and wastewater (Simpson 2008). A number of studies have investigated the effectiveness of adsorption for NAs removal by using various types of adsorbents including: petroleum coke (Gamal El-Din et al. 2011, Small Christina et al. 2012, Zubot et al. 2012); Granular activated carbon (GAC) (Mohamed et al. 2008, Islam et al. 2015); sawdust-based activated carbons (Iranmanesh et al. 2014); organic reach soil (Janfada et al. 2006); activated petroleum coke (Small Christina et al. 2012) and carbon xerogel (Benally et al. 2019). Generally, activated carbon has been investigated more frequently among other adsorbents for NAs removal from OSPW due to its higher surface area and greater adsorption capacity (up to 32 mg g^{-1}) (Quinlan and Tam 2015, Benally et al. 2019). Despite the high porosity and large specific surface area of activated carbon which resulted in its high adsorption efficiency, the cost for preparing, using and regenerating commercial activated carbons is considered a large obstacle (Çeçen and Aktaş 2011).

1.2.5.2 Coagulation/flocculation

Coagulation/flocculation is a common pre-treatment step in municipal and industrial wastewaters treatment that aims to remove the suspended solids, colloidal particles and

insoluble organics (Pourrezaei et al. 2011). The process has been applied successfully at large-scale for treating various types of industrial wastewater including petroleum refineries' wastewater (Santo et al. 2012). An enhanced coagulation process developed by using alum and cationic polymer polyDADMAC was successfully applied for the treatment of OSPW and was able to remove 37% of classical NAs and 86% of oxidized NAs (Pourrezaei et al. 2011). Recently, polyaluminum chloride was also applied as coagulant for OSPW remediation and but it showed low removals for NAs despite the high turbidity removal of over 96% (Wang et al. 2015). Coagulation/flocculation has proven to be a useful pre-treatment step for OSPW remediation given its potential to improve the performance of main treatment step, such as membrane filtration (Loganathan et al. 2015). Electro-coagulation has also been applied for the removal of NAs and resulted in considerable removal of up to 93% (Quinlan and Tam 2015). Although, coagulation/flocculation has shown positive results in treating OSPW, there are still a number of limitations associated with using this process. These limitations include the need for expensive chemicals, the production of large amounts of sludge and the high operating costs (Quinlan and Tam 2015).

1.2.5.3 Membrane filtration

Membrane technology has been used successfully for more than three decades for the removal of pollutants from industrial wastewaters (Allen 2008b, Alpatova et al. 2013). Membranes can produce high quality effluent at high throughput, making them strong candidates for OSPW treatment (Alpatova et al. 2013). A number of studies have investigated the use of various types of membranes for OSPW treatment. A bench-scale flat sheet membrane system was able to maintain a acceptable permeates fluxes while achieving

NA removals of over 95%, but the fouling was severe at the end (Peng et al. 2004). In another study, a commercial ceramic ultrafiltration membrane was used for OSPW treatment but resulted in limited NAs removals compared to the high removal for particulates (Alpatova et al. 2014). Forward osmosis was also applied successfully to reduce the volume of OSPW by using dilute brackish basal depressurization water (BDW) as draw solution and resulted in more than 40% reduction in the volume of OSPW (Zhu et al. 2017). Generally, the main limitation facing the use of membrane filtration processes is membrane fouling (Peng et al. 2004). Therefore, in order to apply membrane technology successfully for the remediation of OSPW, it would likely require the combination of other processes with it to reduce the fouling, such as coagulation/flocculation (Kim et al. 2012, Alpatova et al. 2014).

1.2.5.4 Biological processes

Biological treatments are considered the most popular and widespread processes for wastewater treatment. They have been well-studied for many decades, and they have a great cost advantages that, so far, could not be overcome by other processes (Ganzenko et al. 2014). Despite the toxicity of OSPW to many organisms, as discussed earlier in this chapter, biodegradation by indigenous microbial communities from the tailing ponds has been pursued extensively for OSPW treatment (Herman et al. 1994, Brown and Ulrich 2015, Xue et al. 2018). Different microorganisms native to tailing ponds were used successfully to degrade commercial NA mixtures (Clemente et al. 2004). The relationship between NAs structures and their biodegradability was investigated for both OSPW and commercial NAs mixture (Han et al. 2008). It has also been reported that the native NAs present in OSPW mixture are more recalcitrant to biodegradation compared to the commercial NAs mixtures

(Scott et al. 2005, Han et al. 2008). Different suspended growth and biofilm biological reactors have been applied for OSPW treatment and resulted in promising results (Choi et al. 2014, Xue et al. 2018). Suspended growth aerobic batch reactor with microbial communities native to tailing bonds were able to achieve NAs removal of 22.2% after 73 days of treatment (Dong et a. 2015). Integrated fixed-film activated sludge reactor (IFAS) and moving bed biofilm reactor (MBBR) reactors, on the other hand, were able to achieve NAs removals of 56.7% and 70.6%, respectively (Huang et al. 2017).

A number of microorganisms have shown the ability to degrade and metabolize NAs from OSPW including Nitrosomonas, Arenimonas, Mycobacterium, Limnobacter, Mesorhizobium, Nitrosospira, Bradyrhizobiaceae, and Comamonas Alcaligenes faecalis (Quinlan and Tam 2015). However, similar to many other toxic and/or refractory organic pollutants, the biodegradation of NAs is a very slow and inefficient, therefore, the process needs to be coupled with other processes in order to be considered viable. Ozonation has been frequently studied as a pre-treatment for the biodegradation of OSPW (Han et al. 2008, Martin et al. 2010, Xue et al. 2018). Recently, a number of hybrid biological processes have been proposed for OSPW remediation such as biological-granular activated carbon (Bio-GAC) which combines adsorption with biodegradation (Islam et al. 2015), and membrane bioreactor (MBR) which combines membrane separation with biodegradation (Xue et al. 2016).

1.2.5.5 Advanced oxidation processes (AOPs)

Advanced oxidation processes (AOPs) have gained a wide recognition as an effective treatment option for the degradation of recalcitrant organic pollutants in water and wastewaters. Various advanced oxidation processes have been studied for the degradation

of NAs in OSPW, among them the use of ozone has been reported more frequently (Brown and Ulrich 2015, Quinlan and Tam 2015, Xue et al. 2016). Scott and co-workers were the first group to attempt treating OSPW with ozonation more than a decade ago and they found that ozonation successfully removed NAs by more than 95% and removed the toxicity of OSPW (Scott et al. 2008b). Following that, a number of studies have utilized ozone for treating OSPW with results indicating enhanced biodegradability (Martin et al. 2010), high removal of NAs (Scott et al. 2008b, Wang et al. 2013), and toxicity reduction (Garcia-Garcia et al. 2011, Wang et al. 2013). The principal limitation associated with ozonation for OSPW treatment is the need for applying impractical high ozone doses to achieve the needed NAs removal and biodegradability enhancement which is not economically feasible (Scott et al. 2008b, Wang et al. 2013). A combined O_3/H_2O_2 process has been investigated recently for OSPW treatment and has shown higher NAs removal efficiency compared to ozonation alone (Afzal et al. 2015, Wang et al. 2016c). Other types of AOPs that have been investigated for OSPW treatment include: microwave treatment (Mishra et al. 2010); UV/chlorine process (Shu et al. 2014); UV/hydrogen peroxide (Wang et al. 2016c); and Fenton processes (Zhang et al. 2017). Although most of the studied AOPs have shown positive results in terms of NAs removal from OSPW, all of them were restricted either by the high required doses or other technical restrictions such as the OSPW's alkaline pH in the case of Fenton or the turbidity of OSPW in the case of UV-based AOPs. Ferrate (VI) chemical oxidation was also investigated for the degradation of OSPW organics and achieved NAs removal of up to 78.4%, however the required chemical dose for the treatment was very high (400 mg/L) (Wang et al. 2016b).

1.2.6 Electrochemical oxidation processes

The traditional definition of advanced oxidation processes (AOPs) was restricted to the processes involving the generation of sufficient amount of hydroxyl radical enough to effectively degrade the pollutants (Glaze et al. 1987). This definition was later expanded to include the electrochemical generation of heterogeneous hydroxyl radicals on the anode surface during Electrochemical advanced oxidation processes (EOAPs) (Brillas et al. 2009).

EOAPs have been used successfully for the degradation of different recalcitrant pollutants (Zanta et al. 2000, Szpyrkowicz et al. 2005, Panizza and Cerisola 2006, 2007, Brillas et al. 2009, Panizza and Cerisola 2009, Sirés et al. 2014, Martínez-Huitle et al. 2015, Särkkä et al. 2015, Moreira et al. 2017, Martínez-Huitle and Panizza 2018). Despite that, they have not been investigated for the treatment of OSPW yet. EOAPs can be classified into anodic and cathodic processes depending on whether oxidants are produced at the anode or cathode (Brillas et al. 2009, Panizza and Cerisola 2009, Sirés et al. 2014, Martínez-Huitle et al. 2015, Martínez-Huitle and Panizza 2018). Cathodic oxidation mainly involves the production of hydrogen peroxide (electroperoxidation) through the reduction of O_2 at cathode (Oturan 2000, Drogui et al. 2001, Brillas et al. 2009, Panizza and Cerisola 2009). Anodic oxidation (AO) is generally referred to as Electro-oxidation (EO). AO involves the generation of oxidants at anode and it has been studied and applied more frequently (Brillas et al. 2009, Panizza and Cerisola 2009, Sirés et al. 2014, Martínez-Huitle and Panizza 2018) [73-79]. The oxidation of pollutants during anodic oxidation can occur through: direct electron transfer (DET) by transferring electrons from the substrate (R) to the anode (Eq. (1.1)); the generation of reactive intermediates from water oxidation such as hydroxyl radicals ($^\bullet OH$) at anode (M) (Eq. (1.2)) and other oxidants that can be generated at anode

from water or dissolved anions such as Cl_2 (Eq. (1.3) and $S_2O_8^{2-}$ (Eq. (1.4)) H_2O_2 (Eq. (1.5)) and ozone (Eq. (1.6)) (Panizza and Cerisola 2009, Sirés et al. 2014, Martínez-Huitle et al. 2015).
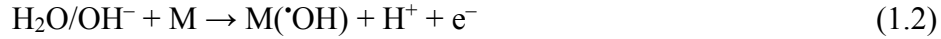
$$R \rightarrow (R^{\bullet})^+ + e^- \qquad (1.1)$$

$$H_2O/OH^- + M \rightarrow M(^{\bullet}OH) + H^+ + e^- \qquad (1.2)$$

$$2Cl^- \rightarrow Cl_2 + 2e^- \qquad (1.3)$$

$$2SO_4^{2-} \rightarrow S_2O_8^{2-} \qquad (1.4)$$

$$2\,A(^{\bullet}OH) \rightarrow 2\,A + H_2O_2 \qquad (1.5)$$

$$3H_2O \rightarrow O_3 + 6H^+ + 6e^- \qquad (1.6)$$

At cathode, on the other hand, hydrogen evolution will occur as a result of the water reduction (Panizza and Cerisola 2009, Martínez-Huitle et al. 2015). The anode material plays great role in defining the oxidation selectivity and involved mechanisms (Panizza and Cerisola 2009). Depending on the oxygen evolution potential and the nature of interaction between the anode surface and generated hydroxyl radicals, whether it is chemosorbed or physisorbed, anode materials have been classified into active and non-active anodes, respectively (Panizza and Cerisola 2009, Sirés et al. 2014, Martínez-Huitle et al. 2015). Active anode materials such as Pt, RuO_2, RuO_2-IrO_2, graphite and carbon generates $^{\bullet}OH$ radicals that are chemosorbed on the anode, which make them not available for reaction away from the anode surface and, therefore, less effective for mineralization (electrochemical conversion). Anodes such as boron-doped diamond (BDD), lead dioxide and antimony-doped tin oxide are considered non-active; they can generates $^{\bullet}OH$ radicals

that are only physisorbed on the anode surface, which make them readily available to completely mineralize pollutants (electrochemical combustion) (Panizza and Cerisola 2009, Sirés et al. 2014, Martínez-Huitle et al. 2015). Graphite has been continuously classified as an active anode due to its low oxygen evolution potentials and poor performance for achieving pollutants mineralization (Panizza and Cerisola 2009). Although graphite anodes have been used extensively before and it was once the standard anode material for the chloralkali process, it is still restricted by the surface corrosion and cannot be effectively used at high voltages (Panizza and Cerisola 2009, Sirés et al. 2014). Graphite, however, as an inexpensive and commercially available anode material, can be an attractive option if the pollutant of concern can be degraded at low current densities where severe corrosion can be avoided (Panizza and Cerisola 2009, Särkkä et al. 2015).

1.3 Research significance

The treatment of OSPW is currently considered a major challenge facing the oil sands industry. Giving the large volumes of accumulated process water in tailings ponds and the expected growth in the production of bitumen from oil sands, finding effective OSPW remediation technologies has become an urgent need. Efforts have been implemented by the oil sands companies, collaborating researchers and the Government of Alberta towards the development of effective treatment technologies. However, most of the current proposed treatment pathways are extremely slow (biodegradation), highly expensive (physical and chemical processes) or have technical restrictions (Fenton and UV-based AOPs) and therefore not feasible to be applied at large scale, as we discussed in previously in Section (1.2.5).

Electro-oxidation (EO) has emerged as novel method for wastewater treatment and recalcitrant organics degradation. Despite the successful application of EO for treating various types of recalcitrant industrial pollutants, till today there has not been any reported study on the application of electro-oxidation for OSPW treatment. Therefore, the aim of this thesis was to investigate the applicability and effectiveness of EO for OSPW treatment. The hypotheses on which this thesis was based include:

- Based on the properties of OSPW; the high TDS concentration and electrical conductivity, EO can be a potential effective and cost-efficient option for OSPW treatment.

- EO will not have any restriction related to OSPW properties similar to Fenton or UV-based AOPs.

- If EO is applied by using inexpensive anode material, such as graphite, and at relatively low current density, it can be a cost-efficient option.

- EO by graphite anode and at low current densities should preferentially degrade the most recalcitrant NAs (cyclic and branched NAs) and decreased their concentrations without resulting in complete mineralisation. Therefore, the application of electro-oxidation should enhance OSPW biodegradability and reduce the acute toxicity.

- Combining low current anodic oxidation with biodegradation should result in an effective and cost-efficient treatment option for OSPW.

1.4 Research objectives

The main objectives of this thesis can be summarized as follow:

(1) Investigate the effectiveness of applying EO using graphite electrodes for degrading NAs, improve their biodegradability and reduce their toxicity. Graphite was selected due to its low cost and relative abundance which make it an attractive material for OSPW treatment by EO at large scales; especially when considering the huge amount of accumulated OSPW in tailing ponds.

(2) Investigate the degradation kinetics of NAs during EO by graphite anode, understand the involved oxidation mechanisms and examine the structure-reactivity relationships during EO by graphite anode. Finding the current density window within which NAs can be degraded electro-chemically and whether the graphite anode corrosion can be avoided are also of great important for this research.

(3) Investigate the effectiveness of EO for degrading the recalcitrant organics in real OSPW. Evaluate and compare the performance of EO by graphite anode and dimensionally stable anode (DSA) for the degradation of the recalcitrant NAs and aromatics in real OSPW. Graphite was selected as low-cost and abundant anode material that, if succeeded in treating OSPW, can be applied successfully at large scale. DSA, on the other hand, is a commercially available active anode that has been used widely for the degradation of different recalcitrant organics. The thesis also looks at the current density window within which the degradation of organics in real OSPW can occur by using the two anode material and compare the energy efficiency and consumption.

(4) Test the hypothesis that EO of OSPW using graphite anode and under low-current density conditions can selectively degrade the most bio-persistent organic fraction in OSPW. The thesis investigates this hypothesis through treating OSPW by EO under different current densities and then incubating untreated and EO-treated OSPW with native

microbial consortium from oil sands tailing ponds. The fate of different organic classes, biodegradation kinetics, oxidation byproducts and the change in the microbial community dynamics will then be examined.

1.5 Thesis organization

The thesis consists of six chapters that were logically organized according to the research stages and objectives presented above.

Chapter 1 contains a general introduction to the research background and objectives. Briefly, it covers a brief review of the oil sands production, OSPW quality, previously investigated treatment options for OSPW, electro-oxidation fundamentals, research significance and objectives and thesis organization. The experimental background, methodologies, results and discussions are presented separately in each subsequent chapter (Chapters 2-5).

Chapter 2 investigates the oxidation of commercial NA mixture by electro-oxidation using graphite electrodes. Different applied current densities were applied for degrading the NAs mixture following that the biodegradation of the residual organics was monitored. The removal of the aliphatic and aromatic fractions in the NAs mixture was evaluated. The selectivity of EO by graphite and biodegradation was specially evaluated from the perspective of the carbon number and number of rings in the commercial NAs mixture. In addition, the acute toxicity of the NAs mixture before and after treatment by EO and biodegradation was evaluated using *Vibrio fischeri* toxicity screening test.

Chapter 3 focuses on investigating the degradation kinetics and structure-reactivity relation of NAs during EO by graphite electrodes. Finding the current density window within which NAs can be degraded and evaluating the corrosion of graphite anode was also included. Different model NA compounds: Cyclohexanecarboxylic acid (CHA), Heptanoic acid (HPA), octanoic acid (OCA), 2-methylheptanoic acid (2mHPA), trans-4-pentylcyclohexane carboxylic acid (TPCA), 1, 3-adamantanedicarboxylic acid (ADA), 4-methyl-1-cyclohexanecarboxylic acid (4mCHA), , 5-cyclohexanepentanoic acid (CHPA), 5-phenylvaleric acid (PVA), 1-adamantaneacetic acid (AAA), dicyclohexylacetic acid (DCHA) and 4-methylheptanoic acid (4mHPA) were selected to simulate the different NA structures. CHA was used for the evaluation of the degradation kinetics and mechanisms during EO by graphite. Cyclic voltammetry was conducted to understand the degradation mechanisms. The surface of anode before and after EO was characterized by scanning electron microscope (SEM) and X-ray photoelectron spectroscopy (XPS) to understand the nature of changes.

Chapter 4 investigates the treatment of real OSPW by EO using two different types of anode materials; graphite and dimensionally stable (Ti/RuO$_2$-IrO$_2$) anode. The degradation of the recalcitrant organics in OSPW by the two anode materials was investigated and compared. UPLC-TOF-MS and Fourier transform infrared (FT-IR) spectroscopy were used to track the removal of NAs and AEF, respectively, while synchronous fluorescence spectrometry (SFS) was used to evaluate the removal of aromatics. The selectivity of NA removal based on carbon number and cyclicity was investigated and compared. The current efficiency and energy consumption were also evaluated and compared.

19

Chapter 5 investigates the hypothesis that EO of OSPW using graphite anode and under low-current density conditions can selectively degrade the most bio-persistent fraction of NAs. In this chapter, coupling low-current EO by inexpensive graphite electrodes and aerobic biodegradation is presented as effective and cost-efficient option for OSPW treatment. OSPW was treated by EO under low current densities and then incubated with native microbial consortium from oil sands tailing ponds. The fate of different organic classes, biodegradation kinetics, and the change in the microbial community dynamics were examined.

Chapter 6 gives a general conclusion of the research findings presented in Chapters 2 to 5. Recommendations for future work are also given in this chapter.

1.6 References

Afzal, A., P. Chelme-Ayala, P. Drzewicz, J. W. Martin, and M. Gamal El-Din. 2015. Effects of Ozone and Ozone/Hydrogen Peroxide on the Degradation of Model and Real Oil-Sands-Process-Affected-Water Naphthenic Acids. Ozone: Science & Engineering **37**:45-54.

Allen, E. W. 2008a. Process water treatment in Canada's oil sands industry: I. Target pollutants and treatment objectives. Journal of Environmental Engineering and Science **7**:123-138.

Allen, E. W. 2008b. Process water treatment in Canada's oil sands industry: II. A review of emerging technologies. Journal of Environmental Engineering and Science **7**:499-524.

Alpatova, A., E.-S. Kim, S. Dong, N. Sun, P. Chelme-Ayala, and M. Gamal El-Din. 2014. Treatment of oil sands process-affected water with ceramic ultrafiltration membrane: Effects of operating conditions on membrane performance. Separation and Purification Technology **122**:170-182.

Alpatova, A., E.-S. Kim, X. Sun, G. Hwang, Y. Liu, and M. Gamal El-Din. 2013. Fabrication of porous polymeric nanocomposite membranes with enhanced anti-fouling properties: Effect of casting composition. Journal of Membrane Science **444**:449-460.

Armstrong, S. A., J. V. Headley, K. M. Peru, R. J. Mikula, and J. J. Germida. 2010. Phytotoxicity and naphthenic acid dissipation from oil sands fine tailings treatments planted with the emergent macrophyte Phragmites australis. Journal of Environmental Science and Health, Part A **45**:1008-1016.

Barrow, M. P., M. Witt, J. V. Headley, and K. M. Peru. 2010. Athabasca Oil Sands Process Water: Characterization by Atmospheric Pressure Photoionization and Electrospray Ionization Fourier Transform Ion Cyclotron Resonance Mass Spectrometry. Analytical Chemistry **82**:3727-3735.

Benally, C., S. A. Messele, and M. Gamal El-Din. 2019. Adsorption of organic matter in oil sands process water (OSPW) by carbon xerogel. Water Research **154**:402-411.

Brillas, E., I. Sirés, and M. A. Oturan. 2009. Electro-Fenton Process and Related Electrochemical Technologies Based on Fenton's Reaction Chemistry. Chemical reviews **109**:6570-6631.

Brown, L. D. and A. C. Ulrich. 2015. Oil sands naphthenic acids: A review of properties, measurement, and treatment. Chemosphere **127**:276-290.

Çeçen, F. and Ö. Aktaş. 2011. Activated carbon for water and wastewater treatment: integration of adsorption and biological treatment. WILEY-VCH Verlag GMBH & Co. KGaA, Weinheim.

Choi, J., G. Hwang, M. Gamal El-Din, and Y. Liu. 2014. Effect of reactor configuration and microbial characteristics on biofilm reactors for oil sands process-affected water treatment. International Biodeterioration & Biodegradation **89**:74-81.

Clemente, J. S. and P. M. Fedorak. 2005. A review of the occurrence, analyses, toxicity, and biodegradation of naphthenic acids. Chemosphere **60**:585-600.

Clemente, J. S., M. D. MacKinnon, and P. M. Fedorak. 2004. Aerobic Biodegradation of Two Commercial Naphthenic Acids Preparations. Environmental Science & Technology **38**:1009-1016.

Clemente, J. S., N. G. N. Prasad, M. D. MacKinnon, and P. M. Fedorak. 2003. A statistical comparison of naphthenic acids characterized by gas chromatography–mass spectrometry. Chemosphere **50**:1265-1274.

de Klerk, A., M. R. Gray, and N. Zerpa. 2014. Unconventional oil and gas: Oilsands. Pages 95-116 Future energy. Elsevier.

Drogui, P., S. Elmaleh, M. Rumeau, C. Bernard, and A. Rambaud. 2001. Oxidising and disinfecting by hydrogen peroxide produced in a two-electrode cell. Water Research **35**:3235-3241.

Frank, R. A., H. Sanderson, R. Kavanagh, B. K. Burnison, J. V. Headley, and K. R. Solomon. 2009. Use of a (Quantitative) Structure–Activity Relationship [(Q)Sar] Model to Predict the Toxicity of Naphthenic Acids. Journal of Toxicology and Environmental Health, Part A **73**:319-329.

Gamal El-Din, M., H. Fu, N. Wang, P. Chelme-Ayala, L. Pérez-Estrada, P. Drzewicz, J. W. Martin, W. Zubot, and D. W. Smith. 2011. Naphthenic acids speciation and removal during petroleum-coke adsorption and ozonation of oil sands process-affected water. Science of The Total Environment **409**:5119-5125.

Ganzenko, O., D. Huguenot, E. D. van Hullebusch, G. Esposito, and M. A. Oturan. 2014. Electrochemical advanced oxidation and biological processes for wastewater treatment: a review of the combined approaches. Environmental Science and Pollution Research **21**:8493-8524.

Garcia-Garcia, E., J. Q. Ge, A. Oladiran, B. Montgomery, M. Gamal El-Din, L. C. Perez-Estrada, J. L. Stafford, J. W. Martin, and M. Belosevic. 2011. Ozone treatment ameliorates oil sands process water toxicity to the mammalian immune system. Water Research **45**:5849-5857.

Glaze, W. H., J.-W. Kang, and D. H. Chapin. 1987. The Chemistry of Water Treatment Processes Involving Ozone, Hydrogen Peroxide and Ultraviolet Radiation. Ozone: Science & Engineering **9**:335-352.

Hagen, M. O., B. A. Katzenback, M. D. S. Islam, M. Gamal El-Din, and M. Belosevic. 2013. The Analysis of Goldfish (Carassius auratus L.) Innate Immune Responses

After Acute and Subchronic Exposures to Oil Sands Process-Affected Water. Toxicological Sciences **138**:59-68.

Han, X., M. D. MacKinnon, and J. W. Martin. 2009. Estimating the in situ biodegradation of naphthenic acids in oil sands process waters by HPLC/HRMS. Chemosphere **76**:63-70.

Han, X., A. C. Scott, P. M. Fedorak, M. Bataineh, and J. W. Martin. 2008. Influence of Molecular Structure on the Biodegradability of Naphthenic Acids. Environmental Science & Technology **42**:1290-1295.

Headley, J. V., K. M. Peru, M. H. Mohamed, R. A. Frank, J. W. Martin, R. R. O. Hazewinkel, D. Humphries, N. P. Gurprasad, L. M. Hewitt, D. C. G. Muir, D. Lindeman, R. Strub, R. F. Young, D. M. Grewer, R. M. Whittal, P. M. Fedorak, D. A. Birkholz, R. Hindle, R. Reisdorph, X. Wang, K. L. Kasperski, C. Hamilton, M. Woudneh, G. Wang, B. Loescher, A. Farwell, D. G. Dixon, M. Ross, A. D. S. Pereira, E. King, M. P. Barrow, B. Fahlman, J. Bailey, D. W. McMartin, C. H. Borchers, C. H. Ryan, N. S. Toor, H. M. Gillis, L. Zuin, G. Bickerton, M. McMaster, E. Sverko, D. Shang, L. D. Wilson, and F. J. Wrona. 2013. Chemical fingerprinting of naphthenic acids and oil sands process waters—A review of analytical methods for environmental samples. Journal of Environmental Science and Health, Part A **48**:1145-1163.

Herman, D. C., P. M. Fedorak, M. D. MacKinnon, and J. W. Costerton. 1994. Biodegradation of naphthenic acids by microbial populations indigenous to oil sands tailings. Canadian Journal of Microbiology **40**:467-477.

Holowenko, F. M., M. D. MacKinnon, and P. M. Fedorak. 2002. Characterization of naphthenic acids in oil sands wastewaters by gas chromatography-mass spectrometry. Water Research **36**:2843-2855.

Hooshiar, A., P. Uhlik, Q. Liu, T. H. Etsell, and D. G. Ivey. 2012. Clay minerals in nonaqueous extraction of bitumen from Alberta oil sands: Part 1. Nonaqueous extraction procedure. Fuel processing technology **94**:80-85.

Iranmanesh, S., T. Harding, J. Abedi, F. Seyedeyn-Azad, and D. B. Layzell. 2014. Adsorption of naphthenic acids on high surface area activated carbons. Journal of Environmental Science and Health, Part A **49**:913-922.

Islam, M. S., Y. Zhang, K. N. McPhedran, Y. Liu, and M. Gamal El-Din. 2015. Granular activated carbon for simultaneous adsorption and biodegradation of toxic oil sands process-affected water organic compounds. Journal of Environmental Management **152**:49-57.

Janfada, A., J. V. Headley, K. M. Peru, and S. L. Barbour. 2006. A Laboratory Evaluation of the Sorption of Oil Sands Naphthenic Acids on Organic Rich Soils. Journal of Environmental Science and Health, Part A **41**:985-997.

Kannel, P. R. and T. Y. Gan. 2012. Naphthenic acids degradation and toxicity mitigation in tailings wastewater systems and aquatic environments: A review. Journal of Environmental Science and Health, Part A **47**:1-21.

Kim, E.-S., Y. Liu, and M. Gamal El-Din. 2012. Evaluation of Membrane Fouling for In-Line Filtration of Oil Sands Process-Affected Water: The Effects of Pretreatment Conditions. Environmental Science & Technology **46**:2877-2884.

Li, C., L. Fu, J. Stafford, M. Belosevic, and M. Gamal El-Din. 2017. The toxicity of oil sands process-affected water (OSPW): A critical review. Science of The Total Environment **601-602**:1785-1802.

Loganathan, K., P. Chelme-Ayala, and M. Gamal El-Din. 2015. Effects of different pretreatments on the performance of ceramic ultrafiltration membrane during the treatment of oil sands tailings pond recycle water: A pilot-scale study. Journal of Environmental Management **151**:540-549.

Lu, W., A. Ewanchuk, L. Perez-Estrada, D. Sego, and A. Ulrich. 2013. Limitation of fluorescence spectrophotometry in the measurement of naphthenic acids in oil sands process water. Journal of Environmental Science and Health, Part A **48**:429-436.

MacKinnon, M. D. and H. Boerger. 1986. Description of Two Treatment Methods for Detoxifying Oil Sands Tailings Pond Water. Water Quality Research Journal **21**:496-512.

Martin, J. W., T. Barri, X. Han, P. M. Fedorak, M. G. El-Din, L. Perez, A. C. Scott, and J. T. Jiang. 2010. Ozonation of Oil Sands Process-Affected Water Accelerates Microbial Bioremediation. Environmental Science & Technology **44**:8350-8356.

Martin, J. W., X. Han, K. M. Peru, and J. V. Headley. 2008. Comparison of high- and low-resolution electrospray ionization mass spectrometry for the analysis of naphthenic

acid mixtures in oil sands process water. Rapid Communications in Mass Spectrometry **22**:1919-1924.

Martínez-Huitle, C. A. and M. Panizza. 2018. Electrochemical oxidation of organic pollutants for wastewater treatment. Current Opinion in Electrochemistry **11**:62-71.

Martínez-Huitle, C. A., M. A. Rodrigo, I. Sirés, and O. Scialdone. 2015. Single and Coupled Electrochemical Processes and Reactors for the Abatement of Organic Water Pollutants: A Critical Review. Chemical reviews **115**:13362-13407.

Masliyah, J., Z. Zhou, Z. Xu, J. Czarnecki, and H. Hamza. 2004. Understanding water-based bitumen extraction from athabasca oil sands. Canadian Journal of Chemical Engineering **82**:628-654.

Mishra, S., V. Meda, A. K. Dalai, J. V. Headley, K. M. Peru, and D. W. McMartin. 2010. Microwave treatment of naphthenic acids in water. Journal of Environmental Science and Health, Part A **45**:1240-1247.

Mohamed, M. H., L. D. Wilson, J. V. Headley, and K. M. Peru. 2008. Novel materials for environmental remediation of tailing pond waters containing naphthenic acids. Process Safety and Environmental Protection **86**:237-243.

Moreira, F. C., R. A. R. Boaventura, E. Brillas, and V. J. P. Vilar. 2017. Electrochemical advanced oxidation processes: A review on their application to synthetic and real wastewaters. Applied Catalysis B: Environmental **202**:217-261.

Osacky, M., M. Geramian, D. G. Ivey, Q. Liu, and T. H. Etsell. 2013. Mineralogical and chemical composition of petrologic end members of Alberta oil sands. Fuel **113**:148-157.

Oturan, M. A. 2000. An ecologically effective water treatment technique using electrochemically generated hydroxyl radicals for in situ destruction of organic pollutants: Application to herbicide 2,4-D. Journal of Applied Electrochemistry **30**:475-482.

Pal, K., L. d. P. Nogueira Branco, A. Heintz, P. Choi, Q. Liu, P. R. Seidl, and M. R. Gray. 2015. Performance of solvent mixtures for non-aqueous extraction of Alberta oil sands. Energy & Fuels **29**:2261-2267.

Panizza, M. and G. Cerisola. 2006. Olive mill wastewater treatment by anodic oxidation with parallel plate electrodes. Water Research **40**:1179-1184.

Panizza, M. and G. Cerisola. 2007. Electrocatalytic materials for the electrochemical oxidation of synthetic dyes. Applied Catalysis B: Environmental **75**:95-101.

Panizza, M. and G. Cerisola. 2009. Direct and mediated anodic oxidation of organic pollutants. Chemical reviews **109**:6541-6569.

Peng, H., K. Volchek, M. MacKinnon, W. P. Wong, and C. E. Brown. 2004. Application on to nanofiltration to water management options for oil sands operation. Desalination **170**:137-150.

Pereira, A. S., M. S. Islam, M. Gamal El-Din, and J. W. Martin. 2013. Ozonation degrades all detectable organic compound classes in oil sands process-affected water; an

application of high-performance liquid chromatography/obitrap mass spectrometry. Rapid Communications in Mass Spectrometry **27**:2317-2326.

Pourrezaei, P., P. Drzewicz, Y. Wang, M. Gamal El-Din, L. A. Perez-Estrada, J. W. Martin, J. Anderson, S. Wiseman, K. Liber, and J. P. Giesy. 2011. The Impact of Metallic Coagulants on the Removal of Organic Compounds from Oil Sands Process-Affected Water. Environmental Science & Technology **45**:8452-8459.

Quinlan, P. J. and K. C. Tam. 2015. Water treatment technologies for the remediation of naphthenic acids in oil sands process-affected water. Chemical Engineering Journal **279**:696-714.

Rogers, V. V., K. Liber, and M. D. MacKinnon. 2002. Isolation and characterization of naphthenic acids from Athabasca oil sands tailings pond water. Chemosphere **48**:519-527.

Ross, M. S., A. d. S. Pereira, J. Fennell, M. Davies, J. Johnson, L. Sliva, and J. W. Martin. 2012. Quantitative and Qualitative Analysis of Naphthenic Acids in Natural Waters Surrounding the Canadian Oil Sands Industry. Environmental Science & Technology **46**:12796-12805.

Rowland, S. J., A. G. Scarlett, D. Jones, C. E. West, and R. A. Frank. 2011. Diamonds in the Rough: Identification of Individual Naphthenic Acids in Oil Sands Process Water. Environmental Science & Technology **45**:3154-3159.

Santo, C. E., V. J. P. Vilar, C. M. S. Botelho, A. Bhatnagar, E. Kumar, and R. A. R. Boaventura. 2012. Optimization of coagulation–flocculation and flotation

parameters for the treatment of a petroleum refinery effluent from a Portuguese plant. Chemical Engineering Journal **183**:117-123.

Särkkä, H., A. Bhatnagar, and M. Sillanpää. 2015. Recent developments of electro-oxidation in water treatment—a review. Journal of Electroanalytical Chemistry **754**:46-56.

Scott, A. C., M. D. Mackinnon, and P. M. Fedorak. 2005. Naphthenic Acids in Athabasca Oil Sands Tailings Waters Are Less Biodegradable than Commercial Naphthenic Acids. Environmental Science & Technology **39**:8388-8394.

Scott, A. C., R. F. Young, and P. M. Fedorak. 2008a. Comparison of GC–MS and FTIR methods for quantifying naphthenic acids in water samples. Chemosphere **73**:1258-1264.

Scott, A. C., W. Zubot, M. D. MacKinnon, D. W. Smith, and P. M. Fedorak. 2008b. Ozonation of oil sands process water removes naphthenic acids and toxicity. Chemosphere **71**:156-160.

Shu, Z., C. Li, M. Belosevic, J. R. Bolton, and M. Gamal El-Din. 2014. Application of a Solar UV/Chlorine Advanced Oxidation Process to Oil Sands Process-Affected Water Remediation. Environmental Science & Technology **48**:9692-9701.

Simpson, D. R. 2008. Biofilm processes in biologically active carbon water purification. Water Research **42**:2839-2848.

Sirés, I., E. Brillas, M. A. Oturan, M. A. Rodrigo, and M. Panizza. 2014. Electrochemical advanced oxidation processes: today and tomorrow. A review. Environmental Science and Pollution Research **21**:8336-8367.

Small Christina, C., C. Ulrich Ania, and Z. Hashisho. 2012. Adsorption of Acid Extractable Oil Sands Tailings Organics onto Raw and Activated Oil Sands Coke. Journal of Environmental Engineering **138**:833-840.

Swart, N. C. and A. J. Weaver. 2012. The Alberta oil sands and climate. Nature Climate Change **2**:134.

Szpyrkowicz, L., S. N. Kaul, R. N. Neti, and S. Satyanarayan. 2005. Influence of anode material on electrochemical oxidation for the treatment of tannery wastewater. Water Research **39**:1601-1613.

Wang, C., A. Alpatova, K. N. McPhedran, and M. Gamal El-Din. 2015. Coagulation/flocculation process with polyaluminum chloride for the remediation of oil sands process-affected water: Performance and mechanism study. Journal of Environmental Management **160**:254-262.

Wang, C., R. Huang, N. Klamerth, P. Chelme-Ayala, and M. Gamal El-Din. 2016a. Positive and negative electrospray ionization analyses of the organic fractions in raw and oxidized oil sands process-affected water. Chemosphere **165**:239-247.

Wang, C., N. Klamerth, R. Huang, H. Elnakar, and M. Gamal El-Din. 2016b. Oxidation of Oil Sands Process-Affected Water by Potassium Ferrate(VI). Environmental Science & Technology **50**:4238-4247.

Wang, C., N. Klamerth, S. A. Messele, A. Singh, M. Belosevic, and M. Gamal El-Din. 2016c. Comparison of UV/hydrogen peroxide, potassium ferrate(VI), and ozone in oxidizing the organic fraction of oil sands process-affected water (OSPW). Water Research **100**:476-485.

Wang, N., P. Chelme-Ayala, L. Perez-Estrada, E. Garcia-Garcia, J. Pun, J. W. Martin, M. Belosevic, and M. Gamal El-Din. 2013. Impact of Ozonation on Naphthenic Acids Speciation and Toxicity of Oil Sands Process-Affected Water to *Vibrio fischeri* and Mammalian Immune System. Environmental Science & Technology **47**:6518-6526.

Wiseman, S. B., Y. He, M. Gamal-El Din, J. W. Martin, P. D. Jones, M. Hecker, and J. P. Giesy. 2013. Transcriptional responses of male fathead minnows exposed to oil sands process-affected water. Comparative Biochemistry and Physiology Part C: Toxicology & Pharmacology **157**:227-235.

Woodworth, A. P. J., R. A. Frank, B. J. McConkey, and K. M. Müller. 2012. Toxic effects of oil sand naphthenic acids on the biomass accumulation of 21 potential phytoplankton remediation candidates. Ecotoxicology and Environmental Safety **86**:156-161.

Xue, J., C. Huang, Y. Zhang, Y. Liu, and M. Gamal El-Din. 2018. Bioreactors for oil sands process-affected water (OSPW) treatment: A critical review. Science of The Total Environment **627**:916-933.

Xue, J., Y. Zhang, Y. Liu, and M. Gamal El-Din. 2016. Treatment of oil sands process-affected water (OSPW) using a membrane bioreactor with a submerged flat-sheet ceramic microfiltration membrane. Water Research **88**:1-11.

Zanta, C. L. P. S., A. R. de Andrade, and J. F. C. Boodts. 2000. Electrochemical behaviour of olefins: oxidation at ruthenium–titanium dioxide and iridium–titanium dioxide coated electrodes. Journal of Applied Electrochemistry **30**:467-474.

Zhang, Y., P. Chelme-Ayala, N. Klamerth, and M. Gamal El-Din. 2017. Application of UV-irradiated Fe(III)-nitrilotriacetic acid (UV-Fe(III)NTA) and UV-NTA-Fenton systems to degrade model and natural occurring naphthenic acids. Chemosphere **179**:359-366.

Zhu, S., M. Li, and M. Gamal El-Din. 2017. Forward osmosis as an approach to manage oil sands tailings water and on-site basal depressurization water. Journal of Hazardous Materials **327**:18-27.

Zubot, W., M. D. MacKinnon, P. Chelme-Ayala, D. W. Smith, and M. Gamal El-Din. 2012. Petroleum coke adsorption as a water management option for oil sands process-affected water. Science of The Total Environment **427-428**:364-372.

2. APPLYING ELECTRO-OXIDATION BY GRAPHITE ANODE FOR COMMERCIAL NAPHTHENIC ACIDS MIXTURE DEGRADATION, BIODEGRADABILITY ENHANCEMENT AND TOXICITY REDUCTION[1]

2.1 Introduction

Canada has the third largest oil reserves known in the world with proven reserves of 165.4 billion barrels of recoverable bitumen (Regulator 2014). The current extraction processes for obtaining bitumen from the oil sands consume large volumes of water. Despite the current high water-recycling rate of more than 80 percent, the fresh water intake for mined oil sands is still as high as 2 to 3 barrels of fresh water for every barrel of upgraded bitumen (He et al. 2011, de Klerk et al. 2014). As a result, large amounts of oil sands process water (OSPW) are generated. Under the currently applied zero discharge approach, oil sands companies do not release their generated OSPW into the receiving environment. Instead, it is sent to constructed tailings ponds to be stored (He et al. 2011). Tailings ponds are growing in volume and number with accumulated amount of OSPW estimated to be more than 1 billion m^3 in 2013 covering an area of more than 220 km^2 (Klamerth et al. 2015, Xue et al. 2018).

OSPW has shown to have toxic impacts on both prokaryotes and eukaryotes (He et al. 2011, Klamerth et al. 2015, Li et al. 2017). Among the different constituents in OSPW, a group of aliphatic and alicyclic carboxylic acids known as naphthenic acids (NAs) have attracted

---

considerable attention because they have been traditionally connected with toxicity of OSPW and they are recalcitrant and can persist in the environment for many years (He et al. 2011, Klamerth et al. 2015, Xue et al. 2018). In addition to OSPW, NAs also exist in petroleum refineries wastewater and are considered problematic because of their toxic and corrosive properties (Whitby 2010, Misiti et al. 2013).

NAs are a complex mixture of alkyl-substituted acyclic and cyclic carboxylic acids. They are generally considered anionic surfactants with pKa values in the range of 5–6 (Misiti et al. 2013). NAs have a general formula of $C_nH_{2n+z}O_x$, where n represents the carbon number, Z is zero or a negative even integer and reflects the hydrogen atoms lost due to ring formation (degree of cyclicity) or double bond equivalent and X is the number of oxygen atoms (X=2 for classical NAs and X>2 for oxidized NAs) (Clemente et al. 2004, Whitby 2010, Misiti et al. 2013, Meshref et al. 2017). Other N and S containing heteroatomic species and aromatic species have also been included in the NA structure range (Meshref et al. 2017).

The treatment of OSPW is considered a great challenge facing the oil sands industry today. Various chemical, physical and biological processes have been investigated for the treatment of OSPW and degradation of NAs. Different biological treatments have been investigated for NA degradation (Clemente et al. 2004, Scott et al. 2005, Han et al. 2008, Quinlan and Tam 2015, Shi et al. 2015, Xue et al. 2018). However, NAs occur naturally as products of the incomplete degradation of petroleum hydrocarbons by the indigenous microbial communities in the reservoirs and therefore the biodegradation of NAs is a very slow and inefficient and the process needs to be coupled with other processes in order to be considered viable (Brown and Ulrich 2015, Quinlan and Tam 2015). Physical processes

such as adsorption (El-Din et al. 2011, Zubot et al. 2012) and membrane filtration (Alpatova et al. 2014, Benally et al. 2018) have also been investigated for NA removal. Different advanced oxidation processes (AOPs) have been applied for the degradation of NAs including ozonation (Garcia-Garcia et al. 2011, Wang et al. 2013b, Islam et al. 2014), combined O_3/H_2O_2 (Afzal et al. 2015), peroxydisulfate/zero valent iron (Drzewicz et al. 2012), UV/chlorine process (Shu et al. 2014), UV/hydrogen peroxide (Afzal et al. 2012a); potassium ferrate (VI) process (Wang et al. 2016b) and Fenton process (Zhang et al. 2016a). However, most of these AOPs were found to have drawbacks. For instance, the UV-based AOPs were limited by the relatively low light transmittance of real OSPW due to the color and turbidity which make a pre-treatment step required (Shu et al. 2014). Fenton process, on the other hand, was restricted by the high natural pH of real OSPW (pH 8) (Zhang et al. 2016a). Potassium ferrate (VI) and peroxydisulfate/zero valent iron processes required high chemicals doses and produced undesired sludges. Ozonation was the most commonly studied process among the other AOPs, but the high required ozone doses limit its application at large scales (Brown and Ulrich 2015, Quinlan and Tam 2015).

Electro-oxidation (EO) has emerged as promising process for wastewater treatment (Chaplin 2014, Ganiyu et al. 2018, Martínez-Huitle and Panizza 2018). In EO, the oxidation of pollutants can occur through (Martínez-Huitle et al. 2015, Moreira et al. 2017): (i) direct transfer of electron at the surface (A) of anode; (ii) reactive oxygen species generated from the water electrolysis at anode such as physiosorbed/chemosorbed •OH generated via Eq. (1), and relatively weaker oxidants like hydrogen peroxide (H_2O_2) and ozone (O_3) formed at the anode surface through Eq. (2) and (3) respectively; (iii) other oxidants that can be generated electrochemically from the ions existing in the solution such

as chloride, sulfate, phosphate and carbonate (Panizza and Cerisola 2009, Martínez-Huitle et al. 2015).

$$A + H_2O \rightarrow A(^\bullet OH) + H^+ + e^- \qquad (2.1)$$

$$2\,A(^\bullet OH) \rightarrow 2\,A + H_2O_2 \qquad (2.2)$$

$$3H_2O \rightarrow O_3 + 6H^+ + 6e^- \qquad (2.3)$$
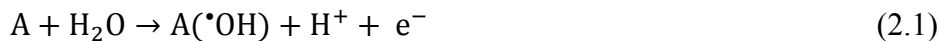
EO has been applied successfully for the degradation of a variety of recalcitrant organic pollutants in wastewater (Panizza and Cerisola 2009, Sirés et al. 2014, Brillas and Martínez-Huitle 2015, Martínez-Huitle and Panizza 2018). The principal advantages EO include ease of operation, small footprint and that chemicals are not needed (Chen 2004). Various types of electrodes have been investigated for EO and it was found that the anode material has a large influence on the process efficiency and selectivity. Some anodes favor the partial and selective oxidation of organics, while other types tend to promote the complete mineralization (Panizza and Cerisola 2009, Moreira et al. 2017). Depending on the oxygen evolution potential and the nature of interaction between the anode surface and generated $^\bullet OH$ radicals, whether it is chemisorbed or physisorbed, anode materials have been classified into active and non-active anodes, respectively (Panizza and Cerisola 2009, Moreira et al. 2017). Anodes with low O_2 evolution over-potentials, such as carbon, RuO_2, IrO_2, and Pt, are classified as active anodes and will only allow partial oxidation of pollutants (Panizza and Cerisola 2009, Rao and Venkatarangaiah 2014). On the other hand, anodes with a high O_2 evolution over-potential (i.e., have poor performance for oxygen evolution reaction), such as boron-doped diamond (BDD), lead dioxide, and antimony-doped tin oxide, are classified as non-active anodes and favor the complete mineralization

of organics (Panizza and Cerisola 2009, Panizza 2010, Rao and Venkatarangaiah 2014, Moreira et al. 2017).

Graphite has been traditionally classified as an active anode material (Panizza and Cerisola 2009, Rueffer et al. 2011, Rao and Venkatarangaiah 2014). It is inexpensive and has a large surface area which made it an attractive option for the removal of organics in electrochemical reactors with three-dimensional electrodes (Panizza and Cerisola 2009, Moreira et al. 2017). However, the main drawback of graphite is that EO at high current densities will generally be accompanied by surface corrosion and that not all the organic pollutants can be degraded at low current densities where corrosion is not prevalent (Rueffer et al. 2011, Moreira et al. 2017). As such, the drawbacks of graphite as anode material (anodic corrosion and low degradation efficiency) can be overcome by performing EO experiments at low current densities and combine the process with other commercially available treatment technologies such as biological treatment, which can further degrade the by-products formed during the EO.

The main objective of this chapter was to investigate the effectiveness of applying low current EO using graphite electrodes for the degradation of commercial mixture of NAs. EO appears to be an attractive option for the treatment of OSPW and degradation of NAs since it does not have the limitations associated with the other AOPs such as the low light transmittance, pH limitation and required chemical additions. This is the first study, to our best knowledge, that investigates the application of EO for NA degradation by using active anode material such as graphite. Considering the nature of graphite anodes which can only promote the partial degradation of organic pollutants, we hypothesize that the application of low voltage EO will result in partial degradation of NAs and, therefore, will reduce the

toxicity and enhance the biodegradability without wasting energy in achieving mineralization. Therefore, combining EO with biological treatments can result in an efficient and energy-effective treatment option for NA-bearing process waters such as OSPW and refinery wastewater. The lower voltages required for the treatment and the use of relatively inexpensive and abundant electrode materials will result in a sustainable and effective process that can overtake the restrictions associated with the other AOPs.

2.2. Materials and methods

2.2.1 Chemicals and materials

A commercial mixture of NAs obtained from Sigma-Aldrich (Oakville, ON, Canada) was used in this study. The NA mixture consists mostly of NAs with 0, 1, 2 and 3 ring NA structures (i.e., Z = 0, -2, -4 and -6) and with carbon numbers (n) in the range between 8 and 18. The exact distribution of the NA mixture is shown in section 3.1. Analytical grade sodium sulfate (($\geq$ 99 %, Sigma-Aldrich, Canada) was used during the experiments. Analytical grade disodium phosphate, monosodium phosphate, sodium hydroxide and sulfuric acid were purchased from Fisher Scientific Canada (Edmonton, Alberta). MilliQ water (18 MΩ•cm, Millipore Corporation) was used for the preparation of all the solutions.

2.2.2 Electro-oxidation experiments

Glass breakers with two-electrodes were used as EO cells for the batch experiments with a total size of 500 mL (Fig. B1). Graphite flat-sheet electrodes (Wale Apparatus, PA, US) were used as anode and cathode. The effective anode surface area was 74 cm^2 and the distance between the anode and cathode inside the reactor was 1.2 cm. Solutions were stirred vigorously during runs by using a magnetic stirrer at 500 rpm to ensure effective

mixing and mass transport within the reactor (Martínez-Huitle 2015). DC power supply (9130, B&K Precision, California, US) with three separated outlets and internal voltammeter and amperometer was used for EO experiments. All the runs were conducted under fixed current (Galvanostatic) conditions, and the changes in voltage were monitored and recorded continuously. A control reactor with an identical setup was operated in parallel with electrodes but without electrical power to exclude any removal arising from adsorption or volatilization.

Three current densities (0.5, 2.5 and 5 mA/cm^2) were selected, based on preliminary runs, to be applied for a total period of 180 minutes with samples being withdrawn periodically. A stock solution of 3.5 g NA/L in 0.01 M NaOH was prepared and used to prepare the buffered solutions. An initial concentration of 35 mg/L of the commercial NA mixture was used to simulate the concentration of NAs in OSPW and petroleum refinery wastewater (Whitby 2010, Misiti et al. 2013, Brown and Ulrich 2015). Experiments were performed at pH 8, to simulate the pH ranges of OSPW and petroleum refinery wastewater, by using phosphate buffer (60 mM Na$_2$HPO$_4$) as an electrolyte.

The specific energy consumption (SEC) per classical NA removed was calculated as follow:

$$SEC = \frac{I.V.t}{(NA_0 - NA_t).V_S} \qquad\qquad (2.4)$$

Where *SEC* is the specific energy consumption per NAs removed (kWh/g NA removed), *I* is the average applied current (A), *V* is the cell voltage (V), *t* is the treatment time (h), V_s is the solution volume (L) and NA$_0$ and NA$_t$ are the initial and final NA concentrations (mg /L), respectively.

2.2.3 Biodegradation assay

Batch experiments were conducted to compare the biodegradability of the raw and EO-pretreated NA mixture solutions under the aerobic condition. The inoculum for these experiments was obtained from a bioreactor contains indigenous microorganisms in the OSPW tailing ponds that was fed with untreated OSPW and maintained for around 2 years. An aliquot of inoculum (2 mL) was concentrated by centrifugation and then added to all treatments to result in identical initial biomass concentration of 22.5 mg MLVSS/L. Erlenmeyer flasks (500 mL) were used as reactors with final liquid incubation volumes of 300 mL. In order to remove residual adsorbed NAs, the inoculum was washed with 0.5 M phosphate buffer (pH 7.2). A salt medium (Bushnell Haas Broth) consisting of (g/ L): 1 Na_2HPO_4; 1 KH_2PO_4; 0.5 NH_4NO_3; 0.29 $MgSO_4.7H_2O$; 0.02 $CaCl_2.2H_2O$; 0.002 $MnSO_4.2H_2O$; 0.002 $FeCl_2$ was added to provide the essential nutrients and no additional carbon source was used. A screwcap was used to close the flask to prevent evaporation of water during the extended incubation period (up to 60 days). The caps were loosened every day for a short period to allow fresh air to flow in to replenish oxygen. Incubations were carried out under aerobic conditions with dissolved oxygen (DO) levels maintained above 4 mg/L at all times by putting the flasks on a shaker at 200 rpm and at room temperature (approximately 21°C). Sterile controls with NA solution only were used.

2.2.4 Water quality analysis

The pH and conductivity of the samples were measured by using a multi-channel pH/conductivity/ion (Accumet excel XL60; Fisher Scientific). DO concentration was measured by a dissolved oxygen meter (Model 50B, YSI Inc., US). Chemical oxygen demand (COD) was determined with HACH COD reagent kits (TNT821, LR, Germany) by

using DR3900 spectrophotometer (HACH, Germany) following the manufacturer's instructions.

2.2.5 Analytical methods

Fourier transform infrared (FT-IR) spectroscopy (Spectrum 100, PerkinElmer Ltd, Bucks, UK) was used to determine the acid extractable fraction (AEF) concentration in OSPW. The samples were filtered using a 0.45 μm nylon filter, acidified to pH 2.0, and then extracted twice with a separation funnel using analytical grade dichloromethane (DCM). The extracted layer was then evaporated to dryness, and then dissolved in a known amount of dichloromethane and analyzed by using FT-IR. The absorbance was measured at 1743 and 1706 cm^{-1}, which represents the monomeric and dimeric carboxylic groups, respectively (Klamerth et al. 2015, Xue et al. 2018).

NA concentration was measured by using ultra-performance liquid chromatography time-of-flight mass spectrometry (UPLC TOF-MS) after filtration by 0.45 μm nylon filter. A sample volume of 1 mL from a mixture consisted of 500 μL OSPW sample, 100 μL of 4.0 mg/L internal standard (myristic acid-1-^{13}C), and 400 μL of methanol was injected into the instrument. Chromatographic separation was done by a Waters UPLC Phenyl BEH column (Waters, MA, USA). The sample analysis was accomplished by a high-resolution time-of-flight mass spectrometry TOF-MS with negative electrospray ionization mode (Synapt G2, Waters, MA, USA). Detailed description of the method can be found in Appendix A. This method was previously developed and has been verified by several publications (Wang et al. 2013b, Wang et al. 2016a, Wang et al. 2016c, Meshref et al. 2017).

Synchronous fluorescence spectra (SFS) was carried out with a Varian Cary Eclipse fluorescence spectrometer (Mississauga, ON Canada) to exam the presence of aromatic

species. Excitation wavelengths ranged from 200 to 600 nm, and emission wavelengths were recorded from 218 to 618 nm. Scanning speed was 600 nm/min and the photomultiplier (PMT) voltage was set at 800 mV.

2.2.6 Toxicity towards *Vibrio fischeri*

The acute toxicity towards *Vibrio fischeri*, a marine luminescent bacterium was measured by using a Microtox® 500 Analyzer (Azur Environmental, Carlsbad, USA) according to the 81.9 % screening test protocol as defined by the manufacturer. The osmotic pressure of the samples was adjusted to maintain the proper osmotic pressure for *Vibrio fischeri*. Samples were tested for 5 and 15 min of exposure. The emitted luminescence was measured and compared to that of the blank sample, which contains 2 % NaCl in deionized (DI) water (pH 6.5–7.0). Phenol standard was used as a positive control to check the sensitivity of the *Vibrio fischeri* before the analysis.

2.3. Results and discussion

2.3.1 Electro-oxidation of NA mixture

Samples of the commercial NA mixture with total initial concentrations of 35 mg NAs/L were exposed to EO under three different current densities (0.5, 2.5 and 5 mA/cm^2) for a period of 180 min. The change in pH was insignificant and the pH remained around 8 due to the use of buffer. The removal of AEF and COD were used as initial performance indicator for evaluating the degree of degradation and transformation during EO. The concentration of AEF has been widely used to evaluate the extent of degradation in OSPW organics, including classical NAs, oxidized NAs, and the other organic compounds that contains carbonyl groups (Garcia-Garcia et al. 2011). As can be seen from Fig. 2.1, the

43

removal rate for both COD and AEF increased with the increase of the applied current density. EO at current densities of 0.5, 2.5 and 5 mA/cm^2 reduced the COD from 89.6 mg/L to 70.0, 65.8 and 62.4 mg/L, respectively. For AEF, on the other hand, the removal rate followed the same trend but with relatively higher rates at 42.2 %, 57.0 % and 67.9 %, respectively. The partial removal of AEF along with COD is a clear indicator for the absence of complete mineralization. Compared to the limited removal of AEF and COD, the removal rate for classical NAs was quite higher (Fig. 2.2). The concentration of classical NAs (O$_2$-NAs) after EO on graphite was reduced from 27.7 mg/L to 6.4, 6.2 and 4.9 mg/L accounting for removal rates of 76.9 %, 77.6 % and 82.4 % at current densities of 0.5, 2.5 and 5 mA/cm^2, respectively. This behaviour of lower AEF removal rates compared to NA removal rates was also observed in previous studies during the degradation of NAs by ozonation (Dong et al. 2015, Zhang et al. 2016b) and can be explained by the fact that the degradation by-products of NAs can contain -CO, -CHO and -COOH groups which still contribute to AEF. It is important to state that the contribution of the adsorption on the surface of the graphite to NAs removal was less than 2%. As can been seen from the commercial NA mixture distribution (Fig. 2.2), acyclic NAs (Z =0) were the dominant species in the mixtures and the cyclicity of NA mixture ranged from Z = 0 to -6 only while the carbon number (n) ranged from 8 to 18. After applying EO, the relative abundance of NAs based on cyclicity showed an increase in the abundance for the acyclic (Z=0) ones which was proportional to the applied current density, while the remaining cyclic species abundance decreased (Fig. 2.3A). This can be considered an indicator for the preference of EO for degrading more cyclic species compared to acyclic. The relative abundance of the NAs mixture based on carbon number, on the other hand, did not show a specific trend for

the degradation (Fig. 2.3B). This can be attributed to the possibility of generating NAs with

lower carbon number when NAs with higher carbon number are electro-oxidized which is a

claim can be supported by dividing Fig. 2.3B into two zones; one zone for NAs with carbon

numbers between 8 and 13, in which the abundance increased after EO, and another zone

with carbon numbers from 14 to 18, in which the relative abundance clearly decreased after

EO.
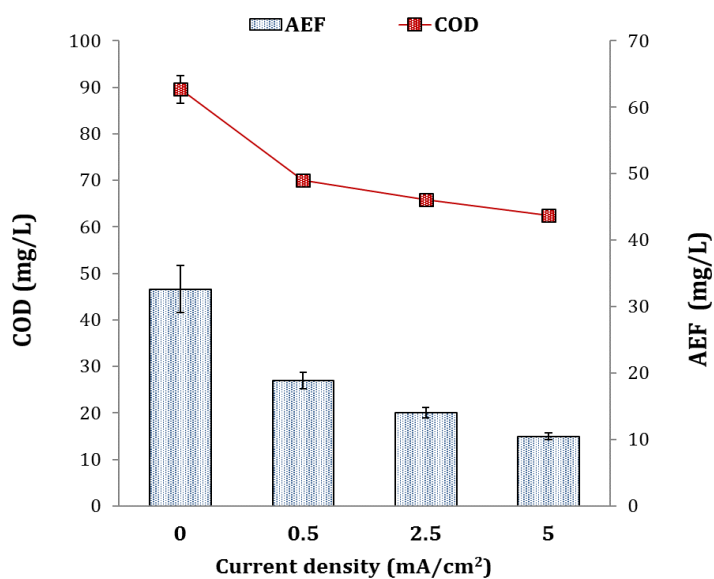
Figure 2.1 Removal of acid extractable fraction (AEF) and chemical oxygen demand

(COD) after 180 min of electro-oxidation.
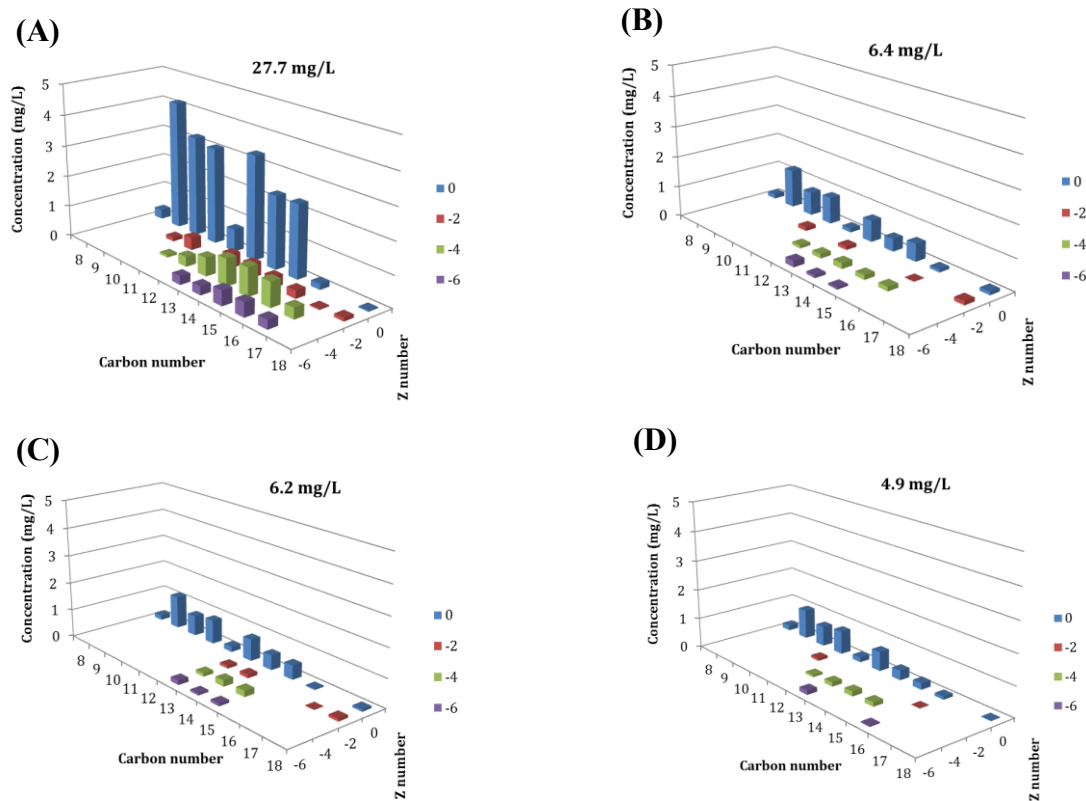
Figure 2.2 Classical NA removal and distribution as a function of applied current density

(A) 0 mA/cm^2; (B) 0.5 mA/cm^2; (C) 2.5 mA/cm^2; and (D) 5 mA/cm^2.

As mentioned earlier, NAs also include oxidized NAs which contain more than 2 oxygen atoms in the structure (i.e., X > 2). Some of these species already existed in the NA mixture (Fig. 4B and 4C), but they can also be generated as products of the oxidation of classical NAs (Martin et al. 2010). The initial concentrations of oxidized (O$_3$ and O$_4$) NAs were much lower than that of classical NAs, 1 and 1.5 mg/L, respectively (Fig. 2.4B and 2.4C).

Despite the low initial concentration of O_3-NAs, there were still considerable removal rates after EO at current densities of 2.5 and 5 mA/cm^2 by 35.2 % and 66.1 %, respectively, with an exception for 0.5 mA/cm^2 which had a slight increase by 8.5 % (Fig. 2.4B). For O_4-NAs, on the other hand, the removal was remarkable at all applied current densities with removals of 57.2 %, 65.4 % and 73.8 % at applied current densities of 0.5, 2.5, and 5 mA/cm^2, respectively. This oxidation behaviour for oxidized NAs was different from that observed during ozonation of commercial NA mixture which showed an increase in the concentration after oxidation (Martin et al. 2010). The difference in the degradation behaviours can be explained by the fact that the oxidation mechanisms are different in ozonation and EO. In ozonation at pH 8, the oxidation occurs both by ozone and via the generated $^\bullet$OH radicals and both contribute to the degradation of NAs (Wang et al. 2013b, Wang et al. 2016c). Therefore, the addition of oxygen atom to the classical NA structure is an expected mechanism that will lead to the generation of oxidized NA species. It has been reported before that the major intermediate by-products resulting from ozonation of NAs in OSPW were oxidized NAs, such as hydroxy- or keto-NAs, and other non-NAs carboxylic acids (Martin et al. 2010, Wang et al. 2013b). In the case of EO on graphite anode, however, the generation of free $^\bullet$OH radicals or ozone is not an expected mechanism, instead the oxidation occurs at the surface of the anode through either direct electron transfer or the generated active surface functional groups (Panizza and Cerisola 2009, Rueffer et al. 2011). Graphite was traditionally considered as an active anode material and was expected to have oxidation behaviour similar to mixed metal oxidizes and Pt anodes. However, Rueffer et al. have recently shown that graphite does not behave neither like metallic active anode nor inactive anode, instead the oxidation behaviour on graphite involved oxygenated functional

groups bonded to the previously oxidized anode surface and not directly to carbon (Rueffer et al. 2011). Therefore, oxidation products other than oxidized NAs were expected and that was why the concentrations of O_3 and O_4 NAs decreased after EO.

(A)

(B)
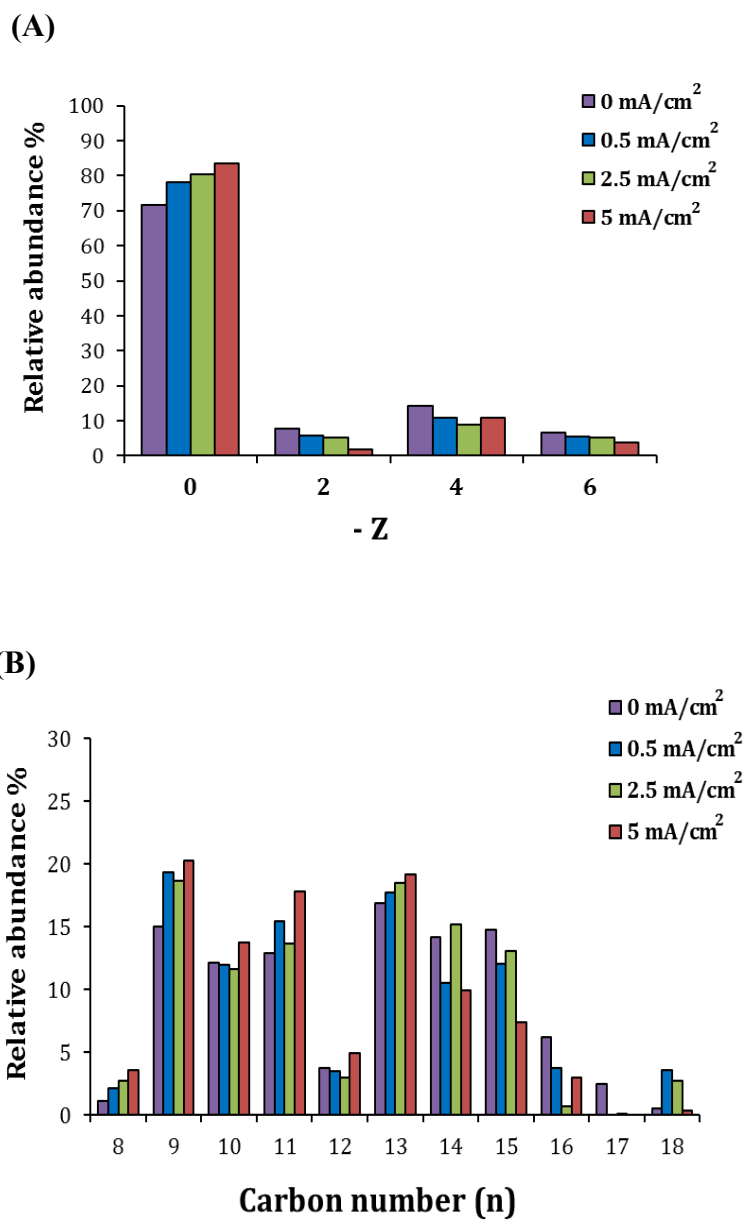
Figure 2.3 Effect of electro-oxidation under different applied current densities on the relative abundance of NAs based on (A) cyclicity (–Z) and (B) carbon number (n).

48
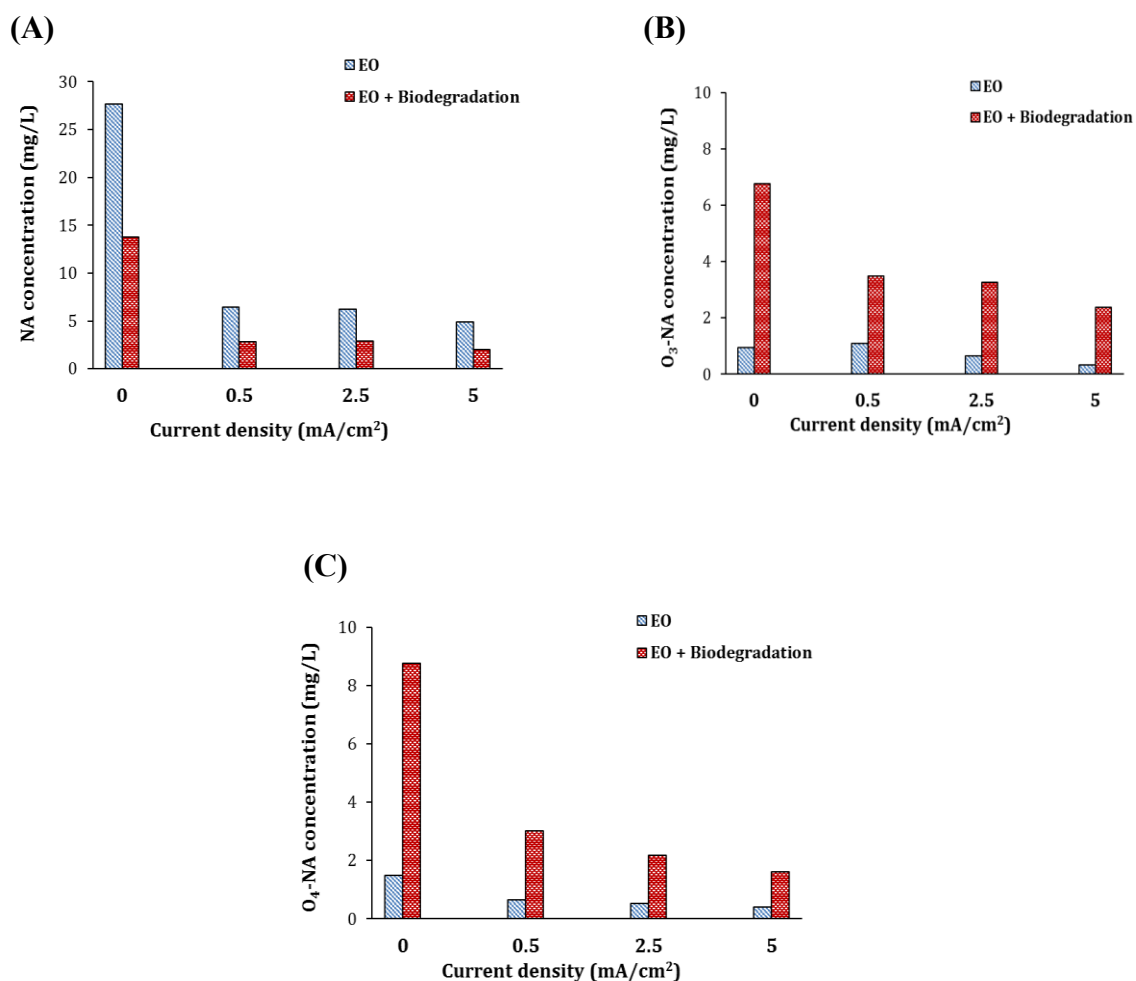
Figure 2.4 Fate of: (A) classical NAs, (B) oxidized (O$_3$) NAs and (C) oxidized (O$_4$) NAs after electro-oxidation (EO) and electro-oxidation followed aerobic biodegradation.

In order to have a rough idea about the energy-efficiency (operating cost) of the EO process and compare it to the other investigated processes, the specific energy consumption (SEC) per classical NA removed was evaluated following Eq. (2.4). As can be seen in Fig. 2.5, SEC for classical NA degradation was 0.086, 0.334 and 0.362 kWh/g NA removed at current densities of 0.5, 2.5, and 5 mA/cm^2, respectively. The increase in SEC with increasing the applied current density was expected due to loss of energy in oxygen

evolution at the anode at higher current densities. Wang et al. have previously reported that ozonation had the lowest capital and operational cost for OSPW treatment and NA degradation when compared to other AOPs such as UV/H_2O_2 and potassium ferrate (VI) process (Wang et al. 2016c).). In order to evaluate the cost-effectiveness of EO in comparison with other AOPs, the energy consumption (main operating cost) of EO was compared with that of ozonation. Vaiopoulou et al. have investigated the degradation of commercial NA mixture by ozonation using a semi-batch system that was connected to an ozonator working at an electrical discharge of (120 V, 60 Hz, 30 W) (Vaiopoulou et al. 2015). The energy consumption for their system per NA removed can be estimated to be 3 kWh/g NA removed when the initial NA concentration was 25 mg/L. By comparing this value with our results, it is obvious that EO by graphite could achieve comparable degradation results while consuming 34 times less energy than ozonation. This is a clear indicator that EO by graphite could be energy and cost efficient option for NA degradation and OSPW treatment if applied at low current density.
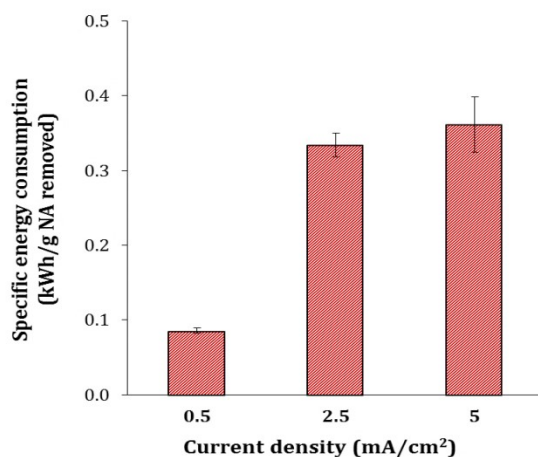
Figure 2.5 Specific energy consumption (SEC) for the degradation of NAs under different applied current densities.

2.3.2 Biodegradation of electro-oxidized NA mixture

In order to assess the effect of EO on the biodegradability of the commercial NA mixture, aerobic biodegradation experiments were conducted in batch mode. Samples containing commercial NA mixture were electro-oxidized for 180 min and then aerobically biodegraded for 60 days to evaluate the impact of EO pre-treatment on the microbial biodegradation performance. The NA concentration and distribution before as well as after biodegradation for electro-oxidized samples at different current densities were compared with each other and with those with no EO pre-treatment. The fate of classical and oxidized NAs after biodegradation is shown in Fig. 2.4. Classical NAs were degraded effectively during biodegradation (Fig. 2.4A). The removal rate for samples without EO pre-treatment was 50.2 % while for the ones with EO pre-treatment were 55.8 %, 53.5 % and 58.9 % for applied current densities of 0.5, 2.5, and 5 mA/cm^2, respectively. This show a clear improvement in the biodegradation performance as a result of the pre-treatment with EO despite the fact the initial concentration in the pre-treated samples were lower than this of the non- pre-treated sample which should actually impact the bioavailability in the electro-oxidized samples and therefore negatively impact the performance. However, it was clear from the results that EO even at current density as low as 0.5 mA/cm^2 was able to improve the classical NA biodegradability (Fig. 2.4A). It is noteworthy to mention that ozonation was investigated before as a pre-treatment before biodegradation for the treatment of commercial NA mixtures (Martin et al. 2010, Vaiopoulou et al. 2015). In both ozonation studies, however, it was found that ozonation did not improve the biodegradation of classical NA portion of the commercial mixtures. Martin et al. found that in most of the cases the biodegradation half-lives were longer in the pre-ozonated commercial NA

samples than the non-ozonated ones, and that with increasing the ozone dose the half-lives increased (Martin et al. 2010). Vaiopoulou et al., on the other side, found that the combination of ozonation-biodegradation achieved the same results for classical NA removal as biodegradation alone and that ozonation did not improve the biodegradation performance (Vaiopoulou et al. 2015). The reason for improved biodegradability of classical NAs in the commercial NA mixture after EO can be explained by the hypothesis that the most bio-persistent fraction of each classical NA species was effectively degraded during EO. It was reported before by that the biodegradability of the NAs in commercial mixtures decreased with the increase of the alkyl branched fraction (Smith et al. 2008, Misiti et al. 2014). Since in our NA mixture, the acyclic ($Z = 0$) NAs fraction was the dominant fraction initially and after EO (Fig. 2.2) and remained the dominant portion after biodegradation (Fig. 2.6), an assumption that there is a considerable branched NA fraction within it can be a reasonable assumption. It should be noted here that even the most advanced analytical equipment available now cannot detect the exact structures of the different species within a complex mixture such as commercial NA mixture. Therefore, our explanation remains an assumption and a detailed investigation by using model NA compounds is needed to deeply investigate that structure reactivity relation, and work is going in our laboratory now to do that. In contrast to the case of classical NAs, oxidized NAs (O_3 and O_4) NAs increased in all the cases after biodegradation (Fig. 2.4B and 2.4C) showing that oxidized NAs were the main products of the biodegradation. It worth to be noted here that in the case of the sample without EO pre-treatment the amount of oxidized NAs (O_3 and O_4) that appeared after biodegradation was almost the same as the amount of classical NAs that disappeared showing that biotransformation other than mineralization

was the major degradation pathway of NAs. In the case of samples with EO pre-treatment, however, the amount of generated oxidized NAs (O_3 and O_4) after biodegradation was always higher than the amount of classical NAs that disappeared, indicating that beside classical NAs other by-products generated during EO were also transformed into oxidized NAs (O_3 and O_4) after biodegradation.
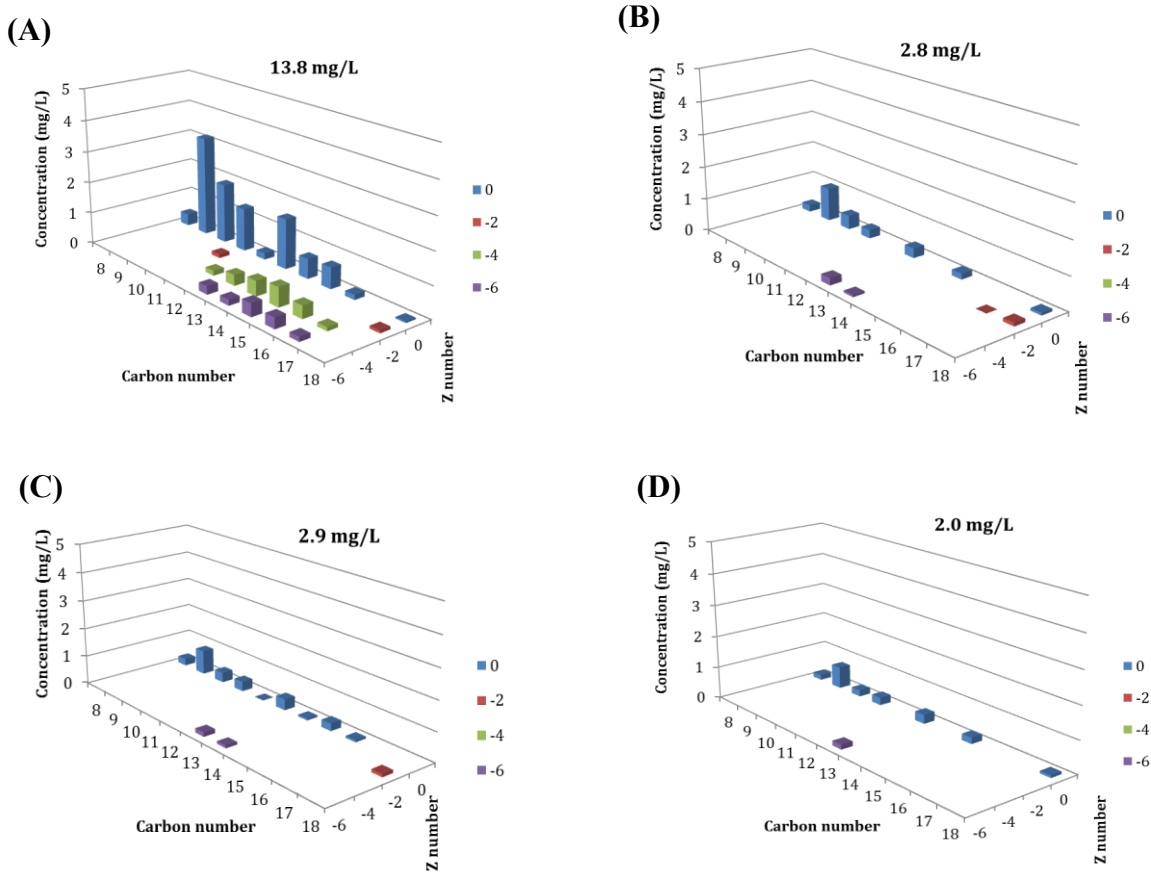
Figure 2.6 Classical NA distribution after electro-oxidation followed by biodegradation ((A) 0 mA/cm^2; (B) 0.5 mA/cm^2; (C) 2.5 mA/cm^2; and (D) 5 mA/cm^2).
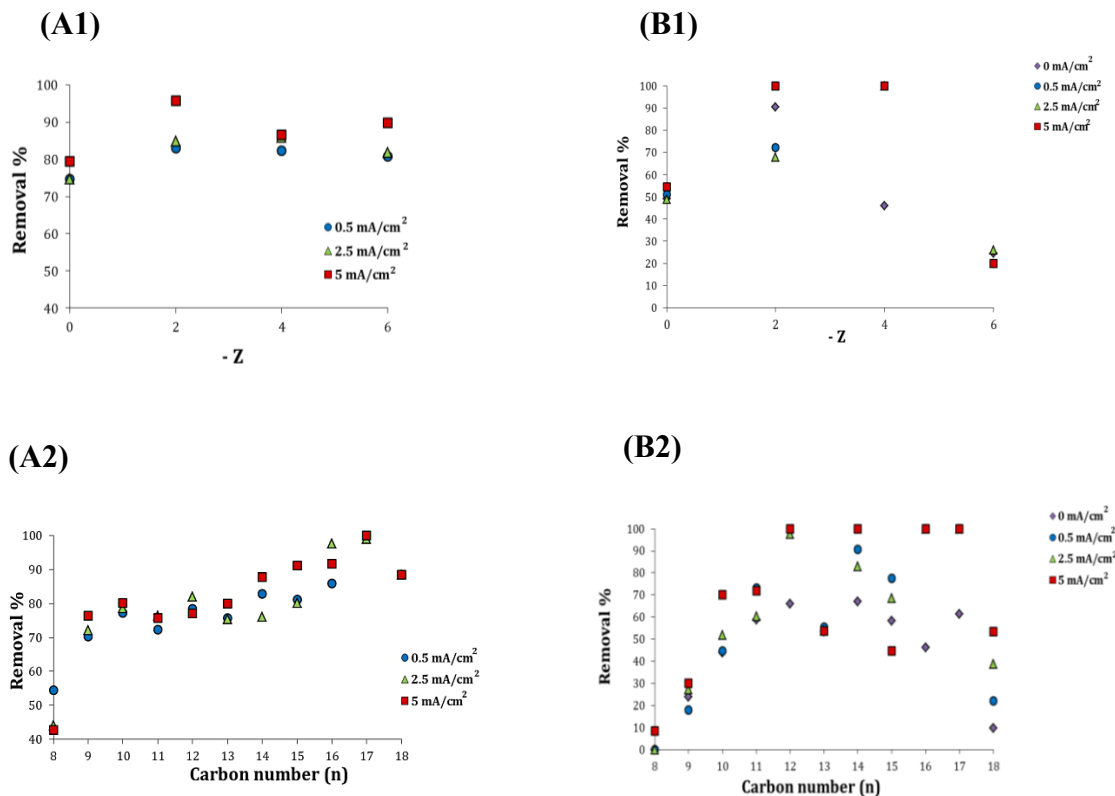
Figure 2.7 The relation between NA removal after: (A) electro-oxidation and (B) combined EO-biodegradation, and (1) cyclicity and (2) carbon number (n) distribution.

In an effort to understand the relation between the removal of classical NAs during EO and biodegradation and its molecular weigh (n) and cyclicity (z), the removal rate for the individual classical NA components were analyzed (Fig. 2.7). As can be seen from Fig. 2.6A1 the lowest removal rate after EO for all the conditions was for the acyclic portion (-Z=0) of the NA mixture and the removal was higher in the case of high -Z (cyclic portion) indicating a clear preference for EO toward the degradation of cyclic species than acyclic. However, it has be noted here that the highest removal rate for all the applied current densities was at (-Z = 2), and that the removal rate was slightly lower at (-Z = 4 and 6) which means that the removal rate did not increase with increasing the cyclicity. This

54

finding was different from what was reported for the other AOPs such as ozonation, O_3/H_2O_2, UV/H_2O_2 and ferrate(VI) which showed a clear trend relating the increase in the degradation rate with the increase in cyclicity (Afzal et al. 2012b, Afzal et al. 2015, Wang et al. 2016c). Which can be explained by the difference in the involved oxidation mechanisms, since EO on graphite generate oxygenated functional groups bonded to the previously oxidized surface instead of free •OH radicals or higher oxides as explained earlier in section 3.1. The relation between the removal rate and carbon number, on the other hand, was clearer with a positive correlation (Fig. 2.7A2). This agreed with the previous AOPs studies which showed a similar trend and can be explained by the idea that the increase in the carbon number means an increase in the sites that available for oxidation and therefore higher rates are expected (Afzal et al. 2012b, Wang et al. 2016c). For the biodegradation step, however, there was no clear relation between the removal rate and cyclicity no matter if there was EO pre-treatment or not (Fig. 2.7B1). As shown in Fig. 2.7B2, the NAs with higher n number had higher removals during biodegradation. The lower removal levels of NAs with low carbon number might be attributed to the bioconversion of NAs with higher n values into NAs with lower n values. Moreover, it was noticed that EO can improve the biodegradation of NAs with higher carbon number more substantially in comparison with NAs with lower carbon number (Fig. 2.7B2).

(A1)

(B1)

(A2)

(B2)

(A3)

(B3)

(A4)

(B4)
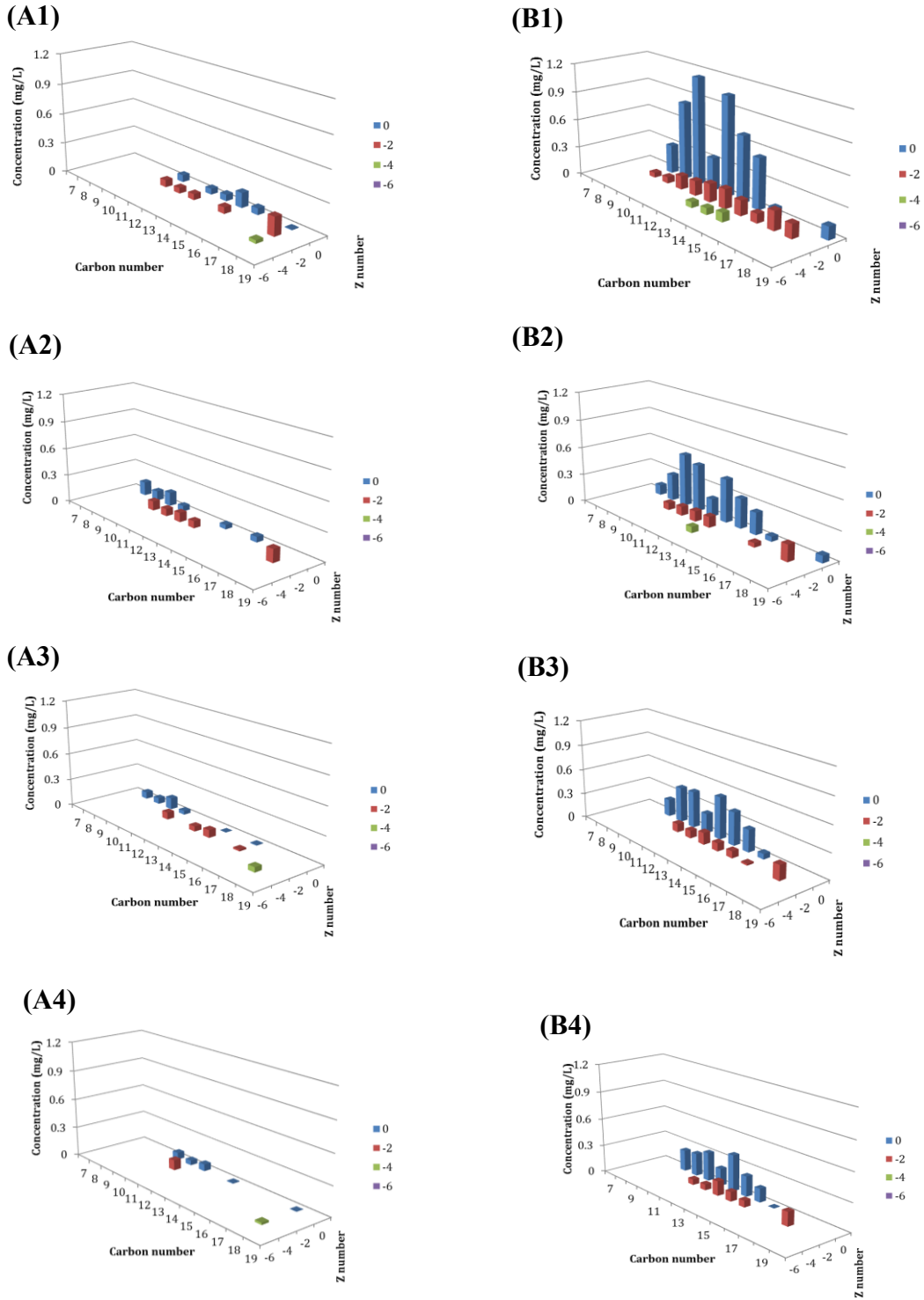
Figure 2.8 Oxidized (O_3) NA distribution after (A) electro-oxidation and (B) electro-oxidation followed by biodegradation ((1) 0 mA/cm^2; (2) 0.5 mA/cm^2; (3) 2.5 mA/cm^2; and (4) 5 mA/cm^2).
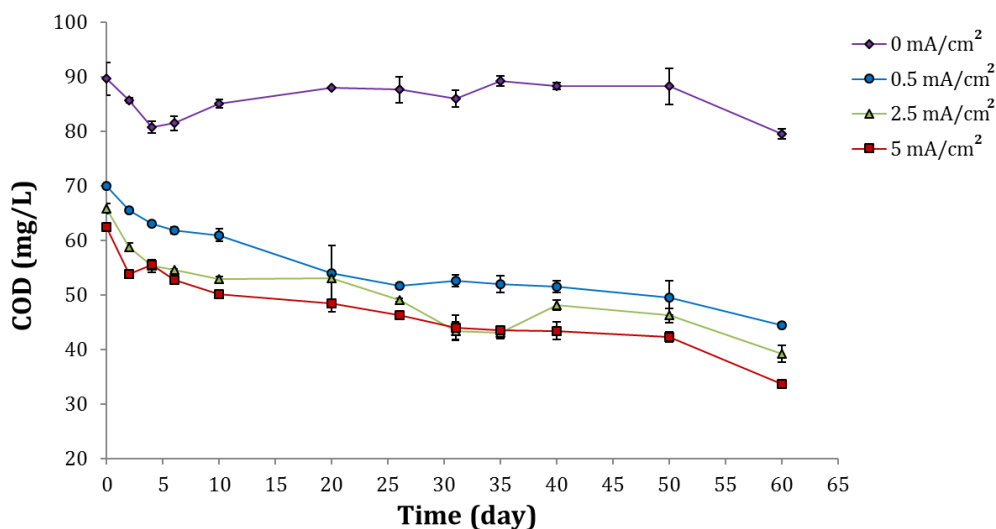
Figure 2.9 COD removal during bio-incubation for 60 days following the electro-

oxidation.

The fate of oxidized NAs (O_3 and O_4) after biodegradation is shown in Fig. 2.4B and 2.4C.

There was a clear increase in the concertation of O_3 and O_4 species in both pre-treated

samples with EO and the ones without pre-treatment. It must be noted here that during

biodegradation, oxidized NAs are generated as results of the degradation of classical NAs

and at the same time it can also be degraded. For oxidized O_3 -NAs the concentration

increased by 7.1 folds after biodegradation in the case without EO pre-treatment, while for

the pre-electro-oxidized samples at current densities of 0.5, 2.5, and 5 mA/cm^2 the

concentration increased by 3.2, 5 and 7 folds, respectively. For oxidized O_4-NAs, on the

other hand, the concentration increased by 5.9 folds for the non-electrolyzed sample, and by

4.7, 4.2 and 4.1 folds for current densities of 0.5, 2.5, and 5 mA/cm^2, respectively. It can be

noted that the increase of oxidized NAs was always higher in the case without EO pre-

treatment compared to the cases with EO pre-treatment which can be attributed to the fact

that the initial concertation of the classical NAs in the case with no EO pre-treatment was very high compared to that for the EO pretreated samples and therefore more classical NAs can be biodegraded to generate oxidized NAs. The distribution of O_3-NA after biodegradation (Fig. 2.8) was very similar to that of classical NAs with acyclic ($z = 0$) and median carbon number being the most abundant species supporting the claim that these are products of bio-insertion of oxygen into the structure of classical NAs, which was the mechanism reported before by Martin et. al (Martin et al. 2010).

Since there was a generation of oxidized NAs during the biodegradation step and due to the possibility that some of these products might be less biodegradable than the original classical NAs, there was a need to evaluate the impact of EO on the biodegradability by using a gross parameter that can include the majority of organics in our commercial NA mixture solution. Therefore, chemical oxygen demand (COD) removal rate during biodegradation experiment was used to evaluate the biodegradability of the different samples. During the biodegradation assay which continued for 60 days, the COD decay rate was faster at the beginning and started slowing from day 10 (Fig. 2.9), which was similar to the trend seen by Han et al. who reported that the biodegradation could be divided into three zones; (1) a lag period, (2) biodegradation of the labile fraction, and (3) remaining persistent fraction (48). Therefore, we used the first 10 days to calculate the COD pseudo 1st order biodegradation rates for the different applied pre-treatment current densities. The COD biodegradation rate constant for the sample without EO pre-treatment was 0.0103 day^{-1} which was increased to 0.0173, 0.0254 and 0.0282 day^{-1} when the samples were pre-treated with EO at current densities of 0.5, 2.5, and 5 mA/cm^2, respectively, which means an increase by 1.7, 2.5 and 2.7 folds in terms of biodegradability. It should also be noted

that the biodegradability improved with increasing the applied current density. This can be considered an indicator that although EO by graphite anodes cannot achieve complete mineralization of NAs, it can actually result in considerable improvement in the biodegradability of NAs through producing more biodegradable intermediates.

2.3.3 Fate of aromatics

As mentioned earlier, the definition of NAs has been expanded to include different hetero atomic and aromatic species that can also be of great concern. In this section, we monitored the fate of the aromatic species in the commercial NA mixture after EO and biodegradation. To investigate the removal of fluorophore aromatics, synchronous fluorescence spectra (SFS) analysis was used. SFS is a selective and surrogate measurement of fluorophore organic compounds that requires the targeted species to have a low-energy transition in order to fluoresce under UV light to be detected (Williams et al. 1983, Shu et al. 2014, Wang et al. 2016c). SFS was employed successfully previously by different researchers to detect aromatics (single-ring and fused-ring aromatics) in OSPW (Shu et al. 2014, Zhang et al. 2015, Wang et al. 2016b, Wang et al. 2016c). However, none of the previous studies that investigated the use of ozone with biodegradation for the treatment of commercial NAs mixtures tried to investigate the fate of the aromatic species. For OSPW, the previous SFS analyses showed the existence of three distinct peaks associated with three different aromatic species; peak (I) at around 270 nm which was associated with one aromatic ring, peak (II) at around 310 nm and was associated with two fused aromatic rings, and peak III at around 330 nm associated with three fused aromatic rings (Shu et al. 2014, Zhang et al. 2015, Wang et al. 2016c).

In the case of our commercial NA mixture, single-ring aromatics (peak at 271 nm) were by far the most dominant species before and after the treatment (Fig. 2.10). EO seemed to be effective for the degradation of aromatic NAs as can be seen from reductions in the peak area at 271 nm (Fig. 2.10A). As we mentioned earlier SFS is a surrogate measurement and cannot give us an exact quantification for the concentrations of these aromatics. Therefore, a semi-quantitative analysis by using the peak area at 271 nm was done to give an idea about the removal of the aromatics fractions (Fig. 2.11). EO was able to achieve reductions of 62.3 %, 63.5 % and 69.6 % when the applied current densities were 0.5, 2.5, and 5 mA/cm^2, respectively (Fig. 2.11). Previous AOPs studies showed that aromatics were degraded by using ozonation, UV/chlorine, UV/H$_2$O$_2$ and ferrate(VI) with single-ring aromatics being the most persistent fraction for oxidation (Shu et al. 2014, Zhang et al. 2015, Wang et al. 2016b, Wang et al. 2016c). Therefore, it is safe to assume here that EO is effective for the degradation of the aromatic fraction, since it was able to degrade the most persistent part of it, single-ring aromatics. .

For biodegradation, on the other hand, aromatics have also been biodegraded effectively in all the cases (Fig. 2.10B). Biodegradation alone without EO pre-treatment was able to achieve 33.5 % aromatics removal (Fig. 2.11). When EO pre-treatments at current densities of 0.5, 2.5, and 5 mA/cm^2 were combined with biodegradation, the aromatics removal increased to 74.9 %, 81.8 % and 88.9 %, respectively. This clearly indicates that combining EO with biodegradation can be an effective option for the degradation of the aromatic fraction in NA-bearing waters.
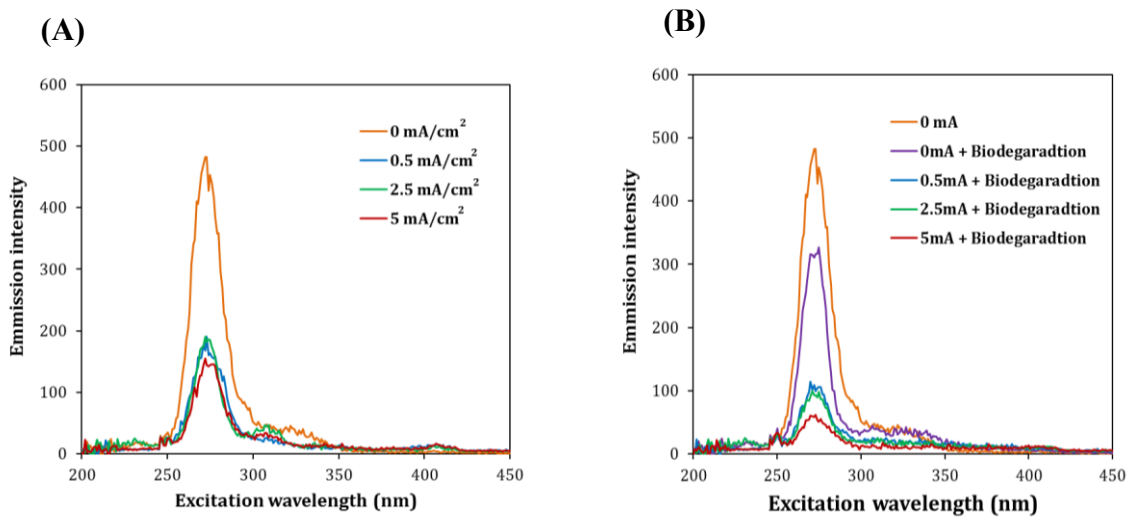
Figure 2.10 SFS analysis to see the fate of fluorescing compounds in the commercial NA mixture after (A) electro-oxidation and (B) combined EO-biodegradation.
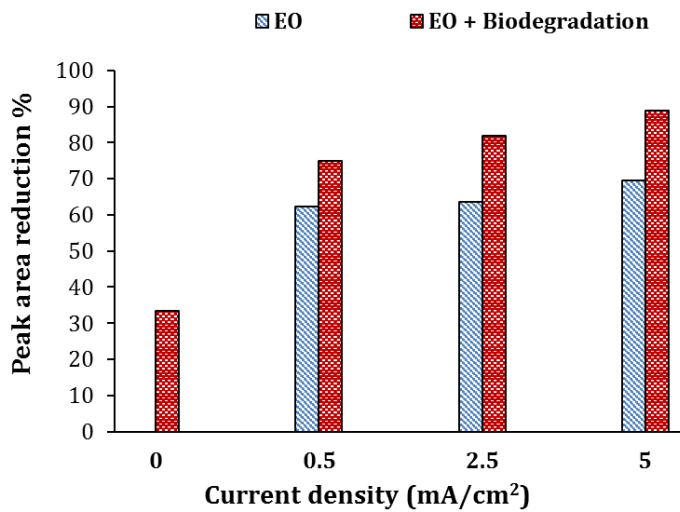
Figure 2.11 Semi-quantitative analysis for the removal efficiency based on the area reduction of the peak at 271 nm.

2.3.3 Toxicity

Finally, the reduction of the acute toxicity of the samples containing NA commercial mixture was evaluated as one of the important parameters for the performance of EO by graphite anode and biodegradation. As an effective pre-screening measurement for acute toxicity, Microtox 81.9 % screening protocol was adopted to evaluate the toxicity toward *Vibrio fischeri*. The marine bacterium *Vibrio fischeri* demonstrated that it could be reasonably used to evaluate the toxicity and have been studied extensively for evaluating the toxicity of OSPW and NA-bearing waters (Martin et al. 2010, Shu et al. 2014, Vaiopoulou et al. 2015, Zhang et al. 2015, Wang et al. 2016c, Zhang et al. 2016b). The initial inhibition level of the samples containing NA commercial mixture was 82.1 % (Fig. 2.12). This value was high compared to the previously reported values for OSPW which were in the range 29-50 % (Shu et al. 2014, Wang et al. 2016c, Zhang et al. 2016b). This can be explained by the reality that the carbon number and cyclicity distribution for our commercial NA mixture (Fig. 2.2A) were different than that reported previously for OSPW (Martin et al. 2010, Shu et al. 2014), and that the toxicity of NAs depends on the molecular structure of NAs (Jones et al. 2011). EO showed positive results in terms of toxicity reduction (Fig. 2.12). EO at current densities of 0.5, 2.5, and 5 mA/cm^2 was able to reduce the inhibition levels to 46.0 %, 34.0 % and 25.0 %, respectively. When ozonation studied for the degradation of commercial NAs, the toxicity of the commercial NA mixture was reported to be reduced in one study (Vaiopoulou et al. 2015), while remained un-affected in another study (Han et al. 2008). The difference between these results could be related to the difference in the used ozone doses between the two studies. However, in our study even at a current density as low as 0.5 mA/cm^2 toxicity was reduced by 44.0 % which means that EO

could be a very effective option for the detoxification of NA-bearing water. Biodegradation, on the other side, was also able to achieve high toxicity reduction even without EO by reducing the inhibition level to 13.0 % (Fig. 2.12). Although more oxidized NAs were generated during biodegradation, it was reported that generated oxidized NAs that contains more ⁻OH groups in their structure are less toxic due to their hydrophilicity which might explain the reduction in the toxicity after biodegradation (Fig. 2.12) (Wang et al. 2013a). What's more, when EO was combined with biodegradation, a complete detoxification was achieved in all the cases (Fig. 2.12). These results could be a clear sign for the effectiveness of combining EO with biodegradation for treating NA-bearing process waters.
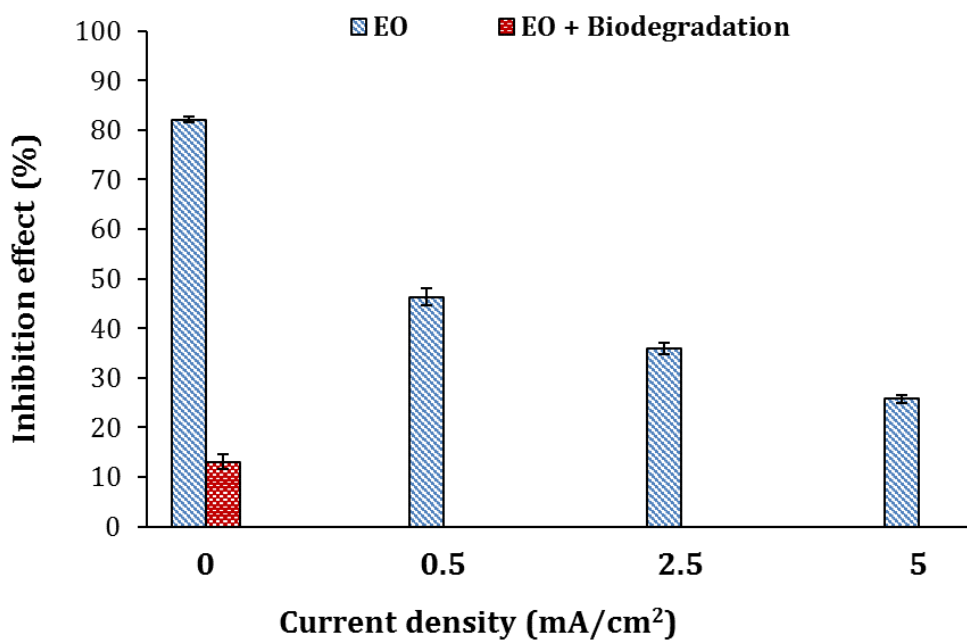
Figure 2.12 The effect of electro-oxidation and combined EO-biodegradation on the toxicity of the commercial NAs mixture towards *Vibrio fischeri*.

2.4. Conclusions

In this study, EO by graphite anodes showed its capability in NA degradation, biodegradability enhancement and toxicity reduction. EO degradation rate for NAs increased with increasing the carbon number (n) and was higher for cyclic NAs than acyclic. The capability of EO in degrading the aromatic species in the NA mixture was also demonstrated. Moreover, it was found that EO enhanced the biodegradability of the NA mixture even at current density as low as 0.5 mA/cm^2. Biodegradation of the raw NA mixture samples resulted in a clear toxicity reduction, however, the combination of EO with biodegradation resulted in a complete detoxification of the samples, showing a synergistic effect of combining these two processes. The study presented here is an important step toward understanding the effectiveness of EO for degrading NAs and the feasibility of using EO as a pre-treatment for aerobic biodegradation to create an effective and energy-efficient treatment option for NA-bearing process waters such as OSPW and refinery effluents.

2.5 References

Afzal, A., P. Chelme-Ayala, P. Drzewicz, J. W. Martin, and M. Gamal El-Din. 2015. Effects of ozone and ozone/hydrogen peroxide on the degradation of model and real oil-sands-process-affected-water naphthenic acids. Ozone: Science & Engineering **37**:45-54.

Afzal, A., P. Drzewicz, J. W. Martin, and M. G. El-Din. 2012a. Decomposition of cyclohexanoic acid by the UV/H$_2$O$_2$ process under various conditions. Science of the Total Environment **426**:387-392.

Afzal, A., P. Drzewicz, L. A. Pérez-Estrada, Y. Chen, J. W. Martin, and M. Gamal El-Din. 2012b. Effect of Molecular Structure on the Relative Reactivity of Naphthenic Acids in the UV/H$_2$O$_2$ Advanced Oxidation Process. Environmental science & technology **46**:10727-10734.

Alpatova, A., E.-S. Kim, S. Dong, N. Sun, P. Chelme-Ayala, and M. Gamal El-Din. 2014. Treatment of oil sands process-affected water with ceramic ultrafiltration membrane: Effects of operating conditions on membrane performance. Separation and purification Technology **122**:170-182.

Benally, C., M. Li, and M. Gamal El-Din. 2018. The effect of carboxyl multiwalled carbon nanotubes content on the structure and performance of polysulfone membranes for oil sands process-affected water treatment. Separation and purification Technology **199**:170-181.

Brillas, E. and C. A. Martínez-Huitle. 2015. Decontamination of wastewaters containing synthetic organic dyes by electrochemical methods. An updated review. Applied Catalysis B: Environmental **166**:603-643.

Brown, L. D. and A. C. Ulrich. 2015. Oil sands naphthenic acids: a review of properties, measurement, and treatment. Chemosphere **127**:276-290.

Chaplin, B. P. 2014. Critical review of electrochemical advanced oxidation processes for water treatment applications. Environmental Science: Processes & Impacts **16**:1182-1203.

Chen, G. 2004. Electrochemical technologies in wastewater treatment. Separation and purification Technology **38**:11-41.

Clemente, J. S., M. D. MacKinnon, and P. M. Fedorak. 2004. Aerobic biodegradation of two commercial naphthenic acids preparations. Environmental science & technology **38**:1009-1016.

de Klerk, A., M. R. Gray, and N. Zerpa. 2014. Unconventional oil and gas: Oilsands. Pages 95-116 Future Energy (Second Edition). Elsevier.

Dong, T., Y. Zhang, M. S. Islam, Y. Liu, and M. Gamal El-Din. 2015. The impact of various ozone pretreatment doses on the performance of endogenous microbial communities for the remediation of oil sands process-affected water. International Biodeterioration & Biodegradation **100**:17-28.

Drzewicz, P., L. Perez-Estrada, A. Alpatova, J. W. Martin, and M. Gamal El-Din. 2012. Impact of peroxydisulfate in the presence of zero valent iron on the oxidation of cyclohexanoic acid and naphthenic acids from oil sands process-affected water. Environmental science & technology **46**:8984-8991.

El-Din, M. G., H. Fu, N. Wang, P. Chelme-Ayala, L. Pérez-Estrada, P. Drzewicz, J. W. Martin, W. Zubot, and D. W. Smith. 2011. Naphthenic acids speciation and removal during petroleum-coke adsorption and ozonation of oil sands process-affected water. Science of the Total Environment **409**:5119-5125.

Ganiyu, S. O., M. Zhou, and C. A. Martínez-Huitle. 2018. Heterogeneous electro-Fenton and photoelectro-Fenton processes: a critical review of fundamental principles and application for water/wastewater treatment. Applied Catalysis B: Environmental.

Garcia-Garcia, E., J. Q. Ge, A. Oladiran, B. Montgomery, M. Gamal El-Din, L. C. Perez-Estrada, J. L. Stafford, J. W. Martin, and M. Belosevic. 2011. Ozone treatment ameliorates oil sands process water toxicity to the mammalian immune system. Water research **45**:5849-5857.

Han, X., A. C. Scott, P. M. Fedorak, M. Bataineh, and J. W. Martin. 2008. Influence of molecular structure on the biodegradability of naphthenic acids. Environmental science & technology **42**:1290-1295.

He, Y., S. B. Wiseman, M. Hecker, X. Zhang, N. Wang, L. A. Perez, P. D. Jones, M. Gamal El-Din, J. W. Martin, and J. P. Giesy. 2011. Effect of ozonation on the estrogenicity and androgenicity of oil sands process-affected water. Environmental science & technology **45**:6268-6274.

Islam, M. S., J. Moreira, P. Chelme-Ayala, and M. Gamal El-Din. 2014. Prediction of naphthenic acid species degradation by kinetic and surrogate models during the ozonation of oil sands process-affected water. Science of the Total Environment **493**:282-290.

Jones, D., A. G. Scarlett, C. E. West, and S. J. Rowland. 2011. Toxicity of Individual Naphthenic Acids to *Vibrio fischeri*. Environmental science & technology **45**:9776-9782.

Klamerth, N., J. Moreira, C. Li, A. Singh, K. N. McPhedran, P. Chelme-Ayala, M. Belosevic, and M. Gamal El-Din. 2015. Effect of ozonation on the naphthenic acids' speciation and toxicity of pH-dependent organic extracts of oil sands process-affected water. Science of the Total Environment **506**:66-75.

Li, C., L. Fu, J. Stafford, M. Belosevic, and M. Gamal El-Din. 2017. The toxicity of oil sands process-affected water (OSPW): a critical review. Science of the Total Environment **601**:1785-1802.

Martin, J. W., T. Barri, X. Han, P. M. Fedorak, M. Gamal El-Din, L. Perez, A. C. Scott, and J. T. Jiang. 2010. Ozonation of Oil Sands Process-Affected Water Accelerates Microbial Bioremediation. Environmental science & technology **44**:8350-8356.

Martínez-Huitle, C. A. and M. Panizza. 2018. Electrochemical oxidation of organic pollutants for wastewater treatment. Current Opinion in Electrochemistry.

Martínez-Huitle, C. A., M. A. Rodrigo, I. Sirés, and O. Scialdone. 2015. Single and coupled electrochemical processes and reactors for the abatement of organic water pollutants: a critical review. Chemical Reviews **115**:13362-13407.

Meshref, M. N., P. Chelme-Ayala, and M. Gamal El-Din. 2017. Fate and abundance of classical and heteroatomic naphthenic acid species after advanced oxidation processes: Insights and indicators of transformation and degradation. Water research **125**:62-71.

Misiti, T., U. Tezel, and S. G. Pavlostathis. 2013. Fate and effect of naphthenic acids on oil refinery activated sludge wastewater treatment systems. Water research **47**:449-460.

Misiti, T. M., U. Tezel, and S. G. Pavlostathis. 2014. Effect of Alkyl Side Chain Location and Cyclicity on the Aerobic Biotransformation of Naphthenic Acids. Environmental science & technology **48**:7909-7917.

Moreira, F. C., R. A. R. Boaventura, E. Brillas, and V. J. P. Vilar. 2017. Electrochemical advanced oxidation processes: A review on their application to synthetic and real wastewaters. Applied Catalysis B: Environmental **202**:217-261.

Panizza, M. 2010. Importance of Electrode Material in the Electrochemical Treatment of Wastewater Containing Organic Pollutants. Pages 25-54 *in* C. Comninellis and G. Chen, editors. Electrochemistry for the Environment. Springer New York, New York, NY.

Panizza, M. and G. Cerisola. 2009. Direct And Mediated Anodic Oxidation of Organic Pollutants. Chemical Reviews **109**:6541-6569.

Quinlan, P. J. and K. C. Tam. 2015. Water treatment technologies for the remediation of naphthenic acids in oil sands process-affected water. Chemical Engineering Journal **279**:696-714.

Rao, A. N. S. and V. T. Venkatarangaiah. 2014. Metal oxide-coated anodes in wastewater treatment. Environmental Science and Pollution Research **21**:3197-3217.

Regulator, A. E. 2014. Alberta's energy reserves 2011 and supply/demand outlook 2012–2021. ST98-2012. ISSN 1910-4235. Alberta Energy Regulator Calgary, Canada.

Rueffer, M., D. Bejan, and N. J. Bunce. 2011. Graphite: An active or an inactive anode? Electrochimica Acta **56**:2246-2253.

Scott, A. C., M. D. Mackinnon, and P. M. Fedorak. 2005. Naphthenic acids in Athabasca oil sands tailings waters are less biodegradable than commercial naphthenic acids. Environmental science & technology **39**:8388-8394.

Shi, Y., C. Huang, K. C. Rocha, M. Gamal El-Din, and Y. Liu. 2015. Treatment of oil sands process-affected water using moving bed biofilm reactors: with and without ozone pretreatment. Bioresource technology **192**:219-227.

Shu, Z., C. Li, M. Belosevic, J. R. Bolton, and M. Gamal El-Din. 2014. Application of a solar UV/chlorine advanced oxidation process to oil sands process-affected water remediation. Environmental science & technology **48**:9692-9701.

Sirés, I., E. Brillas, M. A. Oturan, M. A. Rodrigo, and M. Panizza. 2014. Electrochemical advanced oxidation processes: today and tomorrow. A review. Environmental Science and Pollution Research **21**:8336-8367.

Smith, B. E., C. A. Lewis, S. T. Belt, C. Whitby, and S. J. Rowland. 2008. Effects of Alkyl Chain Branching on the Biotransformation of Naphthenic Acids. Environmental science & technology **42**:9323-9328.

Vaiopoulou, E., T. M. Misiti, and S. G. Pavlostathis. 2015. Removal and toxicity reduction of naphthenic acids by ozonation and combined ozonation-aerobic biodegradation. Bioresource technology **179**:339-347.

Wang, B., Y. Wan, Y. Gao, M. Yang, and J. Hu. 2013a. Determination and Characterization of Oxy-Naphthenic Acids in Oilfield Wastewater. Environmental science & technology **47**:9545-9554.

70

Wang, C., R. Huang, N. Klamerth, P. Chelme-Ayala, and M. Gamal El-Din. 2016a. Positive and negative electrospray ionization analyses of the organic fractions in raw and oxidized oil sands process-affected water. Chemosphere **165**:239-247.

Wang, C., N. Klamerth, R. Huang, H. Elnakar, and M. Gamal El-Din. 2016b. Oxidation of oil sands process-affected water by potassium ferrate (VI). Environmental science & technology **50**:4238-4247.

Wang, C., N. Klamerth, S. A. Messele, A. Singh, M. Belosevic, and M. Gamal El-Din. 2016c. Comparison of UV/hydrogen peroxide, potassium ferrate(VI), and ozone in oxidizing the organic fraction of oil sands process-affected water (OSPW). Water research **100**:476-485.

Wang, N., P. Chelme-Ayala, L. Perez-Estrada, E. Garcia-Garcia, J. Pun, J. W. Martin, M. Belosevic, and M. Gamal El-Din. 2013b. Impact of ozonation on naphthenic acids speciation and toxicity of oil sands process-affected water to Vibrio fischeri and mammalian immune system. Environmental science & technology **47**:6518-6526.

Whitby, C. 2010. Microbial naphthenic acid degradation. Pages 93-125 Advances in applied microbiology. Elsevier.

Williams, A. T. R., S. A. Winfield, and J. N. Miller. 1983. Relative fluorescence quantum yields using a computer-controlled luminescence spectrometer. Analyst **108**:1067-1071.

Xue, J., C. Huang, Y. Zhang, Y. Liu, and M. Gamal El-Din. 2018. Bioreactors for oil sands process-affected water (OSPW) treatment: A critical review. Science of the Total Environment **627**:916-933.

Zhang, Y., N. Klamerth, S. A. Messele, P. Chelme-Ayala, and M. Gamal El-Din. 2016a. Kinetics study on the degradation of a model naphthenic acid by ethylenediamine-N, N'-disuccinic acid-modified Fenton process. Journal of hazardous materials **318**:371-378.

Zhang, Y., K. N. McPhedran, and M. Gamal El-Din. 2015. Pseudomonads biodegradation of aromatic compounds in oil sands process-affected water. Science of the Total Environment **521-522**:59-67.

Zhang, Y., J. Xue, Y. Liu, and M. Gamal El-Din. 2016b. Treatment of oil sands process-affected water using membrane bioreactor coupled with ozonation: A comparative study. Chemical Engineering Journal **302**:485-497.

Zubot, W., M. D. MacKinnon, P. Chelme-Ayala, D. W. Smith, and M. Gamal El-Din. 2012. Petroleum coke adsorption as a water management option for oil sands process-affected water. Science of the Total Environment **427**:364-372.

3. DEGRADATION KINETICS AND STRUCTURE-REACTIVITY RELATION OF NAPHTHENIC ACIDS DURING ANODIC OXIDATION ON GRAPHITE ELECTRODES[1]

3.1 Introduction

The oil sands industry in Northern Alberta is considered one of the main contributors to the Canadian economy (Energy 2013, Regulator 2014). In order to extract bitumen, the molasses-like hydrocarbon mixture that is found mixed in the sands, hot and caustic water needs to be used (Masliyah et al. 2004). The current commercially used extraction technologies consume large volumes of water; in 2015 alone the oil sands industry consumed around 180 million m^3 of fresh water (Operators 2015). As a result, huge quantities of produced water known as oil sands process water (OSPW) are generated and sent to be stored in tailings ponds (Allen 2008). OSPW has been shown to be toxic to various aquatic and terrestrial organisms (Hagen et al. 2012, Wang et al. 2013, Yue et al. 2014, Li et al. 2017). Among the different constituents of OSPW, a group of carboxylic acids known as naphthenic acids (NAs) accounts for almost half of the total organic fraction in OSPW and has been reported to be one of the main causes of its toxicity (Verbeek et al. 1989, Rowland et al. 2011, Li et al. 2017). NAs are known to be very recalcitrant. They are identified as complex mixture of alkyl-substituted acyclic, cyclic and polycyclic carboxylic acids with a general formula of $C_nH_{2n+Z}O_X$, where n represents the number of carbon atoms, Z reflects the hydrogen atoms lost due to ring formation (cyclicity)

($Z \leq 0$) and X is the number of oxygen atoms which refers to either classical NAs (X=2) or oxidized NAs ($X \geq 3$) (Verbeek et al. 1989, Whitby 2010, Rowland et al. 2011, Wang et al. 2013, Meshref et al. 2017). The structure range of NAs has also been expanded to include aromatic compounds, heteroatomic (N or S-containing) compounds and multiple-carboxylated compounds (Kannel and Gan 2012, Wang et al. 2013, Brown and Ulrich 2015, Meshref et al. 2017).

The treatment and release of the accumulated amounts of OSPW is currently considered one of the priorities for oil sands industry. Different processes have been studied for the treatment of OSPW and degradation of NAs (Kannel and Gan 2012, Brown and Ulrich 2015, Quinlan and Tam 2015). Due to the recalcitrant nature of NAs, the biodegradation of NAs in tailing ponds is a very slow and ineffective process with biodegradation half-lives of several years (Scott et al. 2005, Han et al. 2008, Misiti et al. 2014, Xue et al. 2018). Several advanced oxidation processes (AOPs) have been investigated for NAs degradation, including ozonation (Martin et al. 2010, Pérez-Estrada et al. 2011, Wang et al. 2016b), UV/H_2O_2 (Afzal et al. 2012a, Wang et al. 2016b), O_3/H_2O_2 (Afzal et al. 2015), UV/chlorine (Shu et al. 2014) and potassium ferrate (VI) (Wang et al. 2016a, Wang et al. 2016b). Despite its efficiency, the use of AOPs is restrained by the high associated costs. Combining AOPs with biodegradation have been suggested as an effective and cost efficient combination. Ozonation was, by far, the most studied AOP for combination with biodegradation (Scott et al. 2005, Martin et al. 2010, Brown and Ulrich 2015, Zhang et al. 2016b). This combination, however, is still restricted by the high doses of ozone required to improve the biodegradability of OSPW's NAs (Scott et al. 2005, Martin et al. 2010).

Electrochemical advanced oxidation processes (EOAPs) has been used successfully for the degradation of different recalcitrant pollutants (Fockedey and Van Lierde 2002, Martinez-Huitle and Ferro 2006, Panizza and Cerisola 2009, Comninellis and Chen 2010, Rueffer et al. 2011, Chaplin 2014, Moreira et al. 2017). Despite that they have not been investigated for the treatment of OSPW yet. EOAPs can be classified into anodic and cathodic processes depending on whether oxidants are produced at the anode or cathode (Panizza and Cerisola 2009, Sirés et al. 2014, Martínez-Huitle et al. 2015, Moreira et al. 2017). Cathodic oxidation mainly involves the production of H_2O_2 (electroperoxidation) through the reduction of O_2 at cathode (Zöllig et al. 2015). Anodic oxidation (AO), on the other hand, involves the generation of oxidants at anode and it has been studied and applied more frequently (Martinez-Huitle and Ferro 2006, Panizza and Cerisola 2009, Comninellis and Chen 2010, Chaplin 2014, Sirés et al. 2014, Martínez-Huitle et al. 2015, Moreira et al. 2017). The oxidation of pollutants during anodic oxidation can occur through: direct electron transfer (DET) by transferring electrons from the substrate (R) to the anode (Eq. (3.1)); the generation of reactive intermediates from water oxidation such as hydroxyl radicals at anode (M) (Eq. (3.2)); other oxidants that can be generated at anode from water or dissolved anions such as Cl^- and SO_4^{2-} (Eq. (3.3) and (3.4)) (Martinez-Huitle and Ferro 2006, Panizza and Cerisola 2009, Comninellis and Chen 2010, Chaplin 2014, Sirés et al. 2014, Martínez-Huitle et al. 2015, Moreira et al. 2017).

$$R \rightarrow (R^{\bullet})^+ + e^- \qquad\qquad (3.1)$$

$$H_2O/OH^- + M \rightarrow M(^{\bullet}OH) + H^+ + e^- \qquad\qquad (3.2)$$

$$2Cl^- \rightarrow Cl_2 + 2e^- \qquad\qquad (3.3)$$

$$2SO_4{}^{2-} \rightarrow S_2O_8{}^{2-} \tag{3.4}$$
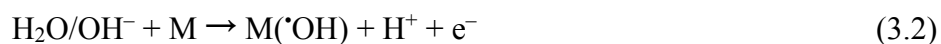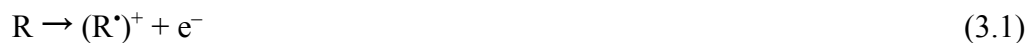
At cathode, on the other hand, hydrogen evolution will occur as a result of the water reduction (Panizza and Cerisola 2009, Comninellis and Chen 2010). The anode material play great role in defining the oxidation selectivity and involved mechanisms (Panizza and Cerisola 2009, Comninellis and Chen 2010). Based on the interaction between the anode surface and the generated $^{\bullet}OH$, anode materials have been classified into active and non-active (Panizza and Cerisola 2009, Sirés et al. 2014, Martínez-Huitle et al. 2015). Active anode materials such as Pt, RuO_2, RuO_2-IrO_2 and carbon generates $^{\bullet}OH$ radicals that are chemisorbed on the anode, which make them not available for reaction away from the anode surface and, therefore, less effective for mineralization (electrochemical conversion). Anodes such as boron-doped diamond (BDD) and lead dioxide are considered non-active; they can generates $^{\bullet}OH$ radicals that are only physisorbed on the anode surface, which make them readily available to completely degrade pollutants (electrochemical combustion) (Martinez-Huitle and Ferro 2006, Panizza and Cerisola 2009, Sirés et al. 2014, Martínez-Huitle et al. 2015, Moreira et al. 2017). Graphite has been continuously classified as an active anode due to its low oxygen evolution potentials and poor performance for achieving pollutants mineralization (Panizza and Cerisola 2009, Rueffer et al. 2011). DET was also proposed as the oxidation mechanism for ammonia, when AO was performed at low voltages using graphite anode (Zöllig et al. 2015). Although graphite anodes have been used extensively before and it was once the standard anode material for the chloralkali process, it is still restricted by the surface corrosion and cannot be effectively used at high voltages (Rueffer et al. 2011, Zöllig et al. 2015, Qiao et al. 2018). Graphite, however, as an inexpensive and commercially available anode material, can be an attractive option if the

pollutant of concern can be degraded at low current densities where severe corrosion can be avoided (Comninellis and Chen 2010, Rueffer et al. 2011, Zöllig et al. 2015, Qiao et al. 2018).

It was reported that there is a strong correlation between the molecular structure of NAs and their chemical, physical and toxicological properties (Han et al. 2008, Jones et al. 2011, de Oliveira Livera et al. 2018). It has been found that the amenability of individual NAs toward oxidation by ozone, UV/H_2O_2 and photocatalysis depended greatly on their molecular structure, with the more complex in structure being more amenable to oxidation (Pérez-Estrada et al. 2011, Afzal et al. 2012b, de Oliveira Livera et al. 2018). The biodegradability of NAs was also found to be strongly connected with their molecular structures, with the side chain branching being an important inhibiter for biotransformation (Scott et al. 2005, Han et al. 2008, Misiti et al. 2014). Moreover, the toxicological properties of NAs have also been shown to depend strongly on molecular structure (Jones et al. 2011, Li et al. 2017). Since, it is clear from the above discussion that all the important treatment parameters for OSPW (resistance to oxidation, biodegradability and toxicity) are strongly correlated with the molecular structure; it is wise to understand the structure–reactivity relationship of NAs in any process proposed for OSPW treatment and NAs degradation.

The main objectives of this chapter were to investigate the degradation of model NA compounds by anodic oxidation on graphite anode; understand the involved oxidation mechanisms; and to examine the structure-reactivity relationships during anodic oxidation by graphite anode. Finding the current density window within which NAs can be degraded electro-chemically and whether the graphite anode corrosion can be avoided are also of

great important for this research. Graphite anode was selected due to its low cost and relative abundance which make it an attractive material for OSPW treatment by AO at large scales; especially when considering the huge amount of accumulated OSPW in tailing ponds.
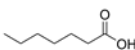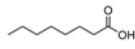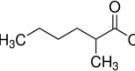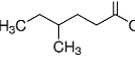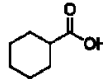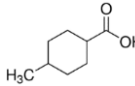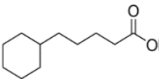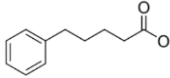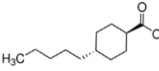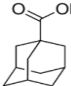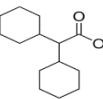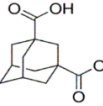
3.2 Materials and methods

3.2.1 Chemicals and reagents

Heptanoic acid (HPA), octanoic acid (OCA), 2-methylheptanoic acid (2mHPA), trans-4-pentylcyclohexane carboxylic acid (TPCA), 1, 3-adamantanedicarboxylic acid (ADA), and 4-methyl-1-cyclohexanecarboxylic acid (4mCHA) were obtained from Tokyo Chemical Industry (TCI) (Tokyo, Japan). Cyclohexanecarboxylic acid (CHA), 5-cyclohexanepentanoic acid (CHPA), 5-phenylvaleric acid (PVA), 1-adamantaneacetic acid (AAA) and dicyclohexylacetic acid (DCHA) were purchased from Sigma-Aldrich (St. Louis, MO, USA). Model compound 4-methylheptanoic acid (4mHPA) was purchased from Narchem Corporation (Chicago). Table 3.1 shows the name, structure, molecular weight, degree of cyclicity and the double bond equivalents (DBE = 1 − Z/2) of each of these model compounds.

Analytical grade 1,4-benzoquinone (BQ) (99%, Sigma-Aldrich, Canada), tert-butyl alcohol (TBA) (99.5%, ACROS Organics, Fisher Scientific, Canada), sodium chloride (> 99%, Fisher Scientific, US) and sodium sulfate (≥ 99%, Sigma-Aldrich, Canada) were used during the experiments. Analytical grade monosodium phosphate, disodium phosphate, sulfuric acid, sodium bicarbonate and sodium hydroxide were purchased from Fisher Scientific Canada (Edmonton, Alberta). MilliQ water (R > 18 MΩ cm, Millipore Corporation) was used for the preparation of all the solutions.

Table 3.1 Name, structure and properties of model NA compounds used during anodic oxidation experiments.

Model compound	Abbrev.	Formula	Structure	M.W.	Z	DBE
Heptanoic acid	HPA	$C_7H_{14}O_2$		130.2	0	1
Octanoic acid	OCA	$C_8H_{16}O_2$		144.2	0	1
2-Methylheptanoic acid	2mHPA	$C_8H_{16}O_2$		144.2	0	1
4-Methylheptanoic acid	4mHPA	$C_8H_{16}O_2$		144.2	0	1
Cyclohexanecarboxylic acid	CHA	$C_7H_{12}O_2$		128.2	-2	2
4-Methyl-1-cyclohexanecarboxylic acid	4mCHA	$C_8H_{14}O_2$		142.2	-2	2
5-Cyclohexanepentanoic acid	CHPA	$C_{11}H_{20}O_2$		184.3	-2	2
5-Phenylvaleric acid	PVA	$C_{11}H_{14}O_2$		178.0	-8	5
Trans-4- pentylcyclohexane carboxylic acid	TPCA	$C_{12}H_{22}O_2$		198.3	-2	1
1-Adamantaneacetic acid	AAA	$C_{11}H_{16}O_2$		180.3	-6	4
Dicyclohexylacetic acid	DCHA	$C_{14}H_{24}O_2$		224.3	-4	3
1,3-Adamantanedicarboxylic acid	ADA	$C_{12}H_{16}O_4$		224.3	-6	N/A

3.2.2 Experimental apparatus and procedure

All AO treatment experiments were conducted in an undivided cylindrical glass reactor of 500 mL capacity equipped with rectangular graphite plate electrodes (7 cm × 2.5 cm × 0.25 cm) and constantly stirred with a PTFE magnetic bar at high speed to ensure homogenization of the solution and enhance mass transport during AO (Fig. B1). Graphite plates (Wale Apparatus, PA, US) were used as electrodes. The two electrodes were placed in the centre of the reactor parallel to each other at electrode distance of 1.2 cm in order to minimize the resistance of the electrolysis medium while maintaining enough space for effective mass transport in the area between electrodes and prevent any gas accumulation. The runs were performed under controlled current conditions (galvanostatic), unless other is stated, and the changes in voltage were monitored and recorded continuously. New set of electrodes were used for each run to exclude any effect that might come from the change of electrodes surface properties. Parallel control reactor with an identical setup was always run with electrodes but without electric field to exclude any removal arising from adsorption or volatilization. DC power station (9130, B&K Precision, California, US) was used to supply power and to monitor voltage, electrode potential and current. Reference Ag/AgCl (saturated) electrode (Accumet, Fisher Scientific, CA), E = +0.201 V vs SHE, was used to measure the anode potentials. Stock solutions of 1.5 g NA/L in 0.01 M NaOH were prepared and used to prepare the different solutions. Initial model NA concentrations of 50 mg/L were used to simulate the concentration of NAs in OSPW (Whitby 2010, Kannel and Gan 2012, Brown and Ulrich 2015, Meshref et al. 2017).

Cyclic voltammetry measurements were carried out by using a Gamry Reference 600 Potentiostat (Gamry, USA) with a three-electrode setup. Graphite rods were used as

working and counter electrodes and saturated Ag/AgCl electrode (Fisher Scientific, CA) was used as reference electrode. The distance between the anode and the standard electrode was set to be 1.2 cm. Voltammograms were recorded at scan rates of 20 mV/s a scan rate low enough to reveal any oxidation beaks (Rueffer et al. 2011) and 10 mM $NaClO_4$ was used as electrolyte medium.

The surface morphology of anodes before and after AO experiment was observed using scanning electron microscope (SEM) (Sigma 300 VP, Zeiss) operating at voltage of 20 kV. The surface functional groups on the anodes were analyzed by X-ray photoelectron spectroscopy (XPS) (AXIS 165, Kratos Analytical) using monochromatized AlKα (1486.6 eV) spectrometer .

3.2.3 Oxidation kinetics and structure-reactivity

To analyze the effect of current density and different operating conditions on the degradation of NAs during AO and to understand the involved oxidation mechanisms, cyclohexanecarboxylic acid (CHA) was selected as a model compound. The degradation of CHA was followed during 180 min under different operating conditions and electrolyte mediums. The effect of molecular structure on the reactivity of NAs was studied by electrolyzing individual solution of twelve different model NA compounds (Table 3.1) under identical experimental conditions for 180 min and the degradation rates were compared. Competitive kinetics plot comparing compounds X and Y was made by plotting $\ln(X_0/X)$ versus $\ln(Y_0/Y)$ for every time point. The plot was linear with a slope equal to the ratio of the rate constants k_X/k_Y (Eq. (3.5)). A slope greater than 1 indicates that X is more reactive than Y and vice versa. All runs were performed in duplicate and were combined

for statistical analysis. Regression analysis was performed using Microsoft Excel and 95% confidence intervals were met for the different slopes.

$$\ln(\frac{X_0}{X}) \Big/ \ln(\frac{Y_0}{Y}) = \frac{k_X}{k_Y} \qquad\qquad (3.5)$$

3.2.4 Analytical methods

The pH and conductivity of the solutions were measured by using a multi-channel pH/conductivity/ion (Accumet excel XL60; Fisher Scientific). A thermometer was used to monitor the solution temperature. Dissolved organic carbon (DOC) was measured by filtering the samples through a 0.45 μm nylon filter and analyze on a Shimadzu TOC analyzer (TOC-LCPH, Shimadzu Corporation). The concentrations of CHA and the rest of the model compounds were measured on a liquid chromatography (LC-MS, Waters, USA) system connected to an ion trap mass spectrometer (Waters Acquity, SQ Detector 2) and operated in negative electro-spray ionization mode (-ESI). The column used for the analysis was C18, 1.7 μm, 2.1× 50 mm (Waters Acquity, Ireland). The column temperature was set at 40°C, the flow rate was 0.4 mL/min and the injection volume was 20 μL. All samples were filtered through a 0.45 μm nylon filter prior to the analysis.

3.3 Results and discussion

3.3.1 Effect of applied current density on the degradation of CHA

CHA is a simple cyclic aliphatic carboxylic acid (Table 3.1) that was used more frequently for the investigation of NAs degradation kinetics during different AOPs (Afzal et al. 2012a, Drzewicz et al. 2012, Afzal et al. 2015, Zhang et al. 2016a). The electrolyte medium used consisted of $NaHCO_3$ (1.5 g/L), NaCl (0.9 g/L) and Na_2SO_4 (0.65 g/L). This was to

simulate the buffered pH (7.8-8.9), conductivity (3-4.1 mS/cm), alkalinity (700-1000 mg/L as CaCO$_3$), sodium (500-700 mg/L), chloride (75-550 mg/L) and sulfate (130-300 mg/L) of real OSPW (Allen 2008, Kim et al. 2012, Shu et al. 2014, Wang et al. 2015). The resulted solution had a buffered pH of 8.5 and conductivity of 4.1 mS/cm.

To investigate the impact of the applied current density on the degradation of CHA, different current densities in the range 0.25 - 20 mA/cm^2 were applied and the decay in the concentration was followed during 180 min runs (Fig. 3.1). The kinetic experiments were performed for 180 min based on preliminary experiment for CHA degradation at 5mA/cm^2 which was conducted for 420 min and showed relatively slower CHA removal rate after 180 min. As can be seen in Fig. 3.1, the degradation of CHA increased steadily with increasing the applied current density and reached 82.1, 74 and 68.7% after 180 min at current densities of 20, 10 and 5 mA/cm^2, respectively. Even at current densities as low as 0.25 and 0.5 mA/cm^2, CHA degradation rates of 12.9 and 29.3%, respectively, were achieved. This indicates that the limiting current density for AO of CHA on graphite is relatively low and that anodic oxidation of NAs on graphite can occur at low current densities ($\leq$ 0.25 mA/cm^2). The degradation of CHA by anodic oxidation on graphite clearly followed a pseudo first order kinetics model with reaction rates increased from 0.00091 min^{-1} to 0.01 min^{-1} when the current density increased from 0.25 to 20 mA/cm^2, respectively (Fig. 3.2). In order to understand the changes at the surface of anode, the voltages were monitored continuously and recorded during the experiments (Fig 3.3). As can be seen in Fig. 3.3, the voltage started increasing during the first couple of min of the experiments before it quickly decreased and then became stable in most of the cases. This behaviour agrees with the results reported by Rueffer et al. (Rueffer et al. 2011) who found

83

that the graphite anode surface get functionalized at the beginning when an electric field is applied and then it became more active for oxidation. This behaviour explains the quick reduction and then stability of the voltage until the end of the run which is because of the quick functionalization at the beginning of electrolysis which led to the reduction in the required voltage to achieve the substrate oxidation. The functionalization depended on the applied current density, and therefore, in the case of 0.25 mA/cm^2 it took 20 min before voltage was stable, whereas at 20 mA/cm^2 it occurred quickly and to higher extent that the voltage was greatly decreased after it (Fig. 3.3). This was also supported by previous report which showed that the oxidation of sulfide by graphite anode was different on previously used anode than on virgin anode (Hastie et al. 2011). It is also important to state that there was neither formation of polymeric byproducts nor coating on the surface of the anode during the electrolysis experiments irrespective of the applied current studied. The initial temperature of solutions was 22±1 ℃, the temperature stayed almost within the same range (22±2 ℃) when the current densities were within the range 0.25 - 5 mA/cm^2. However, it increased to 26 and 29 ℃ at the end of the 180 min runs when the applied current densities were 10 and 20 mA/cm^2, respectively. This behaviour was expected at higher voltages due to the ohmic resistance of the electrodes and the electrolyte.
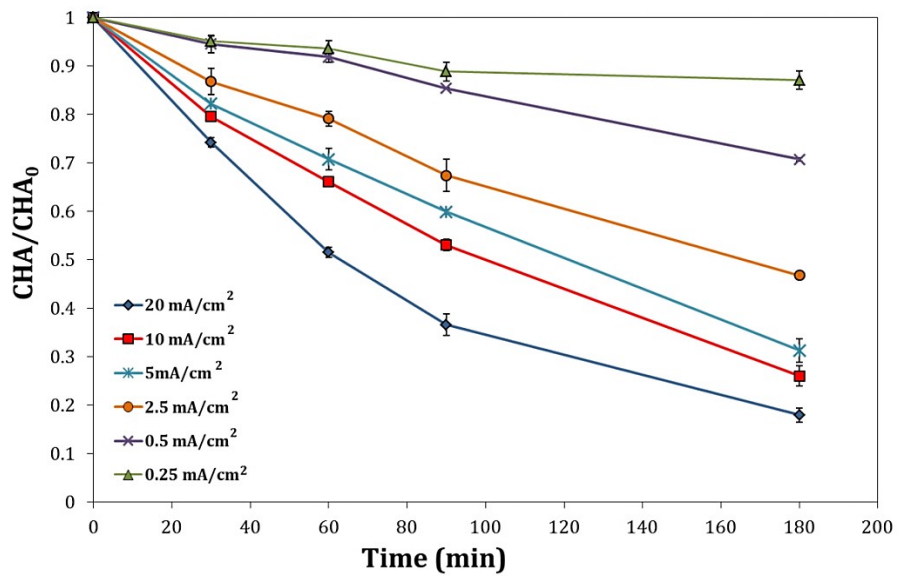
Figure 3.1 Effect of applied current density on the decay of normalized CHA concentration vs. electrolysis time during the anodic-oxidation of 50 mg/L CHA solution using graphite sheet electrodes (electrolyte medium: 1.5 g/L $NaHCO_3$, 0.9 g/L NaCl and 0.65 g/L Na_2SO_4).
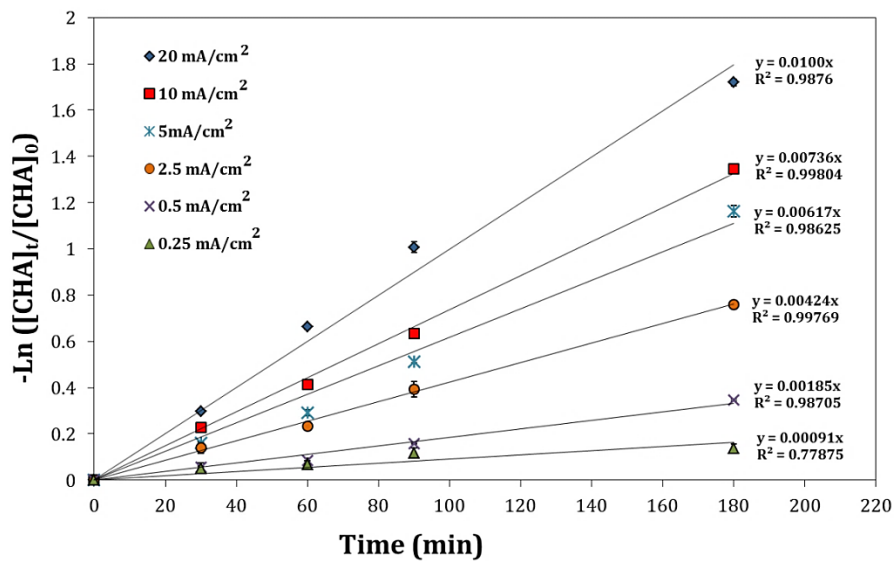
Figure 3.2 Corresponding reaction rates at different current densities for anodic oxidation of CHA reported in Figure 3.1.
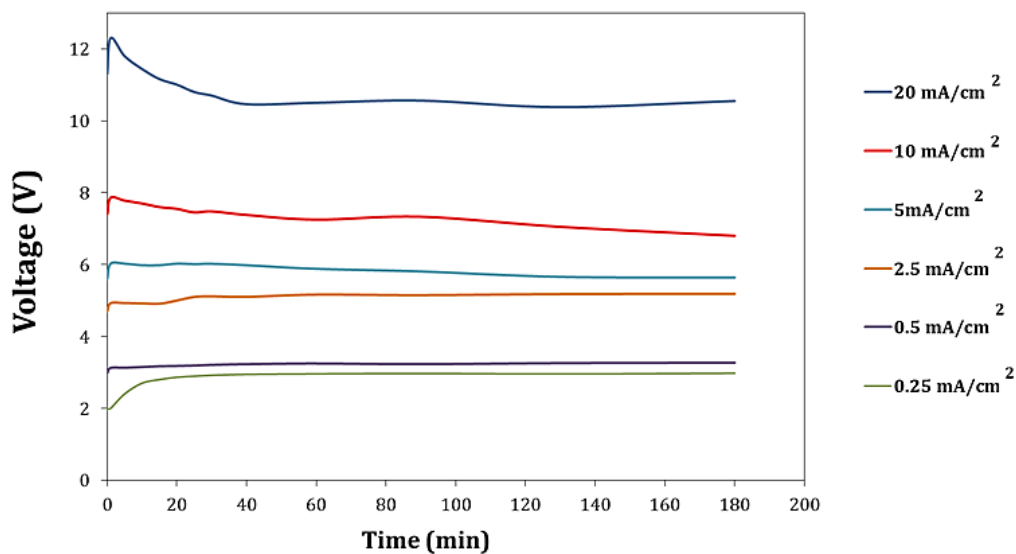
Figure 3.3 Evolution of voltage profiles during anodic oxidation of 50 mg/L CHA solution at different applied current densities using graphite sheet electrodes.

3.3.2 Effect of electrolyte on the degradation of CHA

Since real OSPW has a relatively high alkalinity (700-1000 mg/L as $CaCO_3$), it is important to understand the impact that alkalinity might have on the degradation of NAs during anodic oxidation. To evaluate the effect of carbonate species in the electrolyte on the degradation of CHA, experiments using carbonate and phosphate buffer solutions were done at current density of 5 mA/cm^2 and pH 8 (Fig. 3.4a). As can be seen in Fig. 3.4a, the degradation of CHA was higher in phosphate buffer compared to carbonate buffer. An explanation for this can be that the carbonate buffer species (HCO_3^- and CO_3^{2-}), which are well known radical scavengers, had competed with CHA for radicals at the anode surface. In order to check this explanation, the degradation of CHA in carbonate buffer was performed at different pH (6, 8 and 10) to examine the effect of carbonate species distribution, which should impact degradation rate if they were the scavengers. As can be

seen in Fig. 3.4a, at pH 6, the scavenging effect of the carbonates buffer was less compared with that at pH 10. According to the pH-dependent distribution of carbonate species (pK_{a1} = 6. 4, pK_{a2} = 10.3), at pH 6 the species distribution of H_2CO_3/$HCO_3{}^{2-}$ is around 0.6/0.4. At pH 10, the species became 0.68/0.32 of $HCO_3{}^-$/$CO_3{}^{2-}$. As a result, a more significant scavenging effect from carbonate species is expected at pH 10 because of the introduction of $CO_3{}^{2-}$ and increase of the $HCO_3{}^-$ which are both the main scavengers with higher second order $^\bullet OH$ rate constants (3.9×10^8 M^{-1} s^{-1} and 8.5×10^6 M^{-1} s^{-1}, respectively). Therefore, the scavenging effect of the carbonate ions is clearly the reason for the reduction of CHA degradation rate in carbonate buffer (Shu et al. 2014).

To understand the effect of the chloride and sulfate anions on the degradation of CHA during anodic oxidation on graphite, NaCl and Na_2SO_4 were used as electrolytes and the degradation rates for CHA were compared under different current densities (Fig. 3.4b). As shown in Fig. 3.4b, at low current density (0.5 mA/cm^2) the degradation rate for the case of 0.05M Na_2SO_4 was more than 1.5 times higher than in the cases of 0.05M and 0.1 M NaCl electrolytes. At higher current densities (2.5 and 5 mA/cm^2), on the other hand, the rates for NaCl electrolytes were slightly higher than the rates for 0.05M Na_2SO_4. Increasing the concentration of NaCl from 0.0.5 M to 0.1 M has also resulted in slight increase in the rates. This trend can be explained by considering the generation of reactive species (active chlorine) through equations 3 and 4. The generation of persulfate is not expected when graphite anode is used as the generation of this radical is only possible by anodes that have high oxygen evolution overpotential, such as boron-doped diamond or lead dioxide (Panizza and Cerisola 2009, Comninellis and Chen 2010). The generation of chlorine, however, is well documented when graphite anode is used and graphite itself was a

standard anode for the chloroalkali process (Panizza and Cerisola 2009, Comninellis and Chen 2010, Rueffer et al. 2011). The generation of active chlorine species can explain the improvement in the degradation performance at higher current density and it can also explain the reduction in the performance at lower current density considering that the generation of chlorine can only start at anode potential of 1.6 V and in the case of existence of competitive ions at 1.81V (Zöllig et al. 2015). By checking the anode potentials during the experiments (Fig. 3.5), it can be seen that the anode potential in the case of 0.5 mA/cm^2 was 1.7 V just at the point where chlorine generation start, while the anode potentials were 2.5 and 3 V at current densities of 2.5 and 5 mA/cm^2, respectively. This means that in the case of 0.5 mA/cm^2 chlorine generation will be very inefficient and, therefore, chloride ions will actually compete with CHA at the anode surface resulting in reduced reaction rates. The generation of chlorine can also be supported by looking at the slight improvement in the rate when the concentration of NaCl increased. The degradation of CHA by active chlorine species, however, was not very effective and resulted in slight improvement in both of the cases of higher current densities. This was in agreement with what was reported before that chlorine is not effective for the degradation of NAs (Shu et al. 2014).
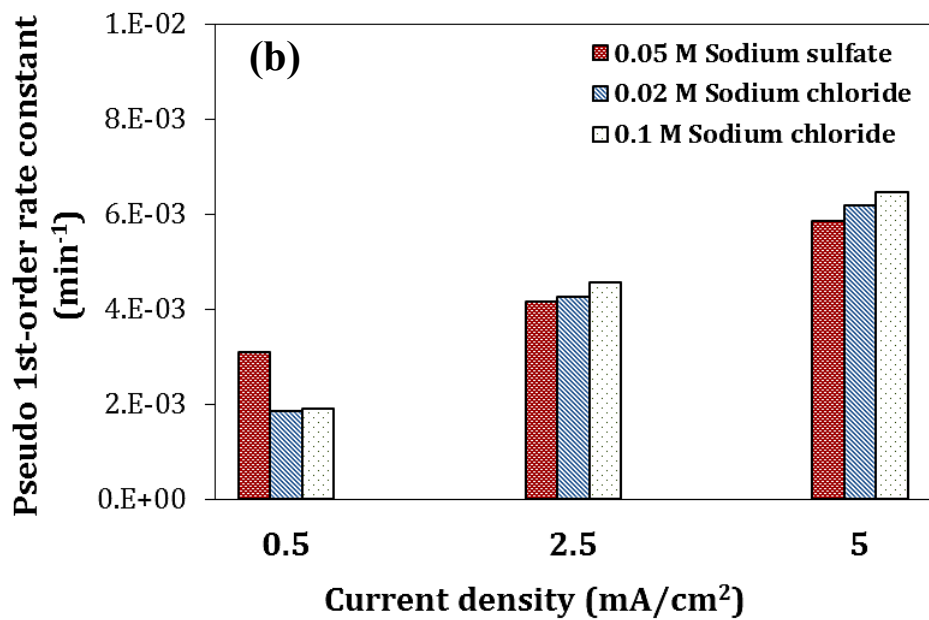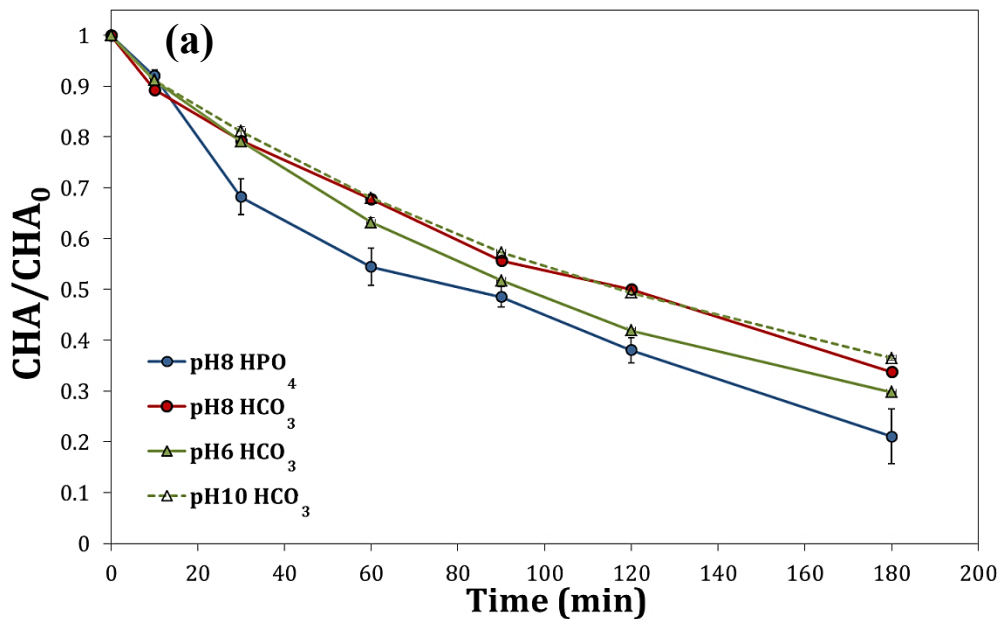
Figure 3.4 Effect of the electrolyte species on the degradation of CHA: (a)

bicarbonate and phosphate buffer (at 5 mA/cm^2); (b) chloride and sulfate anions.
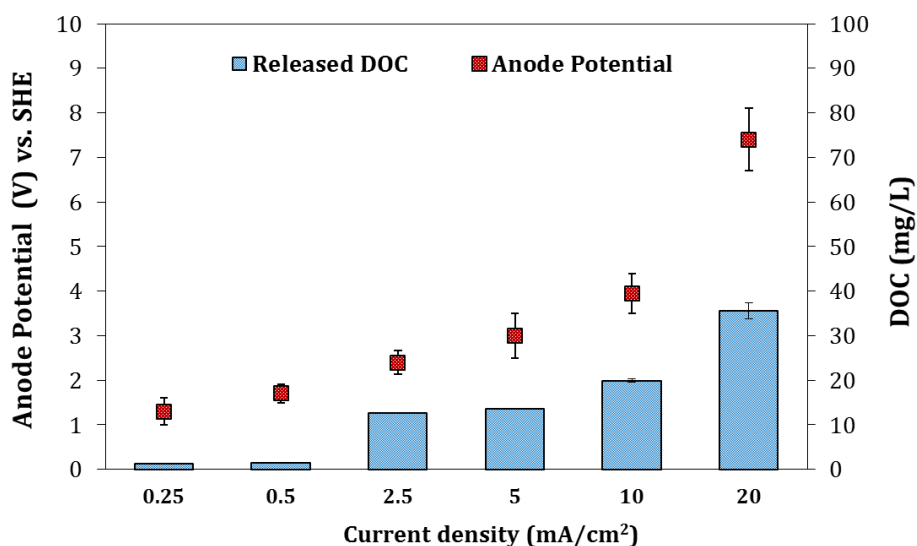
Figure 3.5 The release of DOC from anode during anodic oxidation as function of the applied anode potential.

3.3.3 Effect of applied current density on the anode corrosion

Graphite electrodes are inexpensive and can be used as 3D electrodes with large surface area which make them an attractive option for the removal of organics in electrochemical reactors (Comninellis and Chen 2010, Rueffer et al. 2011, Zöllig et al. 2015). However, the main drawback of anodic oxidation by graphite is that it is usually accompanied by surface corrosion if performed at high current densities and that not all the organic pollutants are oxidizable at low current densities where corrosion is not prevalent (Comninellis and Chen 2010, Rueffer et al. 2011, Zöllig et al. 2015). The corrosion of graphite anode during electro-oxidation was studied extensively when graphite was a standard anode for use in the chloralkali process (Rueffer et al. 2011). This study tried to examine if NAs could be degraded at current densities lower enough to avoid severe corrosion. The level of corrosion at each applied current density was evaluated by measuring the concentration of

90

the released organic carbon, a method that was used previously for this purpose (Rueffer et al. 2011, Qiao et al. 2018). In order to evaluate the release of carbon from graphite anode, control experiments similar to the experiments conducted for CHA degradation were performed by using the same electrolyte but without CHA addition. Dissolved organic carbon was measured at the end of the experiment and plotted against applied current density and anode potential (Fig. 3.5). As can be seen in Fig. 3.5, the release of carbon from anode was negligible at current densities of 0.25 and 0.5 mA/cm^2, with measured DOC level less than 2 mg/L after 180 min. The release of DOC increased starting from 2.5 mA/cm^2 and went up until reaching 35 mg/L at 20 mA/cm^2.
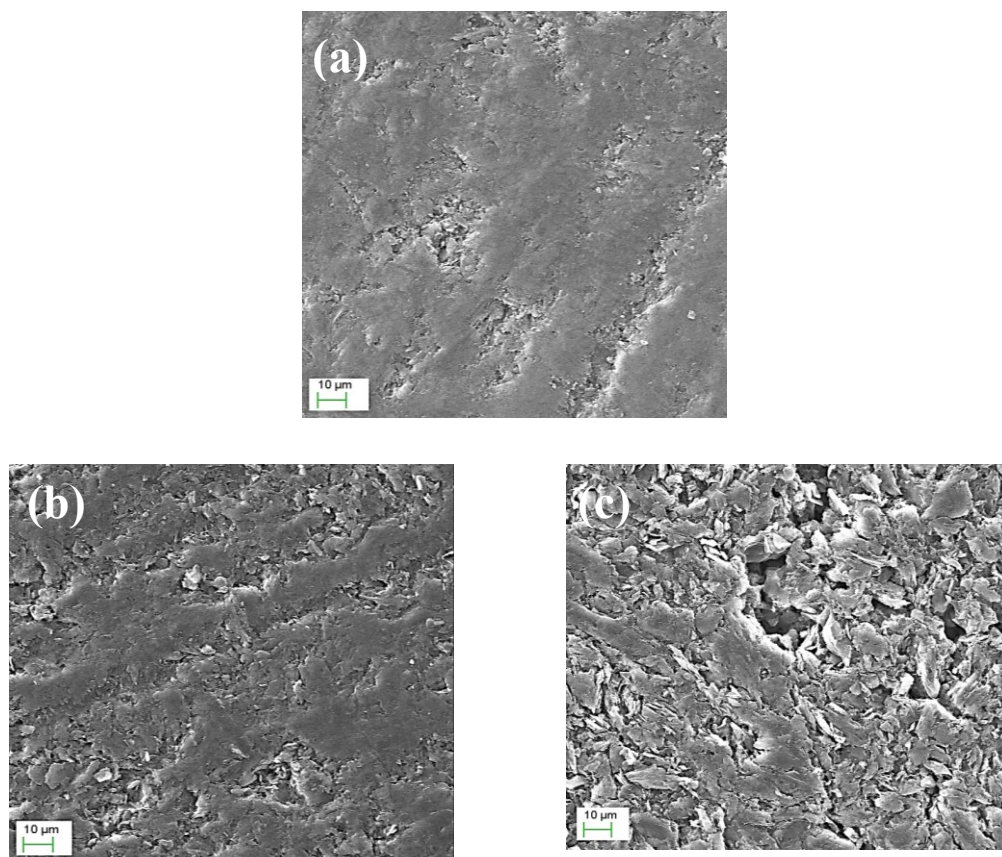
Figure 3.6 SEM images of (a) unused graphite anode and (b and c) graphite anode after 180 min of AO at current densities of 0.5 and 10 mA/cm^2, respectively.

The SEM images of the surface of new anode and the anodes after AO at 0.5 and 10 mA/cm^2 agreed with the DOC results (Fig. 3.6). The SEM images were taken for the lower section of the anodes so that it can be representative of the most severely corroded portion of the surface, if there is any non-uniformity in the corrosion, despite the fact that non-uniformity was not expected to affect due to the short time of the experiment (180 min). The image of anode surface after 180 min of AO at 0.5 mA/cm^2 (Fig. 3.6b) did not show any signs of severe corrosion compared to the new anode surface (Fig. 3.6a). At current density of 10 mA/cm^2, on the other hand, a more deeply pitted surface was observed (Fig. 3.6c) indicating a higher level of surface corrosion. At the end of the experiments, there was change in the color of the solution at current densities of 5, 10 and 20 mA/cm^2 and the color of solution got darker with increasing the applied current density indicating that corrosion has taken place. At current densities between 0.25 and 2.5 mA/cm^2, however, there was no clear change in color. At a current density of 20 mA/cm^2 small graphite particles were noticed in the solution at the end of the experiment, which indicates that graphite exfoliation has taken place at this current density. Additionally, the weight loss of the graphite anodes during electrolysis at 0.25 and 0.5 mA/cm^2 after 180 min was negligible (less than 2 ± 0.5 mg), where at current densities of 2.5 and 5, 10 and 20 mA/cm^2 the weight loss was 11, 13, 18 and 29 mg, respectively. Considering the initial weight of the graphite anodes was 10 ± 1 g, the weight loss recorded in this study could be considered negligible, even at higher current density. Qiao et al. (Qiao et al. 2018) have recently reported that the degradation of surface and release of carbon during AO start at an anode potential of 1.34 V vs. SHE. The pH at which the oxidation occurs was found to play great role in the anode corrosion (Rueffer et al. 2011, Qiao et al. 2018). By looking at the applied

anode potential in Fig. 3.5, it can be seen clearly that the anode potential at current density of 0.25 mA/cm^2 was 1.3V just below the corrosion limiting potential. At 0.5 mA/cm^2 the anode potential was slightly higher than the reported corrosion current density, however, if take into account that the pH during the experiment was 8.5 which is higher than pH of 7 reported by Qiao et al. (Qiao et al. 2018), and by considering that the increase in pH was reported to reduce the corrosion of anode (Rueffer et al. 2011, Qiao et al. 2018) this can explain the negligible corrosion at this current density. These results can be used as an indicator that the degradation of NAs by anodic oxidation on graphite can be performed at current density lower enough to avoid any severe corrosion of anode. It has to be noted that some of the constituents of OSPW (organics and inorganics) might also have a long term corrosive impact on the anode material. However, such corrosion can only occur over an extended periods of time, and investigating such type of corrosion was beyond the focus of this research.

3.3.4 Oxidation mechanisms on graphite anode

The old classical view of electro-oxidation was that it involves the transfer of electron directly from the substrate to the anode or what is known as DET (Panizza and Cerisola 2009, Comninellis and Chen 2010, Rueffer et al. 2011). However, electro-oxidation in water is always associated with the oxidation of water molecules and generation of oxidants (Eqs. (3.1)-(3.4)). Hydroxyl radicals generation, whether physisorbed or chemosorbed, was believed to be the major mechanism for electro-oxidation of pollutants (Martinez-Huitle and Ferro 2006, Panizza and Cerisola 2009, Comninellis and Chen 2010, Chaplin 2014, Sirés et al. 2014, Martínez-Huitle et al. 2015, Moreira et al. 2017). The degradation of organics by the hydroxyl radicals generated from the water discharge during AO is

inevitably accompanied with the undesired side reaction of oxygen evolution which results in reducing the degradation efficiency (Panizza and Cerisola 2009, Comninellis and Chen 2010, Chaplin 2014, Moreira et al. 2017). This parasitic oxygen generation results from the anodic decomposition of the generated hydroxyl radicals as shown by Eq. (3.6) (Panizza and Cerisola 2009, Comninellis and Chen 2010, Rueffer et al. 2011):

$$2M(\bullet OH) \rightarrow 2M + O_2\uparrow + 2H^+ + 2e^- \qquad\qquad (3.6)$$

The generation of oxygen during EO is also related to the nature of anode material. Active anodes generally have lower oxygen evolution potentials compared to inactive anodes (Panizza and Cerisola 2009, Comninellis and Chen 2010, Chaplin 2014, Moreira et al. 2017). Graphite has been widely classified as active anode material that has low oxygen evolution over-potential and low capacity for pollution mineralization due to the limitation of generating physisorbed hydroxyl radicals (Panizza and Cerisola 2009, Comninellis and Chen 2010, Chaplin 2014, Moreira et al. 2017). DET by graphite anode was also reported as main oxidation mechanism for some pollutants below the water discharge potential (Zöllig et al. 2015). Indirect oxidation through the generation of reactive chlorine species by graphite anodes was also a reported mechanism (Panizza and Cerisola 2009, Comninellis and Chen 2010, Rueffer et al. 2011, Chaplin 2014, Moreira et al. 2017). The role of generated chlorine was already discussed in section 3.3.2. Chlorine, if generated, will have a minor positive contribution on the degradation of CHA, as discussed earlier, but it will not be the main mechanism. The limited ability of chlorine to degrade OSPW's NAs and CHA was reported before (Chan et al. 2012, Shu et al. 2014). In addition to that, by taking into account the relatively lower concentration of Cl^- ions used during the first set of experiments (0.015 M) (Fig. 3.1) compared to the concentration used during the second set

94

of experiments (0.05 and 0.1M) (Fig. 3.2b), chlorine generation is not expected to be a main contributor to the oxidation of CHA.

In order to understand the contribution of different oxidation mechanisms in the degradation of NAs by AO on graphite anode, the degradation of CHA was studied under different conditions and with the addition of different radical scavengers (Fig. 3.7). To see if DET was a contributing mechanism for CHA degradation, the degradation of CHA was performed at a fixed voltage below the water oxidation potential (Fig. 3.7). At fixed anode potential (0.85 V), below the water oxidation and oxygen evolution potential by graphite anode, there was no removal of CHA indicating that DET is not a mechanism for the oxidation of CHA on graphite anode (Fig. 3.7). This was also supported by the cyclic voltammograms (Fig. 3.8) which did not show any oxidation peak for CHA in the water stability region. This was expected, since only very few pollutants were reported to be oxidizable by direct electron transfer on graphite (Comninellis and Chen 2010, Zöllig et al. 2015).
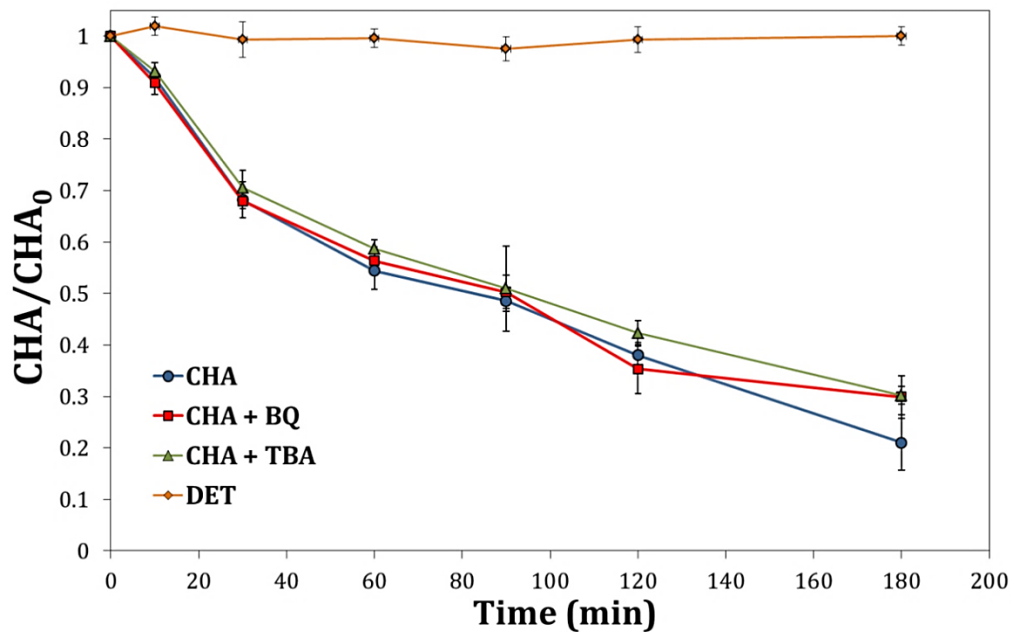
Figure 3.7 Effect of the addition of ˙OH radical probes (5 mM) and direct electron transfer mechanism on the decay of normalized CHA concentration vs. electrolysis time during the anodic-oxidation of 50 mg/L CHA solution at 5 mA/cm^2 and pH 8 using graphite sheet electrodes.
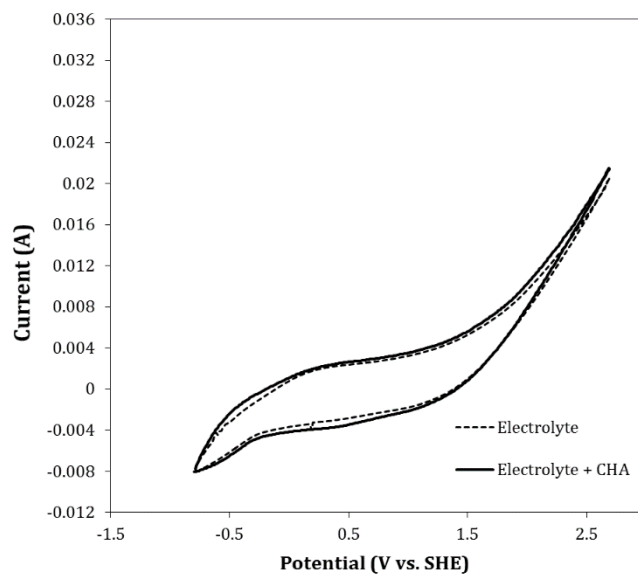
Figure 3.8 Cyclic voltammograms obtained at graphite anode for (10 mM) NaClO$_4$ electrolyte and (Electrolyte + 0.5 g/L CHA) at 20 mV/s fixed sweep rate.

To investigate the role of free $^\bullet$OH in the degradation of CHA during anodic oxidation by graphite, tert-Butyl alcohol (TBA) was chosen as a non-selective radical scavenger. TBA can react with both physisorbed (free) and chemosorbed $^\bullet$OH radicals at rates $6.0 \times 10^8\,M^{-1}\,s^{-1}$ and $10^5\,M^{-1}\,s^{-1}$, respectively (George 1988). 1,4 Benzoquinone (BQ), on the other hand, was selected as a selective radical scavenger that can react quickly with free $^\bullet$OH radicals $(6.6 \times 10^9\,M^{-1}\,s^{-1})$ and resist the degradation by chemosorbed $^\bullet$OH radicals generated during electro-oxidation by active anodes (Schuchmann et al. 1998). As can be seen in Fig. 3.7, the addition of 5 mM TBA, an amount that is enough to scavenge radicals and reduce the rate without causing severe fouling to the surface of anode, did not result in any reduction in the degradation rate of CHA. This clearly indicates the absence of the generation of physisorbed (free) •OH radicals during electro-oxidation with graphite anode, a behaviour that was expected due to the fact that graphite is classified as an active anode material that cannot generate free $^\bullet$OH radicals (Panizza and Cerisola 2009, Comninellis and Chen 2010). The addition of BQ, on the other hand, was expected to result in the reduction of the degradation rate for CHA, since BQ is a known scavengers for radicals that are generated by inactive electrodes (Schuchmann et al. 1998, Rueffer et al. 2011) and graphite is classified as an active anode material (Panizza and Cerisola 2009, Comninellis and Chen 2010, Chaplin 2014, Moreira et al. 2017). However, the results were totally different as the addition of BQ did not impact the degradation rate of CHA. This indicated that the degradation of CHA on graphite did not occur through the generated chemisorbed $^\bullet$OH radicals and that graphite did not generate the same radicals as the other active metallic anodes such as Pt and DSA. This conclusion was supported by an investigation done by Rueffer et al. (Rueffer et al. 2011) who pointed out that graphite does not behave neither

97

like metallic active anode nor like inactive anode. The researchers found that the oxidation behaviour on graphite anode involved oxygenated functional groups bonded to the previously oxidized anode surface and not directly to carbon atoms, which behaved differently than those generated on metallic active and inactive anodes (Panizza and Cerisola 2009, Rueffer et al. 2011). XPS analysis was conducted to examine the existence of such oxygenated functional groups on the surface of graphite anode. Fig. 3.9a and 3.9b show the C1s XPS spectrum for graphite anode before and after AO, respectively. The spectrum for the unused graphite anode shows a main peak at 284.2 and a small one at 286.5 (Fig. 3.9a). The spectrum for the anode after 180 min of AO shows four peaks which are located at 284.2, 286.5, 287.5, and 288.7 eV, respectively, as shown in Fig. 3.9b. Generally, the main peak (in both cases) at around 284.2 eV corresponds to graphitic carbon (graphitic C=C and C-C), the peak around 286.5 eV is attributed to the carbon in C–OH group, the peak around 287.5 eV belongs the carbon in the C=O group, and the peak at 288.7 eV corresponds to the carbon in COOH groups (Yue et al. 1999, Miao et al. 2014, Qiao et al. 2018). Details about the relative content of each functional group are listed in Table 3.2 It is clear from Fig. 3.9 and Table 3.2 that the relative content of oxygen-containing groups (COH, CO, and COOH) increased significantly and that the graphite anode display less graphitic character after it was subjected to AO.
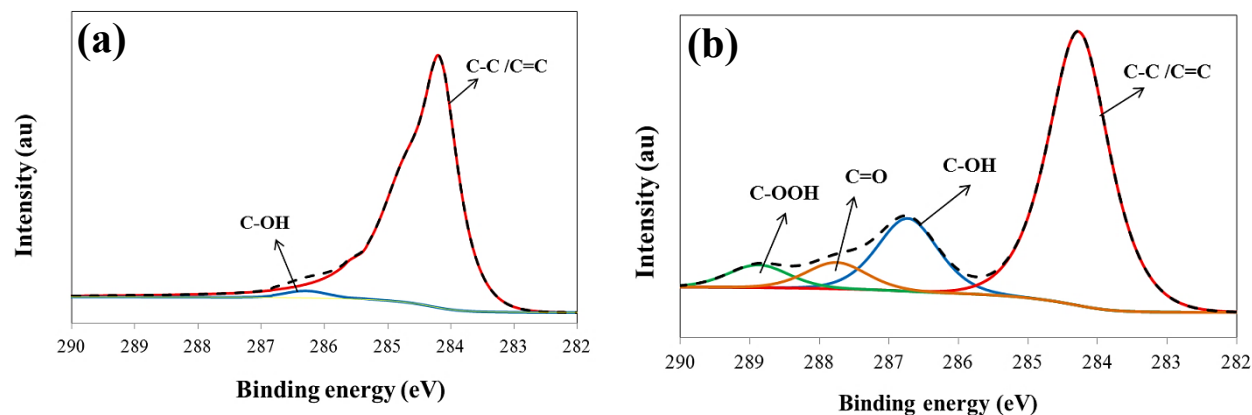
Figure 3.9 C1s XPS spectra of (a) new graphite electrode and (b) graphite anode after 180 min of AO at a current density of 5 mA/cm^2 (electrolyte medium: 1.5 g/L NaHCO$_3$, 0.9 g/L NaCl and 0.65 g/L Na$_2$SO$_4$).

Table 3.2 The relative content of different functional-groups on the surface of graphite anode before and after AO.

Peak	Functional groups	Unused anode	Anode after AO
C1s	C=C/C-C	98.2	76.2
	C-OH	1.8	12.6
	C=O	-	6.4
	COOH	-	4.8

The results obtained from the XPS analysis (Fig.3.9) and the use of radicals scavengers TBA and BQ (Fig. 3.7) were in agreement with the view of Rueffer et al. (Rueffer et al. 2011). Therefore, the oxidation of CHA by AO on graphite anode is expected to occur through oxygenated species generated on the surface of graphite anode and not through chemosorbed (high metal oxides) or physisorbed hydroxyl radicals.

99

3.3.5 Structure-reactivity relationship

CHA, as a simple model NA compound, was used in the previous parts to investigate the degradation of NAs during AO by graphite. Real OSPW, however, contains many different NAs with more complicated molecular structures. It was found that the molecular structure of NAs is strongly connected with their oxidation resistance, biodegradability and toxicity. Therefore, it is wise to understand the structure–based selectivity of any process proposed for OSPW treatment and NAs degradation. In order to understand the relationship between the molecular structures and reactivity during AO on graphite anode, different model NA compounds (Table 3.1) that have different structures were electro-oxidized using graphite anode and the degradation rates were compared.

3.3.5.1 Effect of carbon number

The degradation of two linear NA compounds was compared to determine the effect of carbon number on the susceptibility toward anodic oxidation on graphite anode (Fig. 3.10a). An increase by one carbon atom in the structure was shown to result in an increase in the degradation rate by 1.181. The same phenomenon was also observes in the case of cyclic NAs (Fig. 3.10b). An increase by one carbon atom in case of cyclic NAs resulted in an increase by 1.109 in the degradation rate. These findings agreed with what was reported for other AOPs and it can be attributed to the increase in the number of oxidation sites and number of hydrogen atoms available for abstraction (Pérez-Estrada et al. 2011, Afzal et al. 2012b, Wang et al. 2016a, de Oliveira Livera et al. 2018). Since ring-opening is not a required for linear NAs degradation, the increase in the reaction rate due to increase in the carbon number was higher than in the case monocyclic NAs (1.181 and 1.109, respectively). The same trend was also reported during photocatalytic degradation of NAs (de Oliveira

Livera et al. 2018). It was reported that NAs with more carbons tend to be more hydrophobic and, therefore, can be more toxic (Afzal et al. 2012b). This could be a positive indicator that AO by graphite anode can selectively degrade the relatively more toxic compounds in OSPW.

3.3.5.2 Effect of alkyl branching and tertiary carbon location

Alkyl branching has shown to have a negative effect on the reactivity of organic compounds towards ˙OH radicals, but this effect decreases with increasing branch distance from the carboxylate functional group (Afzal et al. 2012b). To investigate the effect of alkyl branching on the reactivity of NAs toward AO on graphite anode, the degradation of three isomers NA compounds was investigated and compared: linear octanoic acid (OCA) and two methyl substituted heptanoic acids (2mHPA and 4mHPA) were compared (Fig. 3.10c and 3.10d). The α-substituted 2mHPA was clearly less reactive than linear OCA (*slope* = 0.924) (Fig. 3.10c). On the other hand, 4mHPA was significantly more reactive than OCA (*slope* = 1.245) (Fig. 3.10d). This trend can be explained by looking into the stability of the generated intermediate species from the oxidation of those NAs. It was found that the reactivity of carboxylic acids toward oxidation depends on the stability of the intermediate organic radicals resulting from the abstraction of hydrogen. The more stable the intermediate, the more reactive the acid (Hewgill and Proudfoot 1976, Afzal et al. 2012b). By adding an alkyl branch to the molecular structure of the linear acid, a tertiary carbon will be introduced. Compared to primary and secondary carbons, tertiary carbon-centered radicals are more stable (Anbar et al. 1966). Therefore, the rate is expected to increase with the introduction of alkyl branching. However, the distance of the tertiary carbon from the carboxylate group can also play important role in the stability of the intermediate radicals.

It was reported that the presence of a carboxylate group can result in a clear reduction in the reactivity of the hydrogen atoms at α position due to its electron-withdrawing capacity (Hewgill and Proudfoot 1976, de Oliveira Livera et al. 2018). This can explain the reduction in the reactivity in the case of 2mHPA. Similar results were obtained by using ozone and UV/H_2O_2 AOPs (Pérez-Estrada et al. 2011, Afzal et al. 2012b). The biodegradability of NAs was also found to be strongly hindered by the addition of side branching (Scott et al. 2005, Han et al. 2008, Misiti et al. 2014). Therefore, our results here can be considered as an indicator that anodic oxidation by graphite will be able to selectively degrade the recalcitrant part in OSPW and improve the biodegradability.

3.3.5.3 Effect of cyclicity

The effect of cyclicity on the reactivity of NAs during AO by graphite anode was studied by comparing the degradation of different linear, monocyclic and polycyclic model NA compounds. Linear HPA was compared to monocyclic CHA (Fig. 3.11a). Both of the compounds have the same carbon numbers. As can be clearly seen in Fig. 3.11a, monocyclic CHA was significantly more reactive than linear heptanoic acid (HPA) with a slope of more than 1.345. In order to deeply understand this high reactivity toward cyclic compounds, another two compounds were compared. OCA was compared with monocyclic 4mCHA (Fig. 3.11b), both had the same carbon number. The result was also similar to the previous one and 4mCHA was significantly more reactive than OCA (*slope* = 1.263). The reason for this higher reactivity probably lies in the introduction of tertiary carbon in both of the cyclic cases. The reactivity of H atoms on these tertiary carbons is higher than the reactivity of H atoms on primary and secondary carbons in linear compounds. This, as explained in the previous section, can result in higher reactivity during oxidation. The result

is even more impressive in that both of the linear NAs had 2 more hydrogen atoms in their structures, yet they were less reactive than their monocyclic counterparts. The same trend of reactivity toward cyclic compounds was found during the oxidation of NAs by using ozonation, UV/H_2O_2 and photo-catalysis (Pérez-Estrada et al. 2011, Afzal et al. 2012b, de Oliveira Livera et al. 2018).

In order to examine the effect of poly-cyclicity on the reactivity of NAs, the degradation of monocyclic trans-4- pentylcyclohexane carboxylic acid (TPCA) was compared with bicyclic dicyclohexylacetic acid (DCHA) and tricyclic 1-adamantaneacetic acid (AAA). Contrary to the comparison of linear and monocyclic NAs, it was shown that monocyclic TPCA was more reactive than bicyclic DCHA (Fig. 3.11c) despite the fact that DCHA has more carbons and hydrogen atoms than TPCA (Table 3.1). On the other hand, tricyclic 1-adamantaneacetic acid (AAA) was even significantly less reactive than monocyclic TPCA (Fig. 3.11d), despite the fact that AAA has three tertiary carbons in comparison with two tertiary carbons in the case of TPCA. This indicates a clear trend of decreasing reactivity with increase in the number of rings beyond one ring. A possible explanation for that can be that the polycyclic structures can imposes barriers toward the formation of the carbon-centered intermediate radical at the tertiary carbon locations (Anbar et al. 1966). Another important factor that might explain this phenomenon is by considering that the energies of adamantyl tertiary C–H bonds (such as in AAA) are similar to the energy of a secondary C–H bond in an unstrained molecule (Kruppa and Beauchamp 1986). These results are different from the results obtained by using ozonation for NAs degradation (Pérez-Estrada et al. 2011) but it agrees with that obtained by using UV/H_2O_2 (Afzal et al. 2012b). This

103

might indicate that the radicals generated by graphite anode, although they are not hydroxyl radicals, but they behave closer to hydroxyl radicals rather than ozone.
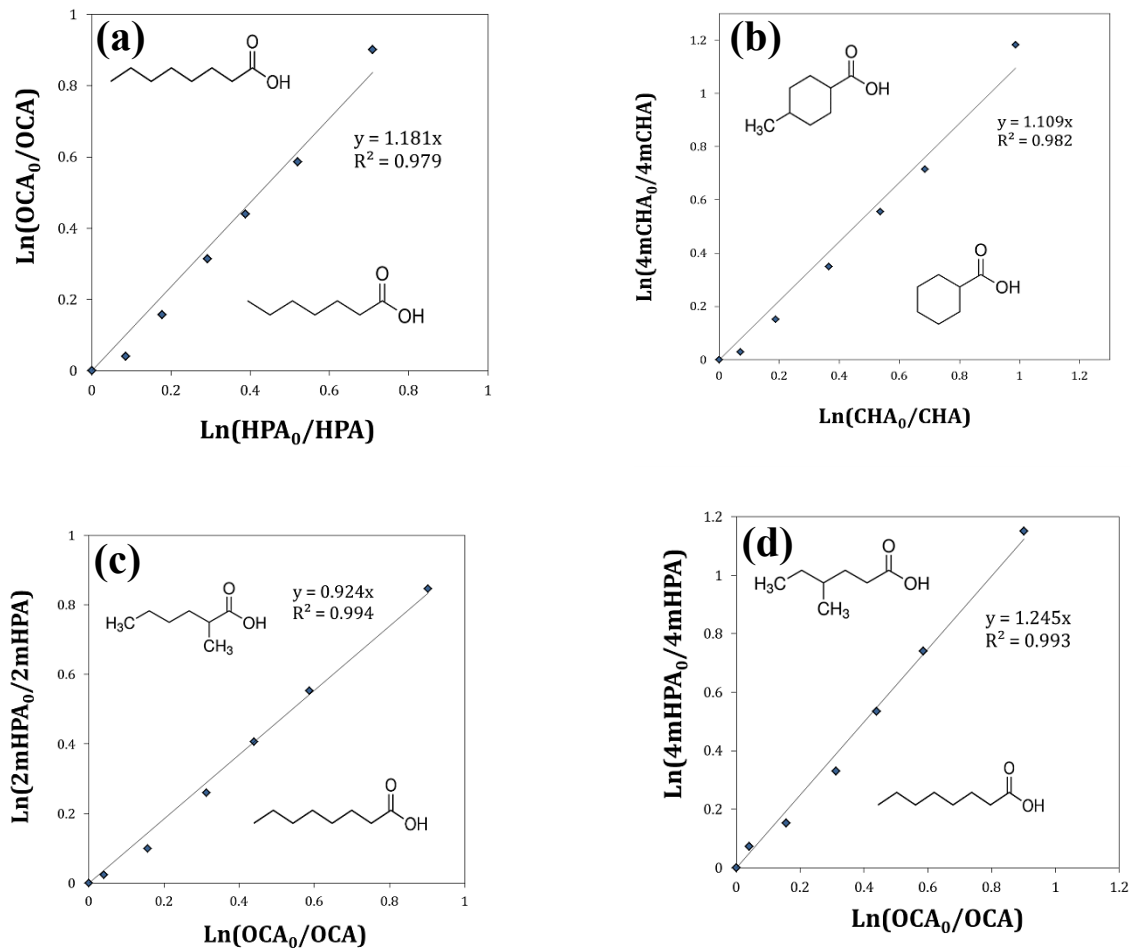
Figure 3.10 Relative kinetics for model NA compounds during anodic oxidation at fixed current density of 5 mA/cm^2 and pH 8 to examine the effect of (a and b) carbon number and (c and d) alkyl branching.
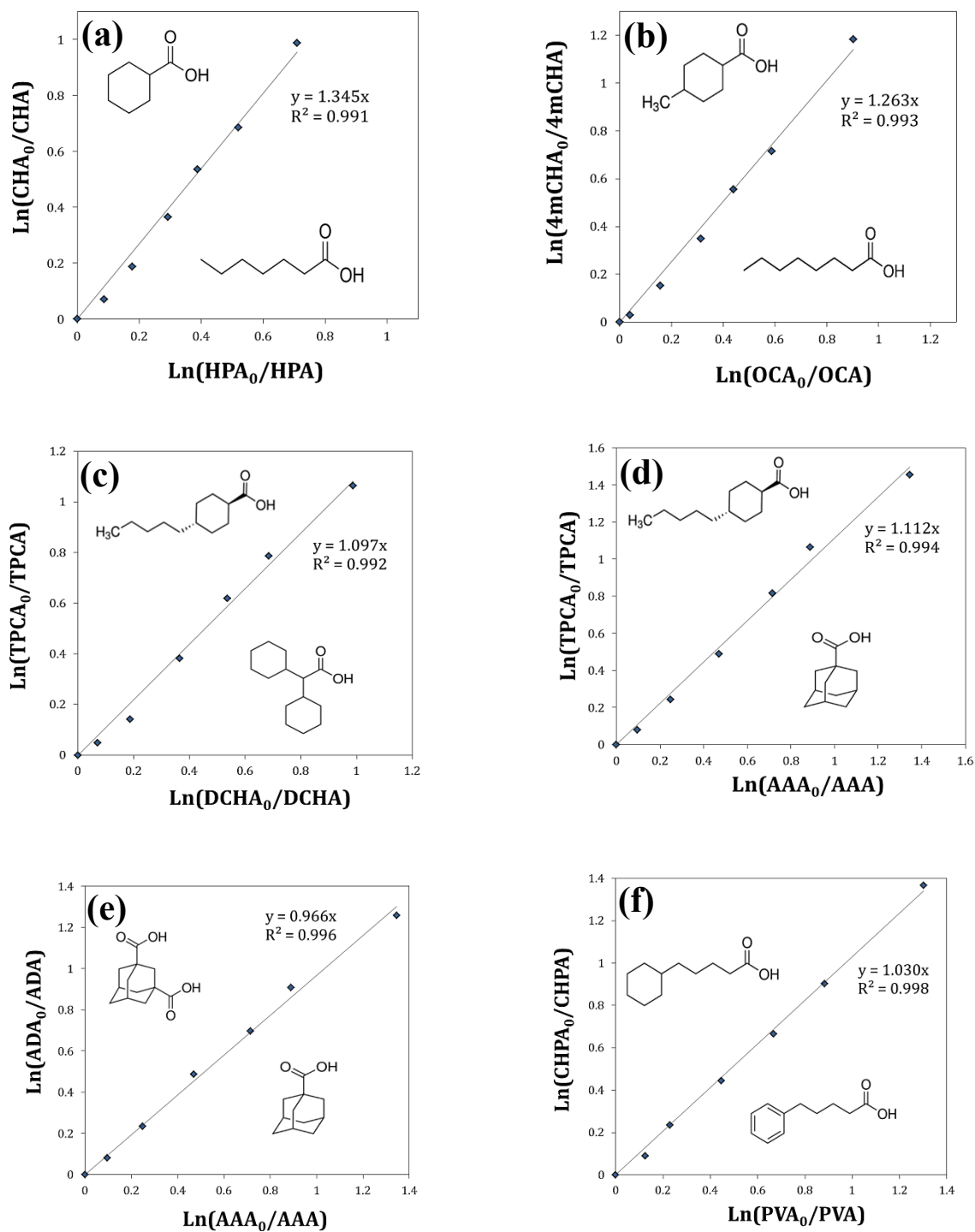
Figure 3.11 Relative kinetics for model NA compounds during anodic oxidation at fixed current density of 5 mA/cm^2 and pH 8 to examine the effect of (a, b, c and d) cyclicity, (e) multiple-carboxylate groups and (f) ring saturation.

3.3.5.4 Effect of multiple-carboxylate and ring saturation

To study the effect of multiple carboxylate group on the reactivity of NAs during AO, the tricyclic 1-adamantaneacetic acid (AAA) was compared with a similar tricyclic 1,3-adamantanedicarboxylic acid (ADA) that has exactly the same structure but with one more carboxylate group (Fig. 3.11e). As can be seen from Fig. 3.11e, the introduction of additional carboxylate group has resulted in a clear reduction in the reactivity during AO with graphite anode. This can be explained by considering three factors: (i) the addition of carboxylate group in the diamond structure of ADA resulted in the introduction of quaternary carbon that has no H atoms for abstraction in the place of a tertiary carbon that has a very reactive H atom which means less reactivity; (ii) ADA has two less hydrogens in its structure compared to AAA and, therefore, it is normal to be less reactive; and (iii) similar to what discussed in section 3.5.2, the presence of an electron-withdrawing group such as a carboxylic group (COOH) can decrease the rate of abstraction from the C–H bond at α position (Minakata et al. 2009). Therefore, the addition of another carboxylic group will lead to more reduction in the total reactivity.

The effect of the ring saturation on the reactivity of NA compounds was also investigated by comparing aliphatic monocyclic 5-cyclohexanepentanoic acid (CHPA) with aromatic monocyclic 5-phenylvaleric acid (PVA) (Fig. 3.11f). The two compounds have a similar structures and carbon numbers with the ring saturation being the only difference. As shown in Fig. 3.11f, the aromatic ring was slightly less reactive than the aliphatic ring. This observation was not expected due to the fact that the aromatic ring has 4 more tertiary carbons than in the aliphatic ring and, therefore, PVA was expected to be more reactive than CHPA. This unexpected trend, however, can be explained by the stability that the

106

conjugated double bond systems can offers, which can reduce the rate of electron transfer reactions (de Oliveira Livera et al. 2018). Other possible explanations can be by the fact that CHPA has 6 more hydrogens than PVA and that PVA has one quaternary (non-reactive) carbon.

3.4 Conclusions

In this study, the degradation of different model NAs compounds during AO on graphite anode was investigated. The degradation of CHA increased with increasing the applied current density and followed clear pseudo first-order kinetics. Carbonate species in the electrolyte medium had scavenging effect on the degradation rate. Chloride and sulfate ions had a minor role in the degradation of CHA. DET mechanism had no contribution in the degradation of CHA. Graphite was found to behave differently from both, active and inactive anodes in terms of the type of oxidants generated on the surface of anode. It was found that the main degradation mechanism for CHA during anodic oxidation by graphite anode was through the generation of oxygenated functional groups at the anode surface. The findings of the structure-reactivity study showed that NAs with higher number of carbons were preferentially degraded by AO. Branched NAs were more reactive than non-branched NAs only if the branch existed far enough from the carboxylate group. It was found that monocyclic NAs were more reactive than linear NAs but any increase in the cyclicity beyond one ring resulted in reduced reactivity. Aliphatic NA compounds were found to be more reactive during AO than aromatic compounds and the existence of more than one carboxylate group in the structure reduced the reactivity. The kinetics and structure-reactivity analysis have shown that AO by graphite can be an attractive option for OSPW treatment and biodegradability enhancement. The application of AO using graphite

107

in combination with biotransformation is currently being studied in our laboratory as a potential OSPW reclamation technique.

3.5 References

Afzal, A., P. Chelme-Ayala, P. Drzewicz, J. W. Martin, and M. Gamal El-Din. 2015. Effects of ozone and ozone/hydrogen peroxide on the degradation of model and real oil-sands-process-affected-water naphthenic acids. Ozone: Science & Engineering **37**:45-54.

Afzal, A., P. Drzewicz, J. W. Martin, and M. Gamal El-Din. 2012a. Decomposition of cyclohexanoic acid by the UV/H2O2 process under various conditions. Science of the Total Environment **426**:387-392.

Afzal, A., P. Drzewicz, L. n. A. Pérez-Estrada, Y. Chen, J. W. Martin, and M. Gamal El-Din. 2012b. Effect of molecular structure on the relative reactivity of naphthenic acids in the UV/H2O2 advanced oxidation process. Environmental science & technology **46**:10727-10734.

Allen, E. W. 2008. Process water treatment in Canada's oil sands industry: I. Target pollutants and treatment objectives. Journal of Environmental Engineering and Science **7**:123-138.

Anbar, M., D. Meyerstein, and P. Neta. 1966. Reactivity of aliphatic compounds towards hydroxyl radicals. Journal of the Chemical Society B: Physical Organic:742-747.

Brown, L. D. and A. C. Ulrich. 2015. Oil sands naphthenic acids: a review of properties, measurement, and treatment. Chemosphere **127**:276-290.

Chan, P. Y., M. Gamal El-Din, and J. R. Bolton. 2012. A solar-driven UV/Chlorine advanced oxidation process. Water research **46**:5672-5682.

Chaplin, B. P. 2014. Critical review of electrochemical advanced oxidation processes for water treatment applications. Environmental Science: Processes & Impacts **16**:1182-1203.

Comninellis, C. and G. Chen. 2010. Electrochemistry for the Environment. Springer.

de Oliveira Livera, D., T. Leshuk, K. M. Peru, J. V. Headley, and F. Gu. 2018. Structure-reactivity relationship of naphthenic acids in the photocatalytic degradation process. Chemosphere **200**:180-190.

Drzewicz, P., L. Perez-Estrada, A. Alpatova, J. W. Martin, and M. Gamal El-Din. 2012. Impact of peroxydisulfate in the presence of zero valent iron on the oxidation of cyclohexanoic acid and naphthenic acids from oil sands process-affected water. Environmental science & technology **46**:8984-8991.

Energy, A. 2013. reality check on the shale revolution Hughes, J. David. Nature (London, United Kingdom) **494**:307-308.

Fockedey, E. and A. Van Lierde. 2002. Coupling of anodic and cathodic reactions for phenol electro-oxidation using three-dimensional electrodes. Water research **36**:4169-4175.

George, V. 1988. Critical review of rate constants for reactions of hydrated electrons, hydrogen atoms and hydroxyl radicals (OH/O) in an aqueous solution. J. Phys. Chem. Ref. Data **17**:513-886.

Hagen, M. O., E. Garcia-Garcia, A. Oladiran, M. Karpman, S. Mitchell, M. G. El-Din, J. W. Martin, and M. Belosevic. 2012. The acute and sub-chronic exposures of goldfish to naphthenic acids induce different host defense responses. Aquatic toxicology **109**:143-149.

Han, X., A. C. Scott, P. M. Fedorak, M. Bataineh, and J. W. Martin. 2008. Influence of molecular structure on the biodegradability of naphthenic acids. Environmental science & technology **42**:1290-1295.

Hastie, J., D. Bejan, and N. J. Bunce. 2011. Oxidation of sulfide ion in synthetic geothermal brines at carbon‑based anodes. The Canadian Journal of Chemical Engineering **89**:948-957.

Hewgill, F. R. and G. M. Proudfoot. 1976. Regioselective oxidation of aliphatic acids by complexed hydroxyl radicals. Australian Journal of Chemistry **29**:637-647.

Jones, D., A. G. Scarlett, C. E. West, and S. J. Rowland. 2011. Toxicity of individual naphthenic acids to Vibrio fischeri. Environmental science & technology **45**:9776-9782.

Kannel, P. R. and T. Y. Gan. 2012. Naphthenic acids degradation and toxicity mitigation in tailings wastewater systems and aquatic environments: a review. Journal of Environmental Science and Health, Part A **47**:1-21.

Kim, E.-S., Y. Liu, and M. Gamal El-Din. 2012. Evaluation of membrane fouling for in-line filtration of oil sands process-affected water: the effects of pretreatment conditions. Environmental science & technology **46**:2877-2884.

Kruppa, G. H. and J. Beauchamp. 1986. Energetics and structure of the 1-and 2-adamantyl radicals and their corresponding carbonium ions by photoelectron spectroscopy. Journal of the American Chemical Society **108**:2162-2169.

Li, C., L. Fu, J. Stafford, M. Belosevic, and M. Gamal El-Din. 2017. The toxicity of oil sands process-affected water (OSPW): a critical review. Science of the Total Environment **601**:1785-1802.

Martin, J. W., T. Barri, X. Han, P. M. Fedorak, M. Gamal El-Din, L. Perez, A. C. Scott, and J. T. Jiang. 2010. Ozonation of oil sands process-affected water accelerates microbial bioremediation. Environmental science & technology **44**:8350-8356.

Martinez-Huitle, C. A. and S. Ferro. 2006. Electrochemical oxidation of organic pollutants for the wastewater treatment: direct and indirect processes. Chemical Society Reviews **35**:1324-1340.

Martínez-Huitle, C. A., M. A. Rodrigo, I. Sirés, and O. Scialdone. 2015. Single and coupled electrochemical processes and reactors for the abatement of organic water pollutants: a critical review. Chemical reviews **115**:13362-13407.

Masliyah, J., Z. J. Zhou, Z. Xu, J. Czarnecki, and H. Hamza. 2004. Understanding water-based bitumen extraction from Athabasca oil sands. The Canadian Journal of Chemical Engineering **82**:628-654.

Meshref, M. N., P. Chelme-Ayala, and M. Gamal El-Din. 2017. Fate and abundance of classical and heteroatomic naphthenic acid species after advanced oxidation

processes: Insights and indicators of transformation and degradation. Water research **125**:62-71.

Miao, J., H. Zhu, Y. Tang, Y. Chen, and P. Wan. 2014. Graphite felt electrochemically modified in H2SO4 solution used as a cathode to produce H2O2 for pre-oxidation of drinking water. Chemical Engineering Journal **250**:312-318.

Minakata, D., K. Li, P. Westerhoff, and J. Crittenden. 2009. Development of a group contribution method to predict aqueous phase hydroxyl radical (HO•) reaction rate constants. Environmental science & technology **43**:6220-6227.

Misiti, T. M., U. Tezel, and S. G. Pavlostathis. 2014. Effect of alkyl side chain location and cyclicity on the aerobic biotransformation of naphthenic acids. Environmental science & technology **48**:7909-7917.

Moreira, F. C., R. A. Boaventura, E. Brillas, and V. J. Vilar. 2017. Electrochemical advanced oxidation processes: a review on their application to synthetic and real wastewaters. Applied Catalysis B: Environmental **202**:217-261.

Operators, O. S. M. 2015. Water Allocation and Water Use by Year; OSIP Data Library; Government of Alberta.

Panizza, M. and G. Cerisola. 2009. Direct and mediated anodic oxidation of organic pollutants. Chemical reviews **109**:6541-6569.

Pérez-Estrada, L. A., X. Han, P. Drzewicz, M. Gamal El-Din, P. M. Fedorak, and J. W. Martin. 2011. Structure–reactivity of naphthenic acids in the ozonation process. Environmental science & technology **45**:7431-7437.

Qiao, M.-X., Y. Zhang, L.-F. Zhai, and M. Sun. 2018. Corrosion of graphite electrode in electrochemical advanced oxidation processes: Degradation protocol and environmental implication. Chemical Engineering Journal **344**:410-418.

Quinlan, P. J. and K. C. Tam. 2015. Water treatment technologies for the remediation of naphthenic acids in oil sands process-affected water. Chemical Engineering Journal **279**:696-714.

Regulator, A. E. 2014. Alberta's energy reserves 2011 and supply/demand outlook 2012–2021. ST98-2012. ISSN 1910-4235. Alberta Energy Regulator Calgary, Canada.

Rowland, S. J., A. G. Scarlett, D. Jones, C. E. West, and R. A. Frank. 2011. Diamonds in the rough: identification of individual naphthenic acids in oil sands process water. Environmental science & technology **45**:3154-3159.

Rueffer, M., D. Bejan, and N. J. Bunce. 2011. Graphite: An active or an inactive anode? Electrochimica Acta **56**:2246-2253.

Schuchmann, M. N., E. Bothe, J. von Sonntag, and C. von Sonntag. 1998. Reaction of OH radicals with benzoquinone in aqueous solutions. A pulse radiolysis study. Journal of the Chemical Society, Perkin Transactions 2:791-796.

Scott, A. C., M. D. Mackinnon, and P. M. Fedorak. 2005. Naphthenic acids in Athabasca oil sands tailings waters are less biodegradable than commercial naphthenic acids. Environmental science & technology **39**:8388-8394.

Shu, Z., C. Li, M. Belosevic, J. R. Bolton, and M. Gamal El-Din. 2014. Application of a solar UV/chlorine advanced oxidation process to oil sands process-affected water remediation. Environmental science & technology **48**:9692-9701.

Sirés, I., E. Brillas, M. A. Oturan, M. A. Rodrigo, and M. Panizza. 2014. Electrochemical advanced oxidation processes: today and tomorrow. A review. Environmental Science and Pollution Research **21**:8336-8367.

Verbeek, A., W. Mackay, and M. MacKinnon. 1989. A toxicity assessment of oil sands wastewater: a toxic balance. Can. Tech. Rep. Fish. Aquat. Sci:196-207.

Wang, C., A. Alpatova, K. N. McPhedran, and M. G. El-Din. 2015. Coagulation/flocculation process with polyaluminum chloride for the remediation of oil sands process-affected water: Performance and mechanism study. Journal of environmental management **160**:254-262.

Wang, C., N. Klamerth, R. Huang, H. Elnakar, and M. Gamal El-Din. 2016a. Oxidation of oil sands process-affected water by potassium ferrate (VI). Environmental science & technology **50**:4238-4247.

Wang, C., N. Klamerth, S. A. Messele, A. Singh, M. Belosevic, and M. Gamal El-Din. 2016b. Comparison of UV/hydrogen peroxide, potassium ferrate (VI), and ozone in oxidizing the organic fraction of oil sands process-affected water (OSPW). Water research **100**:476-485.

Wang, N., P. Chelme-Ayala, L. Perez-Estrada, E. Garcia-Garcia, J. Pun, J. W. Martin, M. Belosevic, and M. Gamal El-Din. 2013. Impact of ozonation on naphthenic acids

speciation and toxicity of oil sands process-affected water to Vibrio fischeri and mammalian immune system. Environmental science & technology **47**:6518-6526.

Whitby, C. 2010. Microbial naphthenic acid degradation. Pages 93-125 Advances in applied microbiology. Elsevier.

Xue, J., C. Huang, Y. Zhang, Y. Liu, and M. Gamal El-Din. 2018. Bioreactors for oil sands process-affected water (OSPW) treatment: A critical review. Science of the Total Environment **627**:916-933.

Yue, S., B. A. Ramsay, R. S. Brown, J. Wang, and J. A. Ramsay. 2014. Identification of estrogenic compounds in oil sands process waters by effect directed analysis. Environmental science & technology **49**:570-577.

Yue, Z., W. Jiang, L. Wang, S. Gardner, and C. Pittman Jr. 1999. Surface characterization of electrochemically oxidized carbon fibers. Carbon **37**:1785-1796.

Zhang, Y., N. Klamerth, and M. Gamal El-Din. 2016a. Degradation of a model naphthenic acid by nitrilotriacetic acid–modified Fenton process. Chemical Engineering Journal **292**:340-347.

Zhang, Y., J. Xue, Y. Liu, and M. Gamal El-Din. 2016b. Treatment of oil sands process-affected water using membrane bioreactor coupled with ozonation: A comparative study. Chemical Engineering Journal **302**:485-497.

Zöllig, H., C. Fritzsche, E. Morgenroth, and K. M. Udert. 2015. Direct electrochemical oxidation of ammonia on graphite as a treatment option for stored source-separated urine. Water research **69**:284-294.

4. DEGRADATION OF THE RECALCITRANT ORGANICS IN REAL OIL SANDS PROCESS WATER BY ELECTRO-OXIDATION USING GRAPHITE AND DIMENSIONALLY STABLE ANODES[1]

4.1 Introduction

The oil sands industry in Alberta, Canada, is considered the key driver for the providence economic prosperity and one of the main contributors to the country's economy (Giesy et al. 2010). Despite that, it is attracting a lot of public concern and scientific focus because it consumes large amounts of water and, subsequently, generates large volumes of process water (Allen 2008b). The extraction of the extra-heavy and viscous crude oil (bitumen) from the mined sand ores occurs by using caustic hot water through what is known as Clark process (Masliyah et al. 2004, Allen 2008a, b). This extraction process depends mainly on water and despite the high water-recycling rate, 80-90%, the fresh water intake is still (2–3) m^3 water for every m^3 of upgraded bitumen (Masliyah et al. 2004, de Klerk et al. 2014, Klamerth et al. 2015). This water-intensive process leads to the generation of large amounts of oil sands process water (OSPW) which is sent to be stored in tailings ponds in accordance with the currently implemented zero discharge practice (Allen 2008a, Klamerth et al. 2015). The amount of impounded OSPW is growing rapidly with an estimated amount of more than trillion liters in tailings ponds (Xue et al. 2018), making the treatment and discharge of OSPW an urgent challenge facing the oil sands industry today.

---

[1] A version of this chapter will be submitted to a peer-review journal as: Abdalrhman, A. S. and M. Gamal El-Din. Degradation of the organics in real oil sands process water by electro-oxidation using graphite and dimensionally stable anodes. 2019 Chemical Engineering Journal

OSPW is a complex mixture of different organic and inorganic constituents. It is generally classified as brackish water with high salinity and alkalinity (Allen 2008a). The organic fraction in OSPW consists mainly of naphthenic acids (NAs), including classical, oxidized and heteroatomic species, and aromatic compounds that include a small portion of polyaromatic hydrocarbon (PAH) (Yue et al. 2015, Wang et al. 2016, Li et al. 2017). NAs refer to a group of alkyl-substituted acyclic and cycloaliphatic carboxylic acids with the general formula $C_nH_{(2n+Z)}O_x$ where n is the number of carbon atoms in the structure, Z indicates the hydrogen deficiency due to rings formation and/or double bonds introduction (Z is zero or a negative even integer), and x is the number of oxygen atoms which refers to either classical NAs (x=2) or oxidized NAs (x≥3) (Kannel and Gan 2012). NAs are leached from oil sands into the water during the bitumen extraction and processing and they keep accumulating in the water due to the water recycling practice (Brown and Ulrich 2015). NAs are known to be very recalcitrant and they account for almost half of the organic fraction in OSPW (Xue et al. 2018). Although some NAs occur naturally in different crude oils, those in oil sands deposits are more complex and recalcitrant as they are products of the biodegradation of mature petroleum in bitumen deposits (Scott et al. 2005, Brown and Ulrich 2015).

OSPW has been proven to be toxic to a wide range of aquatic and terrestrial organisms through different modes of action including narcosis, immunotoxicity and endocrine disruption (Allen 2008a, Kannel and Gan 2012, Reinardy et al. 2013, Klamerth et al. 2015, Yue et al. 2015, Wang et al. 2016, Li et al. 2017). NAs have been consistently considered the major cause of the toxicity of OSPW (Allen 2008a, Kannel and Gan 2012, Reinardy et al. 2013, Klamerth et al. 2015, Yue et al. 2015, Wang et al. 2016, Li et al. 2017). Within the

117

difference classes of NAs, classical NAs were found to be relatively more toxic than oxidized NAs due to the higher hydrophobicity of classical NAs which leads to higher affinity to the cell membrane (Frank et al. 2009, Wang et al. 2016). It was also found that the aromatic fraction has significant contribution to the toxicity of OSPW especially that these aromatics have higher estrogenic activity (Frank et al. 2009, Reinardy et al. 2013, Yue et al. 2015).

Due to the recalcitrant nature of the organics in OSPW (especially NAs) and their high concentrations, different advanced oxidation processes have been investigated as treatment options (Brown and Ulrich 2015, Quinlan and Tam 2015). Some of these processes include ozonation (Dong et al. 2015, Klamerth et al. 2015, Wang et al. 2016, Meshref et al. 2017), O_3/H_2O_2 (Meshref et al. 2017), UV/chlorine (Shu et al. 2014), UV/H_2O_2 (Afzal et al. 2012, Wang et al. 2016), UV/persulfate (Fang et al. 2018), Fenton (Zhang et al. 2017), photo-Fenton (Zhang et al. 2017) and ferrate (VI) oxidation (Wang et al. 2016). Although some of these processes were able to achieve considerable degradation rates for OSPW's NAs, the required doses were always relatively high and not economically viable at large scales, especially by taking into account the large volumes of currently impounded OSPW that need to be treated (Quinlan and Tam 2015, Wang et al. 2016). Some of these processes also have technical restrictions such as the alkaline natural pH of OSPW (pH 8-9) (Zhang et al. 2017) which making it not suitable for Fenton oxidation based processes and the relatively high turbidity which makes all the UV-based AOPs need pre-treatment step (Shu et al. 2014). Among these different AOPs, ozonation was studied more frequently (Dong et al. 2015, Klamerth et al. 2015, Quinlan and Tam 2015, Wang et al. 2016, Meshref et al. 2017) with some studies focused on using ozonation as pre-treatment for biodegradation (Brown

118

and Ulrich 2015, Dong et al. 2015, Xue et al. 2018). The required doses for improving the biodegradability of NAs, however, were still high and not economically viable.

Electrooxidation (EO) has emerged as efficient process for wastewater treatment that has been applied successfully for the degradation of a wide range of organic pollutants (Brillas et al. 2009, Panizza and Cerisola 2009, Martínez-Huitle et al. 2015, Särkkä et al. 2015, Moreira et al. 2017). It involves the application of electric field in the water sample to be treated by using suitable type of electrode material in order to generate oxidants through the reactions at anode (Brillas et al. 2009, Panizza and Cerisola 2009, Martínez-Huitle et al. 2015, Särkkä et al. 2015, Moreira et al. 2017). EO has the advantages of being effective, simple to operate and does not need addition of chemicals or produce secondary sludge (Särkkä et al. 2015, Moreira et al. 2017). During EO pollutants can be oxidized at the anode either directly by transferring electron to anode (generally a poor mechanism) or indirectly through water discharge at anode surface which leads to the generation of oxidants such as hydroxyl radicals or other reactive oxygen species (Panizza and Cerisola 2009). Other oxidants such as chlorine and persulfate can also be generated from dissolved anions (Cl^- and SO_4^{2-}), in water by using suitable anodes (Brillas et al. 2009, Panizza and Cerisola 2009, Martínez-Huitle et al. 2015, Särkkä et al. 2015, Moreira et al. 2017). The anode material plays great role in determining the efficiency of EO and the type of generated oxidants (Panizza and Cerisola 2009, Martínez-Huitle et al. 2015). Non-active anodes, such as boron-doped diamond (BDD), are effective in generating free hydroxyl radicals which can effectively mineralize organic pollutants. Active anode materials such as graphite, RuO_2 and IrO_2 are capable of generating chemisorbed oxygen which can mainly degrading organic pollutants but not mineralizing them (Panizza and Cerisola 2009, Martínez-Huitle

et al. 2015). Carbonaceous electrodes such as graphite are low-cost, unlike BDD and noble metal electrodes, and have good conductivity, chemical stability and can be used as 3D anodes offering higher surface area (Brillas et al. 2009, Panizza and Cerisola 2009). Anodes made from titanium base and covered with a thin conducting ruthenium oxide and/or iridium oxide layers are commonly known as dimensionally stable anodes (DSA) (Martínez-Huitle et al. 2015). In general, DSAs are relatively more expensive than graphite but still less expensive than BDD and they are stable and have good catalytic abilities for oxygen and chlorine generation (Panizza and Cerisola 2009, Martínez-Huitle et al. 2015). Both graphite and DSA are classified as active anodes and they have been used successfully for the degradation of wide range of recalcitrant organic pollutants (Panizza and Cerisola 2009, Kumar et al. 2015, Särkkä et al. 2015, Moreira et al. 2017).

EO has been applied for the treatment of wide range of industrial wastewaters (Brillas et al. 2009, Panizza and Cerisola 2009, Kumar et al. 2015, Martínez-Huitle et al. 2015, Särkkä et al. 2015, Moreira et al. 2017, Martínez-Huitle and Panizza 2018). However, to our best knowledge, it has not yet been applied for the treatment of real OSPW. By considering the physical characteristics of OSPW, with its relatively high TDS and electrical conductivity, EO could be seen as an attractive option for OSPW treatment. EO will not be restricted neither by the alkaline pH of OSPW like in the case of Fenton, nor by the limited light transmittance such as in the case of UV-based AOPs. Therefore, EO is expected to be an effective option for the treatment of OSPW.

The main objective of this chapter was to investigate the effectiveness of EO for degrading the recalcitrant organics in real OSPW. The chapter focused on evaluating and comparing the performance of EO by using graphite anode and DSA for the degradation of the

different NAs and aromatics in OSPW. Graphite was selected as low-cost and abundant anode material that, if succeeded in treating OSPW, can be applied at large scale especially with considering the large amount of impounded OSPW. DSA, on the other hand, is a commercially available active anode that has been used widely for the degradation of different recalcitrant organics. The chapter also looked at the current density window within which the degradation of organics in OSPW can occur.

4.2 Materials and methods

4.2.1 Source of OSPW

Raw OSPW was collected from an oil sands tailings pond in Fort McMurray, Alberta, Canada, and stored in a cold storage room at 4 °C. Water quality analysis of raw OSPW is summarized in Table 4.1. Cyclohexanecarboxylic acid (CHA) was purchased from Sigma-Aldrich (St. Louis, MO, USA). Dichloromethane (HPLC and Optima grades), sodium chloride, sulfuric acid and hydrochloric acid were obtained from Fisher Scientific (Ottawa, ON, Canada).

4.2.2 Experimental apparatus and procedure

EO experiments were performed using cylindrical undivided glass reactor of 500 mL size constantly stirred with a PTFE magnetic bar to enhance the mass transport and maintain homogenization. The electrodes were in the centre of the reactor parallel to each other at distance of 1.2 cm; to minimize the resistance of the electrolysis and maintain effective mass transport. Graphite plates obtained from Wale Apparatus, (PA, US) were used as anode and cathode for EO by graphite with an effective immersed anode surface area of 41.9 cm^2. For DSA experiment, RuO_2/IrO_2 coated titanium mesh electrodes (coating

thickness of 4 μm) purchased from American Elements (Los Angeles, CA, USA) were used as anode and cathode with an effective immersed surface areas of 42.1 cm². All experiments were performed under controlled current conditions (galvanostatic). Control reactors with an identical setup were always run with electrodes but without electric field to exclude any removal by adsorption or volatilization. DC power station (9130, B&K Precision, California, US) was used to supply power and continuously monitor voltages. Anode potentials were determined using Ag/AgCl (saturated) reference electrode (Accumet, Fisher Scientific, CA), E = +0.201 V vs SHE.

General current efficiency (GCE) for the different applied current densities was calculated using the following equation (Panizza and Cerisola 2009, Kumar et al. 2015):

$$GCE = \frac{(COD_0 - COD_f)F.V_r}{8.I.\Delta t} \text{ x } 100\% \tag{4.1}$$

where, COD_0 and COD_f are the initial and final COD (g/L), F represents Faraday's constant (96,485 C/mol), V_r is the reactor volume (L), I is the applied current (A), Δt is the time (s), and 8 represents the equivalent mass of oxygen (32 g O_2 per mol/4 e⁻).

The specific energy consumption (SEC) per g of NAs removed was calculated as follow (Kumar et al. 2015):

$$SEC = \frac{I.U.t}{(NA_0 - NA_f).V_r} \tag{4.2}$$

where, I is the current (A), U is voltage (V), t is the time (h), NA_0 and NA_f are the initial and final classical NA concentrations (g/L), and V_r is the reactor volume (L).

Table 4.1 **Water quality of raw OSPW.**

Parameter	Value
pH	8.5±0.2
Alkalinity (mg/L as $CaCO_3$)	554±6
Conductivity (mS/cm)	3.1±0.1
Turbidity (NTU)	107
TSS (mg/L)	61.8±4.9
Organic parameters	
COD (mg/L)	188 ± 5.6
DOC (mg/L)	49.9±2.1
Classical Naphthenic acids (O_2-NAs) (mg/L)	24.4
O_3-NAs (mg/L)	16.3
O_4-NAs (mg/L)	17.8
O_5-NAs (mg/L)	3.8
Acid extractible fraction (AEF) (mg/L)	66.5 ±3.2

4.2.3 Water quality analyses

The conductivity and pH of samples were measured using a multi-channel pH/conductivity/ion (Accumet excel XL60; Fisher Scientific). Chemical oxygen demand (COD) was determined using HACH COD reagent kits (TNT821, LR, Germany) using DR3900 spectrophotometer (HACH, Germany) following the manufacturer's instructions. All treated OSPW samples were filtered through 0.45 μm nylon filters (Supelco Analytical, PA, USA) and kept in glass bottles prior analysis.

4.2.4 Analytical methods

The concentration of AEF in OSPW was determined using fourier transform infrared (FT-IR) spectroscopy (Spectrum 100, PerkinElmer Ltd, Bucks, UK) following a method that was previously developed and verified by several studies (Frank et al. 2009, Gamal El-Din et al. 2011, Dong et al. 2015). In brief, samples were acidified to pH 2.0 then extracted twice using analytical grade dichloromethane (DCM) in separation funnels. The extract was evaporated to dryness then dissolved in a known amount of dichloromethane and analyzed by FT-IR for absorbance at 1743 and 1706 cm^{-1}, which represents the monomeric and dimeric carboxylic groups, respectively (Gamal El-Din et al. 2011).

NA concentrations in OSPW were measured using ultra-performance liquid chromatography time-of-flight mass spectrometry (UPLC TOF-MS). Chromatographic separation was performed using Waters UPLC Phenyl BEH column (Waters, MA, USA). The sample analysis was performed using a high-resolution time-of-flight mass spectrometry TOF-MS (Synapt G2, Waters, MA, USA) on negative electrospray ionization mode and myristic acid-1-^{13}C was used as the internal standard. Sample of a mixture consisting of 500 µL OSPW sample, 100 µL of 4.0 mg/L internal standard (myristic acid-1-^{13}C), and 400 µL methanol was injected into the instrument. The column temperature was set at 50 ºC while the sample temperature was 10 ºC. The mobile phases were: (A) 10 mM ammonium acetate in water and (B) 10 mM ammonium acetate in 50/50 methanol/acetonitrile at a 100 µL/min flow rate. The elution gradient was 1% B during 0–2 min; increased from 1% to 60% B during 2–3 min; then increased to 70% B during 3–7 min; went to 95% B during 7–13 min; went down to 1% B during 13–14 min, and hold 1% B until 20 min to equilibrate the column with a flow rate of 100 µL/min. The data

acquisition process was performed using MassLynx (Waters, MA, USA) and data extraction from spectra was done using TargetLynx (Waters, MA, USA). The identification of classical NAs (O_2) and oxy-NAs was based on the empirical formula $C_nH_{2n+z}Ox$ (x=2, 3, 4, 5) where n ranged from 7 to 26 and z from 0 to -18.

The presence of aromatic species was examined by synchronous fluorescence spectra (SFS) using a Varian Cary Eclipse fluorescence spectrometer (Mississauga, ON Canada). Excitation wavelengths ranged from 200 to 600 nm, and emission wavelengths were recorded from 218 to 618 nm. Scanning speed was set at 600 nm/min and the photomultiplier (PMT) voltage was 800 mV.

The concentrations of CHA were measured using an ultra-performance liquid chromatography (UPLC-MS, Waters, USA) system connected to an ion trap mass spectrometer (Waters Acquity, SQ Detector 2) and operated in negative electro-spray ionization mode (-ESI). The column used for the analysis was C18, 1.7 μm, 2.1×50 mm (Waters Acquity, Ireland). The column temperature was set at 40°C, the flow rate was 0.4 mL/min and the injection volume was 20 μL. All samples were filtered through a 0.45 μm nylon filter prior to the analysis. The solvents were: (A) water with 0.1% ammonium acetate and (B) 100% acetonitrile.

4.3 Results and discussion

4.3.1 Effect of applied current density on the removal of COD and AEF

Raw OSPW samples were treated by EO for 90 min using graphite anode and DSA under different applied current densities (0.5, 1, 2, 5, 10 and 20 mA/cm^2). The samples pH did not change significantly after EO and remained in the range (8.1 - 8.6), which was expected

due to the relatively high alkalinity of OSPW which offers a natural (HCO_3^-/CO_3^{2-}) buffer capacity (Shu et al. 2014). To investigate the effectiveness of EO for degrading the organic fraction in OSPW, the removal of COD and AEF were used as performance indicators. The initial COD and AEF concentrations in the raw OSPW were 188 mg/L and 66.5 mg/L, respectively (Table 4.1). As can be seen in Fig. 4.1, the removals of AEF and COD were always partial, indicating the absence of complete mineralization which was expected considering that graphite and DSA are both active anode materials and they are not effective in mineralizing organic pollutants (Panizza and Cerisola 2009, Martínez-Huitle et al. 2015, Särkkä et al. 2015, Martínez-Huitle and Panizza 2018). The removal of COD increased with increasing the applied current density for both graphite and DSA (Fig. 4.1a). In the case of DSA, there was no COD removal below current density of 2 mA/cm^2, while graphite was able to achieve COD removals of 7% and 9.2% at current densities of 0.5 and 1 mA/cm^2, respectively. At higher current densities of 2, 5, 10 and 20 mA/cm^2, both anodes were able to reduce the COD; however, graphite continuously maintained removal rates higher than DSA by 7.4%, 7.7%, 18.2% and 7%, respectively (Fig. 4.1a).

AEF, on the other hand, has been widely used as a gross parameter for the recalcitrant organics in OSPW and is often referred to as the extractable organic fraction (Gamal El-Din et al. 2011, Dong et al. 2015, Alberts et al. 2019). AEF of OSPW contains not only classical and oxidized NAs, but also the other carbonyl-containing organics such aromatics, hetero-atomic (sulfur- and nitrogen-containing) organics, diluents, and other bitumen-based hydrocarbons (Gamal El-Din et al. 2011, Dong et al. 2015). Similar to the case of COD, DSA was not able to achieve removal of AEF below 2 mA/cm^2 while graphite anode removed AEF by 15.6% and 24.3% at 0.5 and 1 mA/cm^2, respectively (Fig. 4.1b). This

clearly indicated that the limiting current density for OSPW's organics oxidation by DSA is much higher than graphite which was able to oxidize the organic fraction even at current density as low as 0.5 mA/cm^2. At current densities of 2, 5, 10 and 20 mA/cm^2, graphite was able to achieve AEF removals of 21.3%, 30.7%, 34.1% and 56.3%, respectively, compared to 7.6%, 16.4%, 24.1% and 60.0% for DSA, respectively (Fig. 4.1b). It can be noted that the AEF removal rate at current densities below 10 mA/cm^2 was always higher than the COD removal for both of graphite and DSA (Fig. 4.1). These higher removals of AEF compared to COD were also previously observed during ozonation of OSPW (Gamal El-Din et al. 2011, Dong et al. 2015). This behaviour can be explained by the conversion of compounds that contribute to AEF (i.e., carbonyl-containing organics) to smaller organic compounds that do not contain carbonyl functional group but can still contribute to COD (Dong et al. 2015). At higher current densities (10 and 20 mA/cm^2), COD removals were slightly higher than the AEF removal which can be attributed to the degradation of the smaller organic compounds that do not contain carbonyl functional group at high current densities. This can also be supported by comparing the performance of graphite to DSA for both COD and AEF removals; graphite maintained higher AEF removals at all the different current densities except at 20 mA/cm^2 where DSA was able to achieve slightly higher removal, contrary to the case of COD. This behaviour can be attributed to the difference in selectivity and oxidation mechanism between graphite and DSA which can result in the preference for targeting carbonyl-containing high molecular weight organics in the case of graphite which contribute to AEF rather than the degradation of short chain low molecular weight by-products that do not contribute to AEF (Abdalrhman et al. 2019a).

127
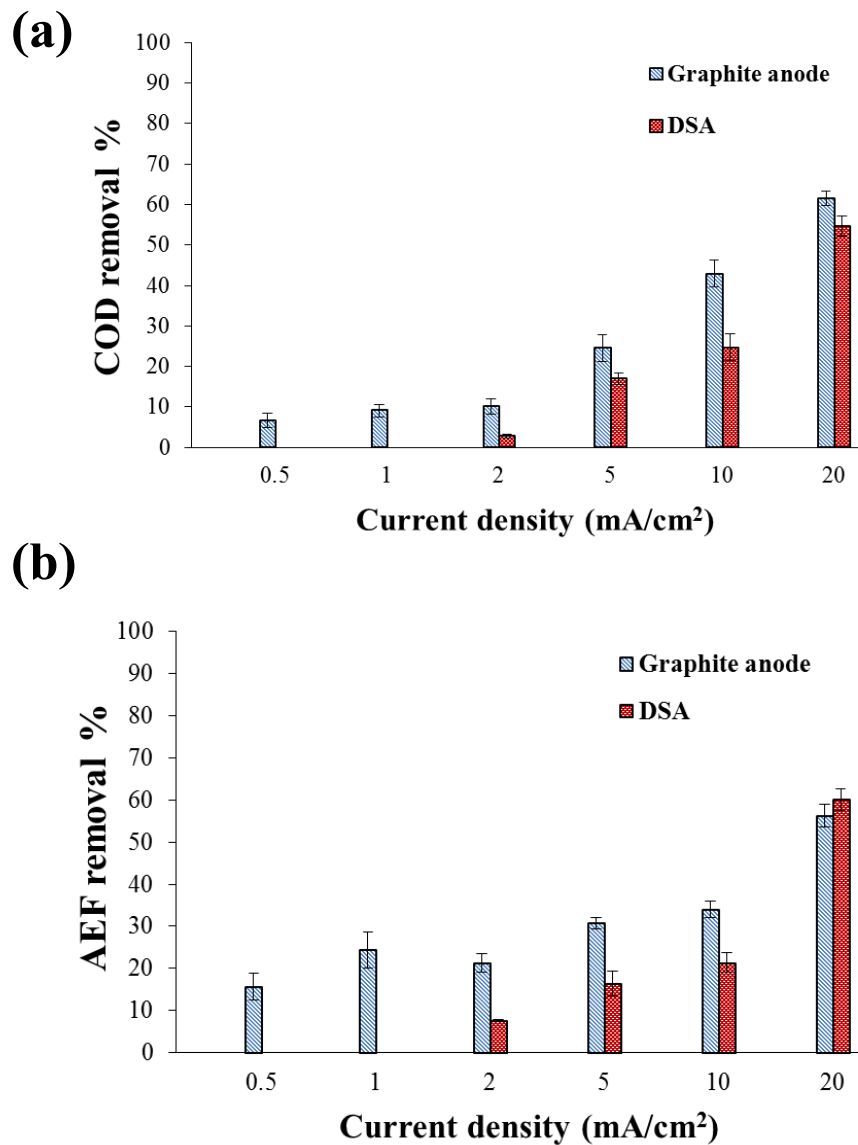
Figure 4.1 The removal of (a) acid extractable fraction (AEF) and (b) COD after 90 min of electro-oxidation by using graphite anode and DSA.

4.3.2 Fate of classical and oxidized NAs during EO

4.3.2.1 Classical NAs

The removal of classical NAs has been used consistently as the main indicator for the efficiency of most of the studied OSPW treatment processes (Kannel and Gan 2012, Shu et

al. 2014, Dong et al. 2015, Quinlan and Tam 2015, Wang et al. 2016). One thing is because of their higher relative abundance. But the most important reason is that classical NAs have been reported to be the most acutely toxic class in OSPW due to their higher hydrophobicity which make them more attachable to the cell membrane (Frank et al. 2009, Yue et al. 2015, Wang et al. 2016). The concentration of classical NAs in the raw OSPW sample was 24.4 mg/L and it was the highest among the other classes (Table 4.1, Fig. 4.2). NA concentrations were measured using ultra-performance liquid chromatography coupled with time-of-flight mass spectrometry which allowed the quantification of the different NA classes with different carbon and Z numbers (Fig. 4.3). As can be seen in Fig. 4.3, classical NAs with carbon number of (12-18) and –Z number (4-12) were the most abundant in the raw OSPW sample and remained the same after treatment. At applied current densities of 2, 5, 10 and 20 mA/cm^2, EO by graphite anode was able to reduce the concentration of classical NAs by 38.4%, 44.7%, 53.7% and 74.6%, respectively (Fig. 4.2a), compared to 13.6%, 24.9%, 38.7% and 83.7%, respectively, for DSA (Fig. 4.2b). At current densities of 0.5 and 1 mA/cm^2, graphite was able to reduce classical NAs by 30.2% and 39.9%, respectively, while DSA did not achieve any removals, confirming the absence of any organic degradation (Fig. 4.2a and 4.2b). This trend in classical NAs removal was similar to that of AEF (Fig. 4.1b), with graphite maintaining higher removal efficiency compared to DSA at all the current density except at 20 mA/cm^2. It should be noted that the removal of NAs for both of the electrodes and at all the applied current densities was higher than the removal of AEF, which was expected due to the fact that some of the degradation by-products of classical-NAs can still contain carbonyl functional groups and, therefore, contribute to AEF (Scott et al. 2005, Dong et al. 2015, Abdalrhman et al. 2019b).
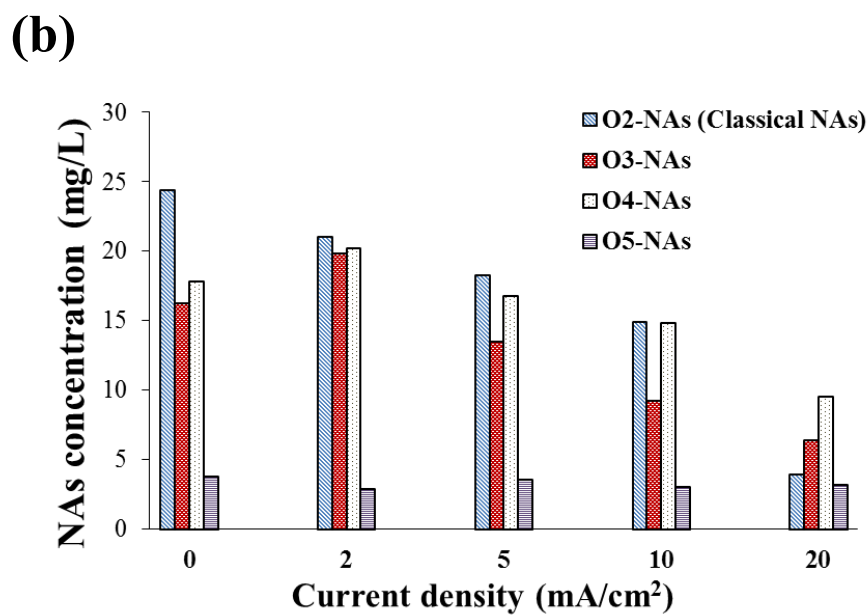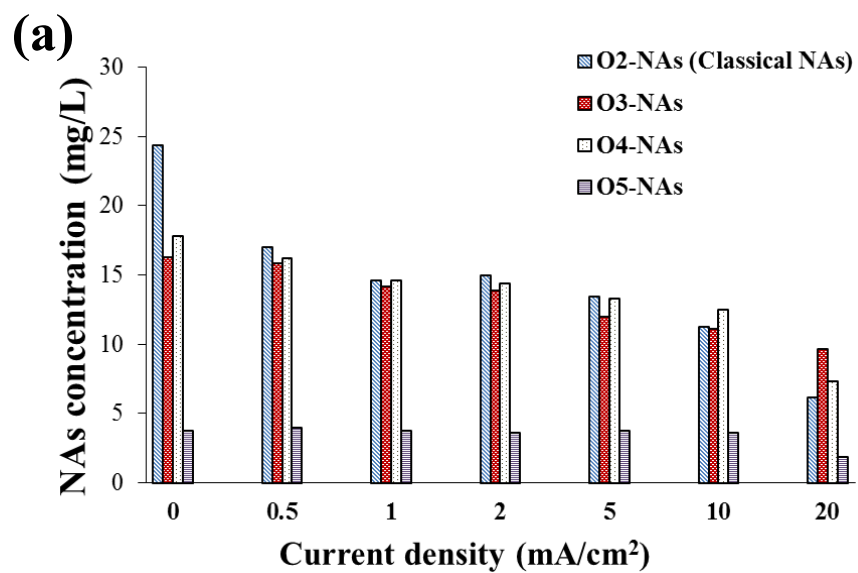
Figure 4.2 Fate of classical-NAs (O_2) and oxidized NAs (O_3, O_4, and O_5) in OSPW after 90 min of electro-oxidation by (a) graphite anode and (b) DSA.
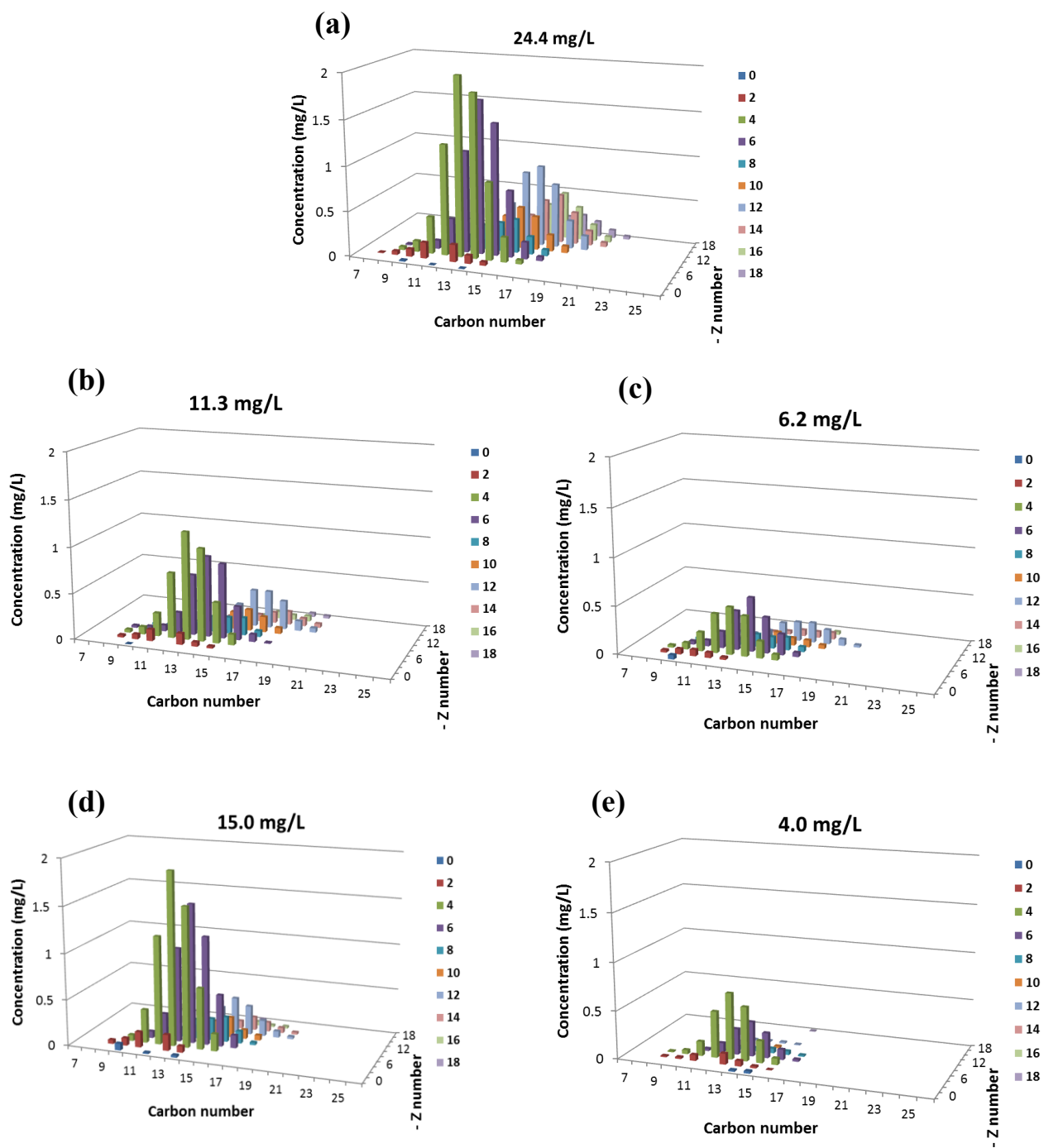
Figure 4.3 Distribution of classical NAs in OSPW: (a) raw OSPW; (b) after EO by graphite at current density 10 mA/cm^2; (c) after EO by graphite at current density 20 mA/cm^2; (d) after EO by DSA at current density 10 mA/cm^2; (E) after EO by DSA at current density 20 mA/cm^2 (EO for 90 min).

In order to better understand and compare the performance of graphite and DSA for the degradation of NAs, the removal of classical NAs was plotted as function of the applied anode potentials (Fig. 4.4). As can be seen in Fig. 4.4, the anode potentials at the same applied current densities were always lower for DSA compared to graphite which can be attributed to higher ohmic resistance of graphite electrodes compared to the metallic DSA which leads to higher voltage requirement for graphite to pass the same current. The first observed removal of classical-NAs by DSA was at an anode potential of 2.5 V (vs. SHE) while graphite was able to remove more than 30% of classical NAs at 1.6 V (vs. SHE) (Fig. 4.4). It should be noted that it was reported before that EO using graphite anode was able to degrade model NA compounds even at anode potential as low as 1.3 V (Abdalrhman et al. 2019a) which indicates that graphite electrode can be effective for degrading NAs even at lower current densities. As a general trend, the removal of NAs increased with the increase in applied potential for both electrodes (Fig. 4.4). The only exception was for graphite when the anode potential increased from 2 to 2.7 V (vs. SHE) which corresponded to current densities of 1 and 2 mA/cm^2, respectively, where there was slight reduction (Fig. 4.4). Similar result was also seen for AEF (Fig. 4.1b). This behaviour can be explained by looking into the inorganic matrix of OSPW which contain high concentration of different anions and cations among them chloride (550 mg/L) (Allen 2008a). The existence of chloride during EO can lead to the electrochemical generation of chlorine according to Eq. (4.3), when the anode potential becomes high enough to allow that, which will react with water to form reactive chlorine species according to Eq. (4.4) and (4.5) based on the pH (Panizza and Cerisola 2009, Moreira et al. 2017). It should be noted that HOCl and OCl$^-$ are both weak oxidants with HOCl being relatively more effective in degrading organics

than OCl⁻. However at pH ranges of OSPW (8.5), the majority of chlorine, if generated, will exist as OCl⁻ (Deborde and von Gunten 2008). The generation of chlorine by EO on graphite was reported to start at an anode potential of 1.81 V and increase with increasing the potential (Zöllig et al. 2015). This means at anode potentials of 2 V, the generation of chlorine will not be high and when increasing the potential to 2.7V, the increase in the potential will be wasted in the generation of chlorine, which will still not be generated at enough amounts, and even if it has been generated enough it will not be effective in degrading NAs. Therefore, increasing the current density from 1 to 2 mA/cm^2 has resulted in reduced removal efficiencies for NAs and AEF.

$$2Cl^- \rightarrow Cl_2 + 2e^- \tag{4.3}$$

$$Cl_2 + H_2O \rightarrow HClO + Cl^- + H^+ \tag{4.4}$$

$$HClO \rightarrow ClO^- + H^+ \tag{4.5}$$
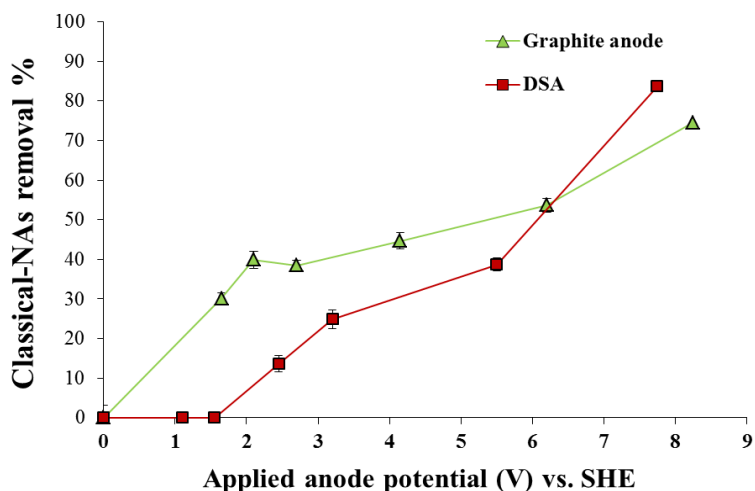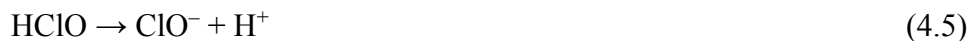
Figure 4.4 The removal of classical-NAs after 90 min of EO by graphite anode and DSA as function of the average applied anode potential.

133

As can be seen in Fig. 4.2 and Fig. 4.4, the removal of classical NAs by graphite anode was always higher than the removal by DSA, except at current density of 20 mA/cm^2 where the applied anode potential exceeded 7V. At this high anode potential DSA was able to achieve removals of NAs and AEF than graphite (Fig.4.1b and Fig. 4.4). This behaviour can be explained by considering the phenomenon of surface corrosion that occurs during EO by graphite at high voltages compared to the highly stable DSA. Corrosion is considered the main drawback of using graphite anodes at high current densities (Panizza and Cerisola 2009, Martínez-Huitle et al. 2015, Qiao et al. 2018). Graphite anode surface can be degraded through the carbon oxidation reaction (COR) which becomes prevalent at high current densities (Qiao et al. 2018, Abdalrhman et al. 2019a). Therefore, at high current densities the efficiency of graphite anode decreased due to the completion from COR.

4.3.2.2 Oxidized NAs

Oxidized NAs are also very recalcitrant and contribute considerably to the toxicity of OSPW [5, 7-9, 15, 18]. Oxidized NAs in the OSPW sample consisted mainly of O$_3$-NAs (NA+ O), O$_4$-NAs (NA+ 2O) and O$_5$-NAs (NA+ 3O) with concentration of 16.3 mg/L, 17.8 mg/L and 3.8 mg/L, respectively (Table 4.1, Fig. 4.2). EO by graphite anode was able to reduce the concentration of oxidized NAs even at current density as low as 0.5 mA/cm^2 (Fig. 2a). The degradation of oxidized NAs by graphite anode increased with the increase in the applied current density with O$_4$-NAs having the highest removal rate and O$_5$-NAs being the least removed species (Fig. 4.2a). This trend can be explained by looking at the relative abundance of oxidized NAs in raw OSPW which show that O$_4$-NAs are the most abundant and O$_5$-NAs the least abundant (Fig. 4.2a). This behaviour for oxidized NAs degradation was different from that observed during other AOPs such as ozonation (Klamerth et al.

134

2015, Wang et al. 2016), ferrate (VI) (Wang et al. 2016) and UV/H_2O_2 (Meshref et al. 2017) which showed that some oxidized NA classes were increased during oxidation at lower oxidants doses while others where decreased. This difference, however, can be explained by the difference in the oxidation mechanisms, since EO using graphite involves the generation of active oxygenated species attached to the carbon surface that behave differently than ozone and $^{\bullet}$OH radicals (Rueffer et al. 2011, Wang et al. 2016).

DSA, on the other hand, behaved slightly different. At low current density (2 mA/cm^2), the concentration of O_3 and O_4-NAs increased significantly while the concentration of O_5-NAs decreased slightly (Fig. 4.2b). At current densities of 5, 10 and 20 mA/cm^2, oxidized NAs were consistently degraded with a rate increased with the increase in the applied current density (Fig. 4.2b). The class that had the highest removal rates by DSA was O_3-NAs while O_5-NAs remained the least removed. This difference in the oxidized NA degradation behaviour between graphite and DSA can be attributed to the difference in the oxidation mechanisms. Although both graphite and DSA are classified as active anodes (Panizza and Cerisola 2009, Martínez-Huitle et al. 2015), the generated oxidants by DSA and graphite were found to be different (Rueffer et al. 2011, Abdalrhman et al. 2019a).

In order to understand and compare the selectivity of EO using graphite and DSA for NA degradation in terms of molecular weight (carbon number) and hydrogen deficiency (−Z), the removal rate for the individual components of classical NAs were analyzed under different current densities (Fig. 4.5). As can be seen from Fig. 4.5a, the removal rate for EO using graphite at the different applied current densities increased with the increase in carbon number. This trend was observed before for different oxidation processes such as photocatalytic oxidation, ozonation, UV/Chlorine, ferrate (VI) and UV/H_2O_2 (Afzal et al.

135

2012, Shu et al. 2014, Wang et al. 2016, de Oliveira Livera et al. 2018). This trend can be explained by the fact that the increase in the carbon number will mean the introduction of new sites available for oxidation and more hydrogen atoms available for abstraction which means more reactivity (Afzal et al. 2012, Shu et al. 2014, Abdalrhman et al. 2019a). In the case of EO using DSA, the trend was more complicated (Fig. 4.5b). At high current density, 20 mA/cm^2, the trend was similar to the case of graphite; removal rate increased with the increase in the carbon number with achieving total removal for the NAs with carbon numbers $\geq$ 17 (Fig. 4.5b). At current densities of 2, 5 and 10 mA/cm^2, there was a removal of NAs with high carbon number (n $\geq$ 17), while at the same time generation of NAs with lower carbon number (Fig. 4.5b). This indicates that in the case of DSA some of the by-products from the oxidation of high carbon number classical-NAs were classical-NAs with low carbon number that still fit the formula ($C_nH_{2n+Z}O_2$). In the case of graphite, however, the oxidation by-products were not NAs. This behaviour can be explained by considering the difference in the oxidation mechanism between graphite and DSA. Although both are classified as active anodes that are not able of generating free $^\bullet$OH radicals (Panizza and Cerisola 2009), it was found that the type of active oxygen species generated at the surface of graphite and DSA behave differently (Rueffer et al. 2011, Qiao et al. 2018, Abdalrhman et al. 2019a). On oxide coated DSA the hydroxyl radicals generated from water discharge at anode (Eq. (4.6)) interact immediately with oxygen already exist in oxide coated anode to form higher metal oxide (Eq. (4.7)) that will be able to oxidize organics. For graphite, on the other hand, the oxidation of organics occurs by oxygen-containing species that are bonded to the previously functionalized anode surface and generated through more complex steps (Rueffer et al. 2011, Qiao et al. 2018, Abdalrhman et al. 2019a).

$$MO_x + H_2O \rightarrow MO_x(\dot{O}H) + H^+ + e^- \qquad\qquad (4.6)$$

$$MO_x(\dot{O}H) \rightarrow MO_{x+1} + H^+ + e^- \qquad\qquad (4.7)$$
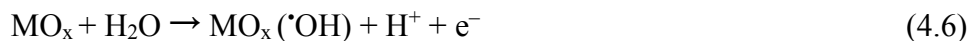
The selectivity of EO for NA degradation based on cyclicity ($-Z$) was relatively similar for graphite and DSA (Fig. 4.5c and 4.5d). EO using graphite and DSA has shown a clear trend of increase in the removal rate with the increase in the cyclicity ($-Z$ number) at the different applied current densities. This increase in the removal, however, was steeper in the case of DSA compared to graphite (Fig. 4.5c and 4.5d) indicating some differences in the selectivity that can be attributed to the previously discussed difference in oxidation mechanisms. A previous study by our group about anodic oxidation by graphite for model NA compound degradation have shown that although cyclic NAs were more reactive than linear ones, but the increase in the cyclicity beyond one ring resulted in reduced reactivity (Abdalrhman et al. 2019a). The results obtained for OSPW NA degradation using graphite anode (Fig. 4.5c) seemed different than that for model NA compounds from the first glance. However, by considering that in the case of OSPW NAs the increase in the $-Z$ number will also result in increase in the carbon number, the increase in the removal rate in the case of graphite anode (Fig. 4.5c) can be attributed to the increase in carbon number rather than the introduction of rings. In the case of DSA, the trend was clearer and the selectivity increased steeply with increasing $-Z$ number (Fig. 4d) showing a trend similar to that obtained during the oxidation of OSPW using ferrate(VI) (Wang et al. 2016). The higher increase in the reactivity with the increase in cyclicity during EO by DSA can be attributed to, increase in carbon number, the fact that the introduction of more rings will result in the introduction of

137

additional tertiary carbons which have higher reactivity toward oxidation by oxidants such as that generated by DSA (Wang et al. 2016, de Oliveira Livera et al. 2018).

The selectivity of EO using graphite and DSA for degradation of oxidized NAs (O_3-NAs and O_4-NAs) was also examined (Fig. 4.6 and Fig. 4.7). As can be seen in Fig. 4.6, the general removal trend for O_3-NAs was similar to that of classical NAs, but with relatively less extend. For O_4-NAs, on the other hand, no clear trends could be seen especially in the case of DSA (Fig. 4.7). This could be attributed to the reality that oxidized NAs, although they are degraded during EO, but they can also be generated as by-products of the oxidation of classical NAs (Fig. 4.2b) which make them difficult to be followed precisely (Wang et al. 2016).
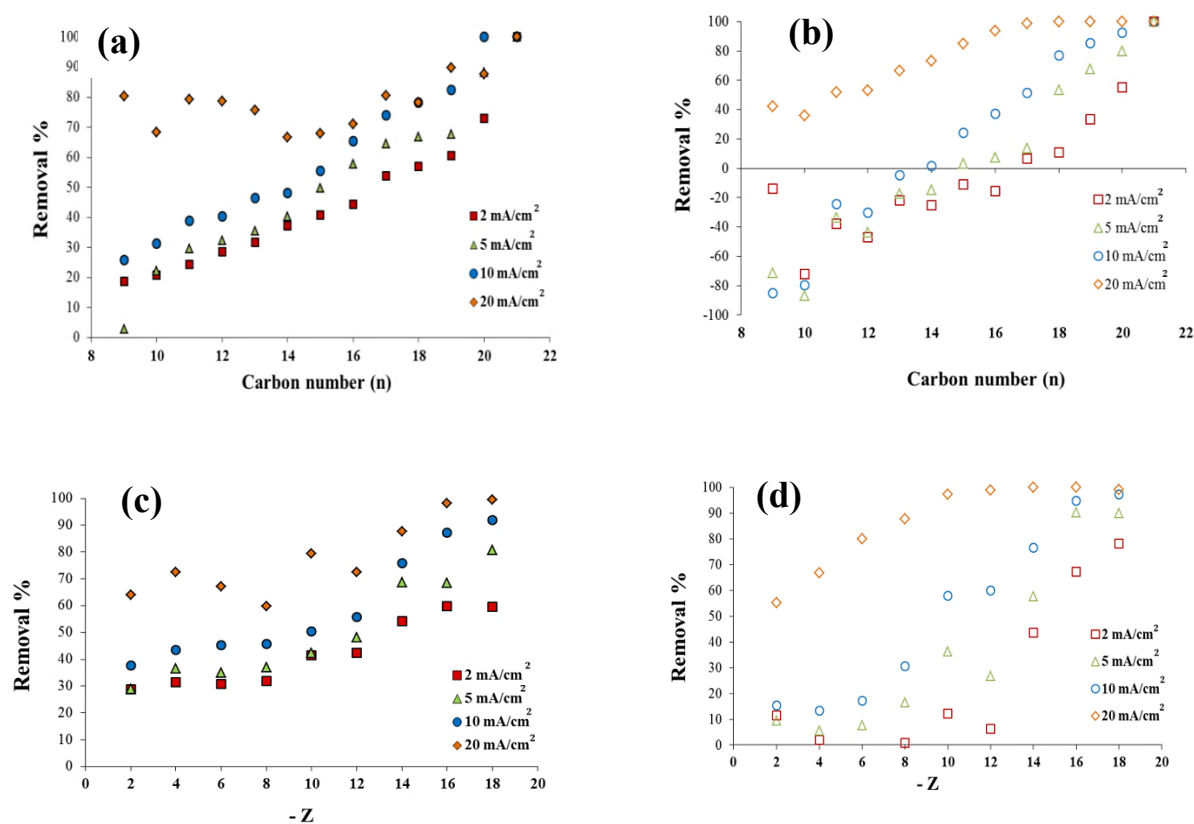
Figure 4.5 Classical-NAs removal after 90 min of EO by (a,c) graphite anode and (b,d) DSA as function of (a,b) carbon number (n) distribution and (c,d) hydrogen deficiency.
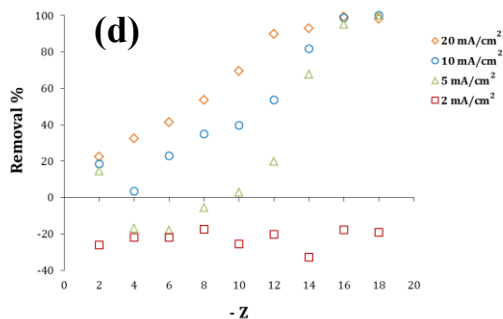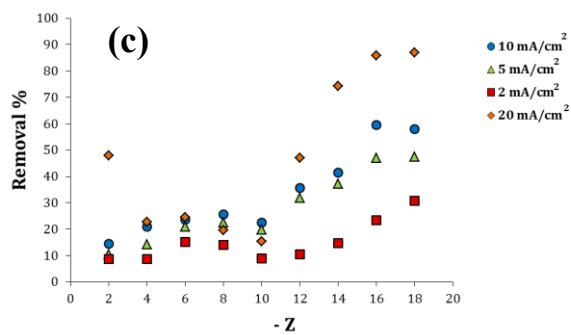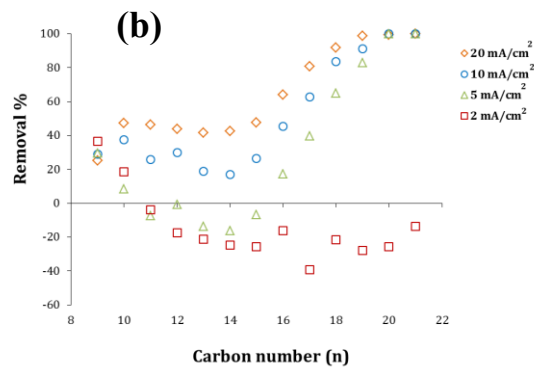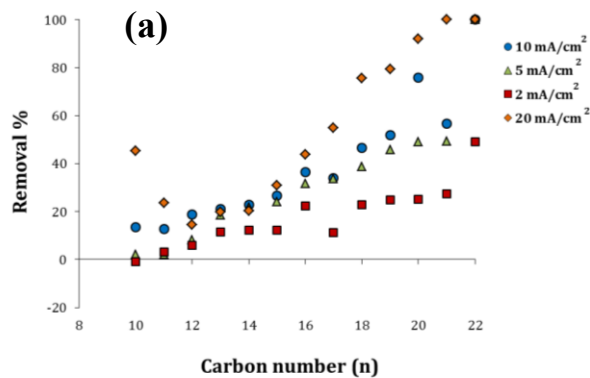
Figure 4.6 Oxidized NAs (O3-) removal after 90 min of EO by (a,c) graphite anode and (b,d) dimensionally stable anode (DSA) as function of (a,b) carbon number (n) distribution and (c,b) hydrogen deficiency.
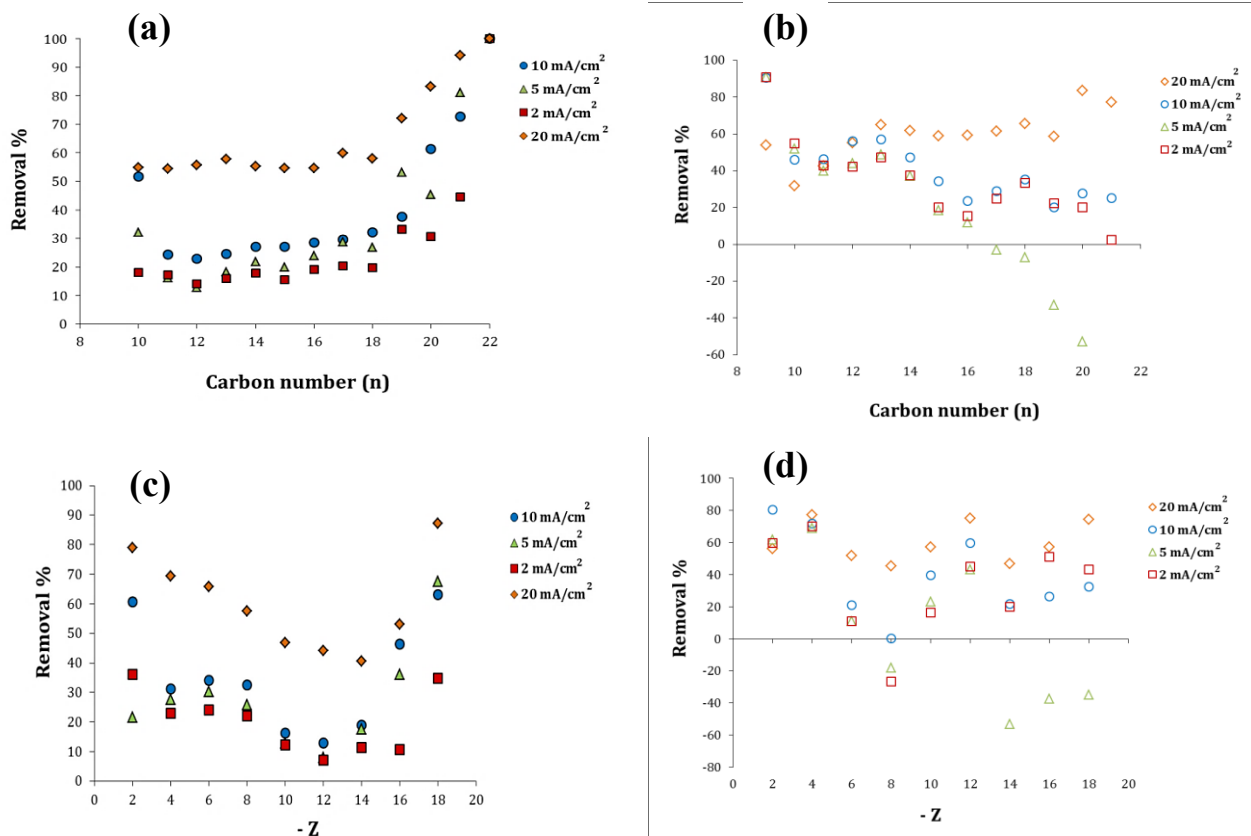
Figure 4.7 Oxidized NAs (O4-) removal after 90 min of EO by (a,c) graphite anode and (b,d) dimensionally stable anode (DSA) as function of (a,b) carbon number (n) distribution and (c,d) hydrogen deficiency.

4.3.2.3 NAs degradation kinetics

In order to investigate the degradation kinetics of OSPW's NAs during EO using graphite anode and DSA, model NA compound, CHA, was used initially. The use of model NA was because of the complex nature of the NA mixture in OSPW and that some NAs will be generated while the other degraded during EO, as was shown earlier. CHA was chosen for this purpose because it is a simple monocyclic NA that has been studied extensively for oxidation of NAs by different AOPs (Afzal et al. 2012, Shu et al. 2014, Zhang et al. 2017, de Oliveira Livera et al. 2018, Fang et al. 2018). As can be seen in Fig. 4.8, the degradation

of CHA by EO followed clear pseudo-first order kinetics for both of graphite and DSA and under the different applied current densities. The degradation rate increased with increasing the applied current density and the rate for graphite anode was always higher than DSA (Fig. 4.8). It should be noted that at 5mA/cm^2 there was no degradation for CHA by DSA and at 20mA/cm^2 the removal by graphite was still higher than DSA. This behaviour was different than that obtained for OSPW where DSA was able to achieve degradation of NAs at 5mA/cm^2 and performed better than graphite at 20mA/cm^2 (Fig. 4.2). This difference can be explained by considering that CHA is a simple monocyclic compound, which means it will be less reactive toward oxidation by DSA which is more effective in degrading the polycyclic NAs as discussed in the previous section. Based on the fit for the pseudo-first order degradation kinetics, the rate constants for the degradation of classical NAs in OSPW have been estimated for graphite and DSA at 10 and 20 mA/cm^2 (Fig. 4.9). As can be seen in Fig. 4.9, the rate constants increased with the increase in carbon and –Z numbers. Some compounds were generated instead of being degraded.
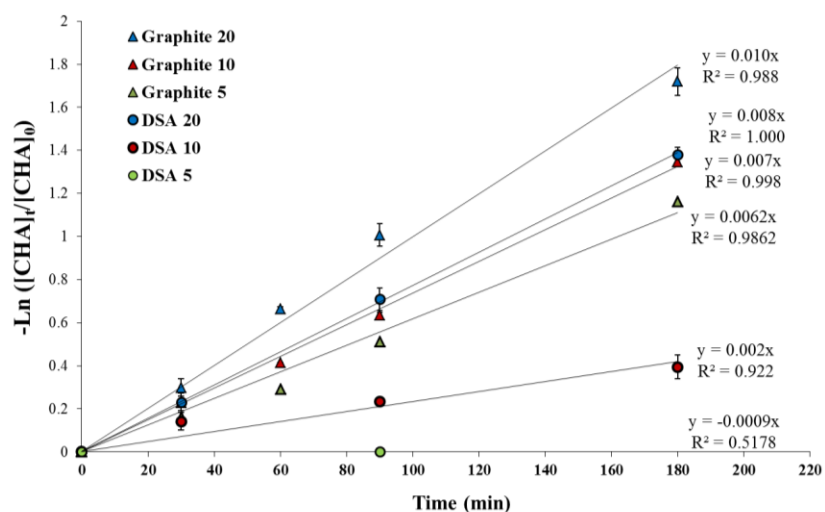
Figure 4.8 Degradation of Cyclohexanoic acid (CHA) by EO on graphite anode and DSA at different current densities; 5, 10 and 20 mA/cm^2 (50 mM NaCl electrolyte and pH 7).
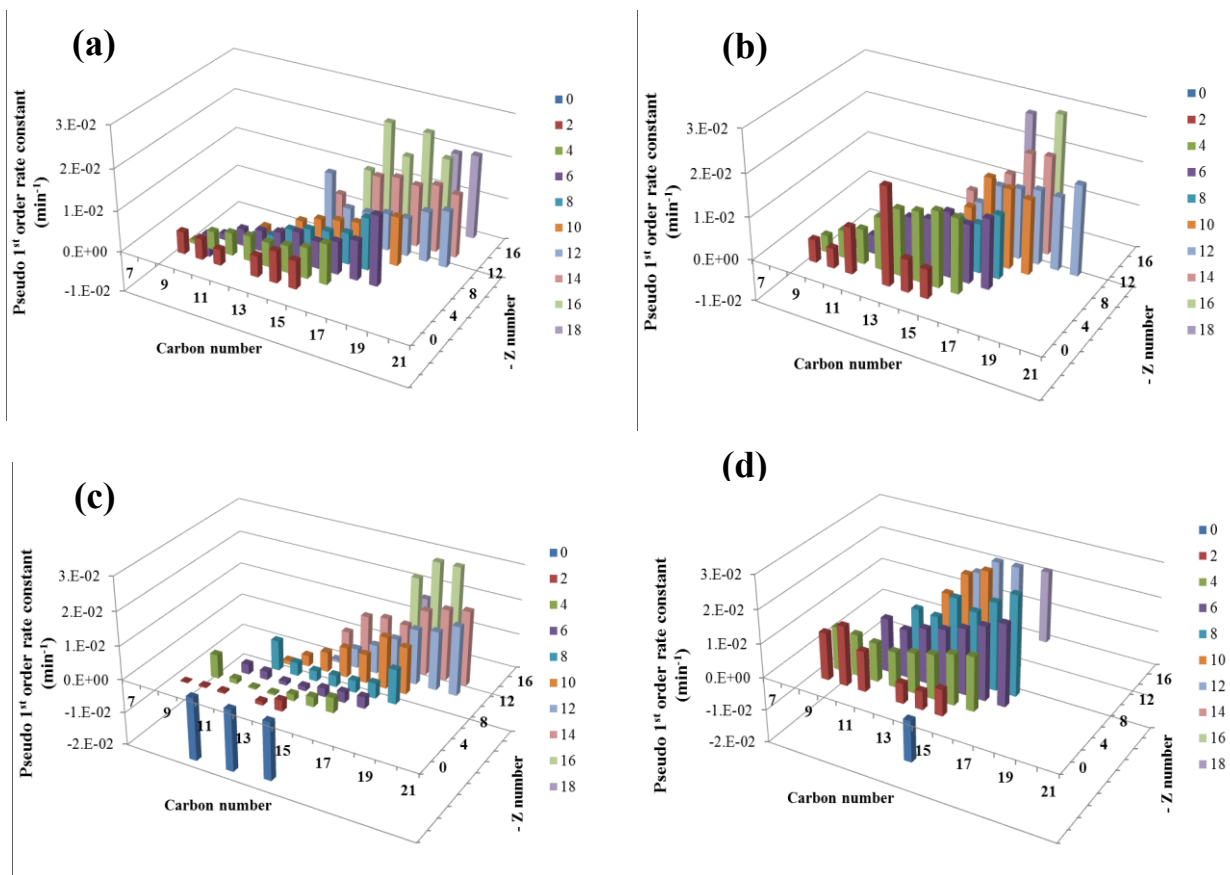
Figure 4.9 Estimated pseudo-first order rate constant for classical-NAs degradation by EO;

(a) graphite anode at 10 mA/cm^2; (b) graphite anode at 20 mA/cm^2; (c) DSA at 10 mA/cm^2;

(d) DSA at 20 mA/cm^2.

4.3.3 Current efficiency and energy consumption

The current efficiency and the specific energy consumption are very important parameters

for comparing the removal performance for different anode materials. General current

efficiency (GCE) represents the electrical charge consumed for the oxidation of organics as

percentage of the total charge consumed during electrolysis that can be calculated using Eq.

(4.1) (Panizza and Cerisola 2009, Kumar et al. 2015). As can be seen in Fig. 4.10a, the

current efficiency of EO using graphite was always higher than that of DSA. The current

efficiency in the case of graphite decreased steadily with increasing the applied current (Fig.

142

4.10a) which can be attributed to parasitic reactions such as oxygen evolution and carbon oxidation that become more prevalent as the current density increase (Panizza and Cerisola 2009, Qiao et al. 2018). For DSA, on the other hand, the efficiency increased slightly when the current density increased from 2 to 5 mA/cm^2, but after that it showed the same decreasing trend as graphite (Fig. 4.10a). The slight increase in the efficiency for DSA in the beginning can be explained by difference oxidation behaviour in the case of DSA compared to graphite, therefore, DSA might require higher potentials to generate enough oxidants.

The specific energy consumption (SEC) represents the amount of energy consumed in (kWh) per every removed g of NAs and can be calculated using Eq. (4.2) (Panizza and Cerisola 2009, Kumar et al. 2015). As can be seen in Fig. 4.10b, SEC increased with the increase in applied current density which is a result of the reduction in current efficiency due to the parasitic reactions. Graphite maintained lower SEC at most of the current density except at 20 mA/cm^2 where DSA was lower. This behaviour was different than the case of GEC, but it can be explained by considering that the COD removal is used for estimating GEC and not NA removal (Eq. (4.1)).

(a)

(b)
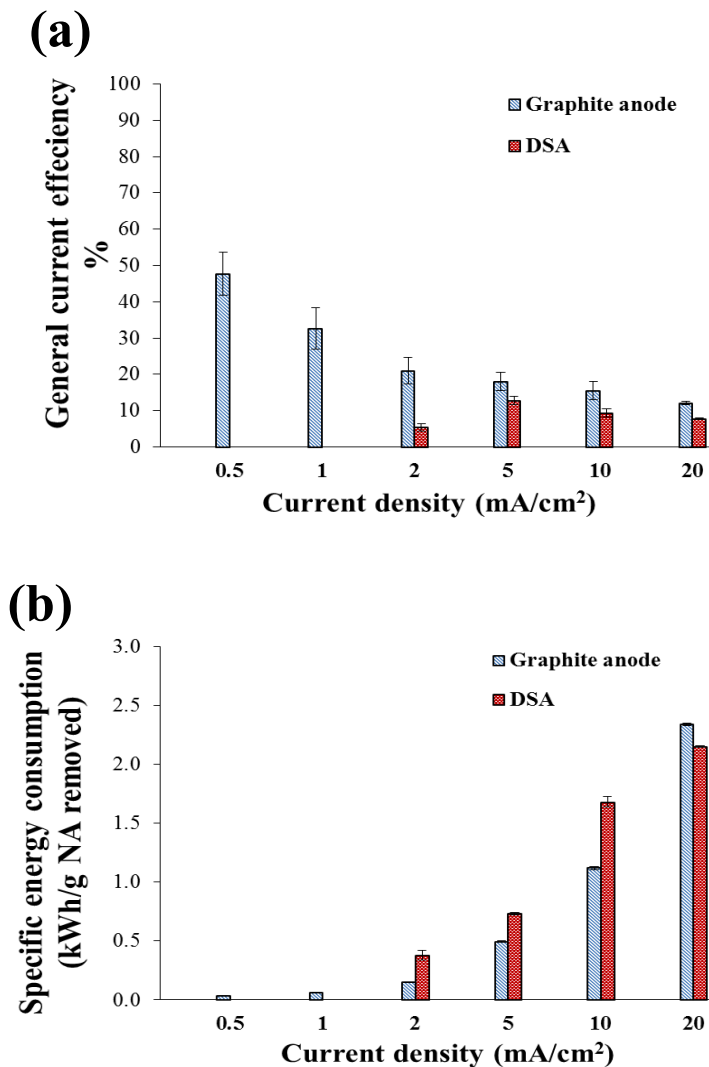
Figure 4.10 (a) General current efficiency and (b) specific energy consumption for the treatment of OSPW by using graphite anode and DSA.

4.3.4 Fate of aromatic organics in OSPW

Another important organic fraction in the matrix of OSPW is the aromatic fraction. The aromatic compounds in OSPW, despite their relative lower concentrations compared to the aliphatic NAs, were found to have considerable contribution to the toxicity of OSPW (Frank et al. 2009, Reinardy et al. 2013, Yue et al. 2015). Synchronous fluorescence spectra (SFS) analysis was used to investigate the removal of aromatics in OSPW (Shu et al. 2014,

Zhang et al. 2015, Wang et al. 2016). As shown in Fig. 4.11, the SFS analysis for the raw OSPW sample showed the existence of three distinct peaks; at 273 nm (I), 317 nm (II) and 325 nm which are associated with single-ring aromatics, two fused aromatic rings, and three fused aromatic rings, respectively (Shu et al. 2014, Zhang et al. 2015, Wang et al. 2016). Single-ring aromatics were the predominant aromatics in OSPW, indicated by the highest peak intensity, which was similar to the previously reported studies (Shu et al. 2014, Zhang et al. 2015).

EO was able to successfully degrade the aromatic fraction in OSPW and the removal rate increased with the increase in the applied current density for both anodes (Fig. 4.11 and 4.12). For EO by graphite anode, the removal of the three types of aromatics was relatively close with two aromatic rings compounds having slightly higher removal rates reaching a maximum removal of 74.6% at current density of 20 mA/cm^2 (Fig. 4.12a). This lower selectivity toward the number of rings was similar to that observed for classical-NAs in section (3.2.3), confirming that graphite anode reactivity increased with increasing the cyclicity no matter whether the rings were aliphatic or aromatic. It should also be noted that increase in the removal rate for aromatics by graphite anode with the increase in the applied density was slight and different than that observed for NAs. This difference, however, can be explained by considering that the abundance of aromatics in the OSPW sample is low compared to NAs.

The performance of DSA for aromatics degradation, on the other side, showed a different trend than the case of graphite anode (Fig. 4.12a and 4.12b). EO using DSA was able to achieve complete removals for two and three rings aromatics and 93.0% removal for single ring aromatics at current density of 20 mA/cm^2. There was a clear increase in the removal

145

rate with the increase in the number of rings (Fig. 4.12b), similar to the trend observed for NAs (Fig. 4.5d), which confirmed the higher reactivity for DSA toward the more cyclic compounds. Contrary to the case of graphite anode, the aromatics removal increased steadily with increasing the applied current density and was higher than that obtained for NAs, despite the higher abundance of NAs, indicating that the oxidants generated at DSA anode were more reactive toward aromatic rings compared to aliphatic ones. This can be explained by the preference of reactive oxygen radicals for aromatics ring-opening through the dioxetane at electron-rich regions available in the aromatic rings (de Oliveira Livera et al. 2018).
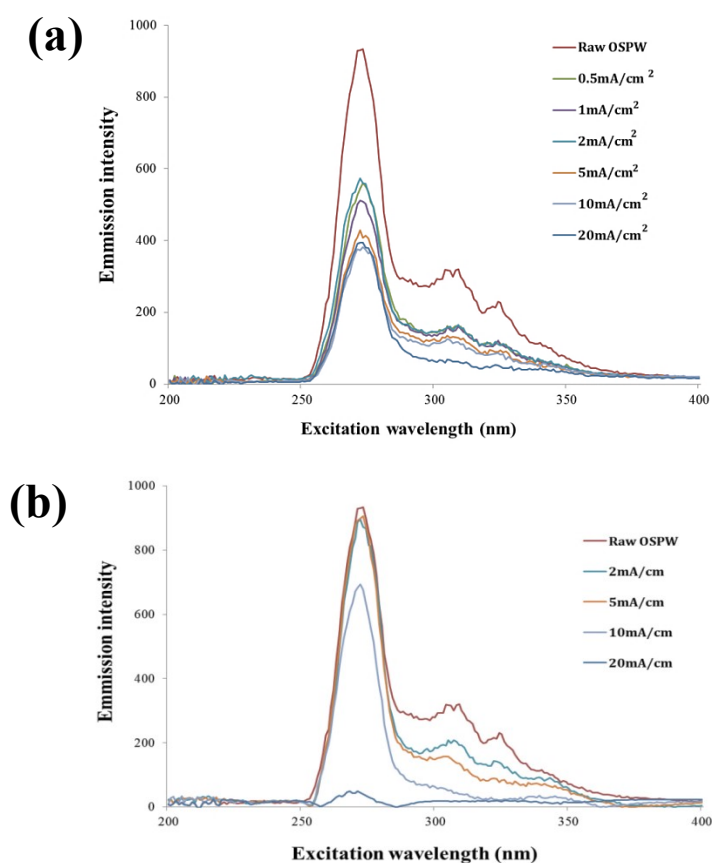
Figure 4.11 SFS analysis for aromatic fluorescing compounds in OSPW after EO by (a) graphite anode and (b) DSA.

146
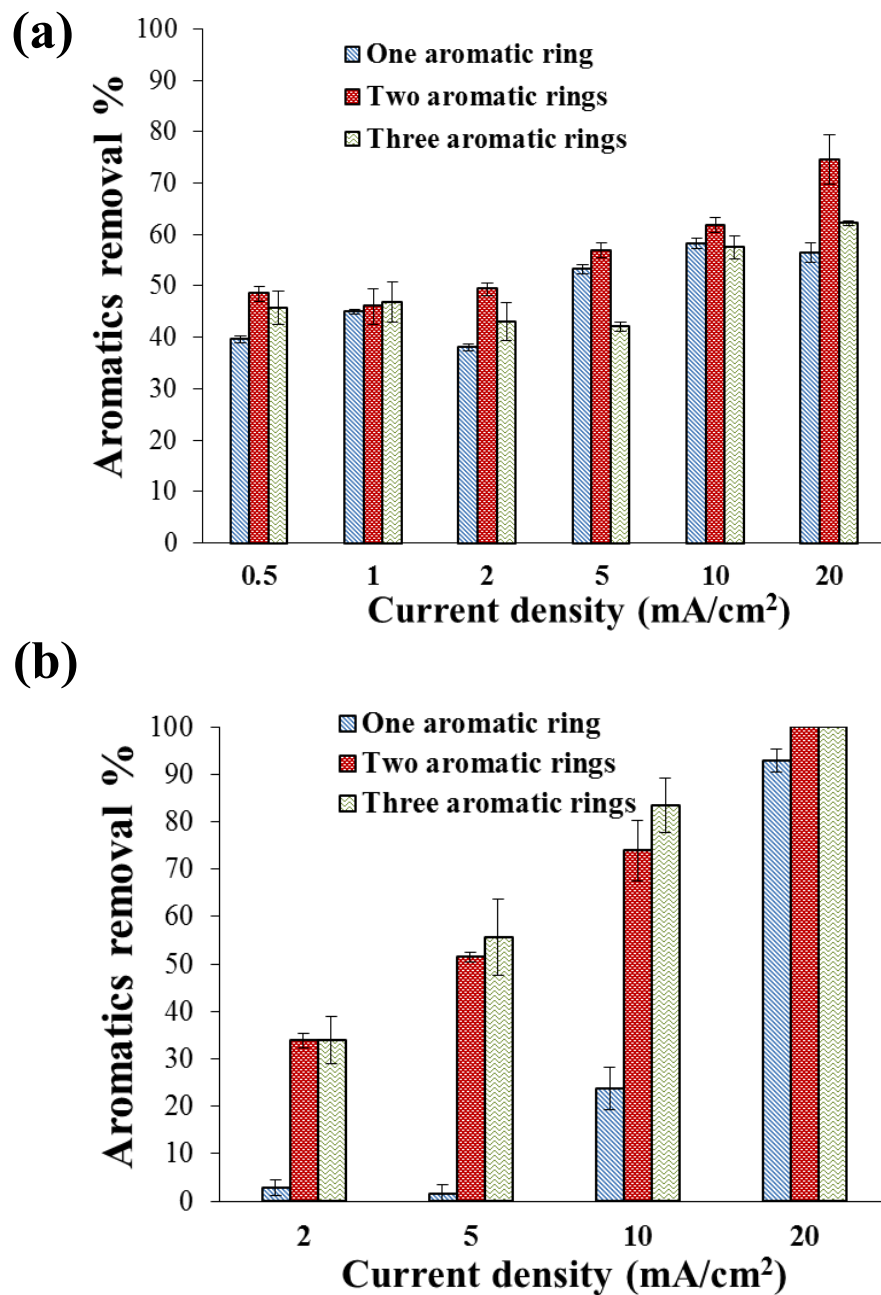
Figure 4.12 Semi-quantitative analysis for the removal of aromatic fluorescing compounds

by EO using (a) graphite anode and (b) DSA.

4.4 Conclusions

This chapter investigated the effectiveness of applying EO using graphite and DSA anodes for the degradation of the recalcitrant organics in OSPW and compared their performances. EO using graphite anode was able to reduce the COD, AEF, classical and oxidized NAs and aromatics in OSPW even at current density as low as 0.5 mA/cm^2. The removal of organics by DSA, on the other hand, did not occur until the current density reached 2 mA/cm^2. The removal of classical NAs by both graphite and DSA increased with the increase in the applied current density and was always higher than the removal of AEF. Graphite anode maintained higher removals of NAs (classical and oxidized) and AEF at most of the applied current densities, except when the applied current reached 20 mA/cm^2 (anode potential > 7V) where DSA showed superior removals. The degradation of NAs by both anodes followed pseudo-first order kinetics. The reactivity of NAs toward oxidation on both anodes increased with the increase of the carbon number. During EO using DSA, low-carbon number NAs were generated as byproducts of the oxidation of high-carbon NAs. EO by graphite was found to be less sensitive towards cyclicity of NAs compared to DSA. Graphite anode maintained higher current efficiency at all applied current densities. Both anodes were able to remove the aromatic compounds with DSA being more selective toward aromatics especially those with multiple aromatic rings. DSA was able to achieve complete removals of two and three rings aromatics and 93.0% removal of single ring aromatics at current density of 20 mA/cm^2 after 90 min of electrolysis, while the highest removal by graphite was 74.6% at similar electrolysis time. For the treatment of OSPW by EO, the results from this chapter indicated that graphite anode can be a more effective

148

option if used at lower current densities. DSA, on the other hand, can be more superior to graphite at higher applied current densities.

4.5 References

Abdalrhman, A. S., S. O. Ganiyu, and M. Gamal El-Din. 2019a. Degradation kinetics and structure-reactivity relation of naphthenic acids during anodic oxidation on graphite electrodes. Chemical Engineering Journal **370**:997-1007.

Abdalrhman, A. S., Y. Zhang, and M. Gamal El-Din. 2019b. Electro-oxidation by graphite anode for naphthenic acids degradation, biodegradability enhancement and toxicity reduction. Science of The Total Environment **671**:270-279.

Afzal, A., P. Drzewicz, L. A. Pérez-Estrada, Y. Chen, J. W. Martin, and M. Gamal El-Din. 2012. Effect of Molecular Structure on the Relative Reactivity of Naphthenic Acids in the UV/H2O2 Advanced Oxidation Process. Environmental Science & Technology **46**:10727-10734.

Alberts, M. E., G. Chua, and D. G. Muench. 2019. Exposure to naphthenic acids and the acid extractable organic fraction from oil sands process-affected water alters the subcellular structure and dynamics of plant cells. Science of The Total Environment **651**:2830-2844.

Allen, E. W. 2008a. Process water treatment in Canada's oil sands industry: I. Target pollutants and treatment objectives. Journal of Environmental Engineering and Science **7**:123-138.

Allen, E. W. 2008b. Process water treatment in Canada's oil sands industry: II. A review of emerging technologies. Journal of Environmental Engineering and Science **7**:499-524.

Brillas, E., I. Sirés, and M. A. Oturan. 2009. Electro-Fenton Process and Related Electrochemical Technologies Based on Fenton's Reaction Chemistry. Chemical Reviews **109**:6570-6631.

Brown, L. D. and A. C. Ulrich. 2015. Oil sands naphthenic acids: A review of properties, measurement, and treatment. Chemosphere **127**:276-290.

de Klerk, A., M. R. Gray, and N. Zerpa. 2014. Chapter 5 - Unconventional Oil and Gas: Oilsands. Pages 95-116 *in* T. M. Letcher, editor. Future Energy (Second Edition). Elsevier, Boston.

de Oliveira Livera, D., T. Leshuk, K. M. Peru, J. V. Headley, and F. Gu. 2018. Structure-reactivity relationship of naphthenic acids in the photocatalytic degradation process. Chemosphere **200**:180-190.

Deborde, M. and U. von Gunten. 2008. Reactions of chlorine with inorganic and organic compounds during water treatment—Kinetics and mechanisms: A critical review. Water Research **42**:13-51.

Dong, T., Y. Zhang, M. S. Islam, Y. Liu, and M. Gamal El-Din. 2015. The impact of various ozone pretreatment doses on the performance of endogenous microbial communities for the remediation of oil sands process-affected water. International Biodeterioration & Biodegradation **100**:17-28.

Fang, Z., P. Chelme-Ayala, Q. Shi, C. Xu, and M. Gamal El-Din. 2018. Degradation of naphthenic acid model compounds in aqueous solution by UV activated persulfate: Influencing factors, kinetics and reaction mechanisms. Chemosphere **211**:271-277.

Frank, R. A., K. Fischer, R. Kavanagh, B. K. Burnison, G. Arsenault, J. V. Headley, K. M. Peru, G. V. D. Kraak, and K. R. Solomon. 2009. Effect of Carboxylic Acid Content on

the Acute Toxicity of Oil Sands Naphthenic Acids. Environmental Science & Technology **43**:266-271.

Gamal El-Din, M., H. Fu, N. Wang, P. Chelme-Ayala, L. Pérez-Estrada, P. Drzewicz, J. W. Martin, W. Zubot, and D. W. Smith. 2011. Naphthenic acids speciation and removal during petroleum-coke adsorption and ozonation of oil sands process-affected water. Science of The Total Environment **409**:5119-5125.

Giesy, J. P., J. C. Anderson, and S. B. Wiseman. 2010. Alberta oil sands development. Proceedings of the National Academy of Sciences **107**:951.

Kannel, P. R. and T. Y. Gan. 2012. Naphthenic acids degradation and toxicity mitigation in tailings wastewater systems and aquatic environments: A review. Journal of Environmental Science and Health, Part A **47**:1-21.

Klamerth, N., J. Moreira, C. Li, A. Singh, K. N. McPhedran, P. Chelme-Ayala, M. Belosevic, and M. Gamal El-Din. 2015. Effect of ozonation on the naphthenic acids' speciation and toxicity of pH-dependent organic extracts of oil sands process-affected water. Science of The Total Environment **506-507**:66-75.

Kumar, S., S. Singh, and V. C. Srivastava. 2015. Electro-oxidation of nitrophenol by ruthenium oxide coated titanium electrode: Parametric, kinetic and mechanistic study. Chemical Engineering Journal **263**:135-143.

Li, C., L. Fu, J. Stafford, M. Belosevic, and M. Gamal El-Din. 2017. The toxicity of oil sands process-affected water (OSPW): A critical review. Science of The Total Environment **601-602**:1785-1802.

Martínez-Huitle, C. A. and M. Panizza. 2018. Electrochemical oxidation of organic pollutants for wastewater treatment. Current Opinion in Electrochemistry **11**:62-71.

Martínez-Huitle, C. A., M. A. Rodrigo, I. Sirés, and O. Scialdone. 2015. Single and Coupled Electrochemical Processes and Reactors for the Abatement of Organic Water Pollutants: A Critical Review. Chemical Reviews **115**:13362-13407.

Masliyah, J., Z. J. Zhou, Z. Xu, J. Czarnecki, and H. Hamza. 2004. Understanding Water-Based Bitumen Extraction from Athabasca Oil Sands. The Canadian Journal of Chemical Engineering **82**:628-654.

Meshref, M. N. A., N. Klamerth, M. S. Islam, K. N. McPhedran, and M. Gamal El-Din. 2017. Understanding the similarities and differences between ozone and peroxone in the degradation of naphthenic acids: Comparative performance for potential treatment. Chemosphere **180**:149-159.

Moreira, F. C., R. A. R. Boaventura, E. Brillas, and V. J. P. Vilar. 2017. Electrochemical advanced oxidation processes: A review on their application to synthetic and real wastewaters. Applied Catalysis B: Environmental **202**:217-261.

Panizza, M. and G. Cerisola. 2009. Direct And Mediated Anodic Oxidation of Organic Pollutants. Chemical Reviews **109**:6541-6569.

Qiao, M.-X., Y. Zhang, L.-F. Zhai, and M. Sun. 2018. Corrosion of graphite electrode in electrochemical advanced oxidation processes: Degradation protocol and environmental implication. Chemical Engineering Journal **344**:410-418.

Quinlan, P. J. and K. C. Tam. 2015. Water treatment technologies for the remediation of naphthenic acids in oil sands process-affected water. Chemical Engineering Journal **279**:696-714.

Reinardy, H. C., A. G. Scarlett, T. B. Henry, C. E. West, L. M. Hewitt, R. A. Frank, and S. J. Rowland. 2013. Aromatic Naphthenic Acids in Oil Sands Process-Affected Water,

Resolved by GCxGC-MS, Only Weakly Induce the Gene for Vitellogenin Production in Zebrafish (Danio rerio) Larvae. Environmental Science & Technology **47**:6614-6620.

Rueffer, M., D. Bejan, and N. J. Bunce. 2011. Graphite: An active or an inactive anode? Electrochimica Acta **56**:2246-2253.

Särkkä, H., A. Bhatnagar, and M. Sillanpää. 2015. Recent developments of electro-oxidation in water treatment — A review. Journal of Electroanalytical Chemistry **754**:46-56.

Scott, A. C., M. D. Mackinnon, and P. M. Fedorak. 2005. Naphthenic Acids in Athabasca Oil Sands Tailings Waters Are Less Biodegradable than Commercial Naphthenic Acids. Environmental Science & Technology **39**:8388-8394.

Shu, Z., C. Li, M. Belosevic, J. R. Bolton, and M. Gamal El-Din. 2014. Application of a Solar UV/Chlorine Advanced Oxidation Process to Oil Sands Process-Affected Water Remediation. Environmental Science & Technology **48**:9692-9701.

Wang, C., N. Klamerth, S. A. Messele, A. Singh, M. Belosevic, and M. Gamal El-Din. 2016. Comparison of UV/hydrogen peroxide, potassium ferrate(VI), and ozone in oxidizing the organic fraction of oil sands process-affected water (OSPW). Water Research **100**:476-485.

Xue, J., C. Huang, Y. Zhang, Y. Liu, and M. Gamal El-Din. 2018. Bioreactors for oil sands process-affected water (OSPW) treatment: A critical review. Science of The Total Environment **627**:916-933.

Yue, S., B. A. Ramsay, J. Wang, and J. Ramsay. 2015. Toxicity and composition profiles of solid phase extracts of oil sands process-affected water. Science of The Total Environment **538**:573-582.

Zhang, Y., N. Klamerth, P. Chelme-Ayala, and M. Gamal El-Din. 2017. Comparison of classical fenton, nitrilotriacetic acid (NTA)-Fenton, UV-Fenton, UV photolysis of Fe-NTA, UV-NTA-Fenton, and UV-H2O2 for the degradation of cyclohexanoic acid. Chemosphere **175**:178-185.

Zhang, Y., K. N. McPhedran, and M. Gamal El-Din. 2015. Pseudomonads biodegradation of aromatic compounds in oil sands process-affected water. Science of The Total Environment **521-522**:59-67.

Zöllig, H., C. Fritzsche, E. Morgenroth, and K. M. Udert. 2015. Direct electrochemical oxidation of ammonia on graphite as a treatment option for stored source-separated urine. Water Research **69**:284-294.

5. LOW-CURRENT ELECTRO-OXIDATION AS A PRE-TREATMENT STAGE TO BIOLOGICAL PROCESS FOR THE DEGRADATION OF RECALCITRANT ORGANICS IN REAL OIL SANDS PROCESS WATER[1]

5.1 Introduction

The extraction of the bitumen from the mined oil sand ores in northern Alberta, Canada, requires huge volumes of hot and caustic water and leads to the generation of large amounts of process water known as oil sands process water (OSPW). Following the currently implemented zero liquid-discharge approach, OSPW is sent to be stored in tailings ponds (Allen 2008). Tremendous volumes of OSPW is currently impounded in tailings ponds, > 10^6 m^3, waiting to be remediated in order to be released into the receiving environment (Scott et al. 2005, Klamerth et al. 2015, Li et al. 2017, Xue et al. 2018). The treatment of OSPW is considered a serious challenge facing the oil sands industry partially because of the huge accumulated amounts, but most importantly due to the recalcitrant nature of the organic pollutants in OSPW (Scott et al. 2005, Xue et al. 2018). OSPW is also known to be toxic to a wide range of aquatic and terrestrial organisms (Li et al. 2017, Xue et al. 2018). Among the different pollutants in OSPW, a group of carboxylic acids known as naphthenic acids (NAs), has attracted most of the attention as they are very recalcitrant, they accounts for almost half of the organic fraction of OSPW, and they have been constantly considered to be the main contributor to the toxicity of OSPW (Scott et al. 2005, Klamerth et al. 2015,

---

[1] A version of this chapter will be submitted to a peer-review journal as: Abdalrhman, A. S., Y. Zhang, and M. Gamal El-Din. Low-current electro-oxidation accelerates the biodegradation of the recalcitrant organics in oil sands process water. 2019 Water Research.

Li et al. 2017, Xue et al. 2018). NAs are a group of alkyl-substituted acyclic, cyclic and polycyclic carboxylic acids that follow the general formula $C_nH_{(2n+Z)}O_x$ with n being the number of carbons in the structure, Z indicates the hydrogen deficiency (Z is zero or a negative even integer) caused by rings formation and/or double bonds introduction, and x refers to the oxygen atoms in the structure, where x=2 for classical NAs and x≥3 for oxidized NAs (Meshref et al. 2017a, Xue et al. 2018). This formula has also been expanded to include nitrogen and sulphur containing NAs in addition to NAs with more than one carboxyl functional groups (Kannel and Gan 2012, Meshref et al. 2017a).

Different physical, biological and chemical processes have been investigated for the treatment of OSPW and degradation of NAs (Brown and Ulrich 2015, Quinlan and Tam 2015, Xue et al. 2018). Despite the recalcitrant and toxic nature of the organics in OSPW, as discussed earlier, biological treatment by indigenous microbial communities from the tailing ponds was investigated more frequently (Clemente et al. 2004, Martin et al. 2010, Brown and Ulrich 2015, Quinlan and Tam 2015, Xue et al. 2018). Biological treatments have been well-studied for decades, and they have the great advantage of being cost effective which, so far, could not be overcome by any other treatment (Ganzenko et al. 2014). Although they were able to achieve NA degradation, but, similar to many other toxic and refractory organic pollutants, the biodegradation of NAs was very slow and inefficient with biodegradation half-lives that can reach several years (Scott et al. 2005, Martin et al. 2010, Xue et al. 2018).

Different advanced oxidation processes (AOPs) were applied successfully for OSPW treatment at the bench-scale level, including ozonation (Wang et al. 2013, Klamerth et al. 2015, Meshref et al. 2017a),UV/chlorine (Shu et al. 2014), UV/H$_2$O$_2$ (Wang et al. 2016b),

UV/persulfate (Fang et al. 2018), photo-Fenton (Zhang et al. 2017) in addition to other AOPs (Brown and Ulrich 2015, Quinlan and Tam 2015). However, the practicality of most of these AOPs at large scale was under serious question either because of the high required chemical doses or due to the natural properties of OSPW such as turbidity and pH which make Fenton and UV-based AOPs less practical (Allen 2008, Brown and Ulrich 2015, Zhang et al. 2017, Fang et al. 2018). Number of studies have proposed the use of ozonation as pre-treatment before biodegradation as a more cost effective treatment option (Scott et al. 2005, Martin et al. 2010, Brown and Ulrich 2015, Dong et al. 2015). Despite the successful results obtained from this combination, the required ozone doses were still high and not economically viable (Martin et al. 2010, Dong et al. 2015).

Electro-oxidation (EO) has shown to be effective for the degradation of many different recalcitrant organic pollutants (Panizza and Cerisola 2009, Kapałka et al. 2010, Martínez-Huitle et al. 2015, Moreira et al. 2017, Martínez-Huitle and Panizza 2018, Abdalrhman et al. 2019b). The performance and selectivity of EO for organics degradation depend greatly on the anode material (Panizza and Cerisola 2009, Kapałka et al. 2010, Martínez-Huitle et al. 2015, Martínez-Huitle and Panizza 2018). Anode materials such as graphite and Ti/ RuO_2 are known as active anodes and can only promote partial degradation of organics. On the other hand, anodes such as doped lead oxides and boron-doped diamond (BDD) are classified as inactive anodes and can unselectively achieve mineralization of organics (Panizza and Cerisola 2009, Kapałka et al. 2010, Martínez-Huitle et al. 2015, Martínez-Huitle and Panizza 2018). Among all the used anode materials for EO, graphite is known to be one of the cheapest anodes materials (Panizza and Cerisola 2009, Kapałka et al. 2010). Graphite anode has previously been used successfully for the degradation of simple model

NA compounds and showed that it can achieve degradation even at current density as low as 0.2 mA/cm^2 (Abdalrhman et al. 2019a).

The main objective of this study was to investigate the hypothesis that EO of OSPW using graphite anode and under low-current density conditions will selectively degrade the most bio-persistent fraction of NAs. Therefore, low-current EO by inexpensive graphite electrodes will lead to improved biodegradability of OSPW's NAs while maintain the economic viability of process. This hypothesis was based on the knowledge that EO by graphite is more selective toward cyclic NAs and those with branches (Abdalrhman et al. 2019a) which are at the same time known to be more recalcitrant toward biodegradation (Han et al. 2008, Misiti et al. 2014). The study investigated this hypothesis through treating OSPW by EO under different current densities and then incubating untreated and EO-treated OSPW with native microbial consortium from oil sands tailing ponds. The fate of different organic classes, biodegradation kinetics, oxidation byproducts and the change in the microbial community dynamics were examined.

5.2 Materials and methods

5.2.1 OSPW and chemicals

OSPW used in this study was collected from active tailings pond in Fort McMurray, Alberta, Canada, and stored in a cold storage room at 4 °C. The characteristics of raw OSPW are presented Table 5.1. The internal standard, myristic acid-1-^{13}C, was purchased from Sigma-Aldrich (Oakville, ON, Canada).

5.2.2 Electro-oxidation experiment

EO treatment was conducted using cylindrical undivided batch reactor of 600 mL total size. The reactor was continuously stirred with a magnetic bar to maintain effective mass transport. Graphite plates obtained from Wale Apparatus, (PA, US) were used as anode and cathode and were positioned parallel to each other at distance of 1.2 cm. The effective anode surface area was 42 cm^2. The electric field was applied under galvanostatic conditions using DC power station (9130, B&K Precision, California, US) and the change in voltage was continuously monitored. Control reactor with an identical setup but without electric field was used to exclude any removals by adsorption or volatilization.

Table 5.1 Water quality of untreated OSPW.

Parameter	Value
pH	8.5
Conductivity (mS/cm)	3.1±0.1
Alkalinity (mg/L as $CaCO_3$)	554±6
Turbidity (NTU)	107
UV_{254} (cm^{-1})	0.597±0.01
TDS (mg/L)	2620±24
Organic parameters	
COD (mg/L)	188 ± 5.6
DOC (mg/L)	49.9±2.1
Classical Naphthenic acids (NAs) (mg/L)	24.36
NAs+O (mg/L)	16.32
NAs+O_2 (mg/L)	17.81
NAs+O_3 (mg/L)	3.83
Acid extractible fraction (AEF) (mg/L)	66.45

5.2.3 Biological incubation

Batch biodegradation incubations for the raw and EO-treated OSPW samples were conducted under aerobic condition for 40 days to evaluate the biodegradability of samples. The microbial consortium used for incubation was obtained from a bioreactor that fed for 2 years with untreated OSPW and contained microbial communities native to oil sand tailings. Erlenmeyer flasks (500 mL) were used as incubation reactors with effective volume of 300 mL. The incubations were conducted in triplicates and sterile (heat-killed) controls were included. Mixed liquor from the bioreactor was collected and a volume of 2 mL was centrifuged, washed twice with 0.5 M phosphate buffer and then added to incubation reactors to result in identical initial biomass concentration of 25 mg MLVSS/L. Nutrients salt medium (Bushnell Haas Broth) containing (g/ L): 1 KH_2PO_4; 1 Na_2HPO_4; 0.5 NH_4NO_3; 0.29 $MgSO_4.7H_2O$; 0.02 $CaCl_2.2H_2O$; 0.002 $FeCl_2$; 0.002 $MnSO_4.2H_2O$ was used to provide the essential needed nutrients but no additional carbon source was added. A screwcap was used to close the flask to prevent evaporation of water. The caps were loosened every day for a short period to allow fresh air to flow in to replenish oxygen. Incubations were carried out under aerobic conditions with dissolved oxygen (DO) levels maintained above 4 mg/L at all times by putting the flasks on a shaker at 200 rpm and at controlled temperature of 21°C. Samples were collected from each reactor for NAs and AEF analysis on days 0, 13, 27, and 40.

5.2.4 Water quality analyses

The conductivity and pH of OSPW samples were measured using a multi-channel pH/conductivity/ion (Accumet excel XL60; Fisher Scientific). Chemical oxygen demand (COD) was measured by HACH COD reagent kits (TNT821, LR, Germany) using DR3900

spectrophotometer (HACH, Germany). Treated samples were filtered through 0.45 μm nylon filters (Supelco Analytical, PA, USA) prior analysis.

5.2.5 Analytical methods

The concentration of acid extractable fraction (AEF) in OSPW was determined using Fourier transform infrared (FT-IR) spectroscopy (Spectrum 100, PerkinElmer Ltd, Bucks, UK) following a previously used method (Gamal El-Din et al. 2011, Dong et al. 2015, Abdalrhman et al. 2019b). The extraction of AEF was performed 3 times in separation funnels using dichloromethane (DCM) after acidifying the samples to pH 2.0. The extract was then evaporated to dryness and dissolved in a known amount of DCM. The DCM samples were then analyzed for monomeric and dimeric carboxylic- containing organics using FT-IR at absorbance 1743 and 1706 cm^{-1}, respectively (Gamal El-Din et al. 2011).

NA concentration was measured using ultra-performance liquid chromatography time-of-flight mass spectrometry (UPLC TOF-MS). The sample analysis was performed using a high-resolution time-of-flight mass spectrometry TOF-MS (Synapt G2, Waters, MA, USA) on negative electrospray ionization mode and myristic acid-1-^{13}C was used as the internal standard. Chromatographic separation was accomplished using Waters UPLC Phenyl BEH column (Waters, MA, USA). The sample analysis was performed using a high-resolution time-of-flight mass spectrometry TOF-MS (Synapt G2, Waters, MA, USA) on negative electrospray ionization mode and myristic acid-1-^{13}C was used as the internal standard. Sample of a mixture consisting of 500 μL OSPW sample, 100 μL of 4.0 mg/L internal standard (myristic acid-1-^{13}C), and 400 μL methanol was injected into the instrument. The column temperature was set at 50 ºC while the sample temperature was 10 ºC. The mobile phases were: (A) 10 mM ammonium acetate in water and (B) 10 mM ammonium acetate in

50/50 methanol/acetonitrile at a 100 µL/min flow rate. The elution gradient was 1% B during 0–2 min; increased from 1% to 60% B during 2–3 min; then increased to 70% B during 3–7 min; went to 95% B during 7–13 min; went down to 1% B during 13–14 min, and hold 1% B until 20 min to equilibrate the column with a flow rate of 100 µL/min. The data acquisition process was performed using MassLynx (Waters, MA, USA) and data extraction from spectra wasdone using TargetLynx (Waters, MA, USA). The identification of classical NAs (O_2) and oxy-NAs was based on the empirical formula $C_nH_{2n+z}O_x$ (x=2, 3, 4, 5) where n ranged from 7 to 26 and z from 0 to -18.

The ion-mobility spectrometry (IMS) was performed in a 15 cm long ion-mobility cell (Tri-Wave®), using pure nitrogen gas (> 99%) as the drift. A transfer cell was used to collect certain amount of ions and a helium gate was used to control the release of these ions into the ion-mobility cell. The number of ions was known and the difference in the number of ions had a threshold of 5%. An electric field (T-wave) was used to separate the ions by moving them counter currently to the gas flow, leading to the ions being drifted based on the cross collision section (CCS). Drift-Scope ver. was used to control ion mobility separation (IMS).

5.2.6 Microbial characterization

PowerSoil® DNA isolation kit (Mo-Bio Laboratories, CA, USA) was used for the extraction of bacterial DNA following the manufacturer instructions. After extraction, the DNA sample was stored at -20 °C before performing the quantitative polymerase chain reaction (qPCR) analysis. A Bio-Rad CFX96 real-time PCR system (Bio-Rad, ON, CA) was used to conduct the qPCR analysis for total bacterial quantification in the samples

before and after biodegradation. Detailed description of the methods can be found in Appendix A-2.

Illumina MiSeq sequencing was used to further understand the changes in the microbial communities after different EO pre-treatment conditions. The sequencing was performed at Research and Testing Laboratory (Lubbock, TX, USA). Following the DNA extraction, amplification of the V1-V2 hypervariable regions of 16S rRNA genes was done using a forward primer 28F and reverse fusion primer 338R prior to sequencing. After denoising (USEARCH application) and chimera removal (UCHIIME in *de novo* mode), the sequences were clustered into operational taxonomic units (OTU) clusters with 100% identity using USEARCH for taxonomic identification. Detailed description of the methods can be found in Appendix A-3.

5.3 Results and discussion

5.3.1 IMS analysis of EO- treated samples

Ion mobility spectrometry is considered a powerful analytical technique that, in combination with UPLC, can separate different NAs classes in OSPW based on the retention time during UPLC and the drift-gas selectivity (Sun et al. 2014, Wang et al. 2016b). As can be seen in Fig. 1a, the IMS analysis of raw OSPW showed that there was three main NAs clusters; classical NAs, oxidized NAs ($NAs+O_x$), and sulfur containing heteroatomic NAs ($NAs + S$). The oxidized NAs cluster in raw OSPW had the highest intensity indicating that they were the most abundant cluster, which agreed with a number of previous studies (Wang et al. 2013, Sun et al. 2014, Klamerth et al. 2015, Meshref et al. 2017b). The treatment of OSPW by EO at current densities of 0.5, 1 and 10 mA/cm^2

resulted in considerable reductions in all the different clusters (Fig. 5.1). It can be noted that the reduction increased with increasing the applied current density, however, there was no complete removal of any of the clusters even at current density as high as 10 mA/cm^2 (Fig. 5.1d). By comparing the removals based on the change of the intensity before and after EO, we can see that there was no clear trend in terms of selectivity toward specific NAs cluster. This behaviour was different than that observed during OSPW treatment by ozonation (Klamerth et al. 2015, Wang et al. 2016b), ferrate (VI) (Wang et al. 2016a) and perexone (Wang et al. 2016b, Meshref et al. 2017b) where there was a clear selectivity toward the heteroatomic sulfur-containing clusters (NAs + S). This difference in reactivity between the aforementioned processes and EO by graphite can be explained by considering that oxidation during EO using graphite occurs through a generated active oxygen species on the surface of anode which are different than ozone, ferrate or free hydroxyl radicals (Wang et al. 2016b, Abdalrhman et al. 2019a). It showed be noted that IMS is a qualitative measurement, quantification of the classical and oxidized NAs removals can be seen in Fig 5.3a and Fig. 5.4a, respectively, and will be discussed in details in the following sections.
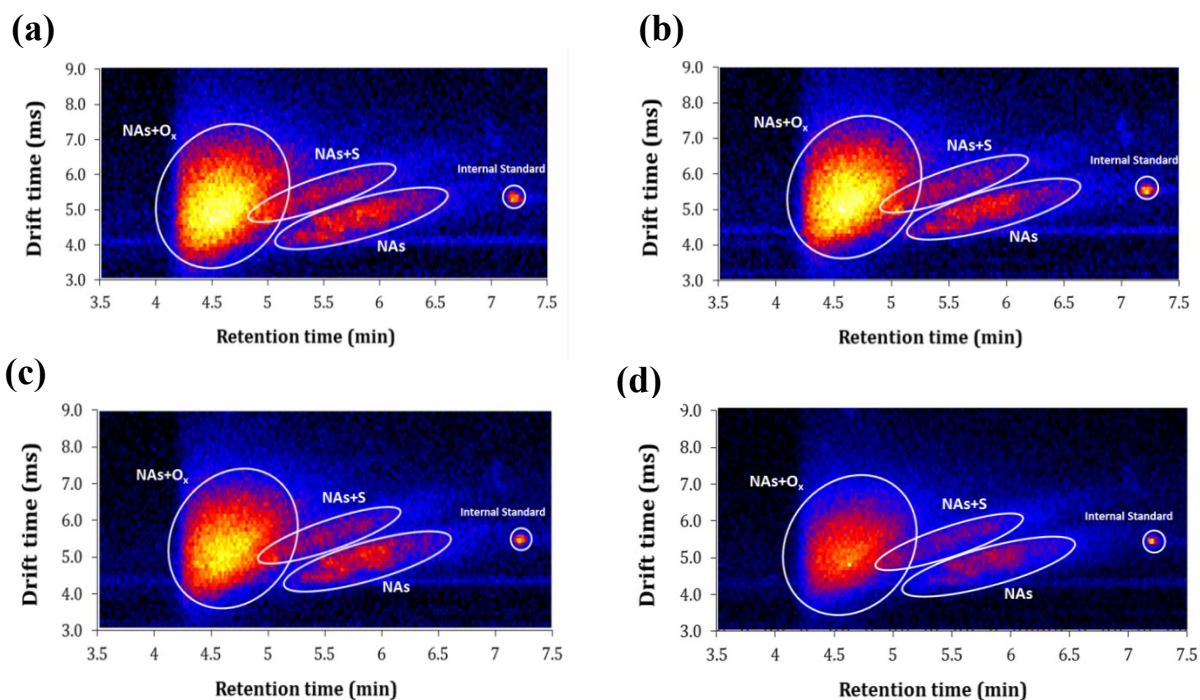
Figure 5. 1 Ion mobility spectra for raw OSPW (a) and OSPW after treatment by EO for 90 min under current densities of; (b) 0.5 mA/cm^2, (c) 1 mA/cm^2 and (d) 10 mA/cm^2.

5.3.2 Fate of classical NAs and AEF during EO and biodegradation

5.3.2.1 Classical NAs and AEF removal by EO

Classical NAs were used extensively as the primary indicator for the efficiency of processes studied for OSPW treatment mainly because they have been found to be more acutely toxic than other classes (Wang et al. 2016b). Classical NAs in raw OSPW had an initial concentration of 24.36 mg/L and consisted of NAs with different carbon number and hydrogen deficiencies but the fraction with those having carbon number between 12 and 17 and −Z number between 2 and 12 were the most abundant (Fig. 5.2). The application of EO by graphite resulted in degrading classical NAs even at current densities as low as 0.2 mA/cm^2 (Fig. 5.3a). Classical NAs removal increased from 19% at 0.2 mA/cm^2 and reached 53.6% at 10 mA/cm^2 (Fig. 5.3a).
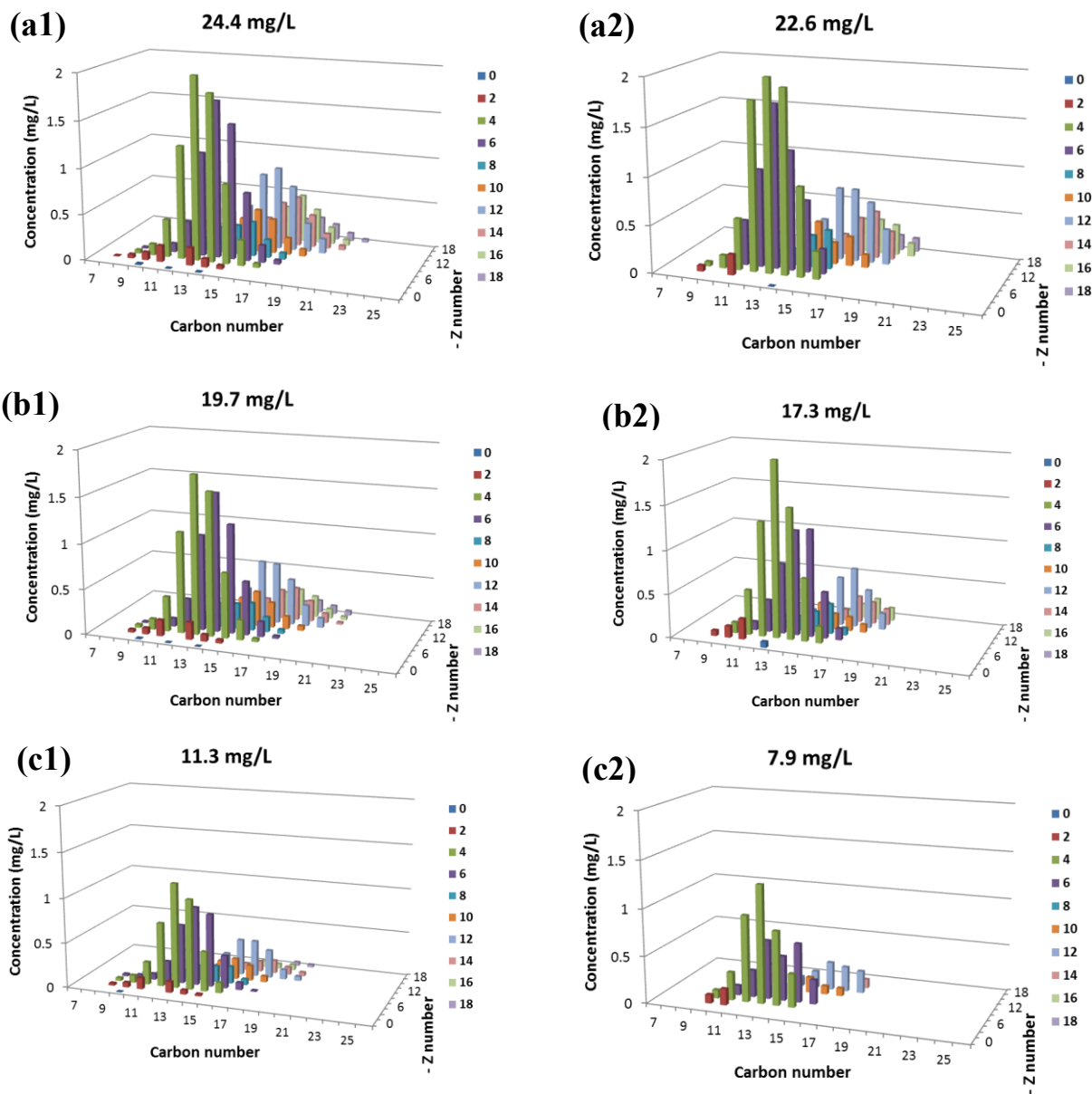
Figure 5.2 Classical NAs distribution in OSPW (1) before biodegradation and (2) after 40 days of biodegradation following EO at current density of: (a) 0 mA/cm^2, (b) 0.2 mA/cm^2 and (c) 10 mA/cm^2.

AEF of OSPW represents all the carbonyl-containing organics including classical NAs, oxidized NAs, aromatics and heteroatomic compounds. The removal of AEF by EO followed similar trend to that of classical NAs but was always lower than classical NAs (Fig. 5.3b). At 0.2 mA/cm^2 EO by graphite removed 6.7% and the removal reached 34.1%

at 10 mA/cm^2. The lower removal of AEF compared to NAs was expected due to the fact that the oxidation by-products of NAs contain alkyl- and keto- NAs that can still contribute to AEF (Dong et al. 2015).
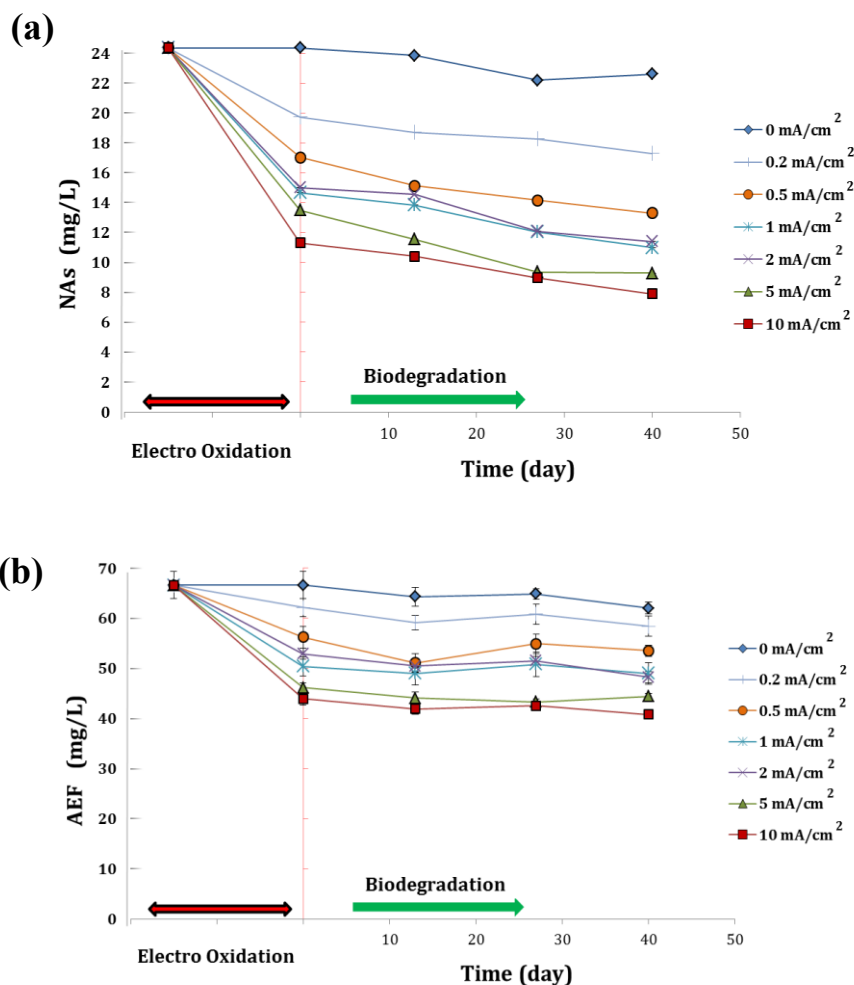
Figure 5.3 The fate of (a) classical NAs and (b) acid extractable fraction (AEF) after 90 min of EO followed by 40 days of aerobic biodegradation.

5.3.2.2 Fate of classical NAs and AEF during biodegradation

Following the application of EO, the treated samples were bio-incubated aerobically for 40 days and the concentrations of classical NAs and AEF were followed with time (Fig. 5.3). The removal of OSPW classical NAs by biodegradation was relatively slower but resulted

in considerable removal percentages after 40 days (Fig. 5.3a). The samples pre-treated with EO showed higher classical NAs removal compared with untreated OSPW sample (Fig. 5.3a). The concentration of classical NAs in the sample without EO pre-treatment dropped from 24.36 mg/L to 22.6 mg/L after 40 days of biodegradation accounting for 7.3 % of removal. Samples with EO pre-treatment, on the other hand, have shown higher removal during the biodegradation step with removals of 12.5%, 21.7%, 25.2%, 23.9%, 30.8% and 29.9% at pre-treatment current densities of 0.2, 0.5, 1, 2, 5 and 10 mA/cm^2, respectively (Fig. 5.3a). The results clearly indicated that the residual NAs after EO were more biodegradable than those removed during EO.

The results for AEF removal during the bio-incubation were less significant in terms of biodegradability enhancement compared to those of classical NAs (Fig. 5.3b). The concentration of AEF remained relatively stable during the bio-incubation period (Fig. 5.3b). After 40 days of biological incubation, the removal of AEF for the sample with no EO pre-treatment was 6.9%, while the removal percentage for EO pre-treated samples were 6.0 %, 4.8%, 8.8% and 7 % at pre-treatment current densities of 0.2, 0.5, 2 and 10 mA/cm^2, respectively (Fig. 5.3b). This behaviour was observed before in the case of ozonation pre-treatment (Dong et al. 2015) and can be explained by the fact that the AEF is a representation for the total amount of carbonyl groups in the OSPW matrix and it was demonstrated before that that biodegradation of NAs can lead to the production of shorter fatty acids or derivatives that contain carboxylic acid groups which can still contribute to AEF (Whitby 2010, Dong et al. 2015).

5.3.3 Fate of oxidized NAs

Following the fate of oxidized NAs concentrations was more complicated since the oxidized NAs in raw OSPW can be consumed while new oxidized NAs can be generated simultaneously. Oxidized NAs in the raw OSPW consisted mainly of O3-NAs, O4-NAs and O5-NAs with concentration of 16.32 mg/L, 17.81 mg/L and 3.83 mg/L, respectively (Table 5.1). As can be seen in Fig. 5.4a, the removal of oxidized NAs, collectively, during EO increased with the increase in the applied current density, showing that they were degraded at a rate higher than the generation rate. It can be noted that at 0.2 mA/cm^2 there was an increase in the concentration of O3- and O5- NAs after EO indicating that some of them were generated as by-products and were not degraded as fast as they were generated (Fig. 5.4a). Similar trend was also observed O5- NAs at 0.5 mA/cm^2. As can be seen in Fig. 5.4a, O4- NAs were removed at all the applied current densities, and they maintained the highest removal rate among other oxidized NAs at current densities below 5mA/cm^2. This behaviour can be partially attributed to their relatively higher abundance, but the difference in reactivity towards EO might also play some role. As a general trend, it can be noted that the fate of NAs during EO by graphite was relatively different than what was reported previously for OSPW treatment by UV/H$_2$O$_2$ and ferrate (Wang et al. 2016a, Wang et al. 2016b). During OSPW treatment by UV/H$_2$O$_2$ and ferrate processes there was an increase in the concentration of oxidized NAs even at high oxidant doses (Wang et al. 2016b). This difference between EO and these processes can also be attributed to the difference in reactivity of oxidized NAs toward the oxidation by different AOPs.
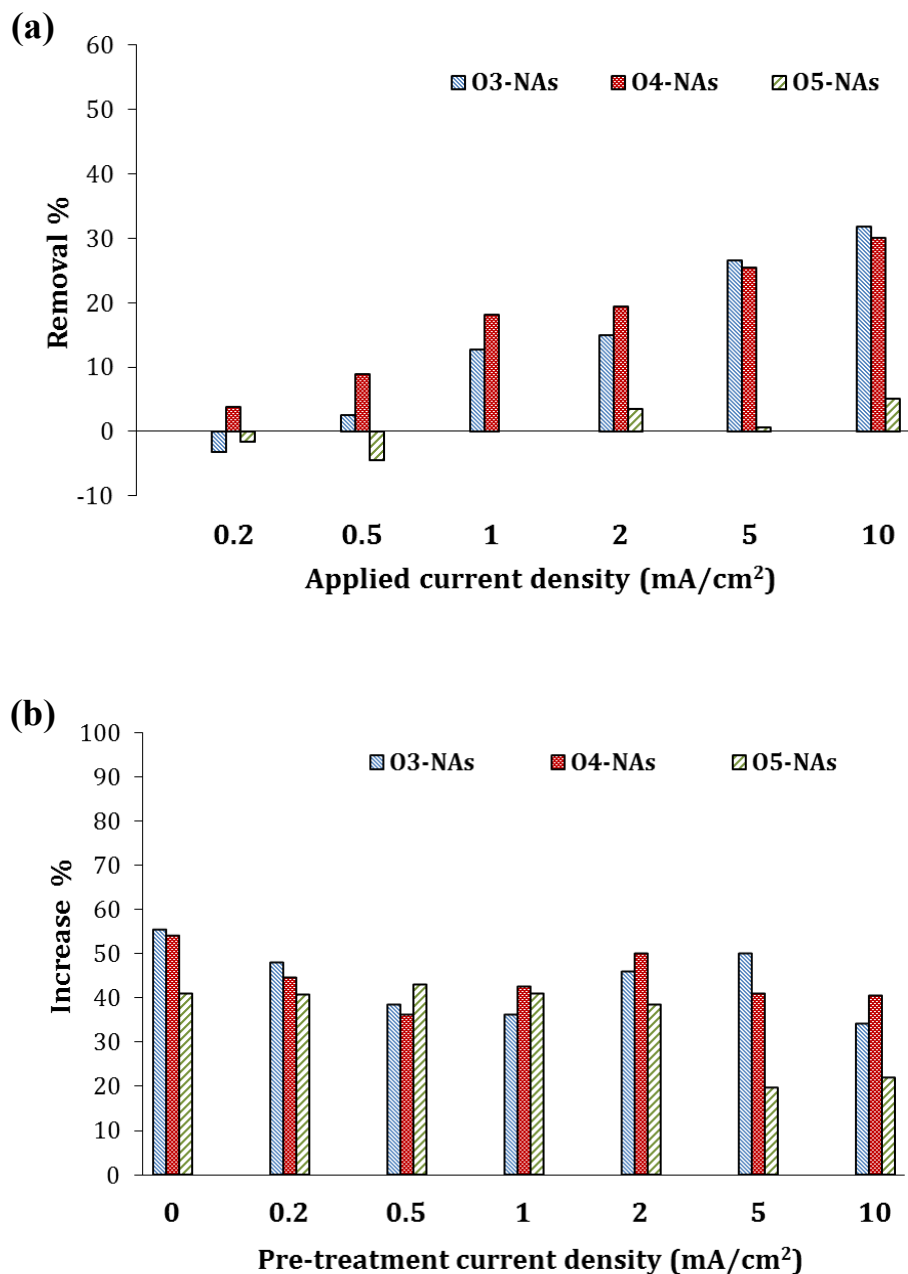
Figure 5.4 The fate of oxidized NAs (O3-NAs, O4-NAs and O5-NAs) after: (a) EO and (b) EO followed by 40 days of biodegradation.

The fate of oxidized NAs during biodegradation was totally different from what was observed during EO. As can be seen in Fig. 5.4b, the concentration of all the different classes of oxidized NAs increased after 40 days of biodegradation, no matter whether the

sample was pre-treated by EO or not. This behaviour was expected as it has been reported previously that oxidized NAs are the main intermediates in the biodegradation of classical NAs (Han et al. 2008, Martin et al. 2010, Whitby 2010). This can clearly support the previously studies which suggest that the mode of microbial biodegradation of classical NAs includes the simple insertion of oxygen which will lead to the generation of oxidized NAs (Han et al. 2009, Martin et al. 2010, Whitby 2010). It can be noted that there was no clear trend for the increase oxidized NAs after bio-incubation neither based on the pre-treatment condition nor the oxidized NAs class.

5.3.4 Influence of EO pre-treatment on the biodegradability of NAs in OSPW

As discussed earlier in this chapter, the main purpose of applying EO was to improve the biodegradability of NAs in OSPW. The applied current densities during EO and the selection of anode material (graphite) were not anticipated to mineralize parent NAs, rather it was anticipated that it will degrade the most bio-persistent fraction. Therefore, the biodegradability of NAs of OSPW was, hypothetically, expected to improve after EO. In order to evaluate the biodegradability of NAs after EO, the biodegradation kinetics were estimated and compared based on the different pre-treatment conditions. The biodegradation of classical NAs was found to follow pseudo-first order kinetics (Fig 5.5). This agreed with a number of previous studies, which confirmed that, the biodegradation of OSPW's NAs followed first order kinetics (Han et al. 2008, Martin et al. 2010). As can be seen in Fig. 5.5, the biodegradation rate constant for classical NAs was clearly increased after pre-treatment by EO. Pre-treating OSPW by EO at current densities of 0.2, 0.5, 1, 5 and 10 mA/cm^2 increased the rate constant by 1.2, 2.5, 2.7, 4.4 and 3.2 folds, respectively (Fig. 5.5). At lower current densities (<2 mA/cm^2), the biodegradation rate increased with

increasing the applied current density. However, at higher current densities this trend was not clear. Among the different applied pre-treatment current densities, the highest increase in the biodegradation rate constant was achieved at 5 mA/cm^2. This might indicate that the increase in the current density to 10 mA/cm^2 resulted in the degradation of NAs that are readily biodegradable as the recalcitrant fraction abundance became lower. The results presented in Fig. 5.5, can clearly support the hypothesis that EO by graphite can selectively degrade the most bio-persistent NAs in OSPW without resulting in complete removals.
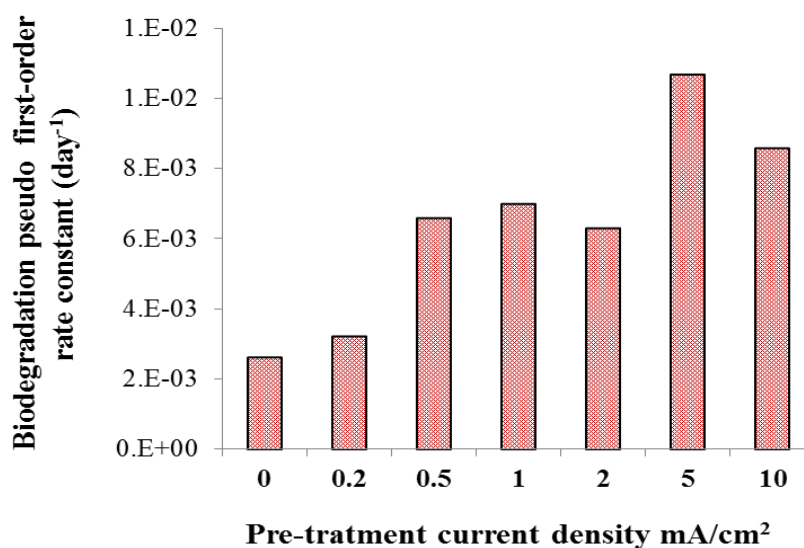
Figure 5.5 Effect of EO pre-treatment current density on the biodegradability of NAs represented as pseudo first order biodegradation rate constant.

In order to further investigate the improvement in biodegradability caused by EO pre-treatment, the change in the biodegradation pseudo first order half-lives based on hydrogen deficiency, (Z number (Fig. 5.6). It was found previously that the impact of ozonation in improving the biodegradability depended on Z number and the used ozone dose (Martin et al. 2010). As can be seen in Fig.5.6, the biodegradation half-lives greatly depended on the Z

number. For NAs with Z= -2, the biodegradation half-life for raw OSPW sample was 154 days (Fig. 5.6a). This half-life was reduced by 1.4, 3 and 4.1 folds when EO pre-treatment was applied at current densities of 0.2, 1 and 5 mA/cm^2. NAs with Z= -4 had the longest half-life among the other Z numbers with around 587 days, and remained the longest even when EO pre-treatment was applied (Fig. 5.6b), but reduced by as high as 1.95 folds at pre-treatment current density of 5 mA/cm^2. Similar reductions were also observed for Z= -6, -8, -10 and -12 as can be seen in Fig. 5.6c, Fig. 5.6d, Fig. 5.6e and Fig. 5.6f, respectively. As can be noted in Fig. 5.6, pre-treatment by EO at 5 mA/cm^2 maintained the highest reductions in half-life for most of Z numbers, except for Z = -8 and -12 where it achieve the second highest reductions. Among the difference Z numbers, the highest reduction in degradation half-life was by 4.5 folds for NAs with Z= -6 and by pre-treatment at 5 mA/cm^2 (Fig. 5.6c). These results further confirmed the improvement in biodegradability of NAs in OSPW.
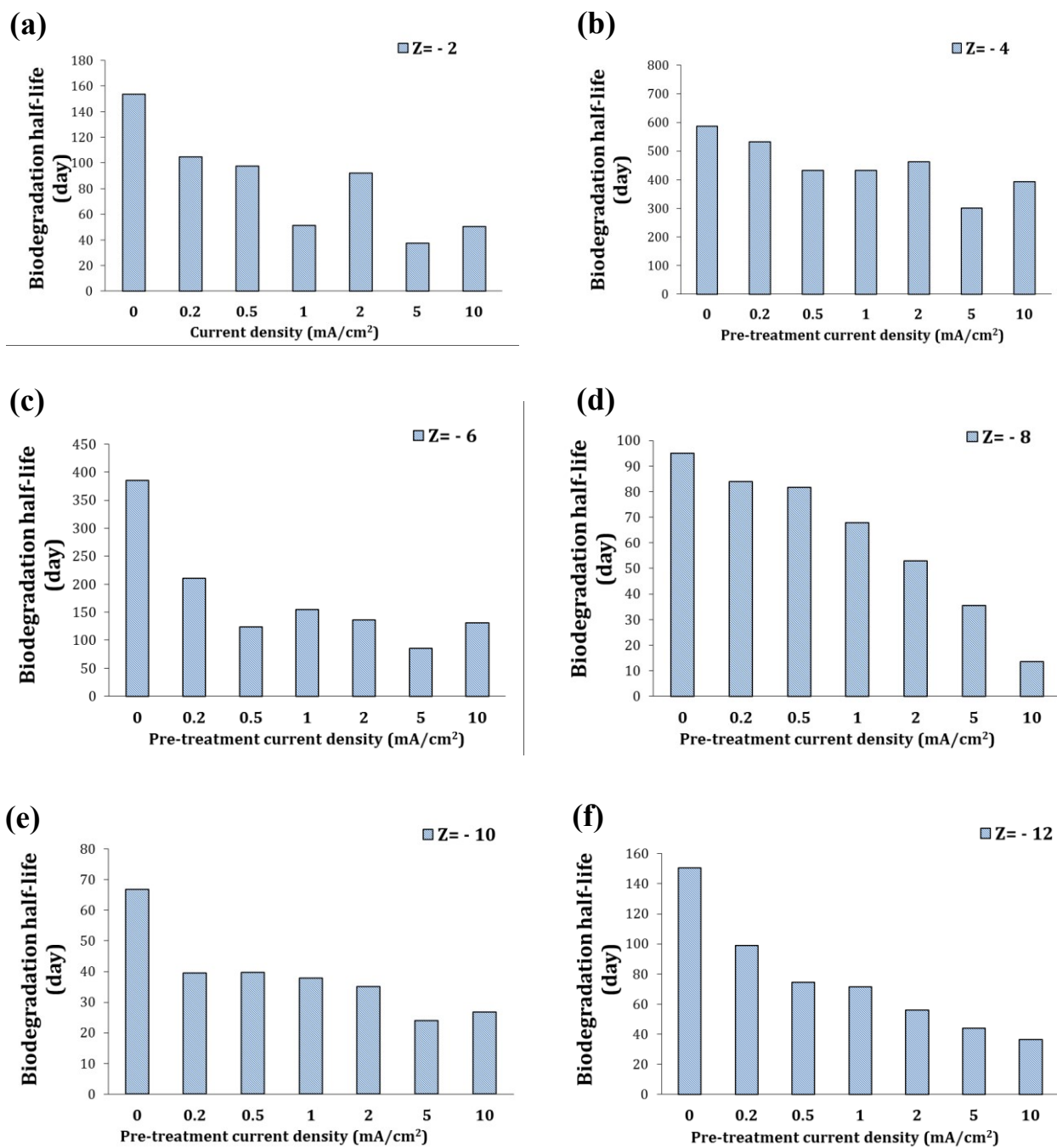
Figure 5.6 NA biodegradation half-lives (days) after different pre-treatment current

densities grouped by Z number: (a) Z = -2, (b) Z = -4, (c) Z = -6, (d) Z = -8, (e) Z = -10, (f)

Z = -12.

5.3.5 Effect of EO pre-treatment on the microbial communities during bio-incubation

Investigating the change of the microbial communities after the biodegradation period can help us understand the reason for the increased biodegradability and the nature of EO treatment by-products. By monitoring the bacterial growth using qPCR, the total number of bacterial cells was quantified and compared for the different pre-treatment conditions (Fig. 5.7). The initial concentration of bacterial cells added to all the bio-incubated sample was 8.5×10^6 cells/mL (Fig. 7). After 40 days of incubation for the raw OSPW sample (without pre-treatment), the number of bacterial cells reached 63.4 folds of the initial number (Fig. 5.7). The final bacterial cells number for all the samples with EO pre-treatment at current densities of 0.2 and 0.5 mA/cm^2 was similar to the sample without EO pre-treatment (Fig. 5.7). In the case of EO pre-treatment at higher current densities (≥ 1 mA/cm^2), however, the cells growth was clearly less than the sample with EO pre-treatment with the growth rate decreasing when the current density increase (Fig. 5.7). This behaviour can be explained by considering the fact that OSPW contains high concentration of chloride (Allen 2008). Therefore at current densities higher than 0.5 mA/cm^2 chlorine is expected to be generated and the generation will increase with the increase in the applied current density (Abdalrhman et al. 2019a). Although chlorine generation by graphite is not expected to be high and that the generated chorine will react and degrade the organics in OSPW, but residual chlorine is expected to remain after EO. The residual chlorine is expected to affect the microbial cell growth during biodegradation which is the reason for the reduction in the number of cells (Fig. 5.7).
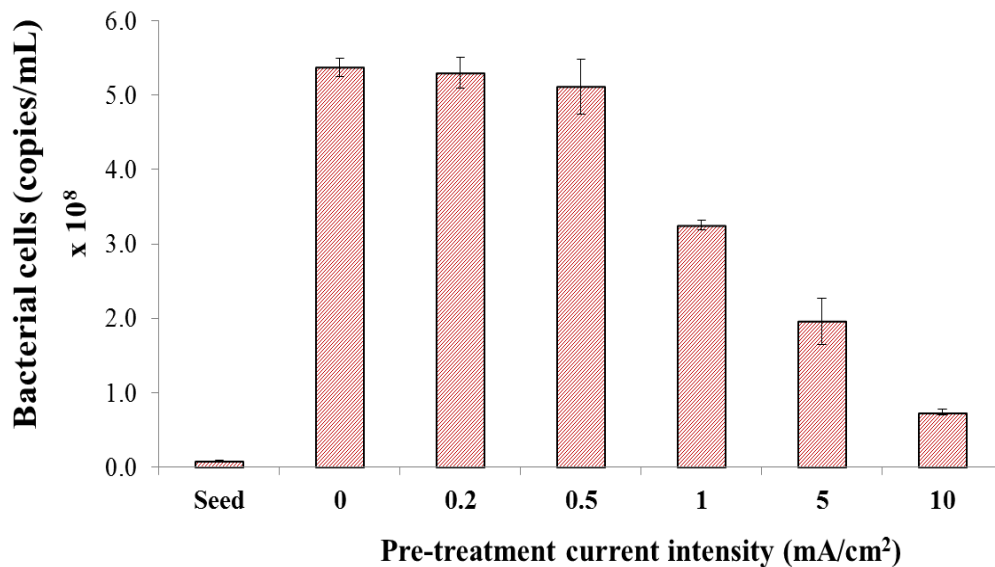
Figure 5.7 Effect of EO pre-treatment current density on the total bacterial growth

quantified by qPCR

MiSeq analysis for the microbial communities in the initial seed and those in the bio-incubated samples was performed (Fig. 5.8). The sequencing analysis was conducted for five samples; the seed, incubated sample with raw OSPW without pre-treatment; EO pre-treated OSPW samples at current densities of 0.2, 1 and 10 mA/cm^2;. Those current densities were selected to represent the lowest, medium and highest pre-treatment current densities applied during the study. The analysis at the phylum level, showed that the dominant phylum before and after biodegradation at different conditions was Proteobacteria (Fig. 5.8a). The domination of Proteobacteria was also observed before in several studies about the biodegradation of OSPW organics (Islam et al. 2015, Xue et al. 2016, Zhang et al. 2018). The abundance of Proteobacteria increased after the biodegradation at all conditions which agreed with a number of previous studies indicated that Proteobacteria play the

176

major role in the biodegradation of the NAs under aerobic conditions (Islam et al. 2015, Whitby 2010, Xue et al. 2016, Zhang et al. 2018). It should be noted that Bacteroidetes was the second abundant phylum in the seed; however, after biodegradation its abundance decreased substantially (Fig. 5.8a). The taxonomic analysis at class level has shown that Betaproteobacteria was the dominant class after biodegradation, although it was less dominant in the seed (Fig. 5.8b). This class could be associated with the degradation of OSPW's NAs as its dominance was also found in other studies (Islam et al. 2015, Zhang et al. 2018).The second most abundant class was Alphaproteobacteria and their relative abundance showed a clear trend of increase with the increase of applied current density in EO pre-treatment (Fig. 5.8b). Alphaproteobacteria, similarly to Betaproteobacteria, is also known to be associated with the degradation of NAs (Skeels and Whitby 2018, Yergeau et al. 2013, Yergeau et al. 2012). This might indicate that the by-products from EO of OSPW's NAs can be degraded more effectively by Alphaproteobacteria and that this class might be responsible for the improved biodegradability observed after EO pre-treatment. Similar increase in the abundance of Alphaproteobacteria was observed in a biofilm reactor when ozonation was used as pre-treatment (Islam et al. 2015). Alphaproteobacteria was also previously found to have higher abundance among the microbial communities in the fine tailings of different tailings ponds and sediments from sites in the Athabasca River and tributary which might indicate its ability to effectively degrade NAs (Yergeau et al. 2012). An analysis at order level for the communities within the Alphaproteobacteria class has shown that Sphingomonadales was the dominant order after biodegradation and its followed a clear trend of increase with the increase of applied current density in EO pre-treatment (Fig. 5.8c). For Betaproteobacteria, on the other hand, although Burkholderiales

177

was the dominant order after biodegradation, the abundance Rhodocyclales showed a clear trend of increase with the increase of applied current density in EO pre-treatment (Fig. 8c). It has to be noted that microorganisms such as Sphingomonadales (Alphaproteobacteria) and Rhodocyclales (Betaproteobacteria) are known for their capability for degrading hydrocarbons and were found to be associated with the degradation of NAs in OSPW (Islam et al. 2015, Skeels and Whitby 2018). Further deeper taxonomic analysis at family and genus levels for Protobacteria class can also be found in Fig. 5.9. A close scrutiny at genus level reveals the dominance of *Hydrogenophaga* after biodegradation. *Hydrogenophaga* showed strong positive correlations with the degradation of PAHs (polycyclic aromatic hydrocarbons) from oil sands mining activities (Yergeau et al. 2012). Interestingly, the abundance of *Sphingobium* increased with applied current density in EO pre-treatment. Sphingobium was also isolated from oil-contaminated soil to degrade aliphatic hydrocarbons (Yergeau et al. 2012). The increase *Sphingobium* abundance might contribute to improved biodegradation of NAs in EO pretreated OSPW.

Although the analysis showed a correlation between the improved biodegradability and microbial orders such as Sphingomonadales (Alphaproteobacteria) and Rhodocyclales (Betaproteobacteria), it has to be noted that the biodegradation of the NAs is known to be a result of the synergistic effect of the whole microbial community rather than a specific class or order.

(a)

(b)

(c)
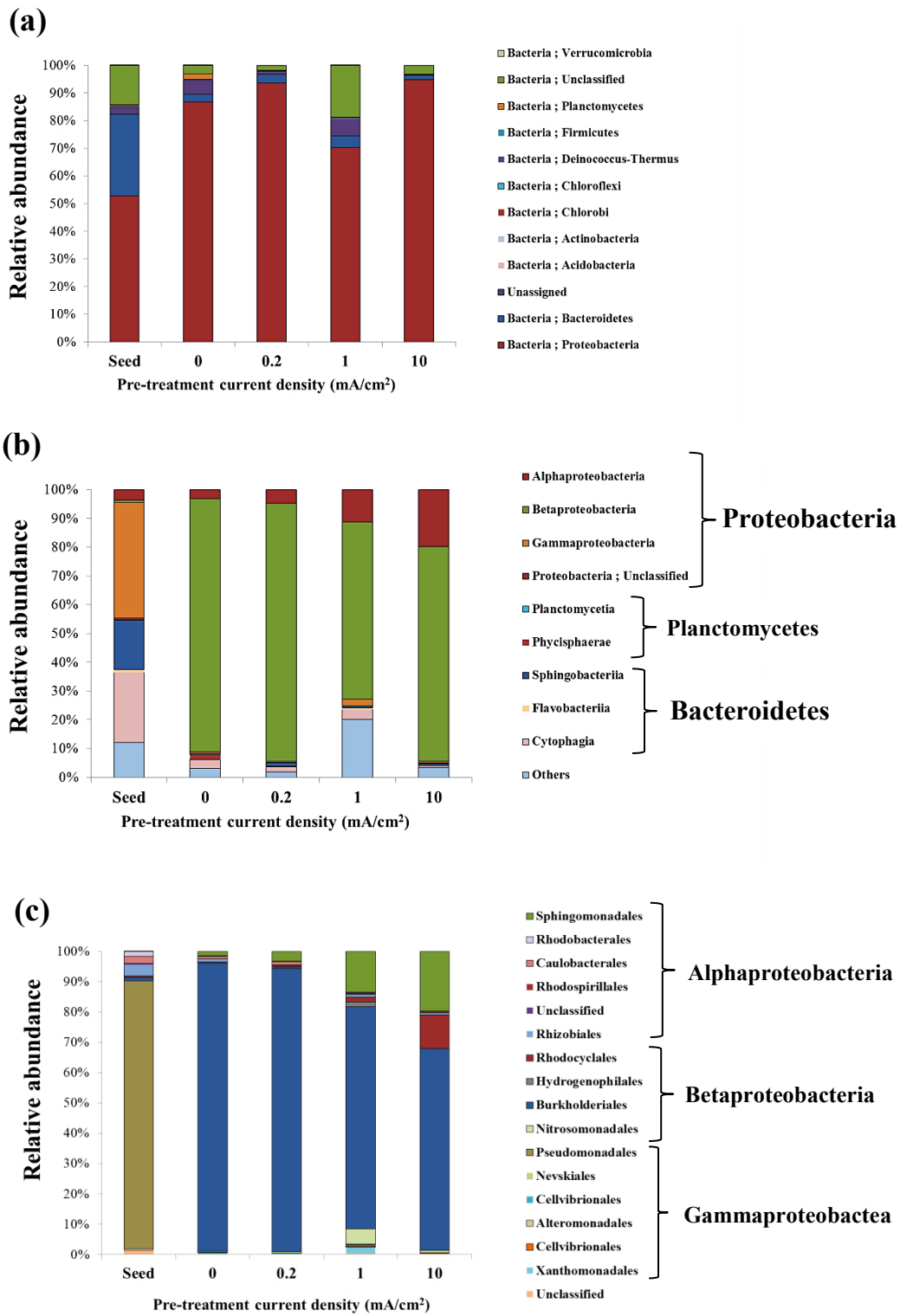
Figure 5.8 Taxonomic classification for the microbial community seed sludge and after 40

days incubation following different pre-treatment current densities at (a) phylum level; (b)

class level for the 3 major phyla; (c) order level for the Proteobacteria class
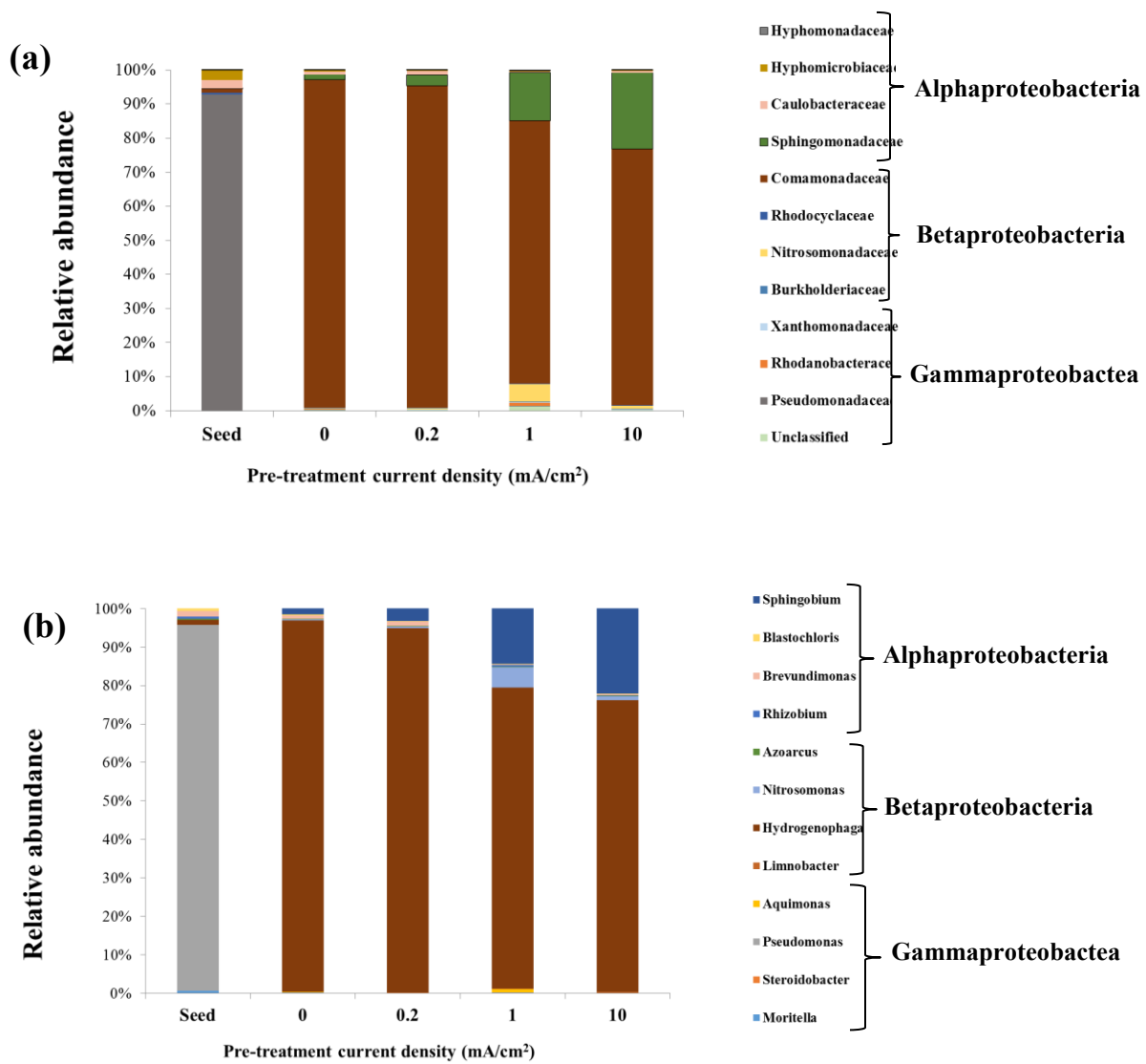
Figure 5.9 Taxonomic classification showing the major (a) families and (b) genera within the Proteobacteria class

5.4 Conclusions

This chapter focused on evaluating the performance of EO by graphite and at relatively low current densities as a pre-treatment before aerobic biological treatment process. The IMS qualitative analysis showed that EO by graphite was able to degrade the different NAs clusters in OSPW including classical, oxidized and heteroatomic NAs. Applying EO even at current density as low as 0.2 mA/cm^2 resulted in reductions in classical NAs and AEF by 19% and 6.7%, respectively. Aerobic bio-incubation for 40 day was able to achieve reductions in NAs by as high as 30.9% when the sample was pre-treated with EO. The removal of AEF during bio-incubation, however, was very slow and limited. Oxidized NAs were degraded during EO and were generated as by-products during biodegradation. It was demonstrated that applying EO as pre-treatment before bio-incubation can increase the biodegradability of classical NAs by up to 4.4 folds. Even at current density as low as 0.2 mA/cm^2, the biodegradation rate constant was increased by 1.4 folds. The analysis for the microbial communities after bio-incubation with different samples showed some differences between the one without EO pre-treatment and those with EO pre-treatments. High abundance of Alphaproteobacteria class and the increase of the abundance of microbial orders such as Sphingomonadales and Rhodocyclales in the EO pretreated samples might be the responsible for the improved biodegradability. This study has shown that low-current EO by graphite anode can be a promising pre-treatment option for OSPW while being routed to in-pit lakes or wetlands where further biodegradation can take place. EO can lead to improved biodegradability of NAs. The lower voltages required, low-cost of graphite electrodes and exclusion of chemicals addition can result in a sustainable and environmental friendly process that can be run by renewable energy.

5.5 References

Abdalrhman, A. S., S. O. Ganiyu, and M. Gamal El-Din. 2019a. Degradation kinetics and structure-reactivity relation of naphthenic acids during anodic oxidation on graphite electrodes. Chemical Engineering Journal **370**:997-1007.

Abdalrhman, A. S., Y. Zhang, and M. Gamal El-Din. 2019b. Electro-oxidation by graphite anode for naphthenic acids degradation, biodegradability enhancement and toxicity reduction. Science of The Total Environment **671**:270-279.

Allen, E. W. 2008. Process water treatment in Canada's oil sands industry: I. Target pollutants and treatment objectives. Journal of Environmental Engineering and Science **7**:123-138.

Brown, L. D. and A. C. Ulrich. 2015. Oil sands naphthenic acids: A review of properties, measurement, and treatment. Chemosphere **127**:276-290.

Clemente, J. S., M. D. MacKinnon, and P. M. Fedorak. 2004. Aerobic Biodegradation of Two Commercial Naphthenic Acids Preparations. Environmental Science & Technology **38**:1009-1016.

Dong, T., Y. Zhang, M. S. Islam, Y. Liu, and M. Gamal El-Din. 2015. The impact of various ozone pretreatment doses on the performance of endogenous microbial communities for the remediation of oil sands process-affected water. International Biodeterioration & Biodegradation **100**:17-28.

Fang, Z., P. Chelme-Ayala, Q. Shi, C. Xu, and M. Gamal El-Din. 2018. Degradation of naphthenic acid model compounds in aqueous solution by UV activated persulfate: Influencing factors, kinetics and reaction mechanisms. Chemosphere **211**:271-277.

Gamal El-Din, M., H. Fu, N. Wang, P. Chelme-Ayala, L. Pérez-Estrada, P. Drzewicz, J. W. Martin, W. Zubot, and D. W. Smith. 2011. Naphthenic acids speciation and removal during petroleum-coke adsorption and ozonation of oil sands process-affected water. Science of The Total Environment **409**:5119-5125.

Ganzenko, O., D. Huguenot, E. D. van Hullebusch, G. Esposito, and M. A. Oturan. 2014. Electrochemical advanced oxidation and biological processes for wastewater treatment: a review of the combined approaches. Environmental Science and Pollution Research **21**:8493-8524.

Han, X., M. D. MacKinnon, and J. W. Martin. 2009. Estimating the in situ biodegradation of naphthenic acids in oil sands process waters by HPLC/HRMS. Chemosphere **76**:63-70.

Han, X., A. C. Scott, P. M. Fedorak, M. Bataineh, and J. W. Martin. 2008. Influence of Molecular Structure on the Biodegradability of Naphthenic Acids. Environmental Science & Technology **42**:1290-1295.

Islam, M. S., Y. Zhang, K. N. McPhedran, Y. Liu, and M. Gamal El-Din. 2015. Next-Generation Pyrosequencing Analysis of Microbial Biofilm Communities on Granular Activated Carbon in Treatment of Oil Sands Process-Affected Water. Applied and Environmental Microbiology **81**:4037.

Kannel, P. R. and T. Y. Gan. 2012. Naphthenic acids degradation and toxicity mitigation in tailings wastewater systems and aquatic environments: A review. Journal of Environmental Science and Health, Part A **47**:1-21.

Kapałka, A., G. Fóti, and C. Comninellis. 2010. Basic Principles of the Electrochemical Mineralization of Organic Pollutants for Wastewater Treatment. Pages 1-23 *in* C. Comninellis and G. Chen, editors. Electrochemistry for the Environment. Springer New York, New York, NY.

Klamerth, N., J. Moreira, C. Li, A. Singh, K. N. McPhedran, P. Chelme-Ayala, M. Belosevic, and M. Gamal El-Din. 2015. Effect of ozonation on the naphthenic acids' speciation and toxicity of pH-dependent organic extracts of oil sands process-affected water. Science of The Total Environment **506-507**:66-75.

Li, C., L. Fu, J. Stafford, M. Belosevic, and M. Gamal El-Din. 2017. The toxicity of oil sands process-affected water (OSPW): A critical review. Science of The Total Environment **601-602**:1785-1802.

Martin, J. W., T. Barri, X. Han, P. M. Fedorak, M. Gamal El-Din, L. Perez, A. C. Scott, and J. T. Jiang. 2010. Ozonation of Oil Sands Process-Affected Water Accelerates Microbial Bioremediation. Environmental Science & Technology **44**:8350-8356.

Martínez-Huitle, C. A. and M. Panizza. 2018. Electrochemical oxidation of organic pollutants for wastewater treatment. Current Opinion in Electrochemistry **11**:62-71.

Martínez-Huitle, C. A., M. A. Rodrigo, I. Sirés, and O. Scialdone. 2015. Single and Coupled Electrochemical Processes and Reactors for the Abatement of Organic Water Pollutants: A Critical Review. Chemical Reviews **115**:13362-13407.

Meshref, M. N. A., P. Chelme-Ayala, and M. Gamal El-Din. 2017a. Fate and abundance of classical and heteroatomic naphthenic acid species after advanced oxidation processes: Insights and indicators of transformation and degradation. Water Research **125**:62-71.

Meshref, M. N. A., N. Klamerth, M. S. Islam, K. N. McPhedran, and M. Gamal El-Din. 2017b. Understanding the similarities and differences between ozone and peroxone in the degradation of naphthenic acids: Comparative performance for potential treatment. Chemosphere **180**:149-159.

Misiti, T. M., U. Tezel, and S. G. Pavlostathis. 2014. Effect of Alkyl Side Chain Location and Cyclicity on the Aerobic Biotransformation of Naphthenic Acids. Environmental Science & Technology **48**:7909-7917.

Moreira, F. C., R. A. R. Boaventura, E. Brillas, and V. J. P. Vilar. 2017. Electrochemical advanced oxidation processes: A review on their application to synthetic and real wastewaters. Applied Catalysis B: Environmental **202**:217-261.

Panizza, M. and G. Cerisola. 2009. Direct And Mediated Anodic Oxidation of Organic Pollutants. Chemical Reviews **109**:6541-6569.

Quinlan, P. J. and K. C. Tam. 2015. Water treatment technologies for the remediation of naphthenic acids in oil sands process-affected water. Chemical Engineering Journal **279**:696-714.

Scott, A. C., M. D. Mackinnon, and P. M. Fedorak. 2005. Naphthenic Acids in Athabasca Oil Sands Tailings Waters Are Less Biodegradable than Commercial Naphthenic Acids. Environmental Science & Technology **39**:8388-8394.

Shu, Z., C. Li, M. Belosevic, J. R. Bolton, and M. Gamal El-Din. 2014. Application of a Solar UV/Chlorine Advanced Oxidation Process to Oil Sands Process-Affected Water Remediation. Environmental Science & Technology **48**:9692-9701.

Sun, N., P. Chelme-Ayala, N. Klamerth, K. N. McPhedran, M. S. Islam, L. Perez-Estrada, P. Drzewicz, B. J. Blunt, M. Reichert, M. Hagen, K. B. Tierney, M. Belosevic, and M. Gamal El-Din. 2014. Advanced Analytical Mass Spectrometric Techniques and Bioassays to Characterize Untreated and Ozonated Oil Sands Process-Affected Water. Environmental Science & Technology **48**:11090-11099.

Wang, C., N. Klamerth, R. Huang, H. Elnakar, and M. Gamal El-Din. 2016a. Oxidation of Oil Sands Process-Affected Water by Potassium Ferrate(VI). Environmental Science & Technology **50**:4238-4247.

Wang, C., N. Klamerth, S. A. Messele, A. Singh, M. Belosevic, and M. Gamal El-Din. 2016b. Comparison of UV/hydrogen peroxide, potassium ferrate(VI), and ozone in oxidizing the organic fraction of oil sands process-affected water (OSPW). Water Research **100**:476-485.

Wang, N., P. Chelme-Ayala, L. Perez-Estrada, E. Garcia-Garcia, J. Pun, J. W. Martin, M. Belosevic, and M. Gamal El-Din. 2013. Impact of Ozonation on Naphthenic Acids Speciation and Toxicity of Oil Sands Process-Affected Water to Vibrio fischeri and Mammalian Immune System. Environmental Science & Technology **47**:6518-6526.

Whitby, C. 2010. Chapter 3 - Microbial Naphthenic Acid Degradation. Pages 93-125 Advances in Applied Microbiology. Academic Press.

Xue, J., C. Huang, Y. Zhang, Y. Liu, and M. Gamal El-Din. 2018. Bioreactors for oil sands process-affected water (OSPW) treatment: A critical review. Science of The Total Environment **627**:916-933.

Xue, J., Y. Zhang, Y. Liu, and M. Gamal El-Din. 2016. Treatment of oil sands process-affected water (OSPW) using a membrane bioreactor with a submerged flat-sheet ceramic microfiltration membrane. Water Research **88**:1-11.

Zhang, Y., P. Chelme-Ayala, N. Klamerth, and M. Gamal El-Din. 2017. Application of UV-irradiated Fe(III)-nitrilotriacetic acid (UV-Fe(III)NTA) and UV-NTA-Fenton systems to degrade model and natural occurring naphthenic acids. Chemosphere **179**:359-366.

Zhang, Y., J. Xue, Y. Liu, and M. Gamal El-Din. 2018. The role of ozone pretreatment on optimization of membrane bioreactor for treatment of oil sands process-affected water. Journal of Hazardous Materials **347**:470-477.

6. CONCLUSIONS AND RECOMMENDATIONS

6.1 Thesis overview

The oil sands reserves in Alberta, Canada, are the third largest oil reserves in the world and considered the key driver for the providence economic prosperity and one of the main contributors to the country's economy. Despite that, it is attracting a lot of public concern and scientific focus because it consumes large amounts of water and, subsequently, generates large volumes of oil sands process water (OSPW). The treatment of OSPW is currently considered a major challenge facing the oil sands industry. Giving the large volumes of accumulated process water in the ponds and the expected growth in the production of bitumen from oil sands, finding effective OSPW reclamation technologies has become an urgent need.

Efforts have been implemented by the oil sands companies, collaborating researchers and the Government of Alberta towards the development of effective treatment technologies. However, most of the current proposed treatment pathways are extremely slow (biodegradation), highly expensive (physical and chemical processes) or have technical restrictions (Fenton and UV-based AOPs) and, therefore, a more effective treatment option needs to be found.

Electro-oxidation (EO) has emerged as effective method for wastewater treatment and recalcitrant organics degradation. Despite the successful application of EO for treating various types of recalcitrant industrial pollutants, till today there has not been any reported study on the application of electro-oxidation for OSPW treatment. By considering the

physical properties of OSPW, especially the high TDS concentration and electrical conductivity, EO can be a potential effective option for OSPW treatment.

The aim of this research was to investigate the applicability and effectiveness of EO for OSPW treatment. The degradation of the recalcitrant organics in OSPW by EO was evaluated with special focus on naphthenic acids (NAs); which are known to be the most abundant and problematic organics in OSPW. This research was conducted at four different stages. In the first stage, EO by graphite electrodes applied for the degradation of commercial NAs mixture; the removal of NAs, the enhancement in the biodegradation of the residual organics in the mixture and the reduction in NAs mixture toxicity were evaluated. In the second stage, the degradation kinetics, structure-reactivity relation of NAs and anode stability during EO by graphite were investigated in detail by using 12 different model NA compounds. In the third stage, the treatment of real OSPW by EO using two different types of anode materials, graphite and dimensionally stable (Ti/RuO$_2$-IrO$_2$) anode, was investigated and compared. In the fourth stage, coupling low-current EO by graphite electrodes and aerobic biodegradation for treating real OSPW was investigated.

6.2 Conclusions

The results obtained in this research show that EO is capable of effectively degrading the recalcitrant organics in OSPW. This study has shown that EO by inexpensive graphite electrodes and at relatively low-current densities can be applied successfully for OSPW treatment. The main conclusions of each chapter are listed below:

Chapter 2: EO by graphite anode for commercial NAs mixture degradation

189

- EO by graphite anode has demonstrated its capability for commercial NAs mixture degradation, biodegradability enhancement and acute toxicity reduction.

- The degradation rate for NAs during EO increased with the increase in carbon number (n) and was higher for cyclic NAs than for acyclic NAs. EO was also capable of effectively degrading the aromatic NAs in the mixture.

- It was found that EO enhanced the biodegradability of the NA mixture even when applied at current density as low as 0.5 mA/cm^2.

- Biodegradation of the raw NA mixture samples resulted in a clear toxicity reduction to *Vibrio fischeri*, however, the combination of EO with biodegradation resulted in a complete reduction of acute toxicity towards *Vibrio fischeri*.of the samples, showing a synergistic effect of combining these two processes.

- This investigation was an important step toward understanding the effectiveness of EO for degrading NAs and the feasibility of using EO as a pre-treatment for aerobic biodegradation to create an effective and energy-efficient treatment option for OSPW.

Chapter 3: Degradation kinetics and structure-reactivity relation of naphthenic acids during anodic oxidation on graphite electrodes

- EO by graphite anode was able to effectively degrade the different selected model NA compounds.

- The degradation of CHA increased with increasing the applied current density and clearly followed pseudo-first-order kinetics.

- Carbonate species in the electrolyte medium had scavenging effect on the degradation rate. However, chloride and sulfate ions had a minor role in the degradation of CHA.

- Graphite was found to behave differently from both, active and inactive anodes in terms of the type of oxidants generated on the surface of anode. It was found that the main degradation mechanism for CHA during anodic oxidation by graphite anode was through the generation of oxygenated functional groups at the anode surface. DET mechanism had no contribution in the degradation of CHA.

- The findings of the structure-reactivity study showed that NAs with higher number of carbons were preferentially degraded by AO. Branched NAs were more reactive than non-branched NAs only if the branch existed far enough from the carboxylate group. It was found that monocyclic NAs were more reactive than linear NAs, but any increase in the cyclicity beyond one ring resulted in reduced reactivity. Aliphatic NA compounds were found to be more reactive during AO than aromatic compounds and the existence of more than one carboxylate group in the structure reduced the reactivity. The kinetics and structure-reactivity analysis have shown that AO by graphite can be an attractive option for OSPW treatment and biodegradability enhancement.

Chapter 4: Degradation of the recalcitrant organics in real oil sands process water by EO using graphite and dimensionally stable anodes

- Graphite and DSA, both, were able to degrade the recalcitrant organics in OSPW.
- EO using graphite anode was able to reduce the COD, AEF, classical and oxidized NAs and aromatics in OSPW even at current density as low as 0.5 mA/cm^2. The

removal of organics by DSA, on the other hand, did not occur until the current density reached 2 mA/cm^2.

- The removal of classical NAs by both graphite and DSA increased with the increase in the applied current density and was always higher than the removal of AEF. Graphite anode maintained higher removals of NAs (classical and oxidized) and AEF at most of the applied current densities except when the applied current reached 20 mA/cm^2 (anode potential > 7V) where DSA showed superior removals. The degradation of NAs by both anodes followed pseudo-first order kinetics.

- The reactivity of NAs toward oxidation on both anodes increased with the increase of the carbon number. During EO using DSA, low-carbon number NAs were generated as byproducts of the oxidation of high-carbon NAs. EO by graphite was found to be less sensitive towards cyclicity of NAs compared to DSA.

- Graphite anode maintained higher current efficiency at all applied current densities.

- Both anodes were able to remove the aromatic compounds with DSA being more selective toward aromatics especially those with multiple aromatic rings. DSA was able to achieve complete removals of two and three rings aromatics and 93.0% removal of single ring aromatics at current density of 20 mA/cm^2 after 90 min of electrolysis, while the highest removal by graphite was 74.6% at similar electrolysis time.

- For the treatment of OSPW by EO, the results from this chapter indicated that graphite anode can be a more effective option if used at lower current densities. DSA, on the other hand, can be more superior to graphite at higher applied current densities.

Chapter 5: Low-current electro-oxidation as a pre-treatment stage to biological process for the degradation of recalcitrant organics in real oil sands process water

- Applying EO by graphite anode at relatively low current densities as a pre-treatment before aerobic biological treatment was successfully evaluated for OSPW treatment.

- The IMS qualitative analysis showed that EO by graphite was able to degrade the different NA clusters in OSPW including classical, oxidized and heteroatomic NAs.

- Applying EO even at current density as low as 0.2 mA/cm^2, resulted in reductions in classical NAs and AEF by 19% and 6.7%, respectively.

- Aerobic bio-incubation for 40 day was able to achieve reductions in NAs as high as 30.9% when the sample was pre-treated with EO. The removal of AEF during bio-incubation, however, was very slow and limited.

- Oxidized NAs were degraded during EO and were generated as by-products during biodegradation.

- It was demonstrated that applying EO as pre-treatment before bio-incubation can increase the biodegradability of classical NAs by up to 4.4 folds. Even at current density as low as 0.2 mA/cm^2, the biodegradation rate constant was increased by 1.4 folds.

- The analysis for the microbial communities after bio-incubation with different samples showed some differences between the one without EO pre-treatment and those with EO pre-treatments. The abundance of Alphaproteobacteria was higher in the samples with EO pre-treatment than in the one with no EO pre-treatment which

might indicate a relation between this class and the improved biodegradability of residual NAs in OSPW.

- This study has shown that low-current EO by graphite anode can be a promising pre-treatment option for OSPW while being routed to in-pit lakes or wetlands where further biodegradation can take place. EO can lead to improved biodegradability of NAs. The lower voltages required and low-cost of graphite electrodes can result in a sustainable and environmental friendly process that can be run by renewable energy. Moreover, the exclusion of the need for chemicals addition will further reduce treatment costs and prevent the production of any additional hazardous wastes.

6.3 Recommendations

Based on the results obtained from this research which suggested that EO can be an attractive option for OSPW treatment, recommendations for future works are proposed here:

- As can be noticed, all of the EO experiments discussed in this thesis were performed by using batch reactors. Batch EO reactors are simple to operate and control and are suitable for kinetics studies, however, in order for EO to be considered for application at large scales, the performance of EO should be evaluated by using a flow-through system. Flow-through reactors are more relevant for large scale application, especially considering the huge volumes of OSPW impounded in tailing pond waiting for treatment. Therefore, evaluating the performance of EO by graphite electrodes using flow-through reactor and the optimization of the reactor conditions should be the next step. Graphite as an anode material has the advantage of being able to be used as a 3D anode material in

backed bed electrochemical reactors, which can be an attractive option for OSPW treatment. This flow through reactor can also help in evaluating the long term impact of the constituents of OSPW (organics and inorganics on the anode corrosion.

- All biological treatment experiments were performed in suspended growth batch rectors. We recommend that EO should also be applied as pre-treatment for biofilm reactors for OSPW treatment. Biofilm reactors have been applied before for OSPW treatment and have showed better performance compared to suspended growth systems, therefore, we believe that coupling EO with biofilm biological treatment might lead to better OSPW treatment performance. Another important aspect that needs to be further expanded for the biological treatment is the characterization of the change in the microbial communities resulting from the application of EO pre-treatment. This can be achieved by extending the operation of reactors for longer period and applying more advanced microbial community characterization techniques such as next-generation sequencing.

- Among the different available anode materials, in this thesis we only used two anode materials (graphite and DSA). Graphite was selected since it is one of the lowest cost anode materials which can be attractive cost-effective anode material for OSPW treatment. DSA, on the other hand, is a well-studied active anode material that has been used widely for the degradation of organics. The investigation of EO by using other anode materials for OSPW treatment and comparing their performances is, however, strongly recommended. Non-active anode materials such as boron-doped diamond (BDD) are known to be very effective in degrading and

mineralizing recalcitrant organics. BDD is also able to generate not only hydroxyl radicals but also other strong oxidants such as sulfate, persulfate and other metallic radicals, if suitable salts and metals exist in the water matrix. By considering the composition of OSPW with high sulfate concentration in addition to the existence of metals, BDD can be an effective anode material for OSPW treatment by EO. Currently, in our laboratory we have started investigating the applicability of EO by BDD for OSPW treatment.

- Coupling EO with other physical or chemical process can also result in a more effective hybrid process that can be applied for OSPW. One of the most attractive combinations for this purpose can be coupling EO with adsorption in a process where EO can be used to simultaneously degrade the organics and regenerate the adsorbents. For this purpose granular activated carbon can be used in a backed bed reactor and low-current densities can be applied.

- Another hybrid electrochemical oxidation processes that can be attractive for OSPW treatment are Electro-Peroxone and Electro-Fenton. Electro-Peroxone combines three effective oxidation processes; peroxone, anodic oxidation and ozonation. In Electro-Peroxone the cathodic reactions can be exploited to produce hydrogen peroxide which then reacts with sparged ozone resulting in the generation of highly active hydroxyl radicals, beside those generated at the anode surface and by the ozone decay. Similar to Electro-Peroxone, Electro-Fenton also involves the cathodic electro-generation of hydrogen peroxide which reacts this time with an iron catalyst, resulting in the generation of large amounts of hydroxyl radicals through the well-known Fenton reaction. Electro-Fenton, besides its high degradation ability, can

also overtake the pH limitation associated with applying the traditional Fenton process for OSPW. That can be achieved through the use of a heterogeneous iron catalyst deposited on the cathode, where it can also be regenerated continuously.

BIBLIOGRAPHY

Abdalrhman, A. S., S. O. Ganiyu, and M. Gamal El-Din. 2019a. Degradation kinetics and structure-reactivity relation of naphthenic acids during anodic oxidation on graphite electrodes. Chemical Engineering Journal 370:997-1007.

Abdalrhman, A. S., Y. Zhang, and M. Gamal El-Din. 2019b. Electro-oxidation by graphite anode for naphthenic acids degradation, biodegradability enhancement and toxicity reduction. Science of The Total Environment 671:270-279.

Afzal, A., P. Chelme-Ayala, P. Drzewicz, J. W. Martin, and M. Gamal El-Din. 2015. Effects of ozone and ozone/hydrogen peroxide on the degradation of model and real oil-sands-process-affected-water naphthenic acids. Ozone: Science & Engineering 37:45-54.

Afzal, A., P. Drzewicz, J. W. Martin, and M. Gamal El-Din. 2012a. Decomposition of cyclohexanoic acid by the UV/H_2O_2 process under various conditions. Science of the Total Environment 426:387-392.

Afzal, A., P. Drzewicz, L. A. Pérez-Estrada, Y. Chen, J. W. Martin, and M. Gamal El-Din. 2012. Effect of Molecular Structure on the Relative Reactivity of Naphthenic Acids in the UV/H_2O_2 Advanced Oxidation Process. Environmental Science & Technology 46:10727-10734.

Alberts, M. E., G. Chua, and D. G. Muench. 2019. Exposure to naphthenic acids and the acid extractable organic fraction from oil sands process-affected water alters the

subcellular structure and dynamics of plant cells. Science of The Total Environment 651:2830-2844.

Allen, E. W. 2008a. Process water treatment in Canada's oil sands industry: I. Target pollutants and treatment objectives. Journal of Environmental Engineering and Science 7:123-138.

Allen, E. W. 2008b. Process water treatment in Canada's oil sands industry: II. A review of emerging technologies. Journal of Environmental Engineering and Science 7:499-524.

Alpatova, A., E.-S. Kim, S. Dong, N. Sun, P. Chelme-Ayala, and M. Gamal El-Din. 2014. Treatment of oil sands process-affected water with ceramic ultrafiltration membrane: Effects of operating conditions on membrane performance. Separation and Purification Technology 122:170-182.

Alpatova, A., E.-S. Kim, X. Sun, G. Hwang, Y. Liu, and M. Gamal El-Din. 2013. Fabrication of porous polymeric nanocomposite membranes with enhanced anti-fouling properties: Effect of casting composition. Journal of Membrane Science 444:449-460.

Anbar, M., D. Meyerstein, and P. Neta. 1966. Reactivity of aliphatic compounds towards hydroxyl radicals. Journal of the Chemical Society B: Physical Organic:742-747.

Armstrong, S. A., J. V. Headley, K. M. Peru, R. J. Mikula, and J. J. Germida. 2010. Phytotoxicity and naphthenic acid dissipation from oil sands fine tailings treatments

planted with the emergent macrophyte Phragmites australis. Journal of Environmental Science and Health, Part A 45:1008-1016.

Barrow, M. P., M. Witt, J. V. Headley, and K. M. Peru. 2010. Athabasca Oil Sands Process Water: Characterization by Atmospheric Pressure Photoionization and Electrospray Ionization Fourier Transform Ion Cyclotron Resonance Mass Spectrometry. Analytical Chemistry 82:3727-3735.

Benally, C., M. Li, and M. G. El-Din. 2018. The effect of carboxyl multiwalled carbon nanotubes content on the structure and performance of polysulfone membranes for oil sands process-affected water treatment. Separation and purification Technology 199:170-181.

Benally, C., S. A. Messele, and M. Gamal El-Din. 2019. Adsorption of organic matter in oil sands process water (OSPW) by carbon xerogel. Water Research 154:402-411.

Brillas, E. and C. A. Martínez-Huitle. 2015. Decontamination of wastewaters containing synthetic organic dyes by electrochemical methods. An updated review. Applied Catalysis B: Environmental 166:603-643.

Brillas, E., I. Sirés, and M. A. Oturan. 2009. Electro-Fenton Process and Related Electrochemical Technologies Based on Fenton's Reaction Chemistry. Chemical reviews 109:6570-6631.

Brown, L. D. and A. C. Ulrich. 2015. Oil sands naphthenic acids: A review of properties, measurement, and treatment. Chemosphere 127:276-290.

Çeçen, F. and Ö. Aktaş. 2011. Activated carbon for water and wastewater treatment: integration of adsorption and biological treatment. WILEY-VCH Verlag GMBH & Co. KGaA, Weinheim.

Chan, P. Y., M. G. El-Din, and J. R. Bolton. 2012. A solar-driven UV/Chlorine advanced oxidation process. Water research 46:5672-5682.

Chaplin, B. P. 2014. Critical review of electrochemical advanced oxidation processes for water treatment applications. Environmental Science: Processes & Impacts 16:1182-1203.

Chen, G. 2004. Electrochemical technologies in wastewater treatment. Separation and purification Technology 38:11-41.

Choi, J., G. Hwang, M. Gamal El-Din, and Y. Liu. 2014. Effect of reactor configuration and microbial characteristics on biofilm reactors for oil sands process-affected water treatment. International Biodeterioration & Biodegradation 89:74-81.

Clemente, J. S. and P. M. Fedorak. 2005. A review of the occurrence, analyses, toxicity, and biodegradation of naphthenic acids. Chemosphere 60:585-600.

Clemente, J. S., M. D. MacKinnon, and P. M. Fedorak. 2004. Aerobic biodegradation of two commercial naphthenic acids preparations. Environmental science & technology 38:1009-1016.

Clemente, J. S., N. G. N. Prasad, M. D. MacKinnon, and P. M. Fedorak. 2003. A statistical comparison of naphthenic acids characterized by gas chromatography–mass spectrometry. Chemosphere 50:1265-1274.

201

Comninellis, C. and G. Chen. 2010. Electrochemistry for the Environment. Springer.

de Klerk, A., M. R. Gray, and N. Zerpa. 2014. Unconventional oil and gas: Oilsands. Pages 95-116 Future Energy (Second Edition). Elsevier.

de Oliveira Livera, D., T. Leshuk, K. M. Peru, J. V. Headley, and F. Gu. 2018. Structure-reactivity relationship of naphthenic acids in the photocatalytic degradation process. Chemosphere 200:180-190.

Deborde, M. and U. von Gunten. 2008. Reactions of chlorine with inorganic and organic compounds during water treatment—Kinetics and mechanisms: A critical review. Water Research 42:13-51.

Dong, T., Y. Zhang, M. S. Islam, Y. Liu, and M. Gamal El-Din. 2015. The impact of various ozone pretreatment doses on the performance of endogenous microbial communities for the remediation of oil sands process-affected water. International Biodeterioration & Biodegradation 100:17-28.

Drogui, P., S. Elmaleh, M. Rumeau, C. Bernard, and A. Rambaud. 2001. Oxidising and disinfecting by hydrogen peroxide produced in a two-electrode cell. Water Research 35:3235-3241.

Drzewicz, P., L. Perez-Estrada, A. Alpatova, J. W. Martin, and M. Gamal El-Din. 2012. Impact of peroxydisulfate in the presence of zero valent iron on the oxidation of cyclohexanoic acid and naphthenic acids from oil sands process-affected water. Environmental science & technology 46:8984-8991.

Energy, A. 2013. reality check on the shale revolution Hughes, J. David. Nature (London, United Kingdom) 494:307-308.

Fang, Z., P. Chelme-Ayala, Q. Shi, C. Xu, and M. Gamal El-Din. 2018. Degradation of naphthenic acid model compounds in aqueous solution by UV activated persulfate: Influencing factors, kinetics and reaction mechanisms. Chemosphere 211:271-277.

Fockedey, E. and A. Van Lierde. 2002. Coupling of anodic and cathodic reactions for phenol electro-oxidation using three-dimensional electrodes. Water research 36:4169-4175.

Frank, R. A., H. Sanderson, R. Kavanagh, B. K. Burnison, J. V. Headley, and K. R. Solomon. 2009. Use of a (Quantitative) Structure–Activity Relationship [(Q)Sar] Model to Predict the Toxicity of Naphthenic Acids. Journal of Toxicology and Environmental Health, Part A 73:319-329.

Frank, R. A., K. Fischer, R. Kavanagh, B. K. Burnison, G. Arsenault, J. V. Headley, K. M. Peru, G. V. D. Kraak, and K. R. Solomon. 2009. Effect of Carboxylic Acid Content on the Acute Toxicity of Oil Sands Naphthenic Acids. Environmental Science & Technology 43:266-271.

Gamal El-Din, M., H. Fu, N. Wang, P. Chelme-Ayala, L. Pérez-Estrada, P. Drzewicz, J. W. Martin, W. Zubot, and D. W. Smith. 2011. Naphthenic acids speciation and removal during petroleum-coke adsorption and ozonation of oil sands process-affected water. Science of The Total Environment 409:5119-5125.

Ganiyu, S. O., M. Zhou, and C. A. Martínez-Huitle. 2018. Heterogeneous electro-Fenton and photoelectro-Fenton processes: a critical review of fundamental principles and application for water/wastewater treatment. Applied Catalysis B: Environmental.

Ganzenko, O., D. Huguenot, E. D. van Hullebusch, G. Esposito, and M. A. Oturan. 2014. Electrochemical advanced oxidation and biological processes for wastewater treatment: a review of the combined approaches. Environmental Science and Pollution Research 21:8493-8524.

Garcia-Garcia, E., J. Q. Ge, A. Oladiran, B. Montgomery, M. Gamal El-Din, L. C. Perez-Estrada, J. L. Stafford, J. W. Martin, and M. Belosevic. 2011. Ozone treatment ameliorates oil sands process water toxicity to the mammalian immune system. Water Research 45:5849-5857.

George, V. 1988. Critical review of rate constants for reactions of hydrated electrons, hydrogen atoms and hydroxyl radicals (OH/O) in an aqueous solution. J. Phys. Chem. Ref. Data 17:513-886.

Giesy, J. P., J. C. Anderson, and S. B. Wiseman. 2010. Alberta oil sands development. Proceedings of the National Academy of Sciences 107:951.

Glaze, W. H., J.-W. Kang, and D. H. Chapin. 1987. The Chemistry of Water Treatment Processes Involving Ozone, Hydrogen Peroxide and Ultraviolet Radiation. Ozone: Science & Engineering 9:335-352.

Hagen, M. O., B. A. Katzenback, M. D. S. Islam, M. Gamal El-Din, and M. Belosevic. 2013. The Analysis of Goldfish (*Carassius auratus L.*) Innate Immune Responses

After Acute and Subchronic Exposures to Oil Sands Process-Affected Water. Toxicological Sciences 138:59-68.

Hagen, M. O., E. Garcia-Garcia, A. Oladiran, M. Karpman, S. Mitchell, M. G. El-Din, J. W. Martin, and M. Belosevic. 2012. The acute and sub-chronic exposures of goldfish to naphthenic acids induce different host defense responses. Aquatic toxicology 109:143-149.

Han, X., A. C. Scott, P. M. Fedorak, M. Bataineh, and J. W. Martin. 2008. Influence of Molecular Structure on the Biodegradability of Naphthenic Acids. Environmental Science & Technology 42:1290-1295.

Han, X., M. D. MacKinnon, and J. W. Martin. 2009. Estimating the in situ biodegradation of naphthenic acids in oil sands process waters by HPLC/HRMS. Chemosphere 76:63-70.

Hastie, J., D. Bejan, and N. J. Bunce. 2011. Oxidation of sulfide ion in synthetic geothermal brines at carbon-based anodes. The Canadian Journal of Chemical Engineering 89:948-957.

He, Y., S. B. Wiseman, M. Hecker, X. Zhang, N. Wang, L. A. Perez, P. D. Jones, M. Gamal El-Din, J. W. Martin, and J. P. Giesy. 2011. Effect of ozonation on the estrogenicity and androgenicity of oil sands process-affected water. Environmental science & technology 45:6268-6274.

Headley, J. V., K. M. Peru, M. H. Mohamed, R. A. Frank, J. W. Martin, R. R. O. Hazewinkel, D. Humphries, N. P. Gurprasad, L. M. Hewitt, D. C. G. Muir, D.

205

Lindeman, R. Strub, R. F. Young, D. M. Grewer, R. M. Whittal, P. M. Fedorak, D. A. Birkholz, R. Hindle, R. Reisdorph, X. Wang, K. L. Kasperski, C. Hamilton, M. Woudneh, G. Wang, B. Loescher, A. Farwell, D. G. Dixon, M. Ross, A. D. S. Pereira, E. King, M. P. Barrow, B. Fahlman, J. Bailey, D. W. McMartin, C. H. Borchers, C. H. Ryan, N. S. Toor, H. M. Gillis, L. Zuin, G. Bickerton, M. McMaster, E. Sverko, D. Shang, L. D. Wilson, and F. J. Wrona. 2013. Chemical fingerprinting of naphthenic acids and oil sands process waters—A review of analytical methods for environmental samples. Journal of Environmental Science and Health, Part A 48:1145-1163.

Herman, D. C., P. M. Fedorak, M. D. MacKinnon, and J. W. Costerton. 1994. Biodegradation of naphthenic acids by microbial populations indigenous to oil sands tailings. Canadian Journal of Microbiology 40:467-477.

Hewgill, F. R. and G. M. Proudfoot. 1976. Regioselective oxidation of aliphatic acids by complexed hydroxyl radicals. Australian Journal of Chemistry 29:637-647.

Holowenko, F. M., M. D. MacKinnon, and P. M. Fedorak. 2002. Characterization of naphthenic acids in oil sands wastewaters by gas chromatography-mass spectrometry. Water Research 36:2843-2855.

Hooshiar, A., P. Uhlik, Q. Liu, T. H. Etsell, and D. G. Ivey. 2012. Clay minerals in nonaqueous extraction of bitumen from Alberta oil sands: Part 1. Nonaqueous extraction procedure. Fuel processing technology 94:80-85.

Iranmanesh, S., T. Harding, J. Abedi, F. Seyedeyn-Azad, and D. B. Layzell. 2014. Adsorption of naphthenic acids on high surface area activated carbons. Journal of Environmental Science and Health, Part A 49:913-922.

Islam, M. S., J. Moreira, P. Chelme-Ayala, and M. Gamal El-Din. 2014. Prediction of naphthenic acid species degradation by kinetic and surrogate models during the ozonation of oil sands process-affected water. Science of the Total Environment 493:282-290.

Islam, M. S., Y. Zhang, K. N. McPhedran, Y. Liu, and M. Gamal El-Din. 2015. Granular activated carbon for simultaneous adsorption and biodegradation of toxic oil sands process-affected water organic compounds. Journal of Environmental Management 152:49-57.

Janfada, A., J. V. Headley, K. M. Peru, and S. L. Barbour. 2006. A Laboratory Evaluation of the Sorption of Oil Sands Naphthenic Acids on Organic Rich Soils. Journal of Environmental Science and Health, Part A 41:985-997.

Jones, D., A. G. Scarlett, C. E. West, and S. J. Rowland. 2011. Toxicity of Individual Naphthenic Acids to *Vibrio fischeri*. Environmental science & technology 45:9776-9782.

Kannel, P. R. and T. Y. Gan. 2012. Naphthenic acids degradation and toxicity mitigation in tailings wastewater systems and aquatic environments: A review. Journal of Environmental Science and Health, Part A 47:1-21.

Kim, E.-S., Y. Liu, and M. Gamal El-Din. 2012. Evaluation of Membrane Fouling for In-Line Filtration of Oil Sands Process-Affected Water: The Effects of Pretreatment Conditions. Environmental Science & Technology 46:2877-2884.

Klamerth, N., J. Moreira, C. Li, A. Singh, K. N. McPhedran, P. Chelme-Ayala, M. Belosevic, and M. Gamal El-Din. 2015. Effect of ozonation on the naphthenic acids' speciation and toxicity of pH-dependent organic extracts of oil sands process-affected water. Science of the Total Environment 506:66-75.

Kruppa, G. H. and J. Beauchamp. 1986. Energetics and structure of the 1-and 2-adamantyl radicals and their corresponding carbonium ions by photoelectron spectroscopy. Journal of the American Chemical Society 108:2162-2169.

Kumar, S., S. Singh, and V. C. Srivastava. 2015. Electro-oxidation of nitrophenol by ruthenium oxide coated titanium electrode: Parametric, kinetic and mechanistic study. Chemical Engineering Journal 263:135-143.

Li, C., L. Fu, J. Stafford, M. Belosevic, and M. G. El-Din. 2017. The toxicity of oil sands process-affected water (OSPW): a critical review. Science of the Total Environment 601:1785-1802.

Loganathan, K., P. Chelme-Ayala, and M. Gamal El-Din. 2015. Effects of different pretreatments on the performance of ceramic ultrafiltration membrane during the treatment of oil sands tailings pond recycle water: A pilot-scale study. Journal of Environmental Management 151:540-549.

Lu, W., A. Ewanchuk, L. Perez-Estrada, D. Sego, and A. Ulrich. 2013. Limitation of fluorescence spectrophotometry in the measurement of naphthenic acids in oil sands process water. Journal of Environmental Science and Health, Part A 48:429-436.

MacKinnon, M. D. and H. Boerger. 1986. Description of Two Treatment Methods for Detoxifying Oil Sands Tailings Pond Water. Water Quality Research Journal 21:496-512.

Martin, J. W., T. Barri, X. Han, P. M. Fedorak, M. Gamal El-Din, L. Perez, A. C. Scott, and J. T. Jiang. 2010. Ozonation of Oil Sands Process-Affected Water Accelerates Microbial Bioremediation. Environmental Science & Technology 44:8350-8356.

Martin, J. W., X. Han, K. M. Peru, and J. V. Headley. 2008. Comparison of high- and low-resolution electrospray ionization mass spectrometry for the analysis of naphthenic acid mixtures in oil sands process water. Rapid Communications in Mass Spectrometry 22:1919-1924.

Martínez-Huitle, C. A. and M. Panizza. 2018. Electrochemical oxidation of organic pollutants for wastewater treatment. Current Opinion in Electrochemistry 11:62-71.

Martinez-Huitle, C. A. and S. Ferro. 2006. Electrochemical oxidation of organic pollutants for the wastewater treatment: direct and indirect processes. Chemical Society Reviews 35:1324-1340.

Martínez-Huitle, C. A., M. A. Rodrigo, I. Sirés, and O. Scialdone. 2015. Single and coupled electrochemical processes and reactors for the abatement of organic water pollutants: a critical review. Chemical Reviews 115:13362-13407.

Masliyah, J., Z. J. Zhou, Z. Xu, J. Czarnecki, and H. Hamza. 2004. Understanding water-based bitumen extraction from Athabasca oil sands. The Canadian Journal of Chemical Engineering 82:628-654.

Meshref, M. N. A., N. Klamerth, M. S. Islam, K. N. McPhedran, and M. Gamal El-Din. 2017. Understanding the similarities and differences between ozone and peroxone in the degradation of naphthenic acids: Comparative performance for potential treatment. Chemosphere 180:149-159.

Meshref, M. N., P. Chelme-Ayala, and M. Gamal El-Din. 2017. Fate and abundance of classical and heteroatomic naphthenic acid species after advanced oxidation processes: Insights and indicators of transformation and degradation. Water research 125:62-71.

Miao, J., H. Zhu, Y. Tang, Y. Chen, and P. Wan. 2014. Graphite felt electrochemically modified in H2SO4 solution used as a cathode to produce H2O2 for pre-oxidation of drinking water. Chemical Engineering Journal 250:312-318.

Minakata, D., K. Li, P. Westerhoff, and J. Crittenden. 2009. Development of a group contribution method to predict aqueous phase hydroxyl radical (HO•) reaction rate constants. Environmental science & technology 43:6220-6227.

Mishra, S., V. Meda, A. K. Dalai, J. V. Headley, K. M. Peru, and D. W. McMartin. 2010. Microwave treatment of naphthenic acids in water. Journal of Environmental Science and Health, Part A 45:1240-1247.

Misiti, T. M., U. Tezel, and S. G. Pavlostathis. 2014. Effect of Alkyl Side Chain Location and Cyclicity on the Aerobic Biotransformation of Naphthenic Acids. Environmental science & technology 48:7909-7917.

Misiti, T., U. Tezel, and S. G. Pavlostathis. 2013. Fate and effect of naphthenic acids on oil refinery activated sludge wastewater treatment systems. Water research 47:449-460.

Mohamed, M. H., L. D. Wilson, J. V. Headley, and K. M. Peru. 2008. Novel materials for environmental remediation of tailing pond waters containing naphthenic acids. Process Safety and Environmental Protection 86:237-243.

Moreira, F. C., R. A. R. Boaventura, E. Brillas, and V. J. P. Vilar. 2017. Electrochemical advanced oxidation processes: A review on their application to synthetic and real wastewaters. Applied Catalysis B: Environmental 202:217-261.

Operators, O. S. M. 2015. Water Allocation and Water Use by Year; OSIP Data Library; Government of Alberta.

Osacky, M., M. Geramian, D. G. Ivey, Q. Liu, and T. H. Etsell. 2013. Mineralogical and chemical composition of petrologic end members of Alberta oil sands. Fuel 113:148-157.

Oturan, M. A. 2000. An ecologically effective water treatment technique using electrochemically generated hydroxyl radicals for in situ destruction of organic pollutants: Application to herbicide 2,4-D. Journal of Applied Electrochemistry 30:475-482.

Pal, K., L. d. P. Nogueira Branco, A. Heintz, P. Choi, Q. Liu, P. R. Seidl, and M. R. Gray. 2015. Performance of solvent mixtures for non-aqueous extraction of Alberta oil sands. Energy & Fuels 29:2261-2267.

Panizza, M. 2010. Importance of Electrode Material in the Electrochemical Treatment of Wastewater Containing Organic Pollutants. Pages 25-54 in C. Comninellis and G. Chen, editors. Electrochemistry for the Environment. Springer New York, New York, NY.

Panizza, M. and G. Cerisola. 2006. Olive mill wastewater treatment by anodic oxidation with parallel plate electrodes. Water Research 40:1179-1184.

Panizza, M. and G. Cerisola. 2007. Electrocatalytic materials for the electrochemical oxidation of synthetic dyes. Applied Catalysis B: Environmental 75:95-101.

Panizza, M. and G. Cerisola. 2009. Direct and mediated anodic oxidation of organic pollutants. Chemical reviews 109:6541-6569.

Peng, H., K. Volchek, M. MacKinnon, W. P. Wong, and C. E. Brown. 2004. Application on to nanofiltration to water management options for oil sands operation. Desalination 170:137-150.

Pereira, A. S., M. S. Islam, M. Gamal El-Din, and J. W. Martin. 2013. Ozonation degrades all detectable organic compound classes in oil sands process-affected water; an application of high-performance liquid chromatography/obitrap mass spectrometry. Rapid Communications in Mass Spectrometry 27:2317-2326.

Pérez-Estrada, L. A., X. Han, P. Drzewicz, M. Gamal El-Din, P. M. Fedorak, and J. W. Martin. 2011. Structure–reactivity of naphthenic acids in the ozonation process. Environmental science & technology 45:7431-7437.

Pourrezaei, P., P. Drzewicz, Y. Wang, M. Gamal El-Din, L. A. Perez-Estrada, J. W. Martin, J. Anderson, S. Wiseman, K. Liber, and J. P. Giesy. 2011. The Impact of Metallic Coagulants on the Removal of Organic Compounds from Oil Sands Process-Affected Water. Environmental Science & Technology 45:8452-8459.

Qiao, M.-X., Y. Zhang, L.-F. Zhai, and M. Sun. 2018. Corrosion of graphite electrode in electrochemical advanced oxidation processes: Degradation protocol and environmental implication. Chemical Engineering Journal 344:410-418.

Quinlan, P. J. and K. C. Tam. 2015. Water treatment technologies for the remediation of naphthenic acids in oil sands process-affected water. Chemical Engineering Journal 279:696-714.

Rao, A. N. S. and V. T. Venkatarangaiah. 2014. Metal oxide-coated anodes in wastewater treatment. Environmental Science and Pollution Research 21:3197-3217.

Regulator, A. E. 2014. Alberta's energy reserves 2011 and supply/demand outlook 2012–2021. ST98-2012. ISSN 1910-4235. Alberta Energy Regulator Calgary, Canada.

Reinardy, H. C., A. G. Scarlett, T. B. Henry, C. E. West, L. M. Hewitt, R. A. Frank, and S. J. Rowland. 2013. Aromatic Naphthenic Acids in Oil Sands Process-Affected Water, Resolved by GCxGC-MS, Only Weakly Induce the Gene for Vitellogenin Production

in Zebrafish (Danio rerio) Larvae. Environmental Science & Technology 47:6614-6620.

Rogers, V. V., K. Liber, and M. D. MacKinnon. 2002. Isolation and characterization of naphthenic acids from Athabasca oil sands tailings pond water. Chemosphere 48:519-527.

Ross, M. S., A. d. S. Pereira, J. Fennell, M. Davies, J. Johnson, L. Sliva, and J. W. Martin. 2012. Quantitative and Qualitative Analysis of Naphthenic Acids in Natural Waters Surrounding the Canadian Oil Sands Industry. Environmental Science & Technology 46:12796-12805.

Rowland, S. J., A. G. Scarlett, D. Jones, C. E. West, and R. A. Frank. 2011. Diamonds in the Rough: Identification of Individual Naphthenic Acids in Oil Sands Process Water. Environmental Science & Technology 45:3154-3159.

Rueffer, M., D. Bejan, and N. J. Bunce. 2011. Graphite: An active or an inactive anode? Electrochimica Acta 56:2246-2253.

Santo, C. E., V. J. P. Vilar, C. M. S. Botelho, A. Bhatnagar, E. Kumar, and R. A. R. Boaventura. 2012. Optimization of coagulation–flocculation and flotation parameters for the treatment of a petroleum refinery effluent from a Portuguese plant. Chemical Engineering Journal 183:117-123.

Särkkä, H., A. Bhatnagar, and M. Sillanpää. 2015. Recent developments of electro-oxidation in water treatment—a review. Journal of Electroanalytical Chemistry 754:46-56.

Schuchmann, M. N., E. Bothe, J. von Sonntag, and C. von Sonntag. 1998. Reaction of OH radicals with benzoquinone in aqueous solutions. A pulse radiolysis study. Journal of the Chemical Society, Perkin Transactions 2:791-796.

Scott, A. C., M. D. Mackinnon, and P. M. Fedorak. 2005. Naphthenic Acids in Athabasca Oil Sands Tailings Waters Are Less Biodegradable than Commercial Naphthenic Acids. Environmental Science & Technology 39:8388-8394.

Scott, A. C., R. F. Young, and P. M. Fedorak. 2008a. Comparison of GC–MS and FTIR methods for quantifying naphthenic acids in water samples. Chemosphere 73:1258-1264.

Scott, A. C., W. Zubot, M. D. MacKinnon, D. W. Smith, and P. M. Fedorak. 2008b. Ozonation of oil sands process water removes naphthenic acids and toxicity. Chemosphere 71:156-160.

Shi, Y., C. Huang, K. C. Rocha, M. G. El-Din, and Y. Liu. 2015. Treatment of oil sands process-affected water using moving bed biofilm reactors: with and without ozone pretreatment. Bioresource technology 192:219-227.

Shu, Z., C. Li, M. Belosevic, J. R. Bolton, and M. Gamal El-Din. 2014. Application of a Solar UV/Chlorine Advanced Oxidation Process to Oil Sands Process-Affected Water Remediation. Environmental Science & Technology 48:9692-9701.

Simpson, D. R. 2008. Biofilm processes in biologically active carbon water purification. Water Research 42:2839-2848.

Sirés, I., E. Brillas, M. A. Oturan, M. A. Rodrigo, and M. Panizza. 2014. Electrochemical advanced oxidation processes: today and tomorrow. A review. Environmental Science and Pollution Research 21:8336-8367.

Small Christina, C., C. Ulrich Ania, and Z. Hashisho. 2012. Adsorption of Acid Extractable Oil Sands Tailings Organics onto Raw and Activated Oil Sands Coke. Journal of Environmental Engineering 138:833-840.

Smith, B. E., C. A. Lewis, S. T. Belt, C. Whitby, and S. J. Rowland. 2008. Effects of Alkyl Chain Branching on the Biotransformation of Naphthenic Acids. Environmental science & technology 42:9323-9328.

Swart, N. C. and A. J. Weaver. 2012. The Alberta oil sands and climate. Nature Climate Change 2:134.

Szpyrkowicz, L., S. N. Kaul, R. N. Neti, and S. Satyanarayan. 2005. Influence of anode material on electrochemical oxidation for the treatment of tannery wastewater. Water Research 39:1601-1613.

Vaiopoulou, E., T. M. Misiti, and S. G. Pavlostathis. 2015. Removal and toxicity reduction of naphthenic acids by ozonation and combined ozonation-aerobic biodegradation. Bioresource technology 179:339-347.

Verbeek, A., W. Mackay, and M. MacKinnon. 1989. A toxicity assessment of oil sands wastewater: a toxic balance. Can. Tech. Rep. Fish. Aquat. Sci:196-207.

Wang, B., Y. Wan, Y. Gao, M. Yang, and J. Hu. 2013. Determination and Characterization of Oxy-Naphthenic Acids in Oilfield Wastewater. Environmental science & technology 47:9545-9554.

Wang, C., A. Alpatova, K. N. McPhedran, and M. Gamal El-Din. 2015. Coagulation/flocculation process with polyaluminum chloride for the remediation of oil sands process-affected water: Performance and mechanism study. Journal of Environmental Management 160:254-262.

Wang, C., N. Klamerth, R. Huang, H. Elnakar, and M. Gamal El-Din. 2016a. Oxidation of oil sands process-affected water by potassium ferrate (VI). Environmental science & technology 50:4238-4247.

Wang, C., N. Klamerth, S. A. Messele, A. Singh, M. Belosevic, and M. Gamal El-Din. 2016b. Comparison of UV/hydrogen peroxide, potassium ferrate(VI), and ozone in oxidizing the organic fraction of oil sands process-affected water (OSPW). Water Research 100:476-485.

Wang, C., R. Huang, N. Klamerth, P. Chelme-Ayala, and M. Gamal El-Din. 2016c. Positive and negative electrospray ionization analyses of the organic fractions in raw and oxidized oil sands process-affected water. Chemosphere 165:239-247.

Wang, N., P. Chelme-Ayala, L. Perez-Estrada, E. Garcia-Garcia, J. Pun, J. W. Martin, M. Belosevic, and M. Gamal El-Din. 2013. Impact of ozonation on naphthenic acids speciation and toxicity of oil sands process-affected water to *Vibrio fischeri* and mammalian immune system. Environmental Science & Technology 47:6518-6526.

Whitby, C. 2010. Microbial naphthenic acid degradation. Pages 93-125, Advances in applied microbiology. Elsevier.

Williams, A. T. R., S. A. Winfield, and J. N. Miller. 1983. Relative fluorescence quantum yields using a computer-controlled luminescence spectrometer. Analyst 108:1067-1071.

Wiseman, S. B., Y. He, M. Gamal-El Din, J. W. Martin, P. D. Jones, M. Hecker, and J. P. Giesy. 2013. Transcriptional responses of male fathead minnows exposed to oil sands process-affected water. Comparative Biochemistry and Physiology Part C: Toxicology & Pharmacology 157:227-235.

Woodworth, A. P. J., R. A. Frank, B. J. McConkey, and K. M. Müller. 2012. Toxic effects of oil sand naphthenic acids on the biomass accumulation of 21 potential phytoplankton remediation candidates. Ecotoxicology and Environmental Safety 86:156-161.

Xue, J., C. Huang, Y. Zhang, Y. Liu, and M. Gamal El-Din. 2018. Bioreactors for oil sands process-affected water (OSPW) treatment: A critical review. Science of the Total Environment 627:916-933.

Xue, J., Y. Zhang, Y. Liu, and M. Gamal El-Din. 2016. Treatment of oil sands process-affected water (OSPW) using a membrane bioreactor with a submerged flat-sheet ceramic microfiltration membrane. Water Research 88:1-11.

Yue, S., B. A. Ramsay, R. S. Brown, J. Wang, and J. A. Ramsay. 2014. Identification of estrogenic compounds in oil sands process waters by effect directed analysis. Environmental science & technology 49:570-577.

Yue, Z., W. Jiang, L. Wang, S. Gardner, and C. Pittman Jr. 1999. Surface characterization of electrochemically oxidized carbon fibers. Carbon 37:1785-1796.

Zanta, C. L. P. S., A. R. de Andrade, and J. F. C. Boodts. 2000. Electrochemical behaviour of olefins: oxidation at ruthenium–titanium dioxide and iridium–titanium dioxide coated electrodes. Journal of Applied Electrochemistry 30:467-474.

Zhang, Y., J. Xue, Y. Liu, and M. G. El-Din. 2016b. Treatment of oil sands process-affected water using membrane bioreactor coupled with ozonation: A comparative study. Chemical Engineering Journal 302:485-497.

Zhang, Y., K. N. McPhedran, and M. Gamal El-Din. 2015. Pseudomonads biodegradation of aromatic compounds in oil sands process-affected water. Science of the Total Environment 521-522:59-67.

Zhang, Y., N. Klamerth, and M. G. El-Din. 2016a. Degradation of a model naphthenic acid by nitrilotriacetic acid–modified Fenton process. Chemical Engineering Journal 292:340-347.

Zhang, Y., N. Klamerth, P. Chelme-Ayala, and M. Gamal El-Din. 2017. Comparison of classical fenton, nitrilotriacetic acid (NTA)-Fenton, UV-Fenton, UV photolysis of Fe-NTA, UV-NTA-Fenton, and UV-H_2O_2 for the degradation of cyclohexanoic acid. Chemosphere 175:178-185.

Zhang, Y., N. Klamerth, S. A. Messele, P. Chelme-Ayala, and M. G. El-Din. 2016a. Kinetics study on the degradation of a model naphthenic acid by ethylenediamine-N, N'-disuccinic acid-modified Fenton process. Journal of hazardous materials 318:371-378.

Zhang, Y., P. Chelme-Ayala, N. Klamerth, and M. Gamal El-Din. 2017. Application of UV-irradiated Fe(III)-nitrilotriacetic acid (UV-Fe(III)NTA) and UV-NTA-Fenton systems to degrade model and natural occurring naphthenic acids. Chemosphere 179:359-366.

Zhu, S., M. Li, and M. Gamal El-Din. 2017. Forward osmosis as an approach to manage oil sands tailings water and on-site basal depressurization water. Journal of Hazardous Materials 327:18-27.

Zöllig, H., C. Fritzsche, E. Morgenroth, and K. M. Udert. 2015. Direct electrochemical oxidation of ammonia on graphite as a treatment option for stored source-separated urine. Water research 69:284-294.

Zubot, W., M. D. MacKinnon, P. Chelme-Ayala, D. W. Smith, and M. Gamal El-Din. 2012. Petroleum coke adsorption as a water management option for oil sands process-affected water. Science of The Total Environment 427-428:364-372.

APPENDIX A. EXPERIMENTAL METHODOLOGY

A-1 Ultra-performance liquid chromatography time-of-flight mass spectrometry (UPLC TOF-MS)

NA concentration was measured using ultra-performance liquid chromatography time-of-flight mass spectrometry (UPLC TOF-MS). The sample analysis was performed using a high-resolution time-of-flight mass spectrometry TOF-MS (Synapt G2, Waters, MA, USA) on negative electrospray ionization mode and myristic acid-1-^{13}C was used as the internal standard. Chromatographic separation was accomplished using Waters UPLC Phenyl BEH column (Waters, MA, USA). The sample analysis was performed using a high-resolution time-of-flight mass spectrometry TOF-MS (Synapt G2, Waters, MA, USA) on negative electrospray ionization mode and myristic acid-1-^{13}C was used as the internal standard. Sample of a mixture consisting of 500 μL OSPW sample, 100 μL of 4.0 mg/L internal standard (myristic acid-1-^{13}C), and 400 μL methanol was injected into the instrument. The column temperature was set at 50 ºC while the sample temperature was 10 ºC. The mobile phases were: (A) 10 mM ammonium acetate in water and (B) 10 mM ammonium acetate in 50/50 methanol/acetonitrile at a 100 μL/min flow rate. The elution gradient was 1% B during 0–2 min; increased from 1% to 60% B during 2–3 min; then increased to 70% B during 3–7 min; went to 95% B during 7–13 min; went down to 1% B during 13–14 min, and hold 1% B until 20 min to equilibrate the column with a flow rate of 100 μL/min. The data acquisition process was performed using MassLynx (Waters, MA, USA) and data extraction from spectra was done using TargetLynx (Waters, MA, USA). The identification

of classical NAs (O_2) and oxy-NAs was based on the empirical formula $C_nH_{2n+z}Ox$ (x=2, 3, 4, 5) where n ranged from 7 to 26 and z from 0 to -18.

A-2 DNA extraction and qPCR detection

PowerSoil® DNA isolation kit (Mo-Bio Laboratories, CA, USA) was used for the extraction of bacterial DNA following the manufacturer instructions. After extraction, The DNA sample was stored at -20 °C before performing the qPCR analysis. A Bio-Rad CFX96 real-time PCR system equipped with a C1000 Thermal Cycler (Bio-Rad, ON, CA) was used to conduct the qPCR analysis. A reaction volume of 20 µL was used for each reaction including 6 µL of sterile water, 1 µL of each primer with a concentration of 10 µM, 10 µL of 2 × SsoFast EvaGreen Supermix, and 2 µL of diluted sample DNA. Forward 341F primer (CCTACGGGAGGCAGCAG) and reverse 534R primer (ATTACCGCGGCTGCTGG) were used to quantify the total bacterial copies number. The qPCR analysis stages consisted of an initial 3 min at 95 °C, followed by 35 cycles of denaturing at 94 °C for 30 s, annealing at 60 °C for 45 s, and extension at 72 °C for 30 s was used to amplify the 16s rDNA genes of total bacteria. All PCR runs used plasmid standards for quantification. Standard plasmids containing target genes were constructed using a TOPO TA Cloning kit (Invitrogen Corporation, Carlsbad, California, USA). Reactions without the DNA template were used as negative controls.

A-3 Next generation sequencing

Illumina MiSeq sequencing was used to further understand the dynamics of the microbial communities after different EO pre-treatment conditions. The sequencing was performed at Research and Testing Laboratory (Lubbock, TX, USA). Following the DNA extraction,

amplification of the V1-V2 hypervariable regions of 16S rRNA genes was done using a forward primer 28F and reverse fusion primer 338R prior to loading them on an Illumina MiSeq instrument. Raw data and analysis data were provided by the company along with instructions on how to analyze the data. After denoising (USEARCH application) and chimera removal (UCHIIME in *de novo* mode), the sequences were clustered into operational taxonomic units (OTU) clusters with 100% identity using USEARCH for taxonomic identification.

APPENDIX B. SUPPORTING FIGURES
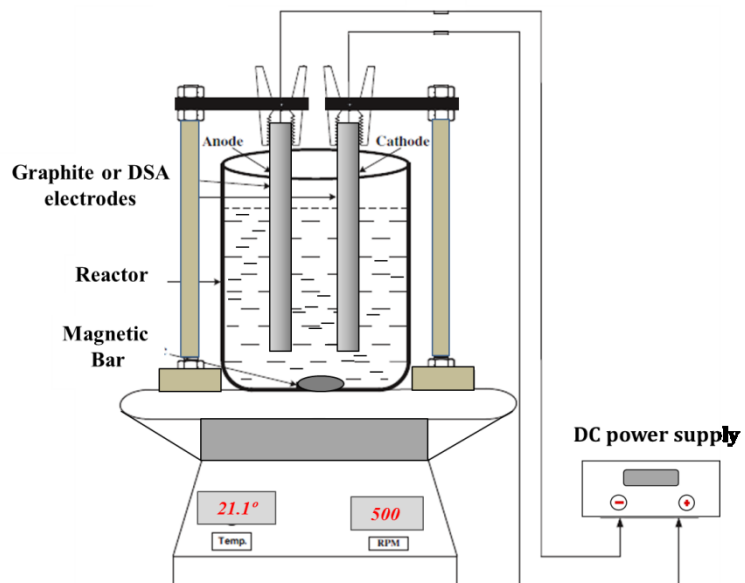
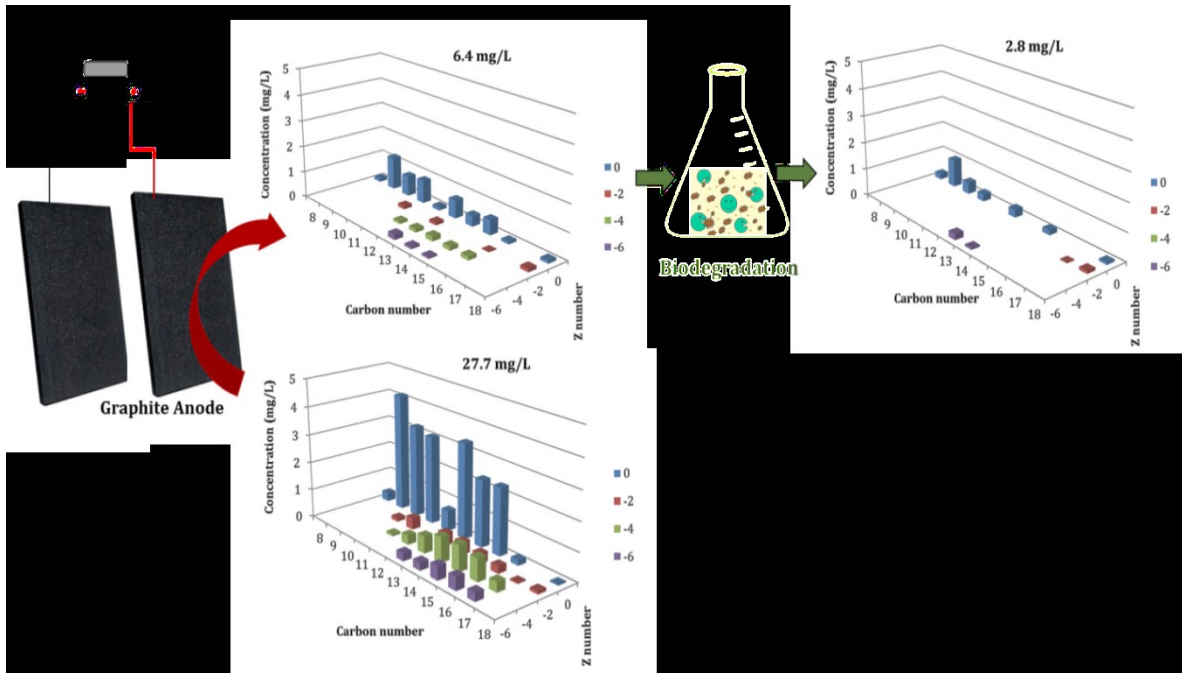**Figure B1** Schematic illustration of the experimental set-up for Electro-oxidation.

Figure B2 Graphical summary of Chapter 2.

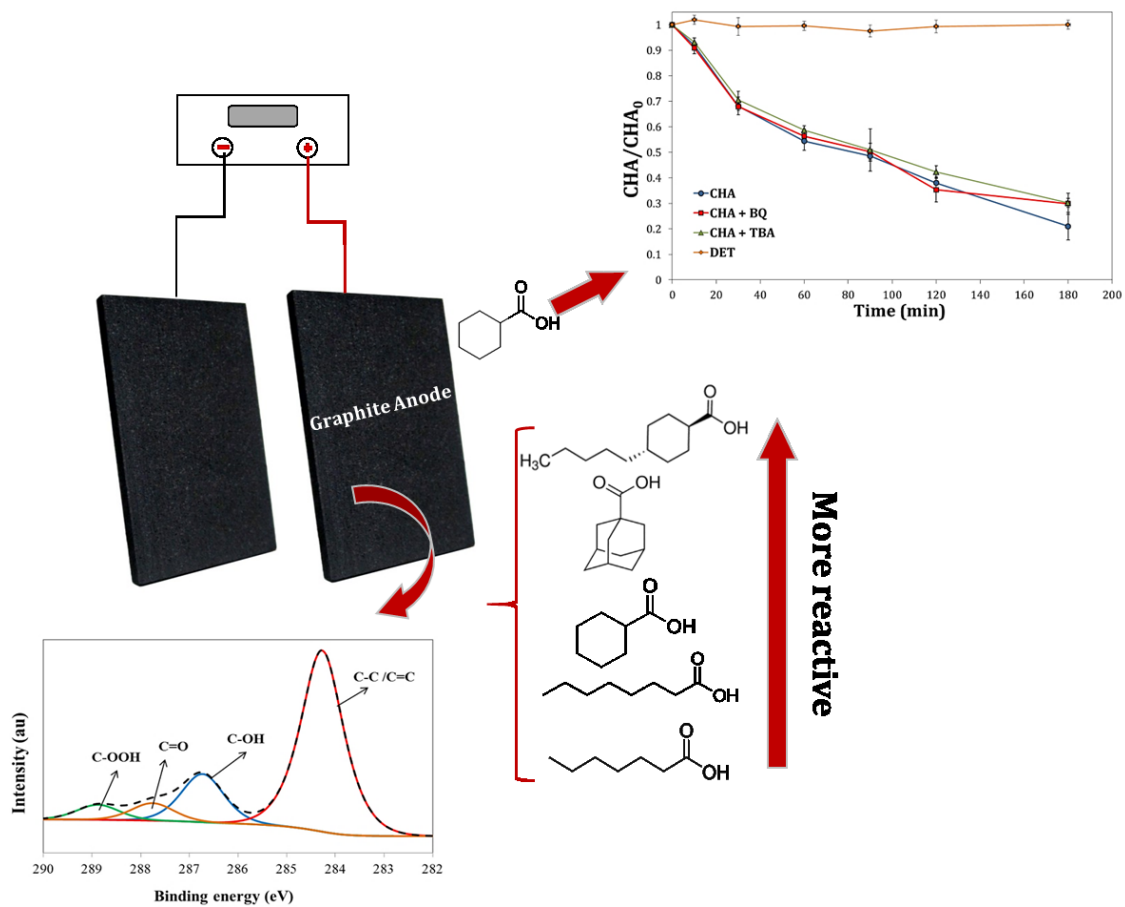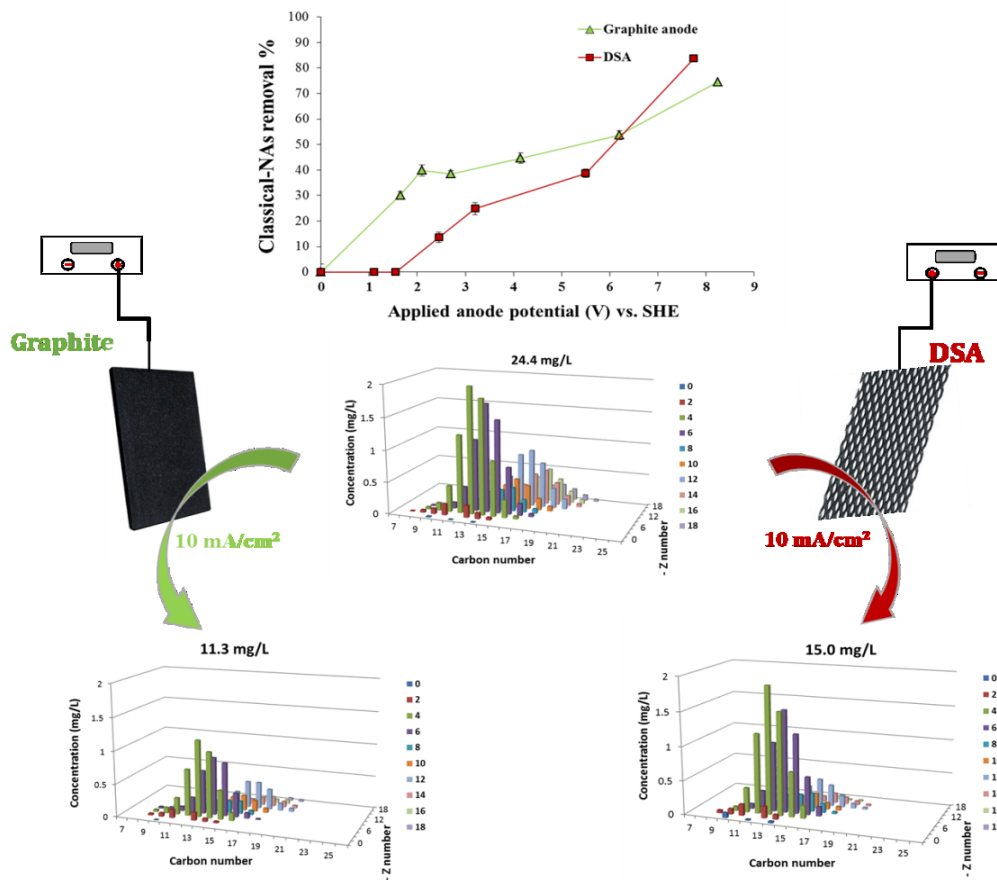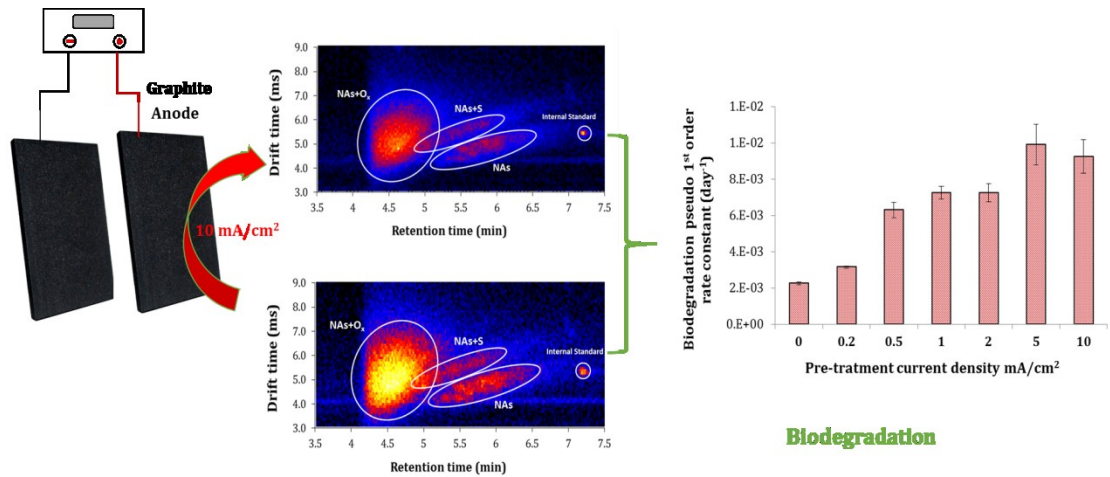**Figure B3** Graphical summary of Chapter 3.

Figure B4 Graphical summary of Chapter 4.

Figure B5 Graphical summary of Chapter 5.